INFLUENCE OF

MANUFACTURING PROCESS PARAMETERS

ON THE PHYSICAL PROPERTIES OF AN

OIL- IN- WATER CREAM

EINFLUSS DER HERSTELLUNGSFAKTOREN AUF DIE

PHYSIKALISCHEN EIGENSCHAFTEN EINER O/W CREME

D I S S E R T A T I O N

der Fakultät für Chemie und Pharmazie
der Eberhard-Karls-Universität Tübingen

zur Erlangung des Grades eines Doktors
der Naturwissenschaften

2007

vorgelegt von

Anja Großmann

INFLUENCE OF

MANUFACTURING PROCESS PARAMETERS

ON THE PHYSICAL PROPERTIES OF AN

OIL- IN- WATER CREAM

EINFLUSS DER HERSTELLUNGSFAKTOREN AUF DIE

PHYSIKALISCHEN EIGENSCHAFTEN EINER O/W CREME

D I S S E R T A T I O N

der Fakultät für Chemie und Pharmazie
der Eberhard-Karls-Universität Tübingen

zur Erlangung des Grades eines Doktors
der Naturwissenschaften

2007

vorgelegt von

Anja Großmann

Für meine Familie

Partial results of this work have been published with permission of Schering AG in the following contributions:

Grossmann, A.,   E. Ceruti, F. Cadei, A. Regola, and R. Daniels. 2007. Influence of the homogenisation time on the physical properties of an o/w cream. *Pharm. Ind.* **69** (6)**:** 730-734.

Grossmann, A.,   F. Cadei, E. Ceruti, A. Regola, and R. Daniels, Influence of the homogenisation time on the physical properties of an o/w cream. (***Poster***) 5th World Meeting on Pharmaceutics, Biopharmaceutics and Pharmaceutical Technology. Geneva. 27-30 March 2006

Grossmann, A.,   F. Cadei, E. Ceruti, A. Regola, and R. Daniels. Influence of the active ingredient on the rheological behaviour of an o/w cream. (***Poster***) 46th symposium AFI. Rimini. 14-16 June 2006 and DPhG Joint meeting. Marburg. 4-7 October 2006

The aim of this study was to examine the manufacturing process of an oil-in-water model cream and to elaborate the relation between critical process parameters and physical properties of the cream. In the past the model cream exhibited some deficiencies such as loss in consistency, separation of watery fluid, and re-crystallisation of drug substance. These instabilities have been directed to be explained and possibly resolved by means of modifying the manufacturing process parameters. Therefore the main emphasis was on pilot scale with batch sizes of 80 kg (placebo) and 40 kg (verum) where a profound knowledge about the process technology was achieved. In addition, placebo batches from lab scale (1.0 kg) as well as verum and pacebo batches from industrial scale (1000 kg) have been the subject of investigation.

For the structural characterisation of the cream, polarized light microscopy, wide and small angle X-ray diffraction, thermogravimetry, differential scanning calorimetry, rheology and physical test methods such as bleeding, electrical conductivity, spreadability and micro-penetration as well as in vitro release were employed. Further, different storage programs (isothermal storage and stress test) provided a broad evaluation of the cream's stability.

Rheological measurements in rotational and oscillatory mode gave the most valuable and detailed results on cream properties and represented an appropriate tool in order to visualize changes in cream properties dependent of manufacturing process parameters. Furthermore, the easily performable physical test methods mentioned above have been proved as being adopted methods for a reasonable cream characterisation regarding the cost-benefit ratio.

Regarding the cream properties and stability, the following as critical retained process parameters have to be investigated: melting time; melting temperature; cooling rate; temperature of API-addition; temperature and duration of final homogenisation; holding time of bulk and finished product as well as filling stress.

The idea of the microstructure is the basis for a reasonable interpretation of the cream behaviour in dependence of the manufacturing process parameters. The structural characterisation of the model cream suggested a gel-matrix comprised by the viscous elastic hydrophilic gel-phase and the lipophilic gel-phase which crystallise separately from each other and intertwine to a fine and complex network immobilizing small oil droplets. This network forms a disordered liquid-crystalline structure of lamellar type, either surrounding the oil droplets or widespread towards the continuous phase. This deformable gel-framework is responsible for the predominantly elastic behaviour of the cream. The cream shows plastic thixotropic flow behaviour with a defined linear viscous elastic region. Water exists as inter-lamellarly bonded water in between crystalline lipid bilayers or entrapped mechanically within

the lipophilic gel-phase or fixed between lipid-layers in the liquid-crystalline state or otherwise present as free bulk water.

The impact from the final homogenisation arose to be the most critical parameter during the manufacturing process. It was proved to irreversibly disorganise already available cream structures formed by crystallisation after cooling. Altered divergence of separately crystallised hydrophilic and lipophilic phases caused water to squeeze out from the gel-matrix and thus reduced the water binding capacity of the cream. Furthermore, the temperature increase in the homogeniser could cause a partially re-melting of crystalline fatty phase components. Hence it was suggested to reduce the final homogenisation time to a minimum in order to alter the cream structure as less as possible but to be attentive to the already available micro textures.

It was also possible to show that the well structured lipophilic gel-network of cetearyl alcohol crystals tolerates a certain mechanical stress as it is applied during tube filling. Rheological results evidenced that the time point of filling is not at all decisive for the final cream properties. Hence, from an economical point of view it is suggested to fill the cream as quickly as possible after manufacturing without a holding time of 10 days. Then the holding time should be applied on the finished product and can be reduced to 5 days. This was shown by rheological results on verum. The mainly suspended active pharmaceutical ingredient (API) azelaic acid (AzA) partially dissolves within the gel-matrix. This slowly dissolution process leads to a drastic decrease in viscosity which reaches its plateau value after approx. 5 days.

Parameters during the melting of the fatty phase components were of secondary importance. This was shown by initial data obtained after 10 days after processing. In order to save energy and time and in order to minimize the instance of chemical decomposition the melting time should be kept short. Further it should be favourable to maintain the melting temperature at the upper limit (75°C) of the default melting range (65-75 °C) in order to avoid occurrence of solidification of lipids when melting near the solidification temperature of surfactant Arlatone 983S and amphiphile Cutina CBS.

A cooling of the hot emulsion in non-linear fashion as generally performed in production may add to the risk of a 'shock'-crystallisation which inhibits the formation of a well structured cream-network widespread towards the continuous phase or surrounding the oil droplets. As an alternative, a more moderate and in particular steady cooling process with a regular formation of both crystalline gel-structures and evenly in the gel-matrix distributed water in consequence, is suggested.

Different API-addition/ final homogenisation temperatures did not influence the physical cream properties in a long time comparison.

Unexpectedly, stability data were in contrast to the storage recommendations (<30 °C). Namely, cream samples were more stable during storage at 40 °C/75 % RH and even more stable during stress test (CT) compared to the isotherm storage at room temperature. Cream samples stored at 25°C/60 % RH generally loss clearly in consistency.

In conclusion of the results of this study an optimized manufacturing process with improved cream properties and with reduced processing times and energy was proposed.

Ziel dieser Arbeit war es, den Herstellungsprozess einer O/W Modell-Creme zu untersuchen und den Zusammenhang zwischen den verschiedenen kritischen Herstellungsparametern und den physikalischen Eigenschaften der Formulierung herauszuarbeiten. Die O/W Creme zeigte in der Vergangenheit in seltenen Fällen Qualitätsmängel wie Konsistenzverlust, Abscheidung von Wasserphase oder Rekristallisationserscheinungen. Aufgabe war es daher, diese Instabilitäten aufzuklären und durch Modifizierung des Herstellungsprozesses möglichst zu beheben. Der Schwerpunkt dieser Untersuchungen lag auf der Herstellung im Pilotmaßstab mit Chargengrößen von 80 kg (Placebo) und 40 kg (Verum). Zusätzlich zu den Pilotuntersuchungen wurden Placebochargen im Labormaßstab (1,0 kg) hergestellt, sowie Verum- und Placebochargen aus dem Produktionsbetrieb (1000 kg) untersucht.

Für die Charakterisierung der Modell-Creme wurden hauptsächlich mikroskopische, röntgendiffraktometrische, thermoanalytische, rheologische und physikalische Methoden wie Synärese, elektrische Leitfähigkeit, Spreitbarkeit und Mikropenetration verwendet. Zudem wurde die Formulierung verschiedenen isothermen Lagerungsprogrammen (25 °C/60 % rF und 40 °C/75 % rF) und einem Schaukeltest (+5 °C/+40 °C/75 % rF) unterzogen, um Rückschlüsse auf deren Kurz- und Langzeitstabilität zu ziehen.

Rheologische Messungen, sowohl im Rotationsexperiment als auch in Oszillation waren hinsichtlich der Beurteilung der Cremeeigenschaften am aussagekräftigsten. Mit beiden Methoden konnten Änderungen in den Produkteigenschaften in Abhängigkeit des Herstellungsprozesses deutlich aufgezeigt werden. Zudem erwiesen sich Methoden wie Synärese, elektrische Leitfähigkeit und Spreitbarkeit hinsichtlich des Aufwand-Nutzen Verhältnisses ebenfalls als gut geeignet für die Charakterisierung der Formulierung.

Kritische Herstellungsparameter und damit Gegenstand der Untersuchung waren Schmelztemperatur/Schmelzzeit; Abkühlrate; Temperatur während der Wirkstoffzugabe; Temperatur und Dauer der Endhomogenisierung; Standzeit der Bulkware/ des Fertigproduktes sowie Abfüllstress.

Die Strukturvorstellung der O/W-Creme bildet die Grundlage für eine rationale Interpretation der Cremeeigenschaften in Abhängigkeit von den Herstellungsfaktoren. Als Strukturmodell wird ein komplexes Gelgerüst, bestehend aus visko-elastischer hydrophiler Gelphase und lipophiler Gelphase angenommen. Die separat voneinander auskristallisierenden Gelgerüste bilden eine ungeordnete flüssig-kristalline lamellare Struktur, welche sowohl die Außenphase durchzieht als auch die Öltröpfchen immobilisiert. Dieses Gelgerüst ist verantwortlich für das vorwiegend elastische Verhalten der Creme. Die O/W-Creme zeigt plastisch thixotropes Verhalten mit einem definierten linear viskoelastischen Bereich (< 30 Pa). Das Wasser ist in diesem Gelgerüst interlamellar zwischen den kristallinen Lipid-Doppelschichten gebunden,

mechanisch im lipophilen Gelgerüst immobilisiert, zwischen den flüssig-kristallinen Lipid-Doppelschichten fixiert oder aber liegt als freies Bulkwasser vor.

Die Dauer der Kalthomogenisierung beeinflusst die Cremeeigenschaften am stärksten. Während des Abkühlens (vor der Endhomogenisierung) kommt es zu einer gleichmäßigen Auskristallisierung zweier separat voneinander vorliegenden Phasen, der hydrophilen und der lipophilen Gelphase. Die nachfolgende Kalthomogenisierung führt zumindest teilweise zu einer irreversiblen Zerstörung der bereits vorhandenen Cremestrukturen. Dies bewirkt ein Verdrängen von Wasser aus dem Gelgerüst, was zu einer erhöhten Synäreseneigung führt. Zudem kann der beachtliche Temperaturanstieg im Homogenisator ein teilweises Schmelzen der kristallinen Fettbestandteile auslösen. Deshalb ist zu empfehlen, die Endhomogenisierung auf ein Minimum zu reduzieren, um die kristallinen Gerüststrukturen der Creme so wenig wie möglich zu verändern.

Es konnte allerdings gezeigt werden, dass das lipophile Kristallgerüst des Cetylstearylalkohols einen moderaten mechanischen Stress, wie er beim Abfüllen auftritt, durchaus zu tolerieren vermag. Die rheologischen Ergebnisse zeigten weiterhin, dass der Zeitpunkt der Abfüllung nicht entscheidend für die endgültigen Cremeeigenschaften ist. Aus Gründen der Zeitersparnis erscheint es daher empfehlenswert, die Creme direkt nach der Herstellung und ohne eine Standzeit von 10 Tagen in Tuben abzufüllen. Die Standzeit sollte dann am Endprodukt d.h. in der Tube erfolgen und kann auf 5 Tage reduziert werden. Das zeigten die rheologischen Ergebnisse am Verum. Der vorwiegend suspendiert vorliegende Wirkstoff Azelainsäure löst sich zu einem geringen Anteil in der Gelmatrix. Dieser langsam stattfindende Lösevorgang führt zu einer deutlichen Abnahme der Viskosität, die nach 5 Tagen ein Plateau erreicht.

Die Parameter während des Schmelzvorganges der Lipidphase zeigten sich von untergeordneter Bedeutung. Für eine zeit- und energiesparende Herstellung, aber auch um eine chemische Zersetzung der Fettbestandteile zu verhindern, wird daher empfohlen, die Schmelzzeit deutlich zu verkürzen. Um ein Erstarren von Emulgator Arlatone 983S und Konsistenzgeber Cutina CBS auszuschliessen, wird zudem eine Temperatur an der Obergrenze (75 °C) des vorgegebenen Schmelzintervalls (65 - 75 °C) empfohlen.

Ein nicht linearer Abkühlvorgang, wie er generell während der industriellen Herstellung erfolgt, kann das Risiko einer schockartigen Kristallisation mit sich bringen. Diese kann wiederum den ungestörten Aufbau von Gelstrukturen verhindern. Alternativvorschlag ist ein moderater und vor allem gleichmäßiger Abkühlprozess (0,5 - 0,75 °C/min), der eine gleichmässige Ausbildung der kristallinen hydrophilen und lipophilen Gelphase erlaubt und damit zu einer gleichmässigen Wasserverteilung innerhalb der Gelmatrix beiträgt.

Unterschiedliche Temperaturen während der Wirkstoffeinbringung bzw. während der Endhomogenisierung beeinflussten kaum die physikalischen Cremeeigenschaften in einem Langzeitvergleich.

Das Lagerverhalten der Creme steht unerwarteterweise im Gegensatz zu den Lagerempfehlungen (< 30 °C). Die Cremeproben zeigten sich stabiler während der Lagerung bei 40 °C/75 % rF bzw. nach Schaukeltest (+5/+40 °C/75 % rF) im Vergleich zur Lagerung bei Raumtemperatur (25 °C/60 % rF). Bei 25 °C/60 % rF gelagerte Cremeproben verlieren generell an Konsistenz.

Für eine Optimierung der Cremeeigenschaften wird schlussfolgernd aus den Ergebnissen dieser Studie ein alternativer, Energie und Arbeitszeit einsparender Herstellungsprozess vorgeschlagen.

List of abbreviations

API	active pharmaceutical ingredient
AzA	azelaic acid
BET	Brunauer, Emmet and Teller (surface analysis)
BP	bulk product
Corresp.	corresponding
CP	cooling process
CR	cooling rate
CR	controlled shear rate
CS	controlled shear stress
CT	cycle test
DAB	German pharmacopoeia (Deutsches Arzneibuch)
DSC	differential scanning calorimetry
DTGA	differential thermogravimetric analysis (first derivate of TGA curve)
FP	finished drug product
Homog.	homogenisation
HT	holding time
ICH	International conference of harmonization
Ind	industrial scale
IPC	in process control
IVR	in vitro release
Lab	lab scale
LTF	technical pharmaceutical lab
LVE	linear visco-elastic region
Ph. Eur. 5	European pharmacopoeia volume 5
Pilot	pilot scale
RT	room temperature
RW 125	Becomix pilot plant (125 L)
SAXD	small angle X-ray diffraction
Sd	standard deviation
SEM	scanning electron microscopy
Std	standard
t_0	10 days after manufacturing date (begin of stability program)
TEM	transmission electron microscopy
TEMP	temperature
TGA	thermogravimetric analysis
T_{onset}	onset temperature
WAXD	wide angle X-ray diffraction
#	batch number

1   INTRODUCTION AND GOAL

The purpose of a semisolid's manufacturer is to consistently produce semisolid systems with long term stability that have a stable microstructure. Concerning this the manufacturing process plays an important role in the quality of a semisolid formulation. Variations in the manufacturing procedures can cause different microstructures and hence changes in the physical cream properties. An inhomogeneous quality of the finished product is therefore the consequence.

The importance of the influence of the manufacturing process on the physical properties and stability of a semisolid formulation has already been showed by different authors.

Alberg (1998) and Kudlek (1996) examined the influence of the manufacturing temperature on the colloidal structure of semisolids. Alberg for instance varied the manufacturing temperature of the model system Wasserhaltige hydrophile Salbe DAB' between 70 °C (according DAB), 50 °C and room temperature (RT) and compared the model creams with regard to structural changes. The creams prepared at RT showed an altered melting behaviour with a lower melting enthalpy compared to creams prepared according DAB. At lower temperatures fatty components are dispersed by mechanical energy, fat globules become visible by TEM. At 70 °C all lipophilic components are molten and because of the higher dispersion grade fat globules are not visible in the TEM-micrograph. Creams prepared at 50 °C led to similar results as creams prepared at RT. A lowering of the manufacturing temperature led indeed to stable creams though their micro structure changed.

Kudlek (1996) demonstrated the temperature dependent distribution of an emulsifier between hydrophilic and lipophilic phase. As a consequence, preparation at 85 °C yielded a lotion whereas at 70 °C a cream was obtained.

The influence of the cooling rate onto the product has been multiply investigated. Timmins (1990) clearly showed lower melting enthalpies of creams manufactured with faster cooling rates which had the same quantitative composition. He reasoned the phenomenon must arrive from a higher organisation of molecules at slow cooling. This in consequence requires more energy for the phase transition. Ecclestone (1990) revealed varying formation of gel-structures dependant on the cooling and dispersing processes. Fast cooling together with low dispersing leads to more fluid systems.

Nürnberg (1968) developed a non ionic o/w cream and obtained homogeneous stable systems by intensive homogenisation whereas manual stirring under cooling led to unstable non homogeneous systems.

Rose (1999) explained the relevance of the manufacturing technology on the colloid structure and stability of a cream.

Brämer (2004), Lashmar (1995) and Asche (1984) pointed out that most semisolids shortly after manufacturing have not obtained their final structure yet, so rheological measurements can lead to less reproducible and representative data.

Folger (1994) pointed out to process parameter changes with scaling up from lab-scale to pilot or industrial scale.

Furthermore creams are influenced by storage temperatures and shear forces. The gel structure may stiffen at lower temperatures, or soften and fluidize at higher temperatures. Shear thinning due to mechanical stress may break down gel structure. Creams possess thixotropic properties that allow recovery of the gel structure upon storage after exposure to shear forces. General indications of instability are the inversion of the emulsion type, coalescence of dispersed phase, syneresis or drop of viscosity and consequently loss of consistency.

Factors inherent to cream composition related to variability of excipients as well as external factors such as packaging, storage time, temperature conditions and shear forces may induce cream instabilities (Kallioinen, 1994).

Various parameters and their interaction complicate the interpretation of physical properties of semisolid systems. Altogether there is a plurality of parameters to be considered influencing the colloidal structure and thus the physical properties of semisolids and also determining their storage stability.

This PhD-thesis focuses on the influence of various process parameters on the physical properties of a model o/w cream containing 20 % (w/w) suspended azelaic acid (AzA) as active pharmaceutical ingredient (API). The o/w cream, used in the treatment of acne and rosacea, is always a marketed product.

In the past, deficiencies in the cream stability occurred. These deficiencies concerned low consistency/viscosity, separation of watery fluid and re-crystallisation of drug substance. Data on critical aspects of the preparation has already been assessed in the past and investigations on manufacturing parameters have been performed in order to ensure the manufacturing of a high-quality product (chapter 2.2.6.). As far as they may originate from the manufacturing process aim of the current study was to identify the causes of the mentioned deficiencies by re-investigating the formulation. The purpose was to understand instability problems and to resolve them at best. Special emphasis was on the most critical manufacturing process parameters cooling rate, homogenisation temperature and number of circulations and their impact on the cream properties. Studies were mainly carried out on pilot scale (40 to 80 kg) on placebo and verum. In view of the study's purpose suitable test methods and stability programs have been established (chapters 3.2 and 3.3).

2   GENERAL PART

2.1 Creams (Ph. Eur. 5)

Creams are multiphase preparations consisting of a lipophilic phase and an aqueous phase. They are formed by incorporation of water into a water-absorbing ointment. The European pharmacopoeia (Ph. Eur. 5) distinguishes between lipophilic and hydrophilic creams.

2.1.1   Lipophilic creams (water-in-oil creams)

The lipophilic gel (hydrocarbon gel, oleo gel, or lipogel) represents the continuous outer phase of lipophilic creams. The lipophilic gel phase gives these creams their spreadability. They contain water-in-oil emulsifying agents such as wool alcohols, sorbitan esters and monoglycerides (Ph. Eur. 5). A typical lipophilic cream is the 'aqueous wool fat ointment' (DAB). Its structure is shown in figure 2-1. In finished products, these are referred to as ointments or rich creams (Daniels and Knie, 2007).
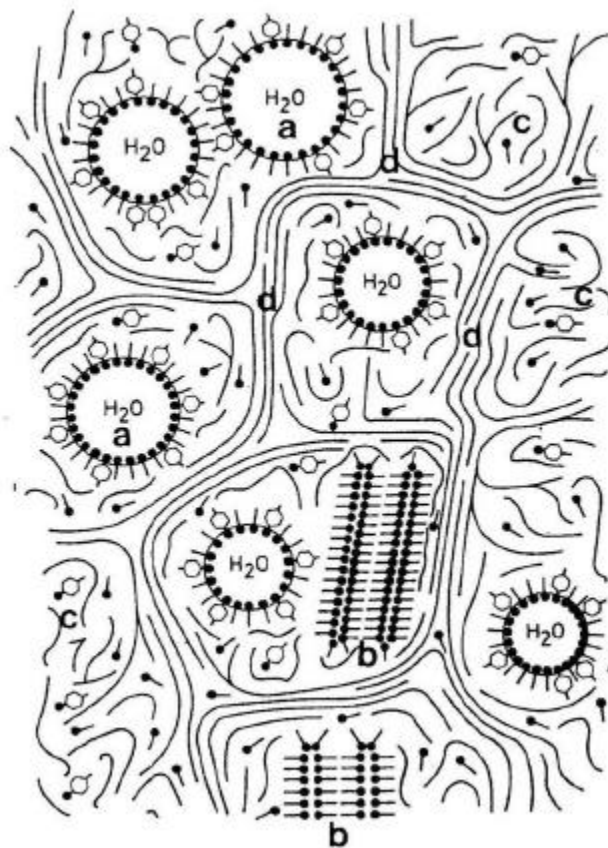
Figure 2-1:   Colloidal structure of a water-in-oil cream (from Niedner, Ziegenmeyer, 1992)

a)   Water droplet stabilised by mixed emulsifiers
b)   Crystals of excess emulsifier
c)   Lipophilic liquid with dissolved emulsifier
d)   Lipophilic gel phase

2.1.2   Hydrophilic creams (oil-in-water creams)

Hydrophilic creams have as the continuous phase the aqueous phase. They contain oil-in-water emulsifying agents such as sodium or trolamine soaps, sulphated fatty alcohols, polysorbates and polyoxyl fatty acid and fatty alcohol esters combined, if necessary, with water-in-oil emulsifying agents (Ph. Eur. 5).

Oil-in-water creams can generally be thought of as mixtures of a hydrogel and an emulsion. They are complex multiple-component preparations and only rarely simple two-phase preparations (Ecclestone, 1990). Although the hydrogel may be formed by a polymer, it is more frequently formed by a swollen, liquid crystal structure of a lamellar arrangement of surfactants. For this purpose, hydrophilic creams contain a mixture of at least two emulsifiers known as 'complex emulsifiers', which combine hydrophilic and lipophilic emulsifiers. The hydrophilic component determines the emulsion type and stabilizes the dispersed oil phase. The lipophilic component crystallizes on its own at room temperature or together with the hydrophilic component, forming a framework that makes the cream easy to spread and stabilizes it (Daniels and Knie, 2007). An example of a typical hydrophilic cream is the 'aqueous hydrophilic ointment DAB' (figure 2-2).
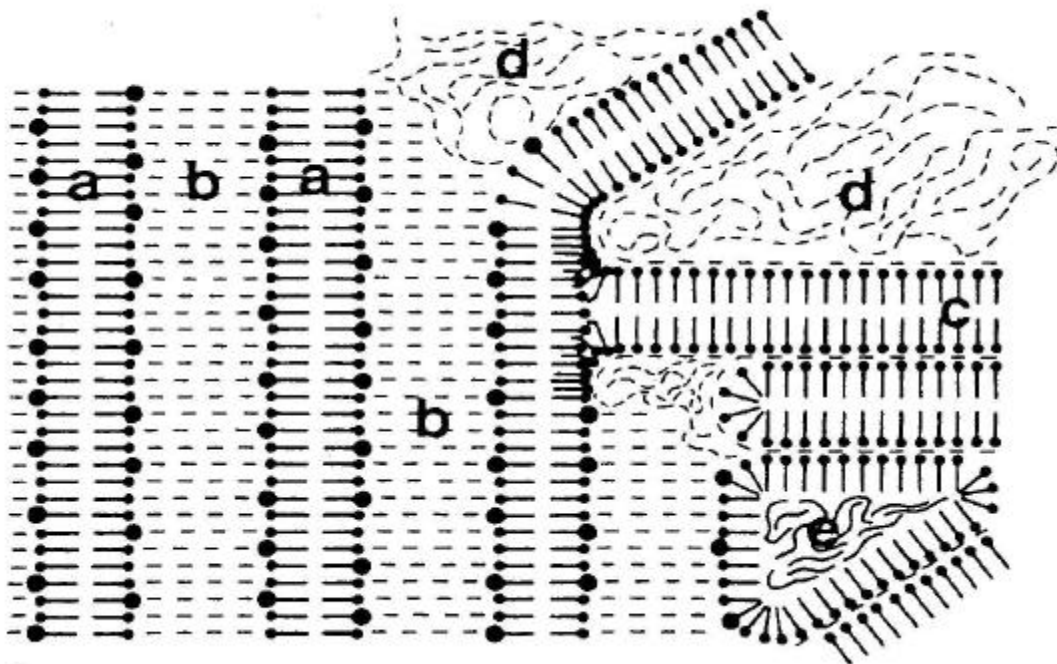
Figure 2-2: Colloidal structure of an oil-in-water cream (from Niedner, Ziegenmeyer, 1992)

        a)   Liquid crystal, lamellar gel structure of emulsifying cetearyl alcohol
        b)   Inter-lamellar fixed water
        c)   Cetearyl alcohol-semihydrate-gel structure
        d)   Bulk water phase
        e)   Lipophilic, disperse phase

They consist of a bulk water phase, a dispersed oil phase and in addition a hydrophilic and a lipophilic gel phase. The fatty amphiphile and the surfactant form a crystalline hydrophilic gel phase. Water molecules enclosed between the bilayers of the hydrophilic gel phase form inter-lamellar water layers. Water molecules available as bulk water are in equilibrium with inter-lamellarly fixed water in the hydrophilic gel phase. Inter-lamellarly fixed water and free bulk water form the continuous phase of the o/w cream. The fatty amphiphile, which doesn't fall part of the bilayers, builds up a lipophilic matrix, the lipophilic gel phase. The dispersed oil phase is mainly immobilized mechanically by the lipophilic gel phase (Kallionen, 1995).

The proportion of the above-described phases of creams depends on the composition of the mixed emulsifier (Kònya et al., 2003). Mixed emulsifiers are composed of an ionic or non-ionic surfactant and fatty amphiphiles. The type of surfactant alters the water binding mechanism in o/w creams. As fatty amphiphiles occur fatty alcohols, fatty acids or monoglycerides. The proportion of surfactant and amphiphile usually varies between 1:2 and 1:20 (Eccleston et al., 1989). These mixed emulsifiers are well-known as ideal stabilizers for semi-solid preparations.

The quantity of bulk and fixed water mainly influence physical properties of creams but they are also important criteria for drug release from o/w creams. It was assumed that increasing the amount of water changes the microstructure of the cream, thus affecting its release properties. A high penetration of the vehicle into the skin is the basis for a high availability of incorporated drug substances.

Oil-in-water creams are indicated for indifferent to fatty skin and can also have a drying effect (Daniels, 2007). In finished products, hydrophilic creams are considered as creams.

2.1.3   Amphiphilic creams

Amphiphilic creams have a bi-coherent structure, meaning that the lipophilic and aqueous phases are continuous (figure 2-3). They thus do not entirely conform to the definition of either a lipophilic or hydrophilic cream, but fall somewhere in between the two. Internal and external phases cannot be discerned and, given their bi-coherence, amphiphilic creams can be diluted with water or lipids. Most such finished products are referred to as creams (Daniels and Knie, 2007). An example of an amphiphilic cream is the 'Basiscreme DAC'.
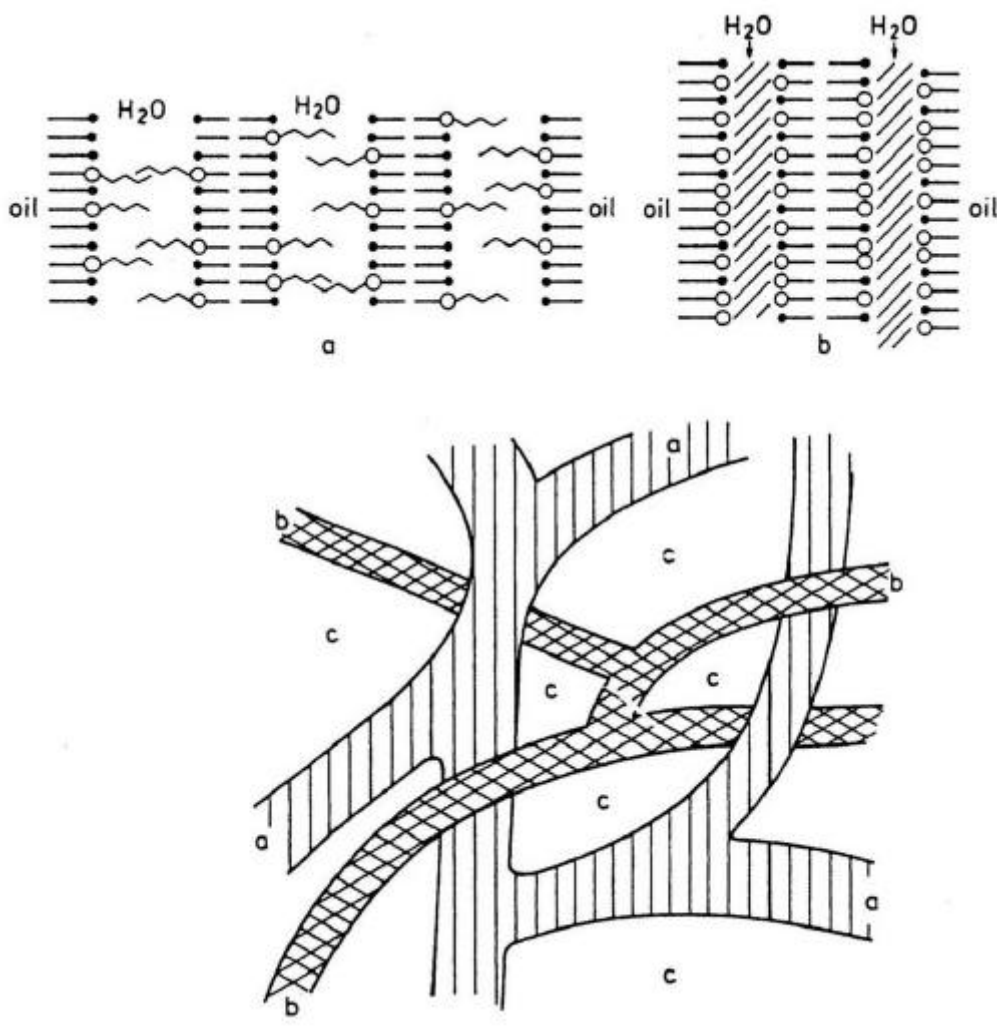
Figure 2-3: Colloidal structure of an amphiphilic cream (from Niedner, Ziegenmeyer, 1992)

        a)   Partly swollen gel structure (emulsifier phase)

        b)   Completely swollen gel structure (water phase)

        c)   Coherent lipid phase

2.2 Manufacturing

In the following chapter and subchapters the manufacturing of o/w creams in general and of the model cream in particular as well as the filling process of the model cream are described. Thereby the appropriate equipment in lab, the pilot and the industrial scale is illustrated. Thereafter the critical process parameters which are supposed to affect the cream quality will be discussed.

2.2.1   Manufacturing procedure of o/w creams in general

Firstly the fatty phase and aqueous phase are prepared separately in the melter and mixer vessels. The fatty phase consists of not only solid and liquid fatty components, but also the fat-soluble emulsifier. The fatty phase is completely melted by heating it up to about 75 °C. Thereafter the fatty phase is filtered through a filter or mesh into the hot mixer by vacuum, pumping or gravitational force.

Similarly, the aqueous phase is heated up to about 75 °C and passed through a filter.

Stirring, it is added to the fatty phase in the mixer, preferably directly into the homogeniser, for a fast dispersion. By operating a fast stirrer and homogeniser, the inner phase (oil) is finely dispersed into the outer phase (water). During the subsequent, moderate, and often stepwise cooling process the cream must be stirred to ensure a soft cream without lumps. Stirrer and blades should ensure a good horizontal and vertical circulation of the mass with an optimal heat exchange within the product. The cooling is supported by a double jacket containing hot or cold water.

Of importance is the solidification temperature of the cream. The optimal effect is obtained with a homogenisation during solidification because the fineness of the emulsion may be retained by solidification. In particular the homogeniser should be used at the beginning of the emulsification and during solidification (Köhler, 1992).

During this so called 'continental' or 'inversion' method, a w/o emulsion is formed at first which then inverts into a o/w cream because of the increasing water phase volume. In lab scale this method is often used since it leads to a fine dispersion of the inner phase. On industrial scale the continental method is less common. There is the so called 'English method' which is exclusively used. In this method the outer phase is provided and the inner phase is added proportionately while stirring the outer phase.

More recent procedures use a low-temperature emulsification. During this energy saving procedure, a cold aqueous phase is dispersed into the hot fatty phase directly through the homogeniser. According to Funke (1972) the processing time may be reduced from 2.5 h to 0.5 h for a 500 kg batch size. Basically for this procedure there is a high fat fraction. If the fat fraction is too low the temperature can fall below the solidification temperature before the complete water phase is added. At higher fat portions on the other hand, saving of time and energy is lost.

2.2.2   Manufacturing procedure of the model o/w cream

Within this PhD-thesis the model o/w cream is manufactured in a Becomix plant where the inner phase is added through the upper part of the mixer into the outer phase i.e. the 'english method' is used. Subsequently the mixture is homogenised by the homogeniser placed at the bottom of the mixer (manufacturing process on pilot scale 2.3.4.3). This procedure was not changed within the scope of this study.

The flow chart in figure 2-4 represents the manufacturing process of the model cream. Processing times are adapted depending on the manufacturing scale. However, the following general steps described are identical for lab, pilot and industrial scale.

The manufacturing process starts with the melting of the fatty phase components at 70 °C and the heating of the aqueous phase up to 70 °C. Both phases have to be free of granulated matters. Then, the fatty phase is added to the aqueous phase and subsequently homogenised at 70 °C. The emulsion is cooled down to 28 °C before the API is added through a suction tube. Thereafter the cream is homogenised. A microscopic check as in process control (IPC) is performed in order to indicate the homogeneous dispersion of the API within the cream. After deaeration the cream is unloaded and stored for at least 10 days before being filled in tubes.
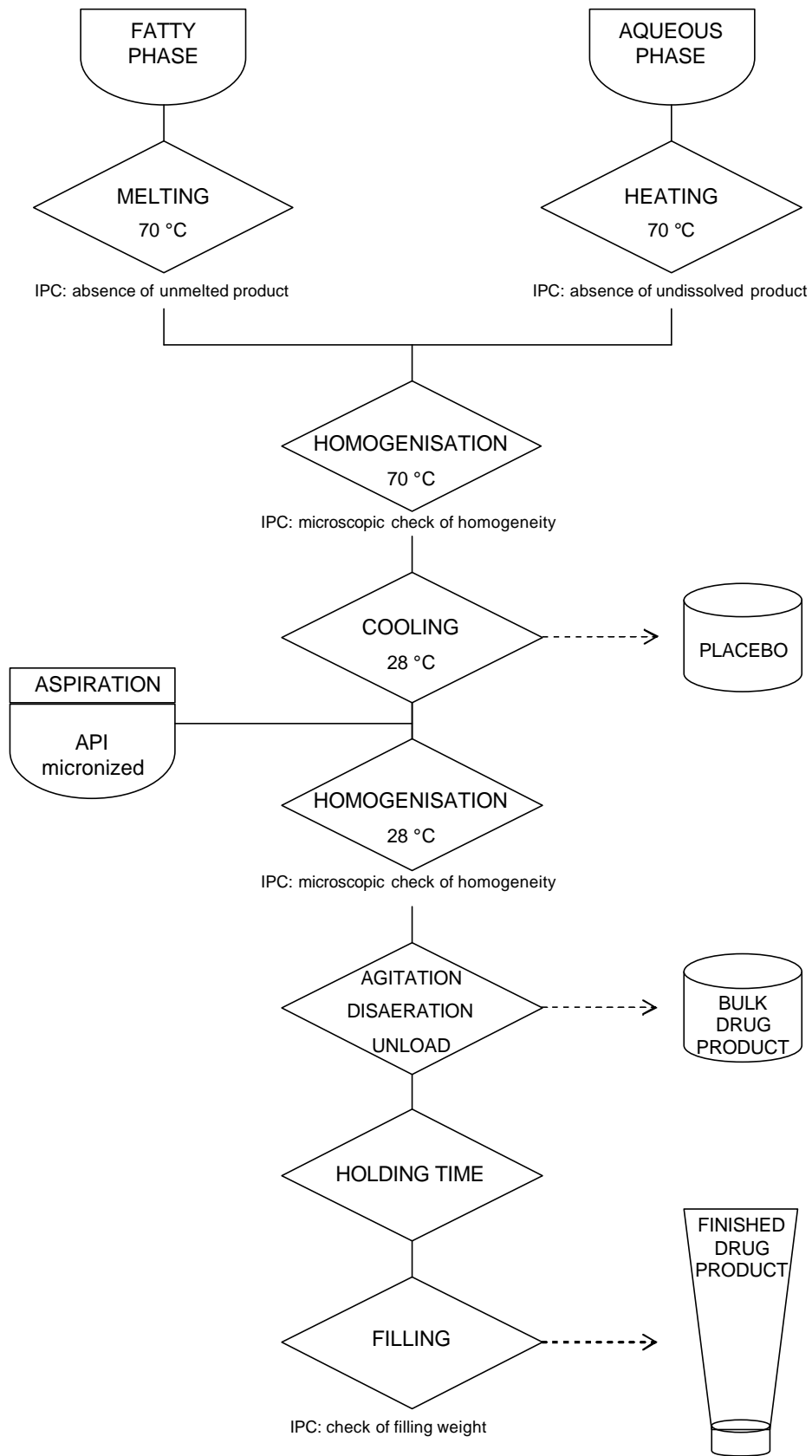
Figure 2-4: Flow chart of the manufacturing process of the model cream

API active pharmaceutical ingredient
IPC in process control

2.2.3   Manufacturing on lab scale

On lab scale, placebo batches with a batch size of 1 kg were prepared. Firstly fatty phase components PCL-Liquid, Cutina CBS and Arlatone 983S were weighed in an appropriate beaker and melted at the predetermined temperature for the predetermined time on a heater with magnetic stirrer. The aqueous phase was prepared in a separate beaker accordingly. The preservative was dissolved in hot water. Propylene glycol and glycerol 85 % were added to the limpid solution.

Thereafter the aqueous phase was homogenised while continuously adding the fatty phase. The mixture was homogenised for 3 min at 6000 rpm by the Ultraturrax T50 (Janke & Kunkel IKA$^{®}$ Labortechnik, Staufen, Germany) (fig. 2-5, left). The emulsion was cooled down in an appropriate lab mixer (fig. 2-5, right) under continuous stirring at 1400 rpm at a vacuum of 76 cm/Hg until deaeration. The mixer consists of a container (self-made) and a stirrer RW 25 (Janke & Kunkel IKA$^{®}$ Labortechnik, Staufen, Germany). After deaeration the cream was cooled down to RT under stirring at 400 rpm.

The cream was filled into tidy closed polyethylene jars (Lameplast S.p.a., Rovereto, Italy) and stored in the climatic cabinet at 25 °C/60 % RH. Each process parameter during the manufacturing process was monitored and documented precisely in a manufacturing batch record. An example record is shown in fig. 2-6.

Figure 2-5:   Ultraturrax T50 (left), Lab mixer RW 25 (right)

Intendis Manufacturing SpA				Pharmaceutical development	
		MANUFACTURING BATCH RECORD			
					Page 1 of 2

PRODUCT NAME: <u>CREAM BASE (PLACEBO)</u>
BATCH SIZE: <u>1 kg</u>
BATCH N°: SHT 292-P04   Target: Investigation of melting parameters

EXCIPIENTS (Item number)	G actual	Batch number	% nominal	g nominal	Signature
Arlatone 983S (1905074)	62,52	56027131	6,250	62,50	
Cutina CBS (1905108)	87,52	56028781	8,250	87,50	
PCL liquid (1905090)	37,60	56011026	3,750	37,50	
Propylene glicol (1905124)	156,42	56027672	15,625	156,25	
Glycerol 85% (1905116)	18,89	56013539	1,875	18,75	
Benzoic acid (1905082)	2,50	56012587	0,250	2,50	
Purified water	635,30	08.05.06	63,500	635,0	

DATE OF PRODUCTION START: <u>08.05.06</u>   DATE OF PRODUCTION END: <u>08.05.06</u>
YIELD g: <u>948,0</u>   YIELD %: <u>94,8</u>

SIGNATURE: DATE: 08.05.06

Intendis Manufacturing SpA		Pharmaceutical development
	MANUFACTURING BATCH RECORD	
		Page 2 of 2

POS	PROCEDURE	DATE	SIGN

1	• Weigh in an adequate beaker:
	     62,5 g ARLATONE 983S
	     87,5 g CUTINA CBS
	     37,5 g PCL-LIQUID
	 • Melt on a hot plate with magnetic stirrer at 65°C for 30min.
	     Actual temperature: *65* °C
	     Actual time: *30* min
	 IPC: visual check for the completeness of the melting: <u>*corresponds*</u>
		08.05.06	

2	• Weigh in a adequate beaker:
	     635,0 g PURIFIED WATER
	 • Heat on a hot plate with magnetic stirrer up to 65-75 °C.
	     Actual temperature: <u>*72*</u> °C
	 • Add **2,5 g BENZOIC ACID** under stirring.
	 IPC: visual check for the completeness of the dissolution: <u>*corresponds*</u>
	 Add **156,25 g PROPYLENE GLYCOL** and
	     18,75 g GLYCEROL 85%
	 • Heat under stirring up to 65-75°C
	     Actual temperature: *72* °C
	 IPC: visual check for the completeness of the dissolution: <u>*corresponds*</u>
		08.05.06	

3	Homogenise the mixture from Pos.2 with the Ultra-Turrax T50 at 6000 RPM while adding continuously Pos.1.	08.05.06	
4	Proceed the homogenisation with Ultra-Turrax T50 for 3min at 6000 RPM. Actual time: <u>*3*</u> min. Actual speed of homogenisation: *6000* RPM	08.05.06	
5	Cool down the emulsion under stirring with the mixer RW25 until the cream is deaerated. Speed of stirring: 1400 RPM Final vacuum: 76 cm/Hg Actual temperature: <u>*42,0*</u> °C Actual speed: <u>*1400*</u> RPM Cool down the cream under stirring at 400 RPM to ambient temperature. Actual speed of stirring: <u>*400*</u> RPM Actual temperature: *26,0* °C **IPC**: microscopic check for homogeneous appearance: <u>*corresponds*</u>	08.05.06	

DATE :   SIGNATURE :

Figure 2-6:   Example of a manufacturing batch record on lab scale

2.2.4   Manufacturing on pilot scale

Lab scale conditions allow to control the process in wide limits in order to obtain a homogeneous quality product. If an investigation of the influences from single process parameters on physical, technological and stability of the cream's properties is desired then manufacturing on lab scale as described before is not sufficient.

The main focus of this PhD study was the manufacturing on pilot scale because of its possibility to vary process parameters under strict controlled conditions. For instance product temperature throughout the whole process, pressure and cooling rate were adjusted manually and kept in close limits. This was very important for a reliable assessment of a possible impact of the investigated parameter on the cream's properties. The pilot plant is very similar to the industrial plant, hence close to practice. In case of changes to process parameters or raw materials the modified process can be scaled up easily without expecting significant changes in the product quality.

Novel products usually first pass the pilot scale before industrial manufacturing starts in order to optimise the desired product characteristics developed previously on a smaller pilot scale or on lab scale. Manufacturing on pilot scale is more reasonable than industrial manufacturing but still near to the industrial product. Once reached the desired product quality and stability the product is ready for scaling up. But also at this final point difficulties can still occur due to changes in the product properties.

Sometimes process parameters have to be once again adjusted. In the worst case, one must go back to lab scale in order to modify the composition or sequence of manufacturing.

2.2.4.1   Pilot plant Becomix RW 125

The pilot plant Becomix RW 125 (A. Berents GmbH & Co KG Mischtechnik, Stuhr, Germany) as shown in figure 2-7 consists of a premixing vessel B2 type MV 125 and a vacuum mixer/homogeniser M1 type RW 125 CD. The plant is semi-automatically operated by a touch screen provided by Berents captive software. All steps of the manufacturing process are started, terminated and controlled from there. Parameters as temperatures, pressures etc. are monitored and adjusted manually in order to keep the desired conditions in very close limits. Major specifications of the Becomix plant RW 125 are listed in table 2-1.
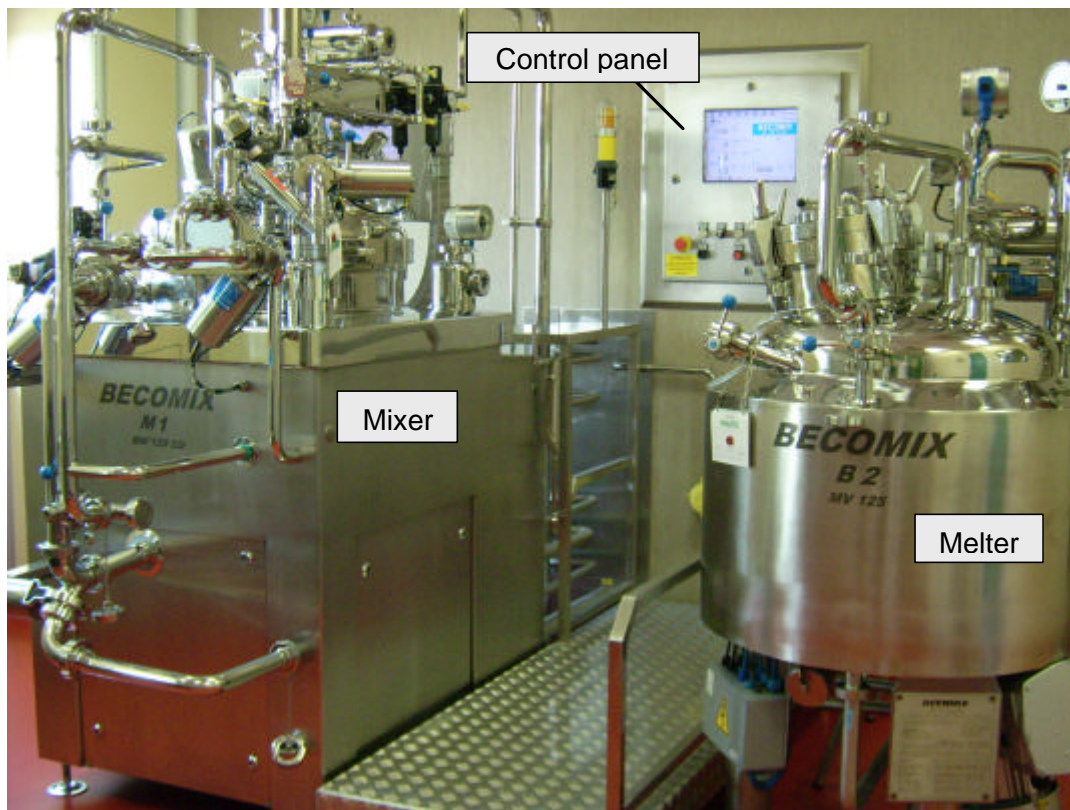
Figure 2-7:   Pilot scale plant Becomix RW 125

Table 2-1:   Specifications of melter and mixer/homogeniser

	Melter B2 MV 125	Mixer M1 RW 125 CD
Batch capacity min [l]	20	30
Batch capacity max [l]	125	125
Stirrer diameter [mm]	150	638
Stirrer velocity [m/s] / [rpm]	2-10 / 255-1274	0,6-3,6 / 18-108
Homogeniser velocity [m/s] / [rpm]	-	5-25 / 845-4227

2.2.4.1.1   Melter

Solid and liquid components are loaded manually into the melter through the top cover which is opened manually. A dissolver blade is placed non-centrically (fig. 2-8) on the bottom of the melter vessel. This shear tool assures an asymmetrical circulation of the product and heat exchange between jacket and product. Stir speed and stir direction are controllable by the control desk.
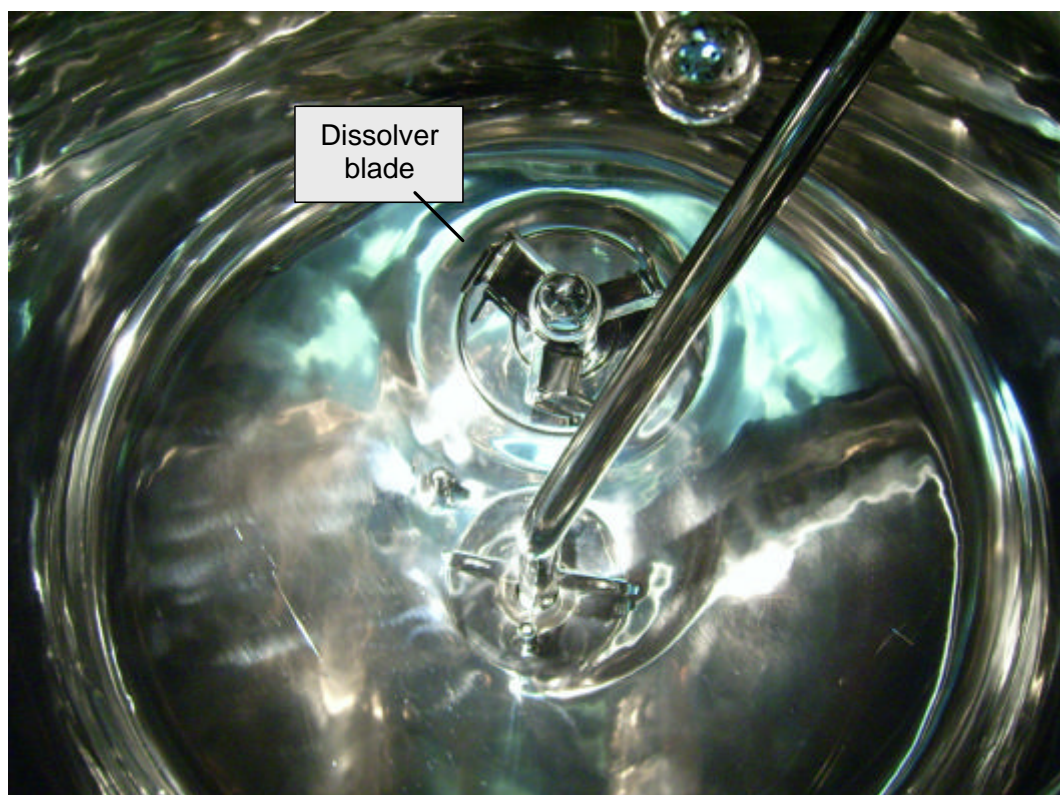
Figure 2-8:   Melting vessel with dissolver blade

2.2.4.1.2   Mixer

The mixer vessel is equipped with a centrally placed horseshoe stirrer fixed on the top cover. The horseshoe stirrer ensures a homogeneous heat exchange by a mainly tangential movement of the high viscous mass. Its combination with blades (stainless steel) and wall scrapers (Teflon) facilitates the circulation of the product (fig. 2-9) by an additionally axial movement. This stirring mechanism assures an intensive circulation of the product in vertical and horizontal direction. Stirring speed and stirring direction (right, left or inversion) are controllable from the control panel.

The vessel is provided with a circulation tube. Liquid excipients are added through this tube applying vacuum. The micronised API is added by aspiration through a suction device (Berents) fitted on the top cover. Mixer and melter vessels are surrounded by a double jacket. Heat exchange medium is hot and cold water. Melter and mixer have integrated temperature sensors at the bottom and in the middle of the vessels. It is possible to work with the jacket or with the product temperature or with both. Actual temperatures at the bottom and middle of the vessel can be displayed on the touch screen. Top covers are provided with a control window with wiper and light in order to visually control the process.
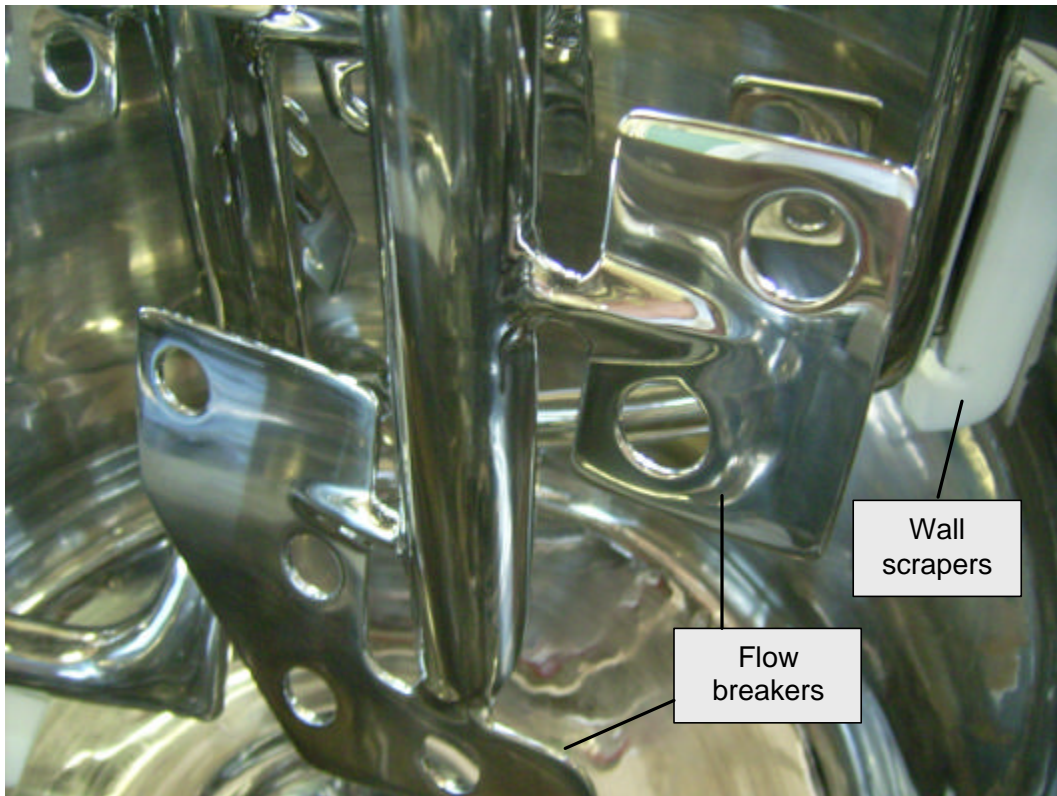
Figure 2-9:   Mixer vessel with horseshoe stirrer, flow breakers and wall scrapers

2.2.4.1.3   *Homogeniser*

The homogeniser as generator of high shear forces serves to emulsify aqueous and fatty phases and to disperse the micronised API into the cream. Fineness of the emulsion and dispersion of solids primarily depend on the homogenisation technique and intensity. Normally, emulsions are homogenised in the vessel (in-line) while products having a higher viscosity such as ointments are homogenised in circulation by means of a circulation tube outside the boiler. The circulation tube connects the centred placed homogeniser at the bottom of the boiler with the upper part of the mixer (fig. 2-10 a).

Starting the circulation tool of the homogenisation process the product circulates passing through homogeniser and circulation pipe before it comes back into the mixer. Homogenisation in circulation generates a particularly good rearrangement of the product.
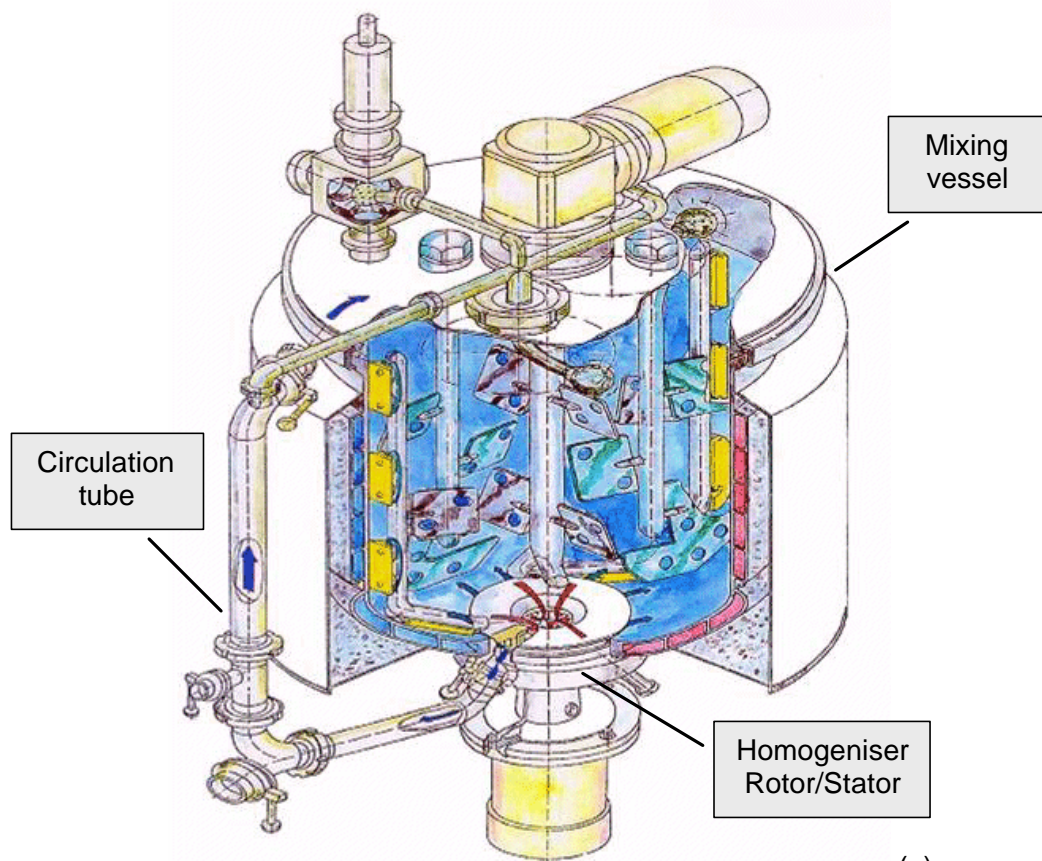
(a)
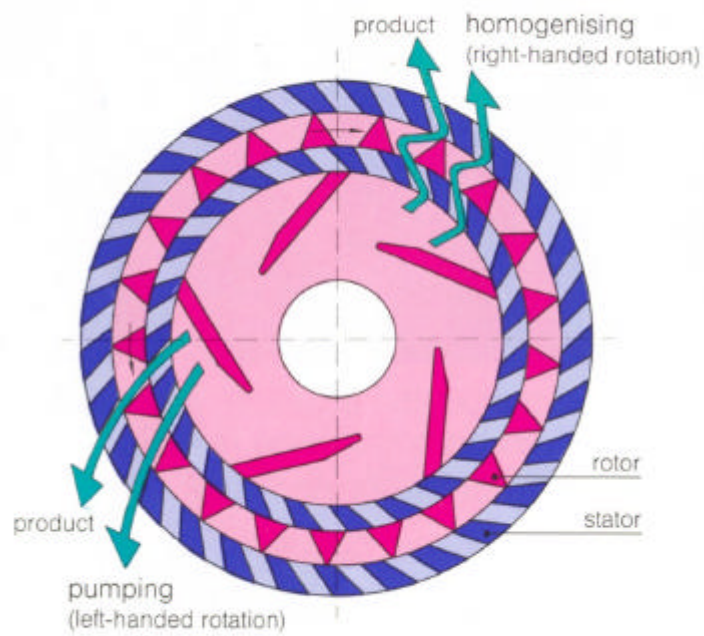
(b)

Figure 2-10:   Mixer vessel with homogeniser (a); Rotor/stator system (b)
                  (from Becomix manual, Berents GmbH & Co KG)

The homogeniser works according to the rotor-stator principle. Two different modes of operation are possible (fig. 2-10 b):

(1)   intensive homogenising during right-handed rotation with high shearing effect

(2)   intensive pump effect during left-handed rotation with low shearing effect.

The cogs of the rotor are placed between two steel blades (stator). The product is directed centrally into the inner blade row of the rotor where flow breakers cause an intensive circulation. Here the product is subjected to high pressure, high shear and gravitational forces between rotor and stator blades. Products with low viscosity e.g. molten or aqueous phases pass through the annulus of 0.5 mm at a high speed creating an intensive mixing effect. Products with high viscosity adhere to the walls of the annulus, leading to a pressure increase and finally to a forced homogenisation via the circulation tube.

Strong shear forces during the first operation mode are used to obtain the finest dispersion of the emulsion up to dimension smaller than 1 µm. This is fulfilled during the emulsification at 70 °C (flow chart fig. 2-4). The second procedure is used in order to have a high throughput of products which are sensitive to shear force. This is the case of powdered drug substance which has to be dispersed homogeneously within the cream base during the final homogenisation step.

2.2.4.2   Standard procedure of manufacturing 40 kg bulk drug product

General steps of the manufacturing process are illustrated in the flow chart in figure 2-4. Batch sizes of the produced pilot scale batches have been 80 kg for placebo and for economy reasons 40 kg for verum.

First of all correctness of excipients, their net weight and batch numbers are checked and recorded. The fatty phase components are loaded manually into the melter. The melting is started by heating the jacket up to 75 °C in order to bring the fatty phase components continuously up to the desired temperature of 70 ± 1 °C. During the heating period a pressure of -0.7 bar (relative pressure) and a stirrer speed of 2.0 m/s are kept. When the fatty phase has achieved the desired temperature of 70 ± 1 °C the complete melting of all raw materials has to be checked. When the fatty phase is exempt from solid matters it is hold at 70 °C for 120 min.

Thereupon the aqueous phase components (purified water, propylene glycol and glycerol 85 %) are loaded into the mixer by a suction tube. During the loading phase the jacket is heated up to 70 °C whilst the stirrer is operated. Benzoic acid is added as powder through the open top cover. The aqueous phase is kept under stirring at 70 ± 1 °C until the fatty phase is ready to get transferred from the melter into the mixer.
Before adding the fatty phase to the aqueous phase, the absence of undissolved product has to be checked. During the transfer from the melter to the mixer the fatty phase goes through a filter membrane of 100 µm before it reaches the aqueous phase through the upper part of the circulation tube.

After mixing for 5 min at 70 °C, 1.3 m/s stirring speed, and -0.6 bar (relative pressure), the emulsion is homogenised in line for 10 min at the maximum speed (25.0 m/s). The vacuum is brought low in order to obtain a better mass flow towards the homogeniser located at the bottom. Thereafter the emulsion is cooled down step by step to the predetermined final temperature at the default cooling rate e.g. 1 °C/min. During the individual cooling steps, product temperature and jacket temperature must be controlled manually in order to keep the required parameters within close limits. Close to the final temperature the vacuum is increased to -1 bar (relative pressure) in order to deaerate the cream base. After halving the cream base (cream discharge by means of a balance) the micronised API is added by a special suction device made by Berents for this kind of powders. After the API-addition process the top cover is elevated and residues are removed carefully with a spatula from wall scrapers and flow breakers and added to the cream.

The cream is mixed for 5 min at maximum vacuum while stirring at 1.3 m/s by inversion. The deaerated cream circulates 8.1 times at maximum homogenisation speed of 25.0 m/s. This corresponds to 7.5 min of homogenisation time. During homogenisation, stirring is carried out in right direction and vacuum is reduced. This procedure facilitates the mass flow towards the homogeniser at the bottom of the mixer. Due to high shear forces during homogenisation the product tends to get heated. Therefore temperature has to be monitored carefully and the jacket of the mixer has to be cooled sufficiently to avoid a temperature rise above the tolerated limit.

The cream is mixed for further 10 min at maximum vacuum - 1 bar (relative pressure) in order to remove residual air. Samples are taken from the mixer by homogenising in left direction pumping mode through the unloading tube. After a further cold homogenisation for 5 min and further mixing for 10 min the residual cream is unloaded through the homogeniser and the yield is determined. Placebo and verum, sampled after different duration of homogenisation were filled into tidy closed polyethylene jars (Lameplast S.p.a., Rovereto, Italy) and stored at 25 °C/60 % RH until investigation.

Indispensable for the manufacturing according to GMP is the manufacturing batch record. In the manufacturing batch record all parameters together with eventually deviations from the procedure during the manufacturing are acquired. Actual parameters recorded automatically during the entire operating process further are plotted by a chart recorder (q.v. chapter 2.2.4.6 Logging of data).

2.2.4.3   Sample testing

Bulk product samples were analysed after 10 days storage at 25 °C/60 % RH by the methods described in chapter 3.2. This relaxation period of 10 days was kept uniformly for any bulk or finished product batch from lab, pilot and industrial scale.

2.2.4.4   Logging of data

Separately recorded protocols for melter and mixer include each activity carried out during the manufacturing process. The time-dependent course of process parameters during the whole manufacturing process for instance jacket temperature, temperature of the product in the middle and at the bottom of melter and mixer, pressures, speeds of stirrer and homogeniser is automatically plotted by a chart recorder. Figure 2-11 shows an example-record which has been partially redrawn from the original. The product temperature on the bottom of the mixer was not redrawn. It ranged consistently 1 °C below the product temperature in the middle of the mixer. Also pressures in melter and mixer as well as speed of the dissolver blade in the melter were not redrawn.
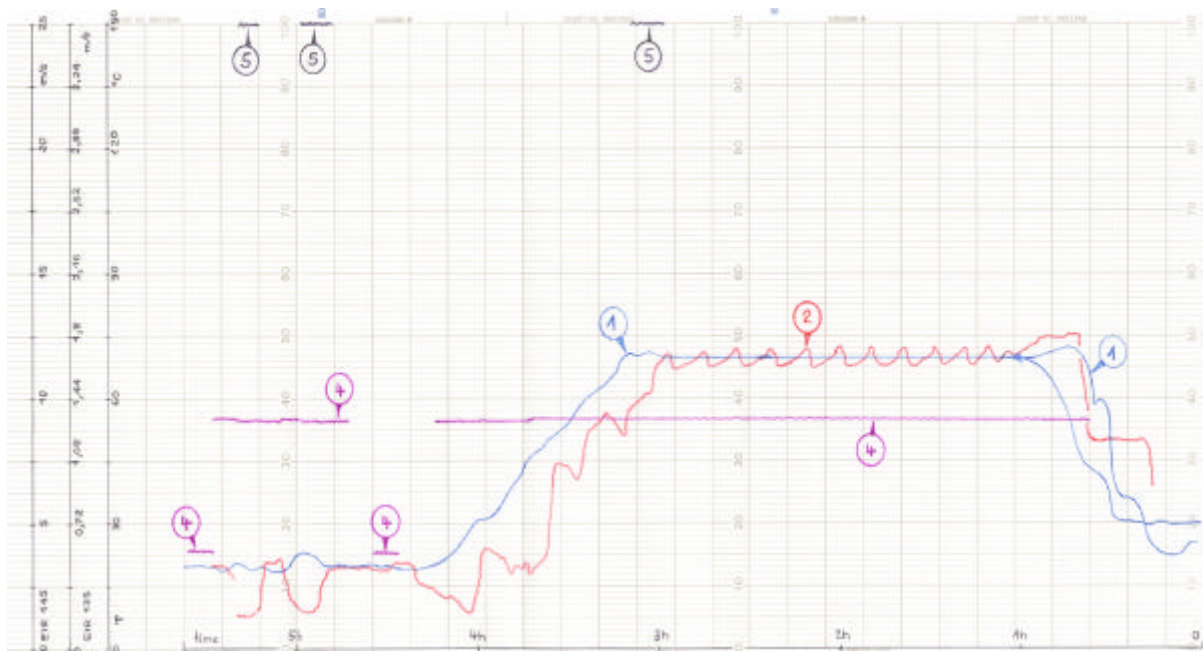
Figure 2-11:   Partially redrawn chart record exemplarily for batch SHT056-P10

1   Product temperature in the middle of the mixer
2   Jacket temperature
3   Product temperature at the bottom of the mixer (not redrawn)
4   Stirrer speed (scale EIR 135)
5   Homogeniser speed (scale EIR 145)

2.2.4.5   In process controls

During the manufacturing process, In Process Controls (IPC) were conducted in order to guarantee that the process proceeds within defined limits. IPCs assure a homogeneous product quality which meets all GMP relevant requirements.

IPCs are the control of temperatures, stirring and homogenising speeds, sequence of addition of excipients, times etc. Excipients are controlled by two people for labelling and quantity. Machines and tools are controlled regarding cleanliness by checking the corresponding label which are taken from the tool and added to the documentation of the batch. In this way the previous product is documented for each machine in case of cross contaminations. Results are signed manually in the batch documentation. Further, microbiological controls of manufacturing ambient are carried out. The microbiological requirements for rooms during manufacturing pharmaceuticals for topical use are maximal 10^2 viable germs/m^3. Ph. Eur 5 defines microbiological requirements for various pharmaceutical dosage forms. Dosage forms for topical application must fulfil the following requirements of microbial count: max. 10^2 aerobic bacteria and fungi, max. 10 enterobacteriaceae, no pseudomonas aeruginosa and no staphylococcus aureus/g or ml. Also the personnel must fulfil the GMP requirements by wearing the appropriate clothes.

2.2.4.6   Filling into the primary packaging material

Bulk batches from pilot and industrial manufacturing were filled into 30 g aluminium tubes (Linhardt Gmbh & Co. KG, Viechtach, Germany) on the fully automatic filler Tonazzi Colibri 601 (V. Tonazzi & Co Srl, Milan, Italy). This filling line (fig. 2-12) consists of a stainless steel hopper with stirrer, auto tube loader, tube orientation station, stations of tube holders with injector unit, closure gripper for heat sealing, grippers for folding and batch number imprinting and ejector unit. The injector is fed by a piston via dosing pump. The filling station is enclosed by a perspex safety cabinet.
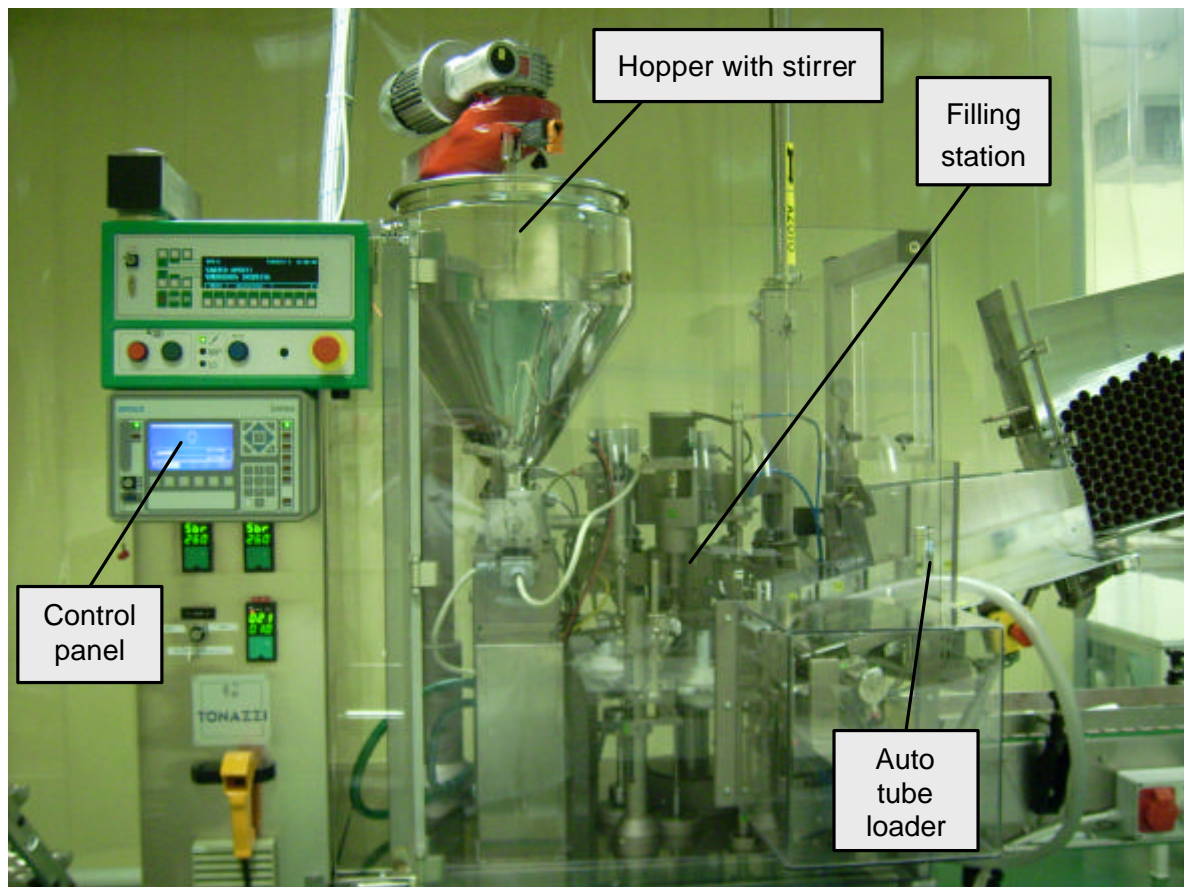
Figure 2-12:   Fully automatic filling line Tonazzi Colibri 601

Figure 2-13 shows tube supply and tube filling (a), whereas tube sealing at 260 °C, double folding and batch number imprint is illustrated in (b). About 200 aluminium tubes (Linhardt) of each batch were filled and stored horizontal in cartons at 25 °C/60 % RH before analysing.
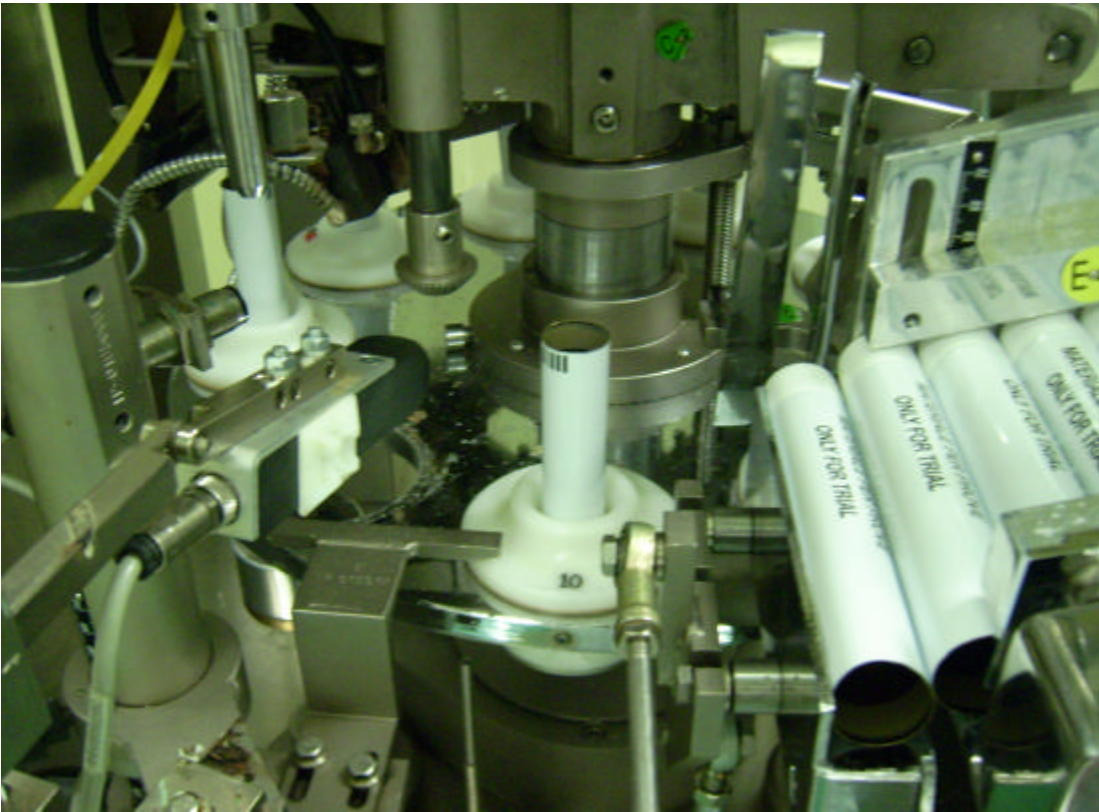
(a)

(b)

Figure 2-13:   Filling process (a); Sealing, folding and imprint (b)

2.2.5   Manufacturing on industrial scale

2.2.5.1   Scaling up

The scaling up normally starts with small quantities of about 1 kg in lab and proceeds then via 50/100 kg batch size to the industrial batch sizes of usually 500 to 1000 kg. The utilised machines should be geometrically and energetically identical. Vessels, homogeniser and stirrer tools shall be identical in shape, type and dimension in order to apply the conditions to the next bigger scale and to assure identical product properties (Liebermann, 1998).

At scaling up usually recipe and process are optimised and validated. This might include slight quantitative changes in the formulation, determination of critical parameters and optimal process times, temperatures, stirrer speeds and physical product properties. Difficulties might occur due to longer cooling times and in consequence longer stirring and homogenisation times especially if the formulation is shear sensitive. This may come along with a lower viscosity. Further the cooling rate influences cream structuring and hence can influence drug release (Köhler, 1992). Finally product and process have to be passed to the manufacturing department. Here the suitability of the product for manufacturing routine will be revealed.

2.2.5.2   Scaling down from Becomix RW 1200 to RW 125

The manufacturing procedure of the model cream was validated the first time in 1990 on a Becomix pilot scale plant. For the current study of the manufacturing process of the model cream, the validated manufacturing procedure on the industrial scale plant Becomix RW 1200 has been adapted to the pilot scale plant Becomix RW 125. The Becomix RW 125 corresponds as far as possible to the Becomix RW 1200 as far as geometry and dynamics are concerned. Instead of a batch size of 1000 kg, batch sizes of 40 kg and 80 kg have been produced. Assembling and functionality of the machines are rather identical. There are some differences regarding homogenisation and stirring speeds due to the different diameters of mixer vessel, stirrer and homogeniser. The technical specifications of both plants are listed in table 2-2.

The possibility of the sequence control on the Becomix RW 125 is favourable for studying the manufacturing process because all process parameters can be set and adjusted manually. This operating mode allows keeping the desired manufacturing conditions at any time of the process. In comparison, the Becomix RW 1200 is controlled fully-automatically and a spontaneous parameter adjustment is not possible.

Table 2-2:   Technical specifications of RW125 and RW1200

Parameter	RW125	RW1200
Diameter anchor stirrer [mm]	638	1236
Diameter homogeniser [mm]	113	166
Diameter agitator blade melter [mm]	150	150

2.2.5.3   Optimization of manufacturing conditions on pilot scale RW 125

In order to obtain a fine emulsion the homogenisation was carried out at the maximum speed possible (25.0 m/s pilot scale vs 26.0 m/s industrial scale). Stirrer speeds of melter and mixer were reduced on pilot scale because of the lower filling level. The homogenisation times during cold homogenisation were transferred 1:1 from RW 1200 with 1000 kg batch size to RW 125 with 80 kg batch size. Passing from 80 kg to 40 kg batch size on the same pilot scale homogenisation times have been halved. Temperatures and pressures were kept identical for both manufacturing scales. Whereas on pilot scale manufacturing temperatures and times were kept strictly in close limits due to investigation issues on industrial scale they range to much wider limits (table 2-3). The cooling rate on pilot scale was homogeneous whereas on industrial scale (chapter 4.4.3) a non-linear profile resulted.

Table 2-3:   Manufacturing process parameters of pilot and industrial scale

Parameter	Pilot scale (80kg)	Industrial scale (1000kg)
Melting time [min]	=120	120-210
Melting temperature [°C]	70 ± 1	70 ± 5
Stirrer speed melter [m/s]	2.0	7.5
Mixing time before hot homog. [min]	5	10
Homogenisation time [min] Homogenisation speed [m/s] Homogenisation temp. [°C]	10 25,0 70 ± 1	10 26,0 70 ± 5
Deaeration time [min]	5	30

Continue Table 2-3:   Manufacturing process parameters of pilot and industrial scale

<u>Stirrer speed mixer [m/s]</u> during cooling and homog. during addition and discharge		1.3 0.6	2.5 1.0
Homogenisator speed unload [m/s]		6.8	10.0
<u>Duration of homogenisation [min]</u> 1st (cold) 2nd (cold)		15 / 7.5 (40kg) 10 / 5 (40kg)	15 10
Cooling rate [°C/min] (std)		1.0 (linear)	0.85 (non-linear)
Cooling steps [°C]	Placebo 70-60 60-45 45-40 40-28	Verum 70-60 60-50 50-40 40-30	70-60 60-45 45-40 40-28
Unload temperature [°C] (std)	28 ± 1	30 ± 1	28 ± 2

2.2.5.4   Determination of circulation times

Within this experiment the respective final homogenisation conditions on pilot and industrial scale (table 2-4) were simulated. The number of circulations was determined on placebo (pilot scale) with a batch size of 80 kg at a product temperature of 28 °C. While homogenising in circulation at a speed of 25.0 m/s four samples were withdrawn from the circulation tube during a period of 10 s and weighted. The output weight/min was converted into the number of circulations/min (circulation times) applied to the batch size of 80 kg. A batch of 80 kg circulates 8.1 times during first homogenisation and 5.4 during second homogenisation (13.5 total circulation times).

The determination of circulation times on RW 1200 was performed with 1000 kg purified water instead of the model cream. Density of the product was neglected. Usually homogenisation was operated under low pressure (0.3 bar below atmosphere pressure). For this purpose at atmosphere pressure (1.01 bar) was operated in order to guarantee that the circulation tube at each time was filled with the product.

Table 2-4:   Determination of circulation times on Becomix RW 125 and RW 1200

Parameter		Unit	RW 125		RW 1200	
Product		-	Placebo		Purified water	
Product temperature		[°C]	28		28	
Over pressure		[bar]	0		0	
Sampling time		[s]	10		10	
Homogeniser circumferential speed speed direction		[m/s] [rpm] [L/R]	25.0 4227 R		26.0 2992 R	
Stirrer circumferential speed speed direction		[m/s] [rpm] [L/R]	1.3 39 R		2.5 38 R	
Batch size		[kg]	80.0		1000.0	
Sample outload	1	[kg]	6.77		88.0	
	2	[kg]	7.26		89.0	
	3	[kg]	8.00		88.0	
	4	[kg]	6.86		87.0	
Mean		[kg]	7.22		88.0	
sd		[kg]	0.56		0.8	
Mean output/min		[kg]	43.34		528.0	
Number of circulations /min (total batch)		-	0.54		0.53	
Total time		[min]	15	10	15	10
Number of circulations (total batch)		-	8.1	5.4	7.9	5.3

The times of circulations on pilot and on industrial scale are almost identical. During the final homogenisation of 15 min the entire mass circulates about 8 times and additional 5 times during further 10 min of cold homogenisation. This experiment confirmed the equivalent conditions during final homogenisation between both manufacturing scales. Hence industrial and pilot scale can be considered as comparable.

2.2.6   Earlier investigations on the formulation

Numerous factors during the life-cycle of a semisolid drug product can influence its physicochemical and stability properties. Different supplier's excipients, active ingredients with different levels of micronisation, variations in the manufacturing techniques or storage conditions might alter the cream quality. Within the complex manufacturing process of a semisolid system there are a lot of parameters which might influence the properties of the final cream and which consequently must be considered as quality determiners.

2.2.6.1   Critical parameters subject to investigation

During the formulation development, several critical parameters have already been assessed. These investigations concerned:

(1)   Particle size and surface charge of the micronised azelaic acid

(2)   Influences from the consistency agent Cutina CBS and
       the emulsifier Arlatone 983S on the cream consistency

(3)   Homogenisation temperature during hot homogenisation

(4)   Holding time of the bulk product

(5)   Final homogenisation time on verum regarding homogeneity of the API

(6)   Addition mode of the API and mode of unloading the cream

3   MATERIALS AND METHODS

3.1   Materials

3.1.1   Composition of the formulation

The o/w cream is composed as shown in table 3-1. The outer aqueous phase of the cream besides purified water contains propylene glycol, glycerol 85 % and the water soluble preservative. The inner fatty phase consists of emulsifier, consistency agent and emollient. The micronized azelaic acid (AzA) is suspended within the oil in water cream base.

Table 3-1:   Composition of the o/w cream (verum and placebo)

Excipient	Verum % (w/w)	Placebo % (w/w)
Azelaic acid micronized	20.0	-
Benzoic acid	0.2	0.250
PEG-5-glycerylstearate (Arlatone 983S)	5.0	6.250
Mixture of glycerylstearate, cetearylalcohol, cetylpalmitate and cocoglycerides (Cutina CBS)	7.0	8.750
Cetearyl octanoate (PCL-liquid)	3.0	3.750
Propylene glycol	12.5	15.625
Glycerol 85%	1.5	1.875
Purified water	50.8	63.500

3.1.2   Active pharmaceutical ingredient

Micronized azelaic acid (Schering AG, D-Berlin), chemical name heptane-1,7-dicarboxylic acid (fig. 3-1) is a white crystalline powder. It is used in the treatment of acne and rosacea because it inhibits the growth of propioni bacteria.

The main fraction is suspended in the formulation. The melting range according USP, class Ia is 105-110 °C. The polymorph azelaic acid is present in its α-modification, less than 5 % occur as β-modification. The solubility of azelaic acid in water is stated with 2.4 g/l at 20 °C (Aldrich). The bibasic acid dissociates in two steps, respective dissociation constants at 25 °C are pk_1 4.53 and pk_2 5.33.
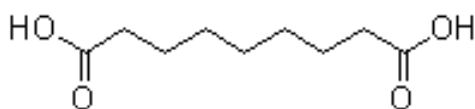
Figure 3-1:   Formula of azelaic acid (AzA)

AzA shows notable surface activity. It lowers the surface tension of purified water by about 12 mN/m. The surface tension of aqueous azelaic acid solution was measured with 60 mN/m (chapter 3.2.9). The surface tension of purified water is stated with 72.8 mN/m at 20 °C (Remington). The BET- surface of AzA crystals was measured with 2.4 m^2/g (chapter 3.2.15). Particle size of the API in the cream matches requirements when no particle is bigger than 60 µm and less than 30 particles between 40 and 60 µm (referred to one representative sample of 2x2 cm).

3.1.3   Excipients

Table 3-2: Excipients of the o/w cream, suppliers and function

Substance	Supplier	Function
Arlatone 983S	Brenntag, D-Mühlheim/Ruhr	Non-ionic emulsifier
Cutina CBS	Cognis, D-Düsseldorf	Co-emulsifier
PCL-liquid	Symrise, D-Holzminden	Emollient
Propylene glycol	BASF, D-Ludwigshafen	Moisturizer
Glycerol 85%	Hedinger, D-Stuttgart	Moisturizer
Benzoic acid	Merck, D-Darmstadt	Preservative

3.1.4   Packaging material

3.1.4.1   Jars

Bulk product samples (BP) were stored in tidy closed 500 g polypropylene jars (Lameplast S.p.a., Rovereto, Italy).

3.1.4.2   Tubes

Finished drug product samples (FP) were stored in 30 g aluminium tubes with a coating of non-porous epoxy resin (Linhardt Gmbh & Co. KG, Viechtach, Germany).

3.2 Methods

3.2.1   Spreadability

Spreadability measurements were performed at 25 °C (in triplicate). A plate with holes of 15 mm diameter and 3 mm height was used. Samples were filled in the holes and smoothed out by means of a spatula. Thereafter the plate was removed. A round Plexiglas plate ($\varnothing$ 80 mm; 20 g) was placed centrically onto the cream and a weight of 200 g was placed onto the plate. After 3 minutes the diameter of the spread cream was measured by a ruler in two directions perpendicular to each other and accordingly the circular area [mm^2] was calculated by $A = \pi/4 \, d^2$. Typical values for creams as mentioned in the literature range from 500 to 4000 mm^2.

3.2.2   Syneresis (bleeding)

Cream samples (in triplicate) with 15 mm diameter and 3 mm height were gently positioned onto a filter paper (Bench Guard Standard, Bibby Sterilin Ltd., Stone, Staffordshire, England) with a high absorbent upper surface, capacity 800 ml/m^2. After 3 hours at 25 °C/60 % RH the diameter [mm] of the leaked fluid was measured and accordingly the circular area [mm^2] was calculated by $A = \pi/4 \, d^2$.

By scattering water soluble methylene blue crystals onto the cream barrel they dissolved in the cream and coloured the leaked fluid blue. By scattering fat soluble sudan red crystals onto the cream they remained on the cream without colouring the leaked fluid.

3.2.3   Electrical conductivity

Electrical conductivity was measured in µS/cm (in triplicate) using a CDM80 conductivity meter equipped with the CDC241-9 glass conductivity cell for viscous media (Radiometer Copenhagen, Denmark) at a product temperature of 25 °C.

3.2.4   Micropenetration

By micro-cone penetrometry according to Klein (Ph. Eur. 5) the depth of immersion of a micro-cone during the runtime of 5 s was measured. The testing kit ('Prüfsatz nach Klein') consists of a micro-cone (7 g), a plunger (16.8 g, length 116 mm) and collecting vessels (volume 4 ml). The samples (in triplicate) were placed into the collecting vessels by means of a spatula without applying any significant shear. The cream was kept during 1 h at 25 °C in the collecting vessels in the thermostat Haake DC1 (Haake Mess-Technik GmbH u. Co, Karlsruhe, Germany). Afterwards the measurement was performed with the penetrometer Petrotest PNR 10 (Petrotest Instruments GmbH + Co. KG, Berlin, Germany). The immersion depth [mm] was tripled and expressed in mm*10^{-1}.

3.2.5   Macroscopic test

The macroscopic appearance was judged visually on the spread cream.

3.2.6   Microscopy

Samples were examined microscopically by the transmitted light microscope Zeiss Axioscop 20 (Carl Zeiss, Oberkochen, Germany) equipped with a polarisation device and using a quartz red filter. The overall magnification was 200. Microscopic pictures were taken by the colour video camera JVC TK-1070E (JVC, Tokyo, Japan) and printed by the video printer Polaroid TX-1100-4 (Polaroid GmbH, Offenbach, Germany).

3.2.7   Differential scanning calorimetry (DSC)

DSC-analyses were performed with a DSC30 (Mettler Toledo GmbH, Giessen, Germany) in triplicate. Samples of 8-10 mg were filled in an aluminium pan using a 1 ml U-100 insulin syringe without needle (Terumo Europe N.V., Leuven, Belgium). The sealed aluminium pan (40 µl) was heated from 25 to 100 °C by 10 °C/min. Normalized melting enthalpies [J/g] and onset temperatures [°C] were evaluated with the $Star^e$ software (Mettler Toledo GmbH, Giessen, Germany).

3.2.8   Thermogravimetric analysis (TGA)

Thermo-gravimetric measurements were carried out in triplicate using a TG50 thermo balance in nitrogen atmosphere with a flow of 200 ml/min in an aluminium pan (40 µl) without lid. Samples of 8-10 mg were filled into the pan as for DSC-measurements and heated from 25 to 100 °C by a heating rate of 5 °C/min. The mass loss [%] referring to the overall sample weight was calculated by means of $Star^e$ software using the 1st derivate (DTGA-curve) of the TGA-curve.

3.2.9   Tensiometry

The surface tension of aqueous azelaic acid solutions was measured with the ring-tensiometer Krüss K12 (Krüss GmbH, Hamburg, Germany). About 500 mg azelaic acid were dissolved in 90 ml purified water and left for 4 hours in an ultrasonic bath. Then the surface tension was measured during 1000 s. Results are mean values from measurements which were performed in triplicate. Surface tension of purified water is 72.8 mN/m at 20 °C (Remington).

3.2.10   X-ray diffraction

3.2.10.1   Wide angle X-ray diffraction (WAXD)

Samples were placed into a sample carrier of aluminium and measured with the goniometer PW1050/25 (Philips, Kassel, Germany). The goniometer was pursued on the x-ray generator PW 1730 with the x-ray tube PW 1877/3 (Ni-filter; CuKα-radiation, λ = 0.154 nm; 45 kV; anode power 20 mA). The measurement was performed by automatic powder diffraction at a run time of 6 hours. From the diffraction angle theta (Θ 2-50 °) the inter-molecular distances were calculated according to Bragg's law: nλ = 2 d sinθ (*l*: wavelength of X-ray; *Q*: half the scattering angle; *d*: distance; *n*: order of reflection).

3.2.10.2   Small angle X-ray diffraction (SAXD) with Kiessig OED

Samples were placed into a cubical sample carrier (TU Braunschweig, Germany) between two x-ray amorphous foils of Kapton (Krempel, Vaihingen, Germany). Interferences were detected by a Kiessig camera OED-50 (Braun, Munich, Germany). To avoid any effects of diffusion the measurement was performed at a pressure of 4 mbar, the measuring time was between 800 and 1000 s. From diffraction angle theta (Θ <2 °) the inter-layer spacings were calculated according to Bragg's law.

Devices:

X-ray generator	: PW 1730 (Philips GmbH)
X-ray tube	: PW 2253/11 (Philips GmbH)
Acceleration voltage	: 40 kV; anode power 35 mA
Radiation	: CuKα, (λ = 1.5418 Å)
Detection	: OED-50 (Fa. M. Braun, D-München)
Analysator	: MCA 8100 (Canberra Electronic, Frankfurt/M.)
Resolution	: 24.5 channels/mm
Distance sample-detector	: 29.5 mm
Gas	: Argon/Methan 90:10

3.2.11   In vitro release

For in vitro release tests the Microette[TM] topical & transdermal diffusion cell system 57-6M (Hanson Research, Chatsworth, USA) consisting of a Franz' cell system Variomag Telesystem of 6 cells, a magnetic stirrer Variomag Telemodul 40S (600 RPM) and a water bath Polyscience was used.

Test conditions:

Membrane: Cuprophan[®] flat membrane Type 150M (Membrana GmbH, Wuppertal, Germany), regenerated cellulose, 11.5 µm thick, pore diameter 0.005 µm

Franz' cell: acceptor volume 7 ml

                  Matrix volume 282.7 mm^3; area of release 176.7 mm^2

Acceptor medium: phosphate buffer 0.066M, pH 8.5

                  9.0 g KH_2PO_4 and 2.5 g NaOH (Merck) were dissolved in 1 l purified water, degased in the ultrasonic heated water bath Bransonic 5200 (Branson Ultrasonics corporation, Danbury, USA) and filtrated by a 0.45 µm regenerated cellulose membrane filter

The cream was filled into the matrix on the membrane of the Franz's cell. In vitro release tests were conducted during 6 h at 32 °C. After 30, 60, 120, 180, 240, 300 and 360 min 0.5 ml of acceptor medium were sampled by means of a 1 ml U-100 insulin syringe (Terumo Europe N.V., Leuven, Belgium) and replaced by buffer solution.

Azelaic acid concentrations were analysed by HPLC 200LC and the UV-VIS detector series 200 (Perkin Elmer, Shelton, USA). Peak identification and evaluation were performed by Turbochrom software Workstation 6.1 (Perkin Elmer Instruments, Norwalk, USA). Concentrations of azelaic acid were calculated using external standard solutions of azelaic acid in phosphate buffer solution 0.066 M; pH 8.5. The coefficient of regression was > 0.9999. Samples were acidified with ortho-phosphoric acid (Merck) in order to maintain a pH < 4.

HPLC conditions:

Stationary phase: Bondapak C18; 300 x 3.9 mm, 10 µm (Waters, Massachusetts, USA)

Mobile phase: acetonitrile for chromatography (Merck) and sodium dihydrogenphosphate monohydrat aqueous solution 1.38 % (w/v); 200:800 (v/v)

                   13.8 g of $NaH_2PO_4*H_2O$ were dissolved in 1 l purified water, degased, filtrated and mixed with CH_3CN

Detector: UV/VIS detector series 200 (Perkin Elmer, Shelton, USA), 200 nm

Flow rate: 2.0 ml/min

Retention time: 6 min

Injection volume: 20 µl (double injection)

Wavelength: 200 nm

3.2.12   Rheology

Rheological measurements were performed with a Haake RheoStress® RS600 (Thermo Electron, Karlsruhe, Germany) using a plate/plate geometry (rotor diameter 35 mm). The gap between rotor and stator plate was generally set to 300 µm based on the biggest particles of about 80 µm found by microscopy. Product and measuring temperature were kept at 20 ± 0.5 °C by the temperature device Haake DC50 (Thermo Electron, Karlsruhe, Germany) and the water bath Haake K10 (Thermo Electron, Karlsruhe, Germany). All parameters during rotation and oscillatory experiments were evaluated using Haake RheoWin® 3.23 software (Thermo Electron, Karlsruhe, Germany).

3.2.12.1   Rotation experiment

3.2.12.1.1   Flow curve

Flow curves were recorded in duplicate under controlled shear rate (CR) after pre-shearing at 100 1/s for 60 s.

Upwards curve: CR, $\dot{g}$ 0-400 1/s, 120 s, 30 data, linear

Downwards curve: CR, $\dot{g}$ 400-0 1/s, 120 s, 30 data, linear

Hysteresis [Pa/s] between upwards and downwards curve and the apparent shear viscosity η_a [mPas] were calculated by the software at the apex of the flow curve at a shear rate of 400 1/s.

3.2.12.1.2   Yield point

The yield point was recorded in duplicate under controlled shear stress (CS). During increasing shear stress τ the deformation γ [-] was measured. As corresponding yield point the bending point of the deformation was calculated by the software.

CS, τ 0.03-200 Pa, 120 s, 120 data, linear

3.2.12.2   Oscillatory measurements

Oscillation measurements (single) were performed within the linear-viscous-elastic (LVE) range. After a waiting time of 300 s complex modulus G* [kPa], storage (elastic) modulus G' [kPa], loss (viscous) modulus G'' [kPa] and phase shift δ [°] were recorded during an oscillating period of 120 s. The respective averages were calculated from 10 data points.

CS, waiting time 300 s, τ 10 Pa, f 1 Hz, 120 s, 10 data

3.2.13 Scanning electron microscopy (SEM)

Samples of micronized azelaic acid were sputted fourfold with gold for 60 s by a sputter-coater (BioRad, Munich, Germany) applying a current of 20 mA and an acceleration voltage of 2.1 kV. Samples were characterised by SEM with the Zeiss microscope DSM 940 (Zeiss, Oberkochen, Germany) using an acceleration voltage of 50 kV. SEM micrographs were taken at 1000-, 2000- and 5000-fold magnification with a frame grabber card Board version 3.1 and the Orion software version 5.11 (E.L.I., Brussels, Belgium).

3.2.14 Surface analysis according Brunauer, Emmet, and Teller (BET)

The surface of micronised API was measured with a Beckman Coulter (Beckman Coulter GmbH, Krefeld, Germany). Measurements were carried out in nitrogen atmosphere at 40 °C for 360 min. Data were evaluated by SA3100 Results software, version 1.00 (Beckman Coulter, Krefeld, Germany).

3.2.15 Storage conditions

Long term and accelerated storage conditions were chosen according to International Conference for Harmonization (ICH) guidelines (EMEA, 2003).

3.2.15.1 *25 °C / 60 % RH (long term)*

Samples were stored at 25 °C / 60 % RH according ICH Guidelines for 6 months in a programmable climatic cabinet AS Biomedical division (Angelantoni Industrie SpA, Massa Martana, Italy). Samples were analysed after 1, 3 and 6 months.

3.2.15.2 *40 °C / 75 % RH (accelerated)*

Samples were stored according ICH Guidelines for 1 month, 3 and 6 months in a programmable climatic cabinet ACS (Angelantoni climatic systems, Massa Martana, Italy) at 40 °C / 75 % RH.

3.2.15.3 *Stress test at +5 °C / +40 °C / 75 % RH*

Temperature during stress tests was changed from +5 °C to +40 °C/75 % RH every 24 hours performing 3 cycles overall (1 cycle takes 48 h).

Bulk product samples were stored in tidy closed plastic containers and finished product samples in the appropriate tubes (chapter 3.1.4). Samples stored at 40 °C/75 % RH and samples from cycle test were stored for 24 hours at 25 °C/60 % RH before analysing.
The typical temperature-time-curves during cycle test, long term and accelerated storage are shown in figure 3-2.
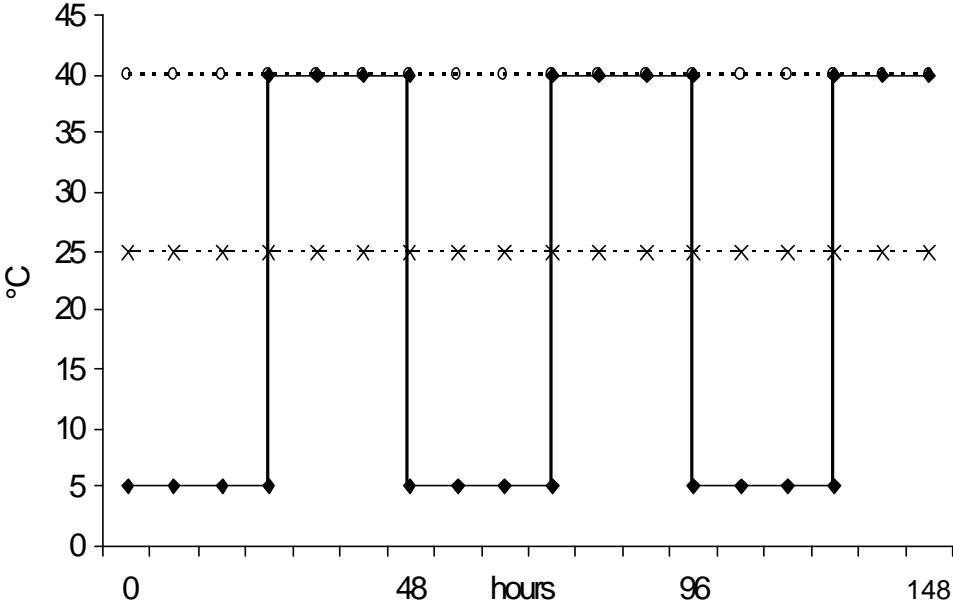
Figure 3-2:   Temperature-time-curves during storage

          --x--   25 °C / 60 % RH up to 6 months
          --o--   40 °C / 75 % RH up to 6 months
          - ♦-   stress test +5 °C / +40 °C/75 % RH

4   RESULTS AND DISCUSSION

First of all, a structural characterisation of the model cream is provided. Afterwards, the main focus will be on the understanding of the influence of selected critical manufacturing parameters on the physical properties of the cream (chapter 4.4). Finally, the emphasis is on changes within the cream properties monitored while storage at different conditions (chapter 4.5).

4.1   Structural characterisation of the model cream

In the following a general characterisation of the structure of the o/w cream is provided by means of X-ray diffraction, thermo-analytical, microscopic and rheological measurements.

4.1.1   Characterisation by X-ray diffraction

4.1.1.1   WAXD

X-ray diffraction in the wide-angle region (2 theta=2-50°) provides information regarding the short-range ordering of molecules. WAXD techniques are able to distinguish between crystalline and liquid-crystalline structures. It is known that hydrocarbon chains in liquid state show a diffuse band termed as halo with its centre at 0.45 nm and additional patterns within the small-angle region. In contrast to the liquid crystalline phase, the α-crystalline gel phase (Lβ) is characterised by a single sharp reflection at 0.415-0.42 nm (Savic et al., 2005).
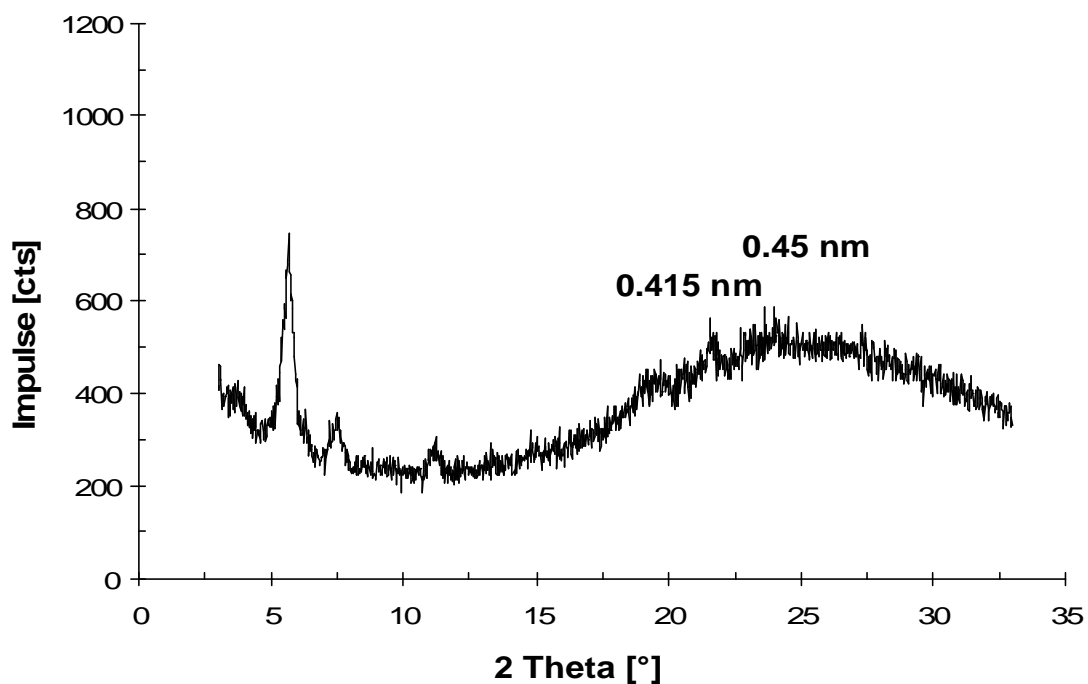
Figure 4-1:   WAXD pattern of placebo, batch # 41166

Figure 4-1 depicts the WAXD pattern of placebo exemplarily for the model cream (WAXD patterns of placebo and verum are identical). The halo, typical for liquid-crystalline phases, was detected in all samples. A weakly pronounced single reflection at 0.415 nm could be detected which could indicate the presence of α-crystalline gel-phase.

Savic (2005) suggested that, during emulsification a certain insertion of alkyl chains of medium chain triglycerides from the oil phase between the alkyl chains of mixed surfactant/fatty alcohol occurs. This disordered liquid-crystalline structure of lamellar type is placed either at the border of the oil droplets or randomly widespread towards the continuous phase.

In figure 4-2 the wide-angle X-ray diffractogram of verum is depicted. The halo and thus liquid crystalline structures are overlapped by interferences of azelaic acid at 2 theta [°]: 5.6 – 8.5 – 19.1 – 22.1 – 23.6 – 28.3 which is mainly present in the α-modification (β-modification = 5 %).
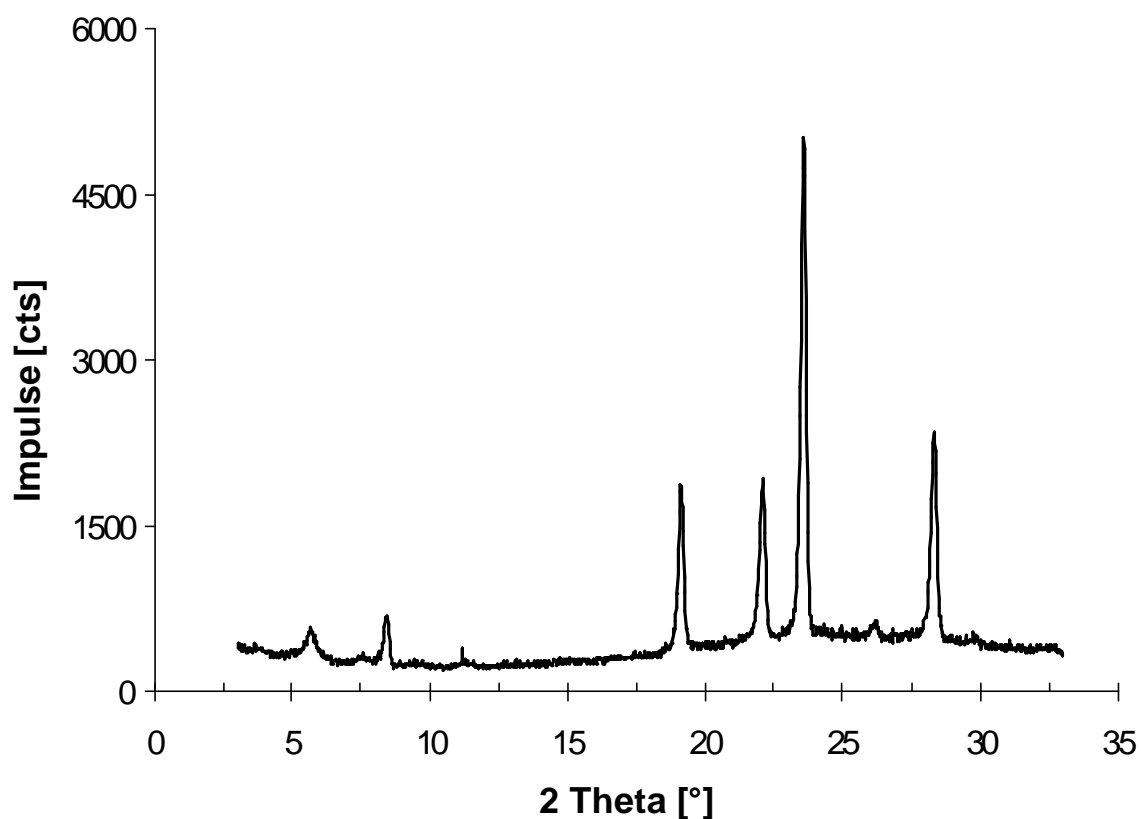
Figure 4-2:   WAXD pattern of verum, batch # 41166

4.1.1.2   SAXD

X-ray diffraction in the small-angle region (2theta <2°) is able to detect the interlayer distances of the liquid-crystalline gel framework (Krischner, 1974, Führer, 1996, Kudlek, 1996). Thereby the broadening of the primary interference on particle surfaces is analysed.

SAXD patterns of verum and placebo are identical. The small angle X-ray pattern is exemplarily depicted for placebo batch # 41166 in figure 4-3. A clear interference (first order) occurs in channel 112 corresponding to the repeated distance of 9.60 nm. After the first order peak follow some sloping interferences between channel 150 and channel 225. They describe the drop of the primary peak. The second clear interference appears between channel 262 and channel 276 corresponding to the repeated distance of 4.62-5.05 nm.
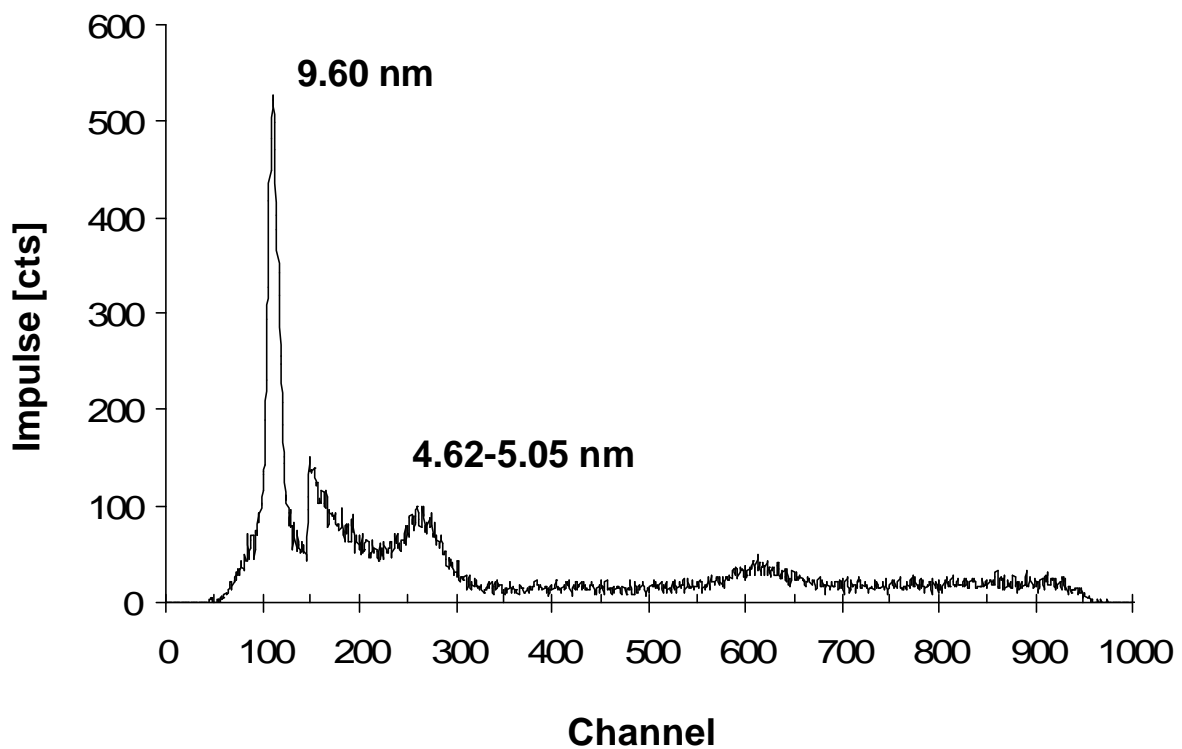
Figure 4-3:   SAXD pattern of placebo, batch # 41166

Literature describes typical orders of interferences for each kind of crystalline structure (Müller Goymann, 1981, Führer and Kudlek, 1996). Whereas the hexagonal phase I shows interferences in the order of $1:1/\sqrt{3}:1/\sqrt{4}:1/\sqrt{7}:1/\sqrt{12}$, lamellar phases show interference maxima in the ratio of 1: 1/2: 1/3: 1/4: 1/5. The interference maxima 9.60 nm and 4.83 nm (averages) could be the hint for a lamellar structure of the o/w cream with the defined inter-lamellar spacing d of 4.83 nm.

But compared to other o/w creams found in literature 4.83 nm would signify a quite small inter-lamellar spacing pointing to a limited water binding capacity in between the double layers (Kudlek, 1996, Bouwstra et. al, 1991). In addition, further order interferences in the ratio 1/3:1/4 etc. are missing and thus this model of colloidal structure alone is less reasonable.

However, the first interference may be due to fully hydrated lamellar liquid crystals (hydrophilic gel-phase). The second interference could be due to cetearylalcohol semi-hydrates within the lipophilic gel-phase (Eccleston et al., 2000). It may be expected that mainly the amphiphilic components PEG-5-glyceryl stearate, glyceryl stearate and cetearyl alcohol are responsible for the construction of the colloidal network (de Vringer, 1986).

Table 4-1 describes main interference peaks and corresponding repeated distances d of various verum and placebo batches.

Table 4-1:   Interlayer spacing d (SAXD) 1st order peak channel 112 (= 9.60 nm) finished drug product (FP) and bulk drug product (BP)

Batch #	Type of product	2nd peak [channel]	Interlayer spacing d [nm]
42171	Verum (FP)	267	4.89
41166	Verum (BP)	270	4.79
41166	Placebo (BP)	268	4.86
42829	Verum (BP)	269	4.83
42829	Placebo (BP)	270	4.79
mean		**269**	**4.83**

4.1.1.3   SAXD of placebo containing different amounts of water

From SAXD patterns the dependency of the repeated distance from the water concentration and thus the water binding mechanism could be derived. 500 g placebo batches with 40, 50, 60, 70, and 80 % water respectively were prepared in lab (chapter 2.3.3). Table 4-2 gives a summary of the interferences. The interlayer spacing d was between 4.93 nm and 4.99 nm. Although the water concentration in the cream rose up to double the interlayer spacing did not increase. This confirms the hypothesis that the model cream is not formed by a four phase system with lamellar structure as supposed by Junginger. Obviously the water is entrapped in various modes within the complex gel-matrix.

Table 4-2:   Interlayer spacing d [nm]; placebo with different water amounts [%]

1st peak in channel 113 (= 9.80 nm)

Water amount [%]	2nd peak [channel]	Interlayer spacing d [nm]
40	268	4.93
50	268	4.93
60	266	4.99
70	269	4.90
80	266	4.99
mean	**267**	**4.95**

4.1.1.4   *Summary of X-ray diffraction*

By WAXD, the liquid-crystalline structure of the formulation with indices of lipid crystals was shown. The overlapping of the diffuse band (ordered lamellar gel matrix) by the interference of α-crystalline gel phase could mean stabilization by liquid crystals organized in the form of layers surrounding the oil droplets. Alkyl chains from œtearyl octanoat could be inserted in between the PEG-5-glycerol stearate/ œtearylalcohol crystals which could be placed at the border of the oil droplets as well as randomly widespread towards the continuous phase. Thus, together with the gel phase they form a disordered liquid-crystalline structure of lamellar type.

SAXD was performed to elaborate in more detail the colloidal structure of the cream. It could be suggested that the model cream be formed by a complex gel matrix. In addition to the hydrophilic gel phase, the lipophilic gel phase is comprised by surplus of cetearyl alcohol semi-hydrates. That means that, along with bulk and inter-lamellar water from hydrophilic gel phase, water could be entrapped within the cetearylalcohol gel-network. It can also be assumed that, bulk oily phase is dispersed in form of oil droplets, whereas some oil, together with mixed crystals of PEG-5-glycerol stearate/ cetearylalcohol provoke lamellar liquid crystalline layers around the droplets. The gel phase could be stabilized predominantly either by electrostatic or steric repulsions.

No distinguished correlation between interlayer spacing d and water concentration could be observed. This confirms a complex and disordered gel matrix comprising of two gel phases separated from each other, the hydrophilic and the lipophilic one.

4.1.2   Thermo analytical characterisation

More and more novel studies about the characterisation of semisolids utilize thermo-analytical methods in examining the structure of semisolids (Niemi et al., 1991, Kallionen et al., 1995; Rose, 1999). It is also known that TGA characterisation could be useful in investigation of water distribution within creams (Junginger et al., 1984). Kònya et al. (2003) studied microstructural changes during application with respect to the stability of the lamellar bilayer. He used TGA in order to study the water bond mechanism in o/w creams and the influence of mixed emulsifiers on the binding of water incorporated in the structure (inter-lamellar or free bulk water). Junginger et al. (1984) assumed that inter-lamellarly fixed water molecules exhibit different physicochemical properties than those of the bulk water phase.

4.1.2.1   TGA

4.1.2.1.1   TGA of placebo

A typical water loss profile of placebo is shown in figure 4-4.
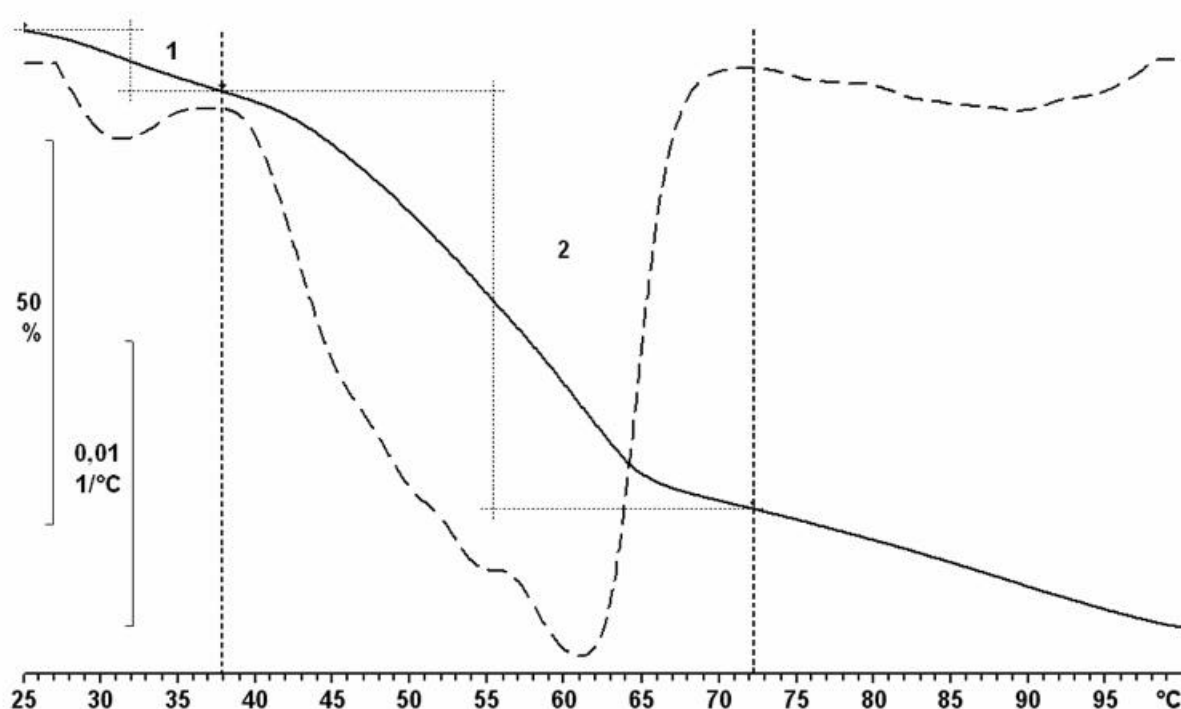
Figure 4-4:   TGA and DTGA-curves of placebo, batch # SHT292-P02
                                mass loss   (full line)
                                rate of mass loss   (dashed line)
                                1   free water
                                2   bound water

Following the evaporation rate (DTGA-curve) two different types of water (two individual steps of water loss) can be differentiated. The evaporation rate of bulk water increases until about 40 °C. At approx. 38°C there is an inflection point in the DTGA-curve. After that temperature the evaporation rate increases strongly up to a temperature of approx. 70 °C responsible for the evaporation of fixed water. The end of the 2nd step is not always clearly detectable because of a missing peak maximum. Thus, when speaking about water binding capacity in this study then the free bulk water is meant corresponding to the first water loss.

4.1.2.1.2   TGA of verum

In figure 4-5 TGA and DTGA curves of verum are shown. An evaluation of free and bound water according to placebo was not possible as far as there was no clear distinction of two peaks.
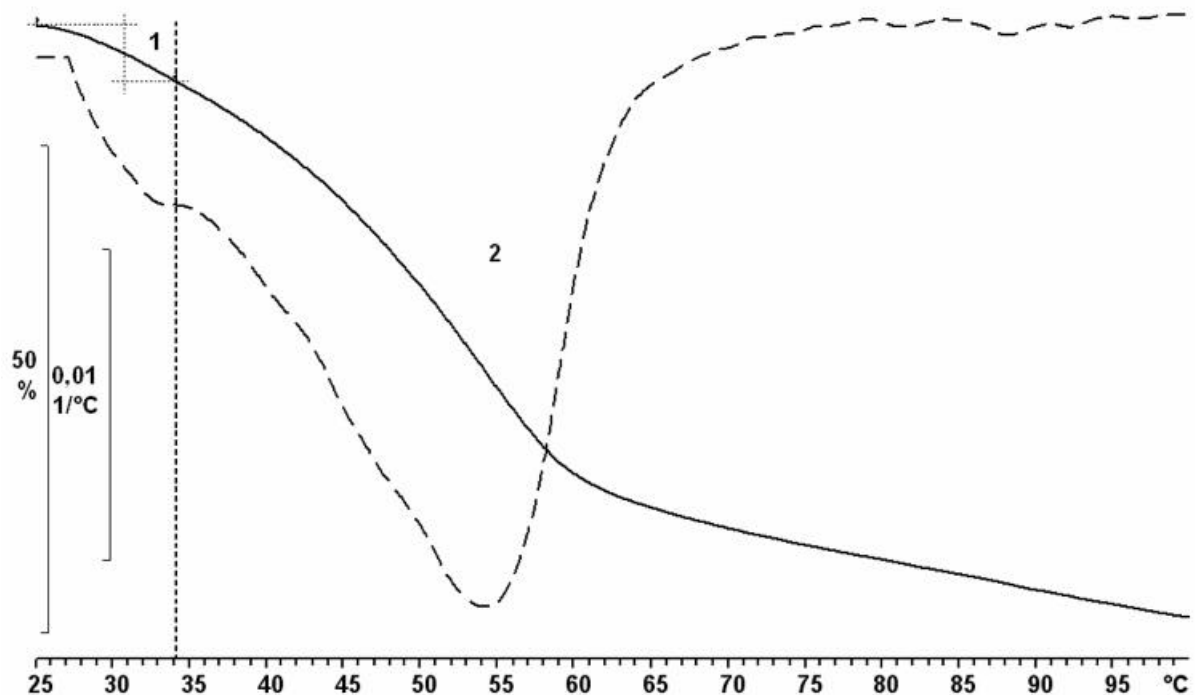
Figure 4-5:   TGA and DTGA-curves of verum
                      mass loss   (full line)
                      rate of mass loss   (dashed line)
                      1   free water
                      2   bound water

4.1.2.1.3   TGA of placebo with 40, 60, and 80 % (w/w) water

In figure 4-6 TGA and DTGA-curves of placebo containing 40, 60 and 80 % water are shown. Increase of the water amount from 40 % to 60 % results in a change in detecting process (the steps become less distinctive). With increasing water amount, a shift to the higher temperatures (1st step: 38 - 42 - 49 °C; 2nd step: 65 - 71 - 76 °C) associated with a higher mass loss becomes evident.

a)
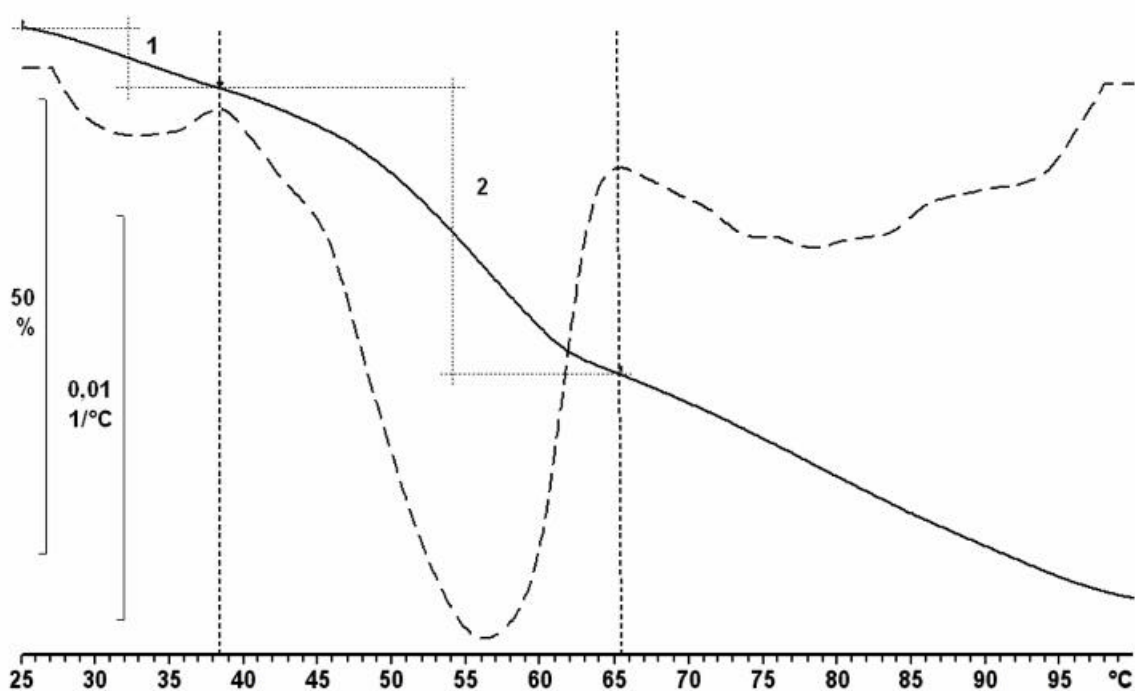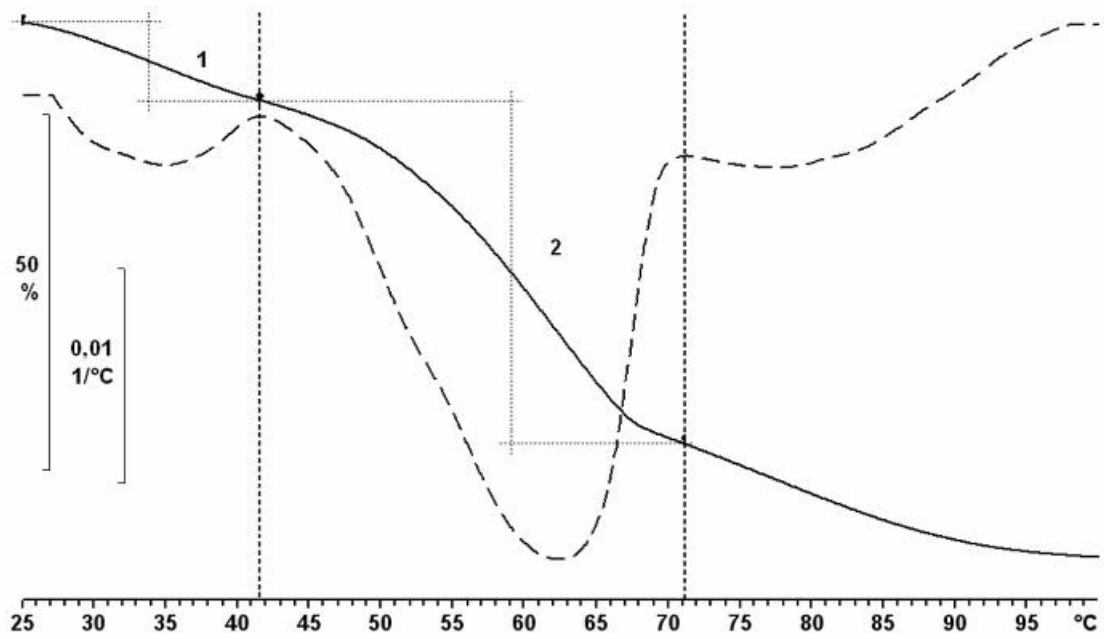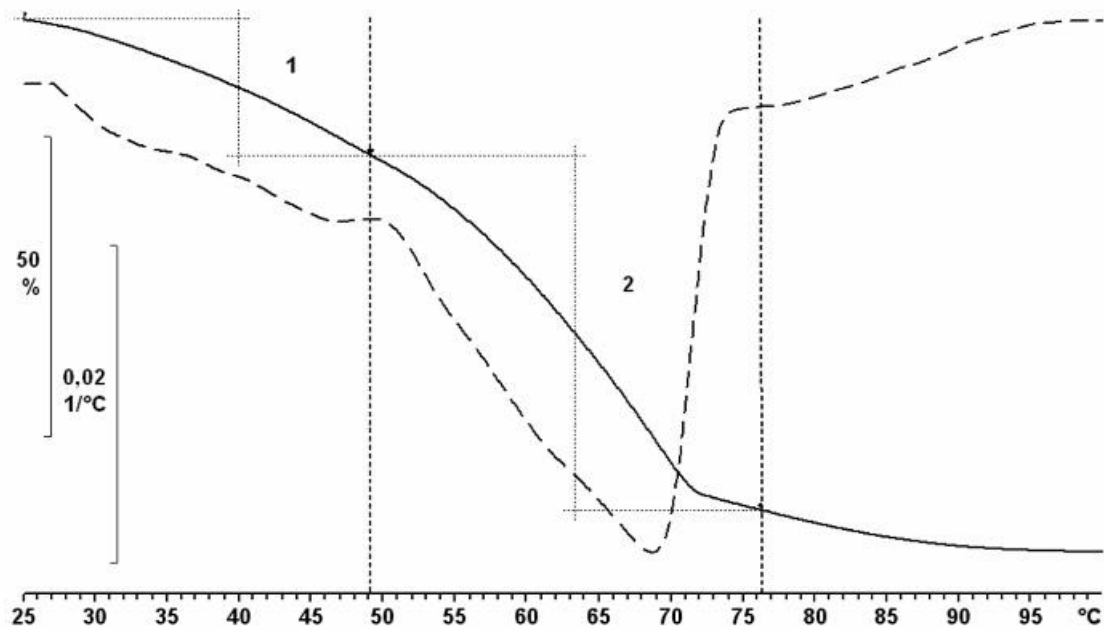
Figure 4-6:   TGA and DTGA-curves of placebo
          a)   containing 40 % water
          b)   containing 60 % water
          c)   containing 80 % water
          1   free water
          2   bound water

Table 4-3 shows free bulk (column 5) and bound water (column 6) in percent from the overall water amount as measured by DTGA. Up to water content of 60 % the ratio does not change significantly. About 20 % of the total water is bulk water. About 80 % is available as bound water. When the total water content exceeds 70 %, this ratio is shifted in favour of free bulk water and at the expense of bound water. Placebo containing 80 % water contains about 30 % free bulk and 70 % bound water.

Table 4-3:   Free, bound and total water of placebo with different water content [%]

1	2	3	4	5	6	7
40	6,77 ± 1,45	32,09 ± 0,93	38,86 ± 2,33	**17,43**	**82,57**	4,74
50	10,99 ± 0,82	39,96 ± 1,03	50,94 ± 0,97	**21,57**	**78,43**	3,64
60	12,04 ± 0,96	48,93 ± 1,92	60,96 ± 2,37	**19,74**	**80,26**	4,07
70	18,14 ± 1,98	53,62 ± 2,05	71,76 ± 0,36	**25,28**	**74,72**	2,96
80	24,75 ± 2,01	56,91 ± 2,43	81,66 ± 0,56	**30,31**	**69,69**	2,30

1   theoretical amount of water in the sample

2   1st mass loss and standard deviation (referred to sample weight)

3   2nd mass loss and standard deviation (referred to sample weight)

4   sum of 1st and 2nd mass loss and standard deviation

5   content of free bulk water (referred to the total amount of water)

6   fraction of bound water (referred to the total amount of water)

7   ratio between bound and free bulk water

4.1.2.1.4   Conclusion of TGA

The water in the cream can be differentiated in free bulk (first water loss) and water which is entrapped within the gel-matrix (second water loss). That the bound water is not only fixed inter-lamellar was shown by SAXD which showed constant inter-layer spacing of placebo containing different water amounts. A lamellar gel-network as proposed by Junginger, with increasing water amount would swell resulting in increasing interlayer distance.

But in the case of the model cream with water amounts between 40 and 60 % the ratio between free and bound water (20:80) remains unchanged. This means that the bound water necessarily has to be entrapped in different ways.

In addition to the inter-lamellar fixed water between crystalline lipid bilayers of the hydrophilic gel, water is bonded within the lipophilic gel and a third part is immobilised by lipid layers in liquid-crystalline state around the oil droplets.

The high water evaporation rate between 40 and 70 °C could be partially due to loss of water entrapped mechanically within the lipophilic gel-phase caused by the melting of cetearyl alcohol semi‑hydrates as well as partially due to the melting of lipid layers in liquid-crystalline state and hydrophilic gel-phase and thus evaporation of water fixed between the lamellae ("depot" water).

Shifting of the ratio in favour of free water and at the expense of bound water (from 20:80 to 25:75 to 30:70) in creams with water contents of 70 and 80 % indicates that lamellae as well as lipophilic gel and liquid-crystalline lipid layers are saturated with water. Excess of water is loosely dispersed within the continuous phase.

Although TGA can be considered useful to distinguish between different bound water in the cream, it could not provide a quantitative determination of free bulk and inter-lamellar bound water in the model formulation because the evaluation of the peak maxima is up to the observer's eye.

4.1.2.2   DSC

DSC analyses provide information about the structural nature of single components and the complex formulation. In the following general characterisation melting temperatures and curve profiles will be considered to gain information about the melting behaviour. Later on, onset temperatures and melting enthalpies of phase transitions will be evaluated for the assessment of process parameters and storage behaviour.

Figure 4-7 shows DSC curves of the fatty phase components responsible for the formation of the gel-structure. The pure emulsifier PEG-5-glycerylstearate shows two marked peaks at 45 °C and at 62 °C. Cutina CBS as mixture of fatty ester and fatty alcohol shows a broad melting interval with a distinctive melting peak at 61 °C and a shoulder at 46 °C. Within the curve profile of the 7:5:3 mixture of the fatty phase components (Arlatone 983S; Cutina CBS; PCL-Liquid) the melting behaviour of Cutina CBS and Arlatone 983S is recognisable. A distinctive peak at 55 °C and a shoulder at 42 °C are visible.

The more complex the mixture (Arlatone 983S < Cutina CBS < fatty phase mixture), the lower the melting temperature of the second peak (62 > 61 > 55 °C).
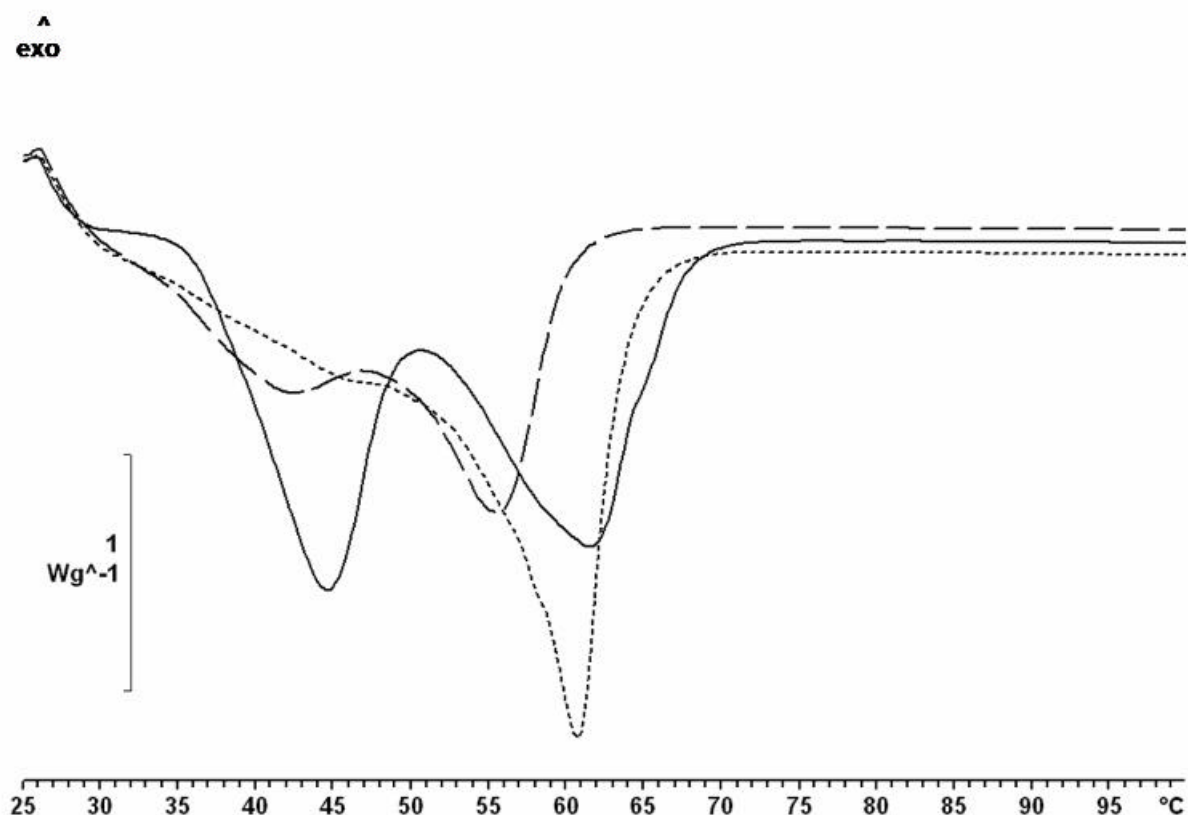
Figure 4-7:   DSC-curves of fatty phase components
                     Full line   Arlatone 983S
                     Dotted line   Cutina CBS
                     Dashed line   Fatty phase mixture*

* fatty phase mixture in the ratio 7:5:3 respectively Arlatone 983S; Cutina CBS; PCL-Liquid

Pure API-crystals melt at 108.12 °C (fig. 4-8). Placebo (fig. 4-9), different from the fatty phase mixture in fig. 4-7, shows a single symmetrical peak with its melting point at 53 °C. Single fatty phase components can not be differentiated within placebo.

The onset temperature of the phase transition of the API from the solid to the liquid state is shifted down from 108.12 °C (in the pure API) to about 70 °C within verum (fig. 4-9). This peak is wider, flatter and less distinctive compared to the melting peak of the pure API. It seems that this endothermal peak is likely due to dissolution of the crystalline API within the hydrophilic and/or lipophilic gel-phase and not to a depression of the melting point by approx. 30 °C. The melting of the fatty phase (first peak) in verum is reduced to a single and less pronounced peak between 43 and 55 °C similar to a plateau. Compared to placebo this melting peak is shifted to lower temperature by approx. 5 °C.
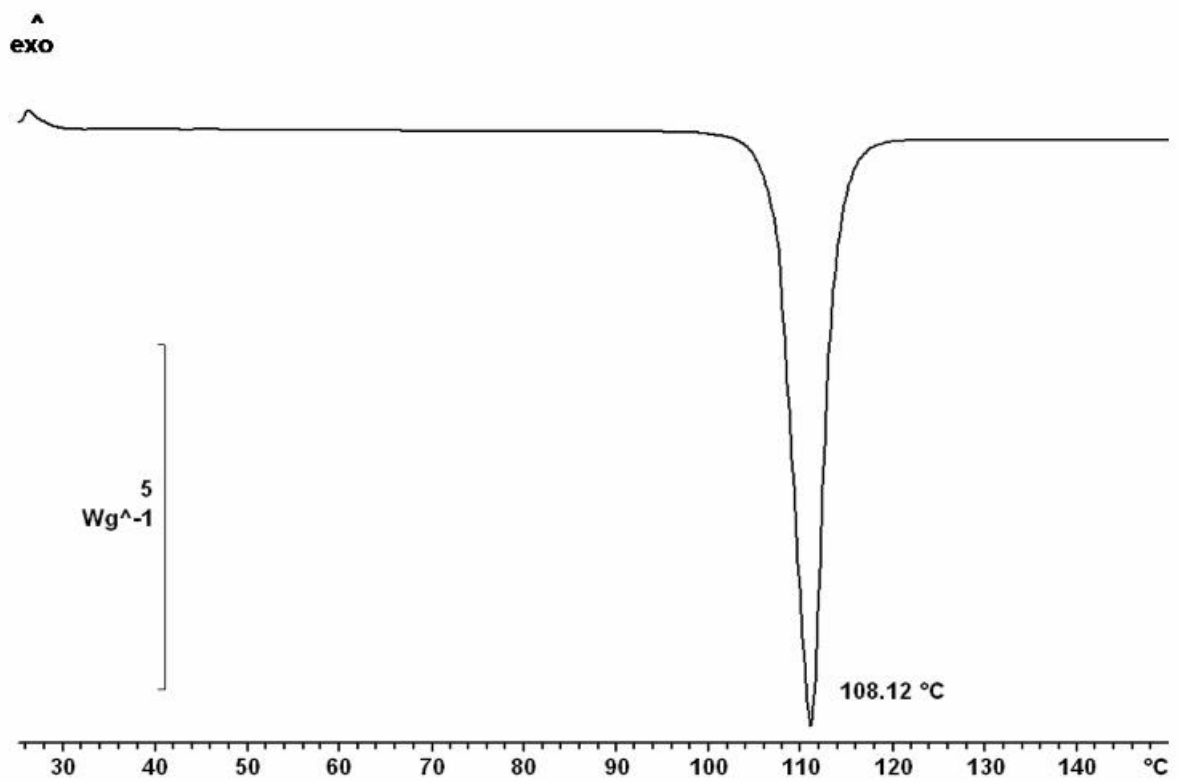
Figure 4-8:　　　DSC-curve of micronized azelaic acid (AzA)
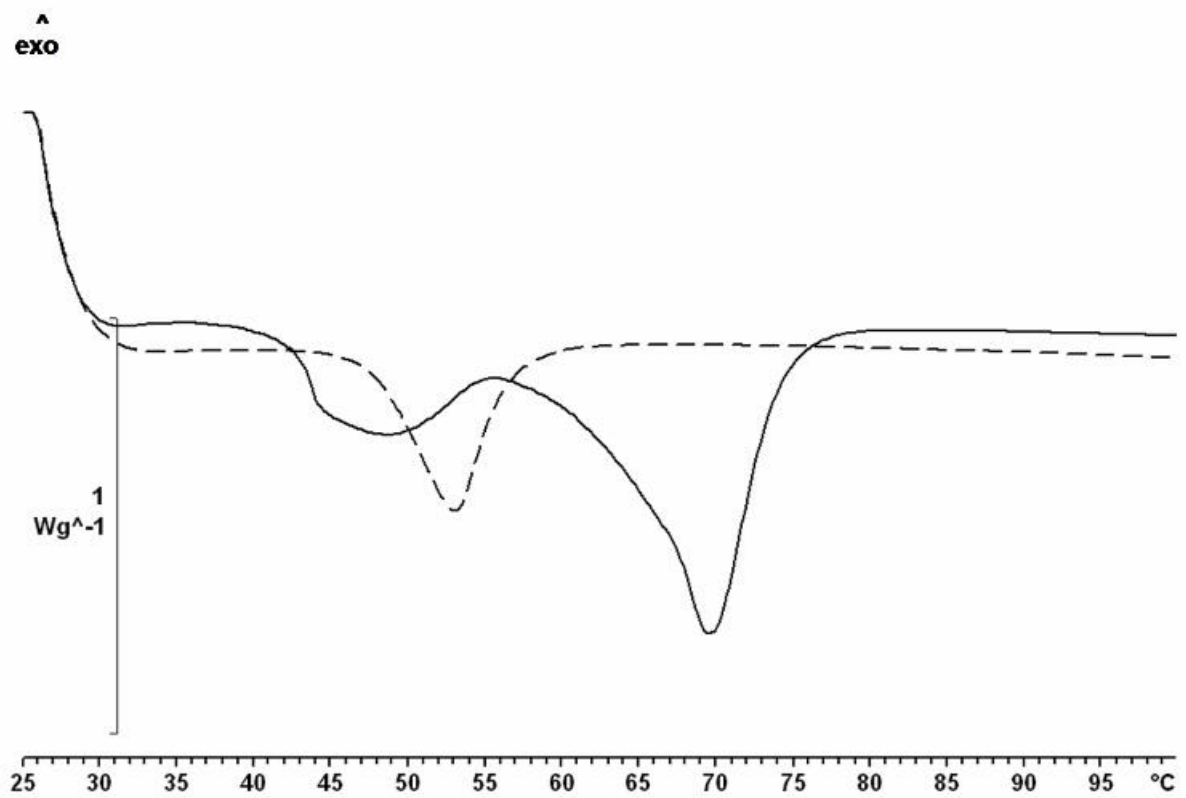
Figure 4-9:　　　DSC-curves of verum (full line) and placebo (dashed line)

4.1.2.3   Summary of DSC

The melting behaviour of the fatty phase components and the API depends on the qualitative and quantitative composition of the sample.

The first shoulder of the fatty phase mixture may correspond to the transition of the free cetearyl alcohol from crystalline to α-crystalline form. Literature indicates two melting peaks for cetearyl alcohol, transformation from crystalline to α-crystalline form (36.5 °C) and transition from α-crystalline to molten form (49.5 °C) (Kudlek, 1996).

Melting profiles of Arlatone 983 S, Cutina CBS and the fatty phase mixture show a pronounced peak between 55-62 °C. The more complex the mixture is, the higher is the depression of this melting peak. Compared to the single components, surfactant PEG-5-glycerolstearate and amphiphile Cutina CBS obviously form a common structure consequently with an altered melting profile. The dominance of the cetearyl alcohol in the DSC curve is in line with WAXD/SAXD diffractograms.

The two endotherm melting peaks in the fatty phase mixture are reduced to a single peak at 53 °C within placebo whereas to a plateau peak with its maximum at about 48 °C in verum. The huge shift down from 108.12 °C (pure AzA-crystals) to 70 °C together with the broadening of the API's melting peak clearly point to a solubilization of AzA-crystals within the gel matrix.

4.1.3   Macroscopic and Microscopic characterisation

The verum is a white, opaque, and smooth cream with API-crystals distinguishable as white dots. The placebo is shiny and smooth and appears less white due to the absence of the API-crystals (fig. 4-10).
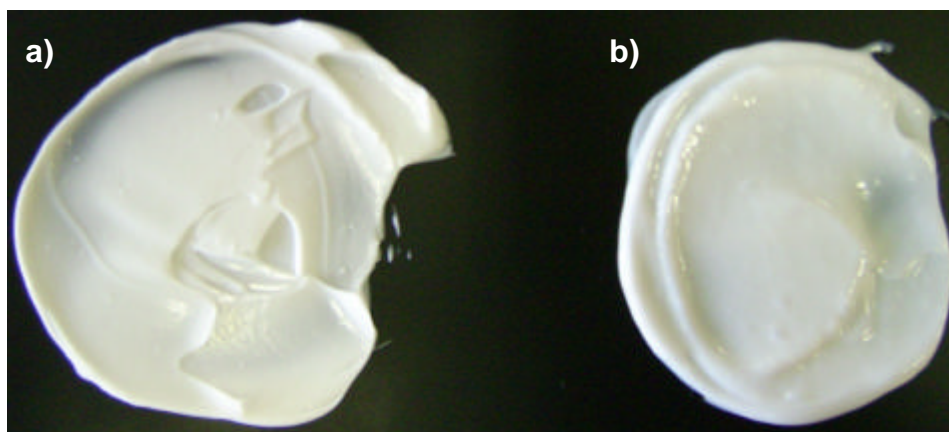
Figure 4-10:   a) verum   b) placebo

Figure 4-11 represents the microscopic picture of the placebo. The drops of the inner oily phase are distinguishable with a mean diameter of about 2 µm. Weakly formed red and blue coloured areas indicate hydrophilic and lipophilic gel phases.

The polarized microscopic picture of the verum (fig. 4-12) shows API-crystals homogeneously dispersed in the cream. These acicular rods appear variously coloured due to polarisation on the crystal's surfaces. Their single dimensions vary between less than 5 µm for the smallest particles to about 20 to 30 µm for the biggest ones.
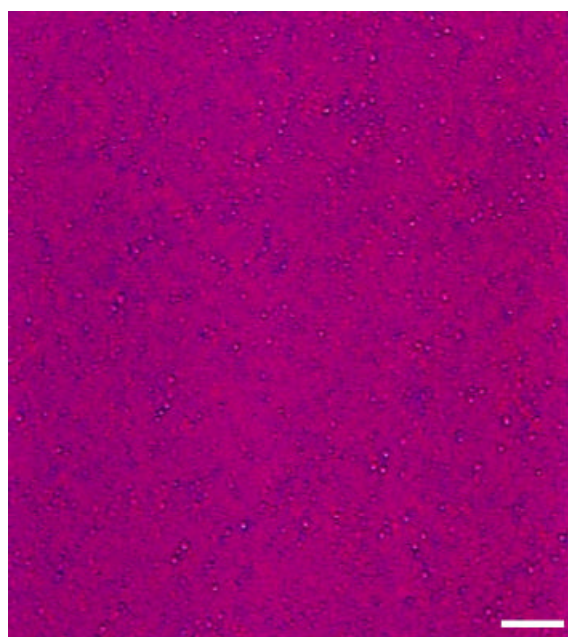
Figure 4-11:   placebo, 200x, bar 32 µm   Figure 4-12:   verum, 200x, bar 32 µm
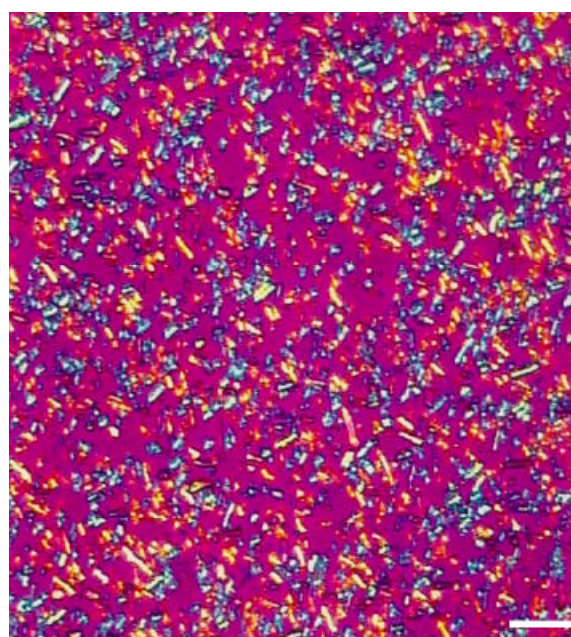
Micronized API-crystals show moderate crystal growth after prolonged storage of the cream at 40 °C/ 75 % RH. The crystals that measure up to 80 µm get a rhomboidal shape. Figure 4-13 shows an example.
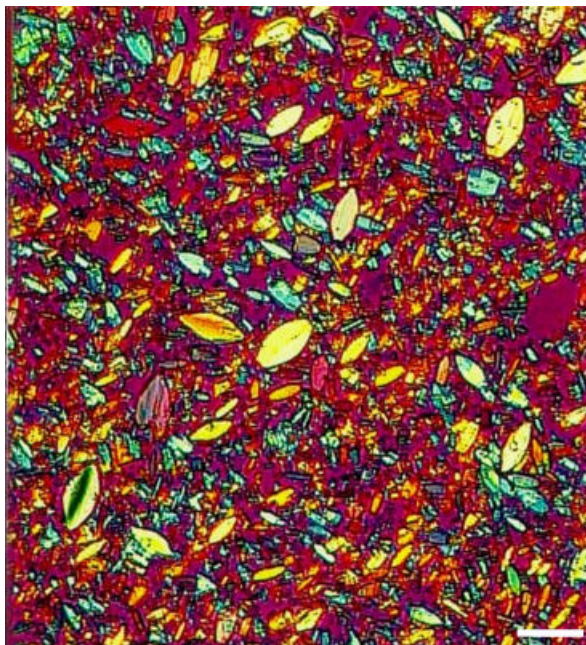
Figure 4-13:   verum after 3 months at 40 °C, 200x, bar 32 µm

The micronised API was characterised by SEM (chapter 3.2.14). Figure 4-14 shows the SEM-micrograph of azelaic acid crystals magnified by 5000. They show a monoclinic prismatic shape with a mean length of about 5 µm. The smallest crystals have dimensions smaller than 2 µm, bigger ones have dimensions of about 20 µm. Agglomerates are absent.
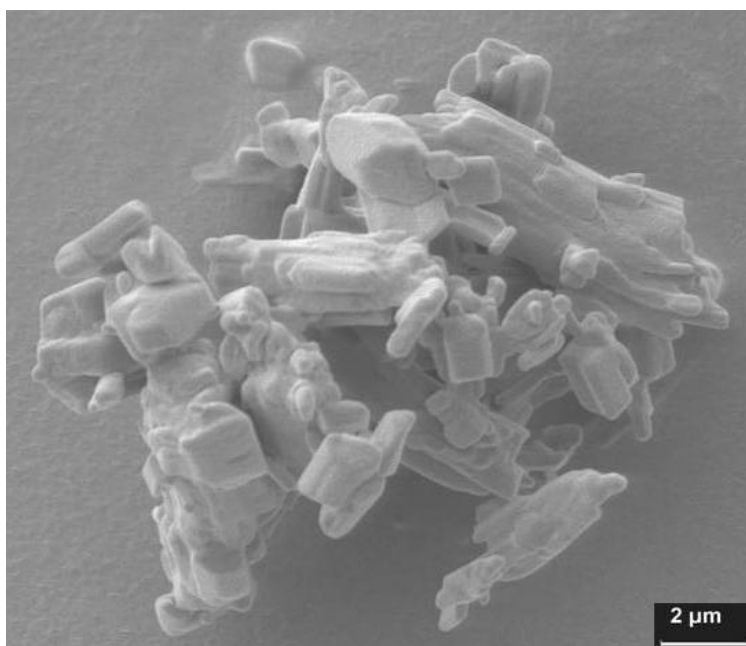
Figure 4-14:   SEM-micrograph of AZA; 500x

4.1.4   Rheological characterisation

Rheological measurements are well suited for the structural characterisation of semisolid dosage forms. These measurements are recommended to be performed after a certain holding time after their preparation. This was pointed out by different authors. Lashmar et al. (1995) for instance noted that often shortly after manufacturing semisolid preparations have not formed their final structure yet, leading to less representative and less reproducible results. Creams show more complex flow behaviour than emulsions (Moore et al., 1986). Therefore the application of an adapted rheological method is very important in order to obtain good interpretable results.

Rheology is also indicative for changes in flow behaviour and viscous-elastic properties and thus for structural changes in dependence on stability interacting factors (Rose, 1999). These results are the basis for stability tests and quality control (Kaiho et al., 1980).

4.1.4.1   Flow behaviour

Flow properties as apparent shear viscosity at the apex of the shear stress curve at 400 1/s, hysteresis between back and forth curve and yield point were investigated by rotational experiment.

4.1.4.1.1   Yield point

The yield point is defined as the minimum required shear force where a substance begins flowing. It can be determined by means of the bending point of the deformation curve increasing the shear stress τ. It provides information on elasticity and mechanical resistance of a sample. Figure 4-15 exemplifies the determination of the yield points of verum and placebo (pilot scale batch # SHT056-P02) with increasing shear stress.

Typical to structural flow behaviour is that substances only start flowing after being subject to a certain shear stress (plastic). Up to the yield point the samples are elastic and the molecules are capable to follow the increasing shear without considerable flow. When the yield point is reached, samples begin to flow and the deformation rises abruptly.

Placebo and verum show similar yield points. Measurements of samples of the same batch as well as measurements between samples of different batches show high relative standard deviations (cv > 10 %). The low reproducibility is a frequent disadvantage when the yield point is determined by rotational experiment. Further it should be mentioned that the measuring period can possibly influence the result.
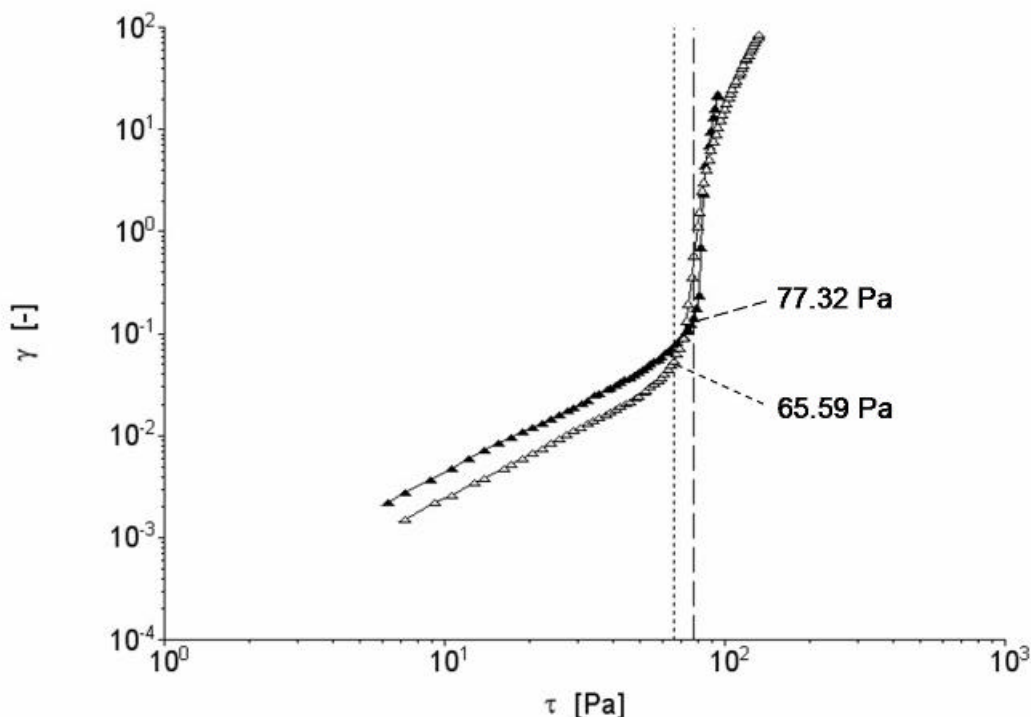
Figure 4-15:   Yield points [Pa], batch # SHT056-P02 (pilot scale std)
                    -▲-   placebo   -△-   verum

4.1.4.1.2   Flow curve

Figure 4-16 represents flow curves of verum and placebo (pilot scale std, # SHT056-P02) in CR mode (controlled shear rate). By a preset shear rate ramp the shear stress reaction of the sample is evaluated. Before increasing the shear rate a defined pre-shear is applied to the sample in order to smooth out the fluctuations at the beginning of the flow curve (chapter 3.2.12.1.1).

All samples, placebo and verum show plastic thixotropic flow behaviour as this is typical for semisolid preparations (Rose, 1999). Both samples are sensitive to shear. The build-up of structure after a shear strain occurs strictly as temporally delayed (hystereses values). Apart from the API verum distinguished from placebo by the final homogenisation.

At the same shear rate placebo clearly shows higher response of the shear stress and hence higher mechanical resistance to shear. Upwards and downwards curves of placebo are a long distance from each other. Placebo curve rises steeply before it reaches its maximum shear stress of 300 Pa at a shear rate of 180 1/s. The shear stress remains at its maximum

between 180 1/s and 225 1/s. At shear rates higher than 225 1/s the shear stress regresses slightly up to the apex.

Obviously, the behaviour is clearly determined by shear induced destruction of structural elements in the cream. This effect is less pronounced within the verum. This might be attributed to 20 % solid API-fraction in verum that gives the system mechanical stability and elasticity. At each time point the curve progression of verum rises and obtains at the apex its maximum shear stress of 200 Pa.
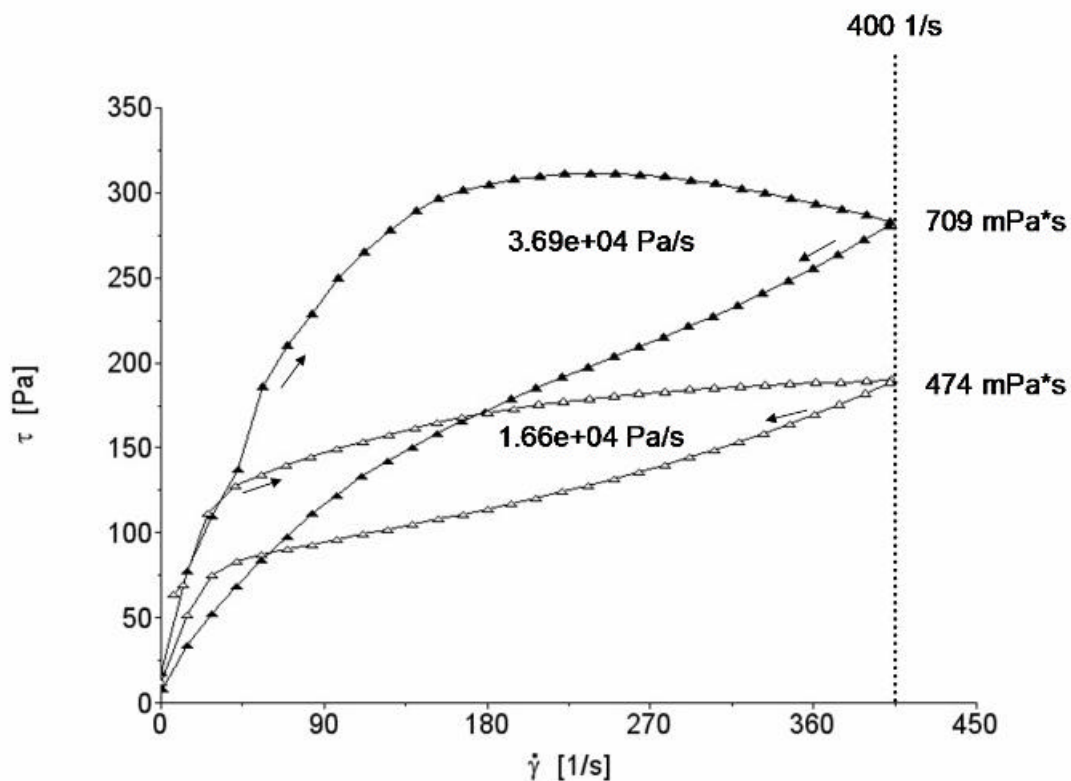
Figure 4-16:   Flow curves, batch # SHT056-P02 (pilot scale std)
                    -▲-   placebo   -△-   verum

In order to compare shear viscosities between the two the apparent shear viscosity at the apex of each thixotropy loop (Eccleston, 1975) was considered. The apparent shear viscosity describes the ratio of shear stress and shear rate. Figure 4-17 shows viscosity curves of verum and corresponding placebo (pilot scale std batch # SHT056-P02).
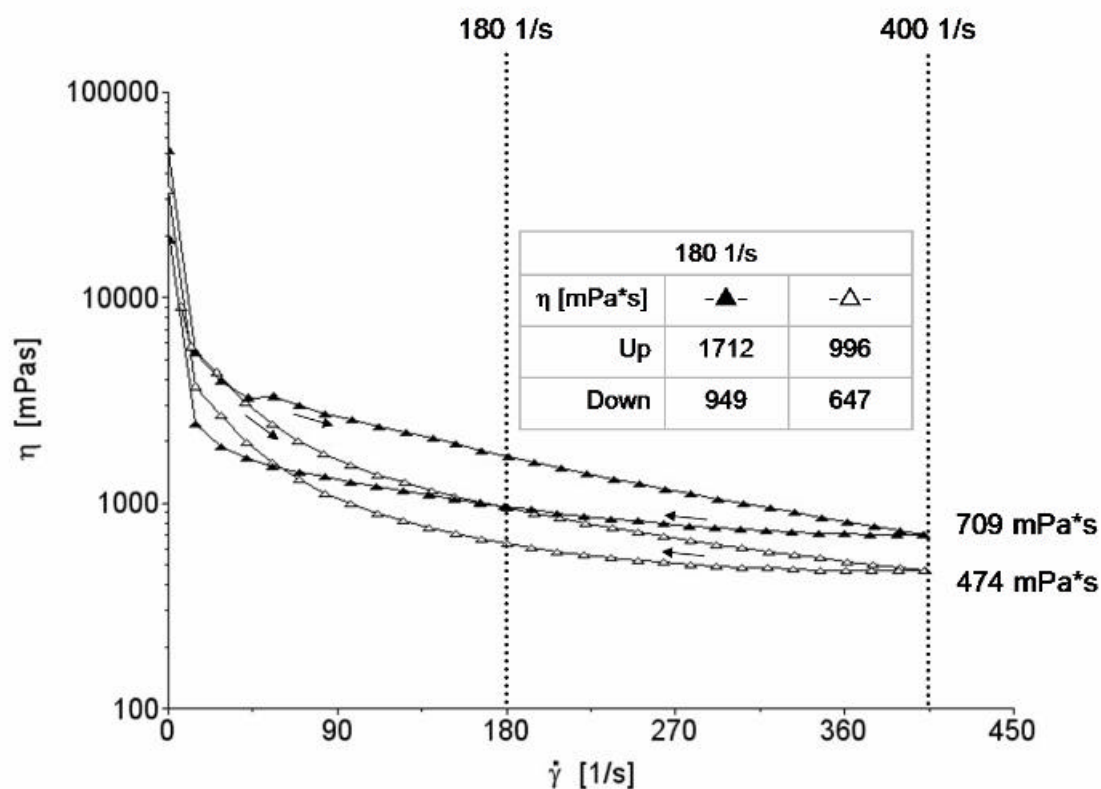
Figure 4-17:   Shear viscosity curves, batch # SHT056-P02 (pilot scale std)

            -▲-   placebo   -△-   verum

With increasing shear rate the verum and placebo viscosities decrease ('shear thinning'). The apparent verum shear viscosity at 400 1/s is 474 mPas whereas placebo shows a shear viscosity at the apex of 709 mPas. By diminution of the shear rate the viscosity is regained only partially. Backward curves are clearly separated from forward curves.

The formulation is very sensitive to shear. In order to clarify if the break down of structure is reversible, placebo and verum were subjected to repetitive shear cycles. Figure 4-18 shows flow curves of placebo (a) and verum (b) after multiple shear rate loops. With increasing number of shear cycles the hysteresis decreases. The most prominent difference is detected between first and second shear rate loop. Finally, after 10 shear rate loops the cream shows almost no hysteresis. Table 4-4 shows hystereses values of verum and placebo with increasing numbers of shear rate loops.
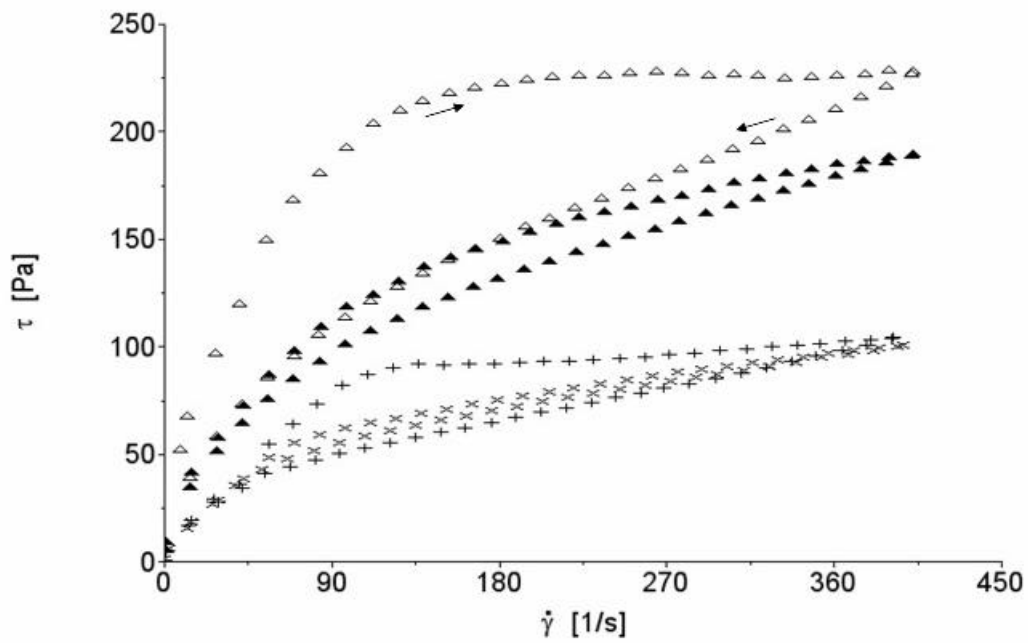
a)
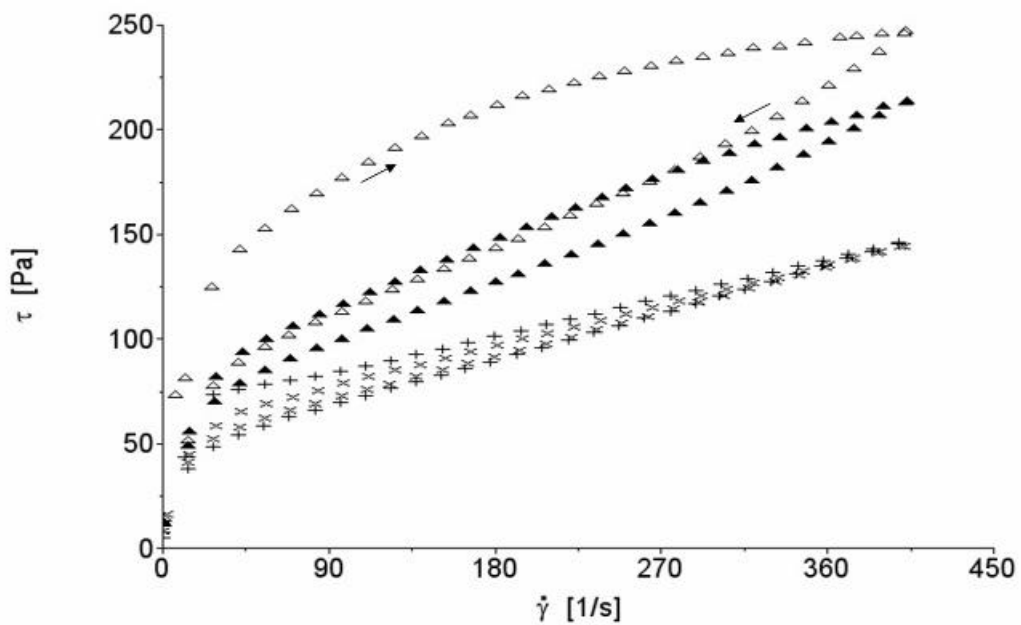
b)

Figure 4-18:   Flow curves, batch # 53179 (ind scale), a) placebo, b) verum
△   1st loop
▲   2nd loop
×   10th loop
+   loop after 10 loops + 3 h rest

After 10 shear rate loops, the cream was allowed a relaxation time of 3 hours. After 3 hours a further shear loop was applied. During the rest period of 3 hours the cream partially restores its micro structure. The cream might possibly regain its initial structure after several hours/days at rest. It would mean that a rheo-destruction occurs.

Anyway, from figure 4-18 it becomes apparent that shearing destroys at least partially irreversibly micro structure as the cream is not able to regain its original structural viscosity.

Table 4-4:   Hystereses [Pa/s], # 53179 (ind scale), placebo and verum

Loop	1st	2nd	10th	loop after 10 loops + 3 h rest
Placebo	2.03e+04	4898	1624	6560
Verum	1.99e+04	6421	1902	4068

4.1.4.2   Summary of flow behaviour

The model cream (verum and placebo) shows plastic thixotropic flow behaviour. Shear viscosity decreases by shearing. This obtained 'shear-thinning' behaviour is a desirable property in creams, since they should be 'thin' during application and 'thick' otherwise. The model cream shows a stable gel structure. This was visible on the high shear stress values during the upwards curve. Thus, hystereses were interpreted as a measure of build-up of micro structure after applied shearing (thixotropy). But the cream is also shear-sensitive. By strong shearing it comes to a structure break-down. By repeatedly applying of shear the structure will be progressively disordered and hysteresis will be progressively lost. After rest the cream restores its structure only slowly and partially. It shows at least partially rheo-destruction of the cream. In this case the resulting hystereses can be interpreted as measure of structure-loss during shearing (Barry, 1974, Martin et al., 1964).

The yield point as a measure of visco-elastic properties of the system was a bad indicator of the physical stability as measurements showed low reproducibilities (cv >10 %). Hence, for the evaluation of critical manufacturing process parameters and assessment of the cream stability the yield point was not considered.

4.1.4.3   Oscillatory behaviour

The oscillation test is capable to determine the visco-elastic properties of a sample simultaneously whereas shearing leads to an integrated characterisation only. In oscillation experiments a sinusoidal shear stress is applied to the sample. The sample will deform. Dependent on the relation of viscous and elastic properties the maximum amplitude of deformation γ_0 is not necessarily reached at the same time as the stress amplitude τ_0. After an applied shear a delay is occurred in the deformation for viscous-elastic compounds such as most semisolid preparations. Therefore viscous-elastic compounds show a phase shift δ between 0 and 90 °. When δ is below 45 ° elastic properties prevail, when δ is higher than 45 ° viscous properties have the overbalance.

For the evaluation of an oscillation experiment the following basic equation is used:

$$\tau_0 = G^* \, \gamma_0$$

By setting the stress amplitude and measuring the deformation amplitude the complex modulus G^* can be calculated. By knowing the frequency and measuring the time at which stress and deformation amplitudes are reached the phase shift δ between both can be calculated:

$$G' = G^* \, \cos\delta$$

G' describes the storage modulus and is a representative for the elastic behaviour and hence for the energy which can be recovered from the system. Loss modulus G'' stands for the dissipated energy and viscous properties.

$$G'' = G^* \, \sin\delta$$

One might be interested in the ratio of viscous and elastic properties. This is commonly done by looking at:

$$G''/G' = \sin\delta/\cos\delta = \tan\delta$$

The phase shift amounts to 45 ° when storage modulus and loss modulus are in equilibrium. Oscillatory parameters are a function of the frequency and consequently a function of the period of the applied shear. Oscillatory measurements have the benefit of maintaining the inner structure of the sample provided that the measurement is carried out within the linear visco-elastic region (Rose, 1999). Within this LVE-region the system is inherently stable, oscillatory characteristics as phase shift and oscillation modules are constant.

4.1.4.3.1   Strain stress sweep

In order to determine the LVE-region a so called strain-stress sweep or amplitude sweep was carried out. Here the amplitude of oscillation is increased without steps keeping the frequency constant. Figure 4-19 shows exemplarily an amplitude sweep for verum and placebo (ind scale batch # 51177). The upper limit of the LVE-region is characterised by the decline of the elastic modulus G'. For both, placebo and verum this drop begins at shear stresses above 30 Pa. Exceeding 100 Pa the structure changes irreversibly and breaks down completely. At the same time phase shifts abruptly rise. The lower phase shifts of verum (18.32 ± 1.51 °) compared to placebo phase shifts (23.14 ± 0.60 °) evidence the higher elasticity of verum explicable with the solid API-fraction of 20 % (w/w). The semisolid cream character with predominantly elastic behaviour (G' > G'') passes over in a fluid system with predominantly viscous character (G'' > G'). The 'cross-over' of G' and G'' occurs at a shear stress of 245 Pa (placebo) whereas at 280 Pa (verum). The 'cross-over' can be taken as yield stress.
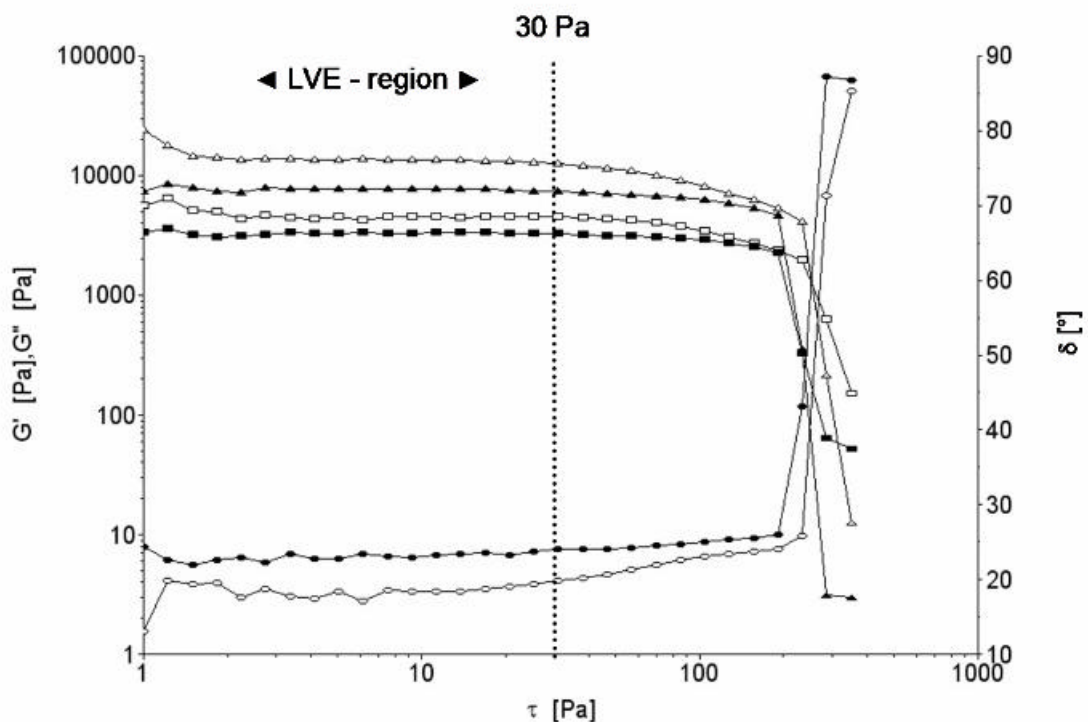
Figure 4-19:   Strain stress sweep, τ = 1-350 Pa, f = 1 Hz, # 51177 (ind scale)

Placebo	Verum	
-▲-	-△-	: Storage modulus G'
-■-	-□-	: Loss modulus G''
-●-	-○-	: Phase shift δ

Table 4-5:   G' [Pa], G'' [Pa] and δ [°] (1-30 Pa) within the LVE-region, batch # 51177

Product	G' [Pa]	G''[Pa]	δ [°]
Placebo	7683 ± 292	3282 ± 114	23.14 ± 0.60
Verum	14352 ± 2670	4704 ± 553	18.32 ± 1.51

4.1.4.3.2   Frequency sweep

The frequency sweep was carried out in order to study the dependency of the frequency within the LVE-region. Therefore the frequency was increased continuously from 0.1 Hz to 30 Hz keeping a constant shear stress of 10 Pa (fig. 4-20).
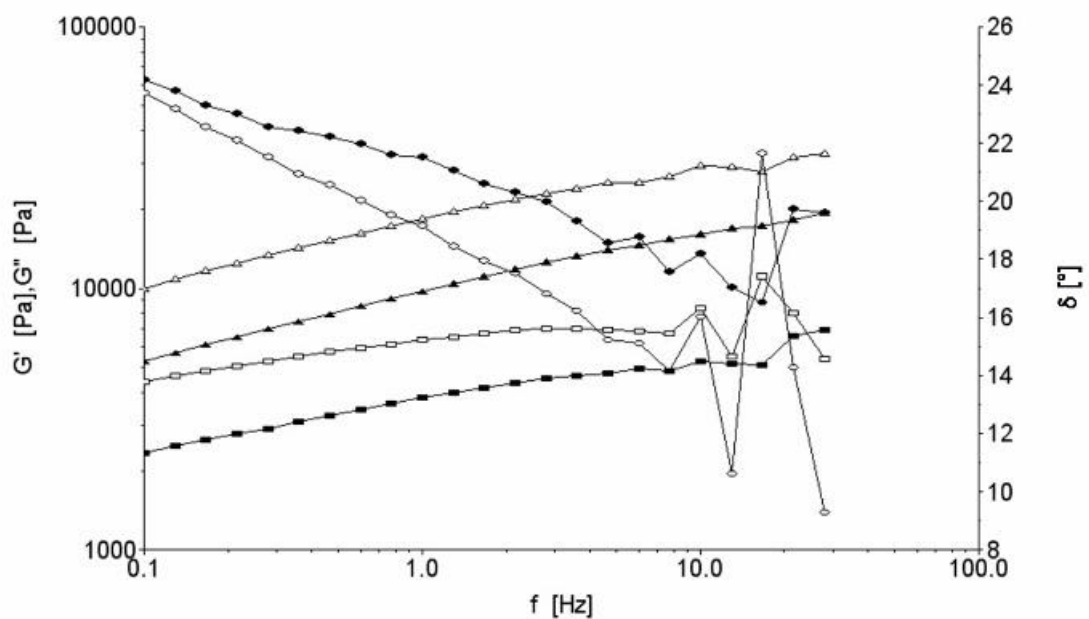
Figure 4-20:   Frequency sweep, τ= 10 Pa, batch # 51177 (ind scale)

Placebo   Verum
-▲-   -△-   : Storage modulus G'
-■-   -□-   : Loss modulus G''
-●-   -○-   : Phase shift δ

As in figure 4-20 exemplarily shown for placebo and verum industrial scale at low frequencies (< 2 Hz) G' and G'' increase linear (G' increases more than G''). Above 2 Hz, G' continues rising whereas G'' remains constant. The elastic behaviour increases because of the incapability of the system to follow high frequencies. The system becomes increasingly stiff. The 'zig-zag' of δ at high frequencies (>10 Hz) is probably caused by API-crystals that are no longer able to follow the high frequency and thus become entangled in one another.

4.1.4.4   Summary of oscillatory test

Oscillatory analyses are designed to not destroy the structure (measurement within the linear visco-elastic region). Therefore it can provide information on the inter-molecular forces. Within the linear visco-elastic region (< 30 Pa) cream samples are inherently stable and the inner structure will not be destroyed.

Based on the oscillatory characterisation test conditions of various samples from industrial, pilot and lab scale with varied manufacturing process parameters and at different storage conditions and storage times uniformly were set as follows:

<u>Parameters for the oscillation time curve</u>

Measuring mode	CS*
Waiting time	300 s
Shear stress	10 Pa
Frequency	1 Hz
Measuring time	120 s
Data	10

*CS   controlled shear stress

4.1.5   Concluding results of structural characterisation

Cognitions obtained from the structural characterisation of the formulation are the base for investigations on the relevance of the manufacturing process. Based on the structural characterisation the following model can be described for the cream. The cream's microstructure is formed by a complex gel-matrix comprised by the visco-elastic hydrophilic gel-phase and the lipophilic gel-network. Liquid lipid crystals in the form of layers surround and stabilize the oil droplets. Oily phase (PCL-liquid) is inserted between alkyl chains of PEG-5-glyceryl stearate/ cetearyl alcohol crystals forming a disordered liquid-crystalline structure of lamellar type, either at the border of oil droplets or widespread towards the continuous phase. Randomly oriented multilayer of complex visco-elastic gel-phase gives the structured continuous phase with increased viscosity, thus contributing to the oil droplets immobilization (Savic, 2005).

The water is inter-lamellar bound between crystalline lipid bi-layer, entrapped mechanically within the lipophilic gel-phase as well as fixed between lipid-layers in liquid-crystalline state and present as free bulk water. With regards to the verum with water content of about 50 % (placebo 63.5 %), the water content of placebo was investigated in the range of 40-80 % (w/w). The ratio between free and 'bound' water is 20:80 up to a water content of 60 %. This is in agreement with SAXD analyses that show a fully hydrated gel-phase of limited swelling with increasing water concentration within the cream. Above 60 % the ratio changes in favour of bulk water to 30:70.

Melting peaks between 55 and 62 °C of Arlatone 983 S, Cutina CBS and the fatty phase mixture (7:5:3 respectively Arlatone 983S: Cutina CBS: PCL-Liquid) show the dominance of the cetearyl alcohol. Placebo shows only a single peak at 53 °C compared to two endotherm melting peaks of the fatty phase mixture. The huge down shift of the melting peak of the API from 108.12 °C (pure API-crystals) to 70 °C (in verum) points to the dissolution of the API within hydrophilic and/or lipophilic gel-phases.

The model cream, like all creams, combines viscous (liquid) and elastic (solid) properties at the same time. The investigated formulation shows predominantly elastic behaviour. Responsible therefore is the deformable gel-framework. Further, the high amount of solids in the verum gives the cream a high mechanical resistance. Structure build-up after an applied shear generally occurs temporally delayed for all investigated formulations (plastic-thixotropic). All samples show a defined linear visco-elastic region (< 30 Pa). The yield point was less suitable as an indicator for visco-elastic stability because of its low reproducibility.

4.2   Investigated manufacturing process parameters

The influence of single manufacturing process parameters on physical, thermo analytical and rheological cream properties as well as in vitro release will be assessed in the following. In addition, the impact on storage stability will be subject to evaluation.

Investigations on the model cream focus on manufacturing process parameters which probably influence the physical properties of the cream. An explanation regarding the choice of the kind of parameter and the values of each single parameter is forwarded in the current chapter. For making a choice of parameters subject to investigations the manufacturing process was analysed at the beginning of this work. The most critical steps have been selected based on experiences and respective parameter values have been set. Mainly there are interests in clarifying regarding the cold homogenisation and the meaning of the holding time.

Table 4-6 summarises critical manufacturing process parameters studied within the scope of this PhD-thesis. Investigations were partially performed on both, verum and corresponding placebo. Other parameters for instance, melting parameters of fatty phase and cooling rate have been studied exclusively on placebo neglecting the impact of the API.

Melting parameters were easily controlled on placebo lab scale. Parameters as cooling rate, circulation times/homogenisation times, temperatures of API-addition/final homogenisation have been investigated on pilot scale trials. Only on pilot scale have parameters been subject to a strict control nonetheless close to production. All investigations were performed on the bulk product. Additionally, holding time investigations have been performed on finished product (30 g aluminium tube).

Table 4-6: Investigated critical parameters

Parameter	Value	Object	Scale
Manufacturing process parameters			
Melting temperature/ Melting time	65 °C/ 30 min 90 °C/ 210 min	Placebo	Lab
Cooling rate	1.0 – 0.5 °C/min * 0.85 °C/min +	Placebo	Pilot
Circulation times	0 – 8.1 – 13.5 †	Verum/ corresp. Placebo	Pilot
Temp API-addition/ Temp final homogenisation	20/20 – 30/30 – 40/40 – 40/30 °C	Verum/ corresp. Placebo	Pilot
Holding time (HT)#	0 – 1 – 2 – 3 – 4 – 5 – 6 – 7 – 8 – 9 – 10 d	Verum/ corresp. Placebo	Pilot/ Ind
Batch size	40 kg / 80 kg	Verum/ corresp. Placebo	Pilot
Raw materials			
Arlatone 983S	56023361 / 56027131	Verum/ corresp. Placebo	Pilot
Cutina CBS	56023256 / 56028781	Verum/ corresp. Placebo	Pilot

* constant cooling rate

+ non-homogeneous cooling gradient (production like)

† final homogenisation time: 80 kg: 0, 15, 25 min 40 kg: 7.5, 12.5 min

performed with bulk and finished product (FP), FP filled after 0 d and 10 d HT

4.3 Impact of process parameters on the cream's properties

4.3.1   Melting time and melting temperature

The melting process of the fatty phase can be expected to be less critical, supposed that all fatty components are completely molten before getting transferred to the aqueous phase. Melting temperatures might have some effect on cream properties in particular if the melting temperature is borderline with the solidification temperature of the fatty phase. If the melting temperature is near the solidification temperature problems might occur during addition of the fatty phase to the aqueous phase due to re-crystallisation of fatty phase components in the cream. Further a loss of fatty phase components in transfer tubes and thus a reduced quantity in the inner phase of the emulsion, emulsifier and consistency agent included are possible. These situations might lead to changed consistency (quality relevant). On the other hand high temperatures and long melting times should be considered for their possible effect on the chemical stability of the fatty phase components.

Therefore two placebo batches, each of 1 kg, were prepared on lab scale simulating two extremes which might occur when preparing the fatty phase (table 4-7). On the one hand, an insufficient melting of fatty phase components has been simulated with a short melting at low temperature. On the other hand, a chemical decomposition of fatty phase components might be caused by a long term melting at high temperature.

The upper limit of the melting time (210 min) and the lower limit of the melting temperature (65 °C) have been taken over by the master formula. Furthermore, 90 °C has been selected as upper temperature extreme and 30 min has been fixed as lower melting time limit respectively.

Table 4-7:   Melting parameters of fatty phase, placebo lab scale, batch size 1 kg

	Batch SHT292-	Melting temperature [°C]	Melting time [min]	Possible Effect
1	P04	65	30	Insufficient melting
2	P06	90	210	Chemical decomposition

The lab scale batches P04 and P06 were prepared according the manufacturing batch record in figure 2-6 (chapter 2.2.3). During addition of the fatty phase to the aqueous phase (batch P04) parts of the fatty phase solidify immediately in the beaker.

Thus it might be possible that portions of the fatty phase re-crystallise and form more or less small lipid aggregates while homogenising.

In figure 4-21 the fine emulsion with drops of the inner oily phase of = 5 µm is shown exemplarily for batch # SHT292-P04. Both creams are homogeneous and show a white opaque and smooth appearance.

Figure 4-21:   SHT292-P04, 200 x, bar 32 µm

Table 4-8 summarises physical, flow, oscillating and thermo analytical properties of the creams. The thermo analytical properties as melting enthalpy and onset temperature as well as the oscillating properties do not show significant differences. Also consistencies (spreadability and micro-penetration) of both creams are comparable with one other.

Batch # P06 is more viscous compared to batch # P04. Batch # P06 with the higher shear viscosity and also shows slightly higher hystereses. Although they show identical electrical conductivities batch # P06 shows lower bleeding accompanied by a lower portion of free water. However, considering the standard deviation the difference in the free water amount is not significant.

The melting temperature of 65 °C (batch # P04) is close to the solidification temperature of the fatty phase components Cutina CBS and Arlatone 983S. Phase transitions in both occur at approx. 60 °C. This was shown by DSC measurements (fig. 4-9 in chapter 4.1.2.2). However, it did not affect the melting enthalpy and onset temperature of batch # P04.

Table 4-8:   Comparison between different melting procedures
SHT292-P04 vs # SHT292-P06, lab scale (1 kg)

Method	Unit	65 °C/30 min P04	90 °C/210 min P06	N° of measurements
Bleeding	mm^2	568 ± 92	450 ± 30	3
Conductivity	µS/cm	18.5 ± 1.0	18.4 ± 0.5	3
Free water	%	11.36 ± 0.46	10.13 ± 1.28	2
Spreadability	mm^2	1731 ± 157	1842 ± 67	3
Micro-penetration	mm*10^{-1}	395 ± 42	357 ± 14	3
Viscosity	mPa*s	569.2 ± 86.3	713.9 ± 61.8	2
Hysteresis	Pa/s*10^4	1.84 ± 0.51	2.32 ± 0.07	2
G'	Pa	7308 ± 155	7786 ± 138	10 data points
G''	Pa	3259 ± 96	3194 ± 121	10 data points
Phase shift	°	24.05 ± 0.94	22.30 ± 0.66	10 data points
Enthalpy	J/g	13.66 ± 0.45	13.51 ± 0.44	2
T_{onset}	°C	46.22 ± 0.54	47.54 ± 1.17	2

4.3.1.1   Summary and conclusion

It can be summarised that the cream with the lower melting temperature tends to have lower viscosity/hysteresis, is contemporaneous less elastic and shows slightly higher tendency to bleeding. On the other hand, results of micro-penetration, spreadability, conductivity, oscillation and DSC do not show differences between both batches.

These data indicate that melting time and melting temperature of the fatty phase do not have a major impact on the appearance and the physical properties of the placebo cream. In the light of this pilot scale trials on verum have not been performed.

4.3.2   Duration of final homogenisation

Comparing hot and cold homogenisation, the later is undoubtedly the more critical step. This was revealed by experiences during manufacturing of semi-solid formulations in general. The final homogenisation step is primarily required to disperse homogeneously the micronised API within the cream base.

The master batch record states that homogenisation for 15 min is performed. If IPC reveal that the API is not homogeneously dispersed homogenisation is performed for further 10 min.

The impact of the homogenisation time was studied on pilot scale batches of placebo (80kg) and verum (40 kg). Homogenisation times of industrial scale have been applied accordingly to pilot scale with the aim to study the shearing effects during homogenisation, primarily on placebo. Secondarily, verum pilot scale batches were homogenised for 7.5 min respectively 12.5 min (7.5 + 5 min).

During the 1st homogenisation step the total cream circulates 8.1 times through the mixer whereas during the 2nd step 5.4 times. This corresponds to a total number of circulations of 13.5. The number of circulations has been verified by batch # SHT292-P03 (table 2-4). It was identical in all investigated verum and placebo pilot scale batches.

4.3.2.1   Placebo with cooling rate of 1.0 °C/min

Samples of two batches were taken before (0 min), after 15 min, and after additional 10 min of homogenisation, respectively. Hence, the total bulk product in the mixer circulated 0, 8.1, and 13.5 times, respectively. The homogenisation was carried out at a product temperature of 28 ± 1 °C and at a homogeniser speed of 25.0 m/s in circulation.

Due to the high shearing during homogenisation the cream heats up. Therefore the jacket temperature was lowered and the product temperature in the middle and at the bottom was controlled continuously (table 4-9). The actual temperatures during final homogenisation deviate not more than 1°C from the target temperature. After homogenisation the jacket temperature was reset immediately in order to avoid cooling below the desired product temperature of 28 °C.

Table 4-9:   Temperatures during final homogenisation (## SHT292-P02/-P03)

Batch #	Duration [min]	T_{theor} [°C]	$T_{actual\ MEAN}$* [°C]	$T_{min\ actual}$ [°C]	$T_{min\ actual}$ [min]	$T_{max\ actual}$ [°C]	$T_{max\ actual}$ [min]
P02	15	28 ± 1	28,7	28	4	29	11
P02	10	28 ± 1	29,0	28	5	30	5
P03	15	28 ± 1	29,3	28	1	30	6
P03	10	28 ± 1	29,0	-	-	29	10

*   temperature measurement every minute

4.3.2.1.1   Consistency

Final homogenisation slightly decreased the spreadability. The differences were not significant as they range within the standard deviations. Micro-penetration was not affected (table 4-10).

Table 4-10:   Spreadability and micro-penetration after different circulation times
                   Means and relative standard deviations (n=2)

Circulation times (Duration of homogenisation in min)	Spreadability [mm^2]	Micro-penetration [mm*10^{-1}]
0 (= 0 min)	1833 ± 109	393 ± 31
8.1 (= 15 min)	1780 ± 276	368 ± 1
13.5 (= 25 min)	1661 ± 123	407 ± 20

4.3.2.1.2   Water binding capacity

In the following the impact of a cold homogenisation on the water binding capacity was assessed. Interestingly, the input of mechanical energy by final homogenisation clearly alters the distribution of bulk water in the cream. This could be determined indirectly by means of bleeding and electrical conductivity. This effect is summarised in fig. 4-22.
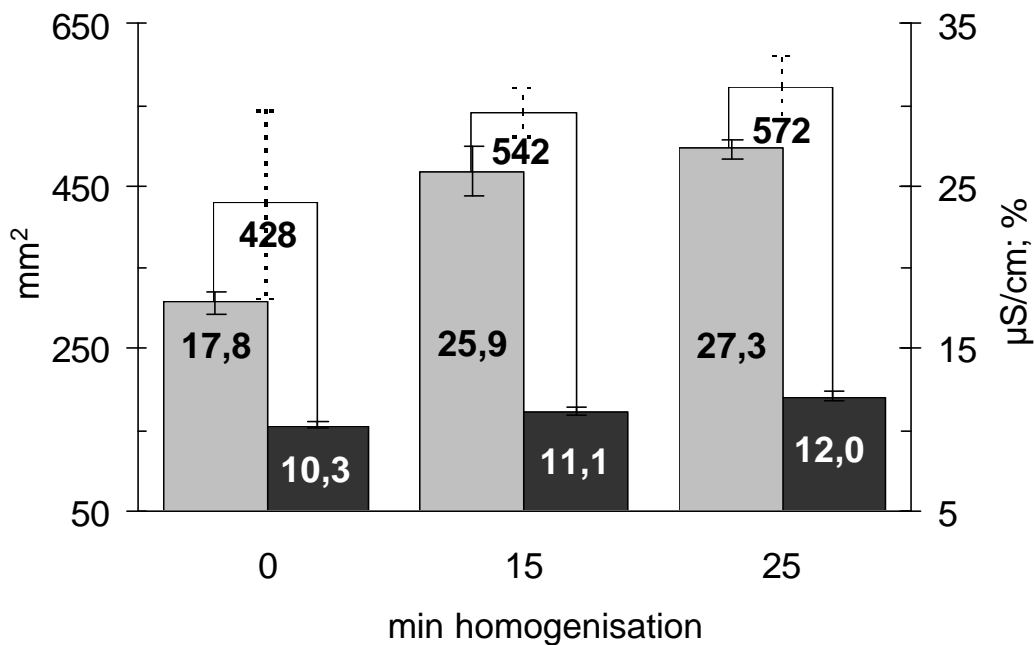
Figure 4-22:   White: bleeding [mm²]
                Grey: electrical conductivity [µS/cm]
                Black: free water loss [%] from total sample weight

Both, bleeding and electrical conductivity increase when the fraction of free bulk water increases. In particular the increase of both parameters becomes visible when comparing not homogenised cream and cream homogenised for 15 min. By increasing the final homogenisation by further 10 min the water binding capacity decreases again. The separated fluid was confirmed as aqueous leakage by means of the 'methylene blue method' (chapter 3.2.2).

Free bulk water in the formulation was determined directly through thermo gravimetric analysis. Thus the TGA result supports the results from bleeding and electrical conductivity. The portion of free bulk water increases from 10.3 % to 11.1 % to 12.0 % referred to total sample weight (table 4-11). Although the individual values of free water are not significantly different among creams homogenised for different times a trend for increasing bulk water with increasing homogenisation could be shown.

Table 4-11:   1ˢᵗ weight loss (= free bulk water) in % from total sample weight

Duration of homogenisation/ Number of circulations	0 min / -		15 min / 8.1		25 min / 13.5	
Sample	P02	P03	P02 H	P03 H	P02 HH	P03 HH
1	9.1	10.8	9.7	11.7	11.4	10.7
2	11.8	9.6	13.2	10.6	10.8	12.3
3	10.2	10.0	9.8	11.3	13.2	13.9
mean (n=3)	10.4	10.1	10.9	11.2	11.8	12.3
sd	1.3	0.6	2.0	0.6	1.2	1.6
mean ± sd (n=6)	10.3 ± 0.9		11.1 ± 1.3		12.0 ± 1.3	

These results demonstrate that the amount of unbound bulk water increases with increasing shearing of the cream. Obviously an extension of the homogenisation time leads to the worsening of the water binding capacity. The longer the time of final homogenisation the higher is the tendency to separate water from the system. The increasing fraction of free bulk water in turn might be the cause for the higher electrical conductivity.

Obviously, final homogenisation provokes a disorganisation of the hydrophilic gel phase. This in turn can speed up the separation of water from the system.

4.3.2.1.3   Melting behaviour

Changes in the melting enthalpy with dependence to the homogenisation could be shown by DSC analysis. From figure 4-23 the notable increase of melting enthalpy when the cream was homogenised for the first 15 min becomes apparent. A supplementary homogenisation for 10 min does not further increase the melting enthalpy. Onset temperatures are aligned with the tendency of melting enthalpies.
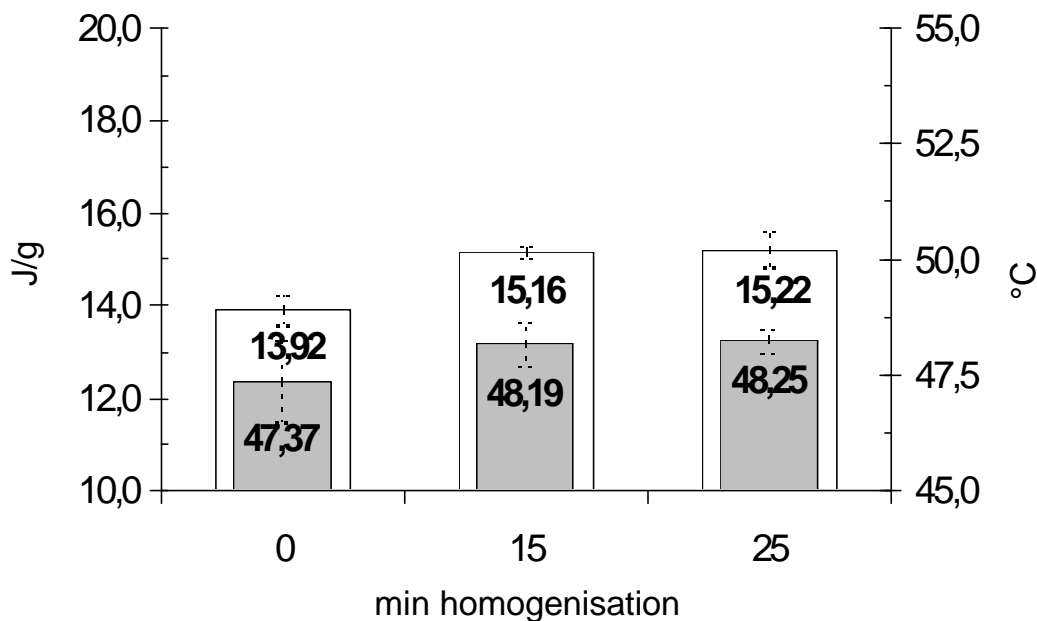
Figure 4-23:   White: normalized melting enthalpy [J/g]
                Grey: onset temperature [°C]

4.3.2.1.4   Rheological properties

Figure 4-24 represents the corresponding flow curves of the investigated creams. All samples show plastic thixotropic flow behaviour. The creams without final homogenisation show a high shear stress τ with increasing shear rate. The steep curve progression demonstrates a well structured and highly shear resistant cream. Upwards and downwards curves are clearly separated from each other.

Recovery of the structure occurs in delay for all systems and evidences the sensitivity of the creams to shear. Curve progressions of homogenised creams are much more flat. At low shear rates the shear stress τ inclines gently while at higher shear rates it reaches a plateau. This clearly indicates that structure has been lost. This is typical for less ordered systems. The progressive curve flattening by extended homogenisation is well visible on the flow curves of batch # P02 (empty symbols). In contrast, curve progressions of batch # P03 homogenised for 15 min and 25 min (filled symbols) are very similar.

By prolonging the homogenisation time a grading is only allusively visible. Most notable is the break down of the structure by changing from 0 to 15 min of homogenisation. This is in accordance with the other parameter.
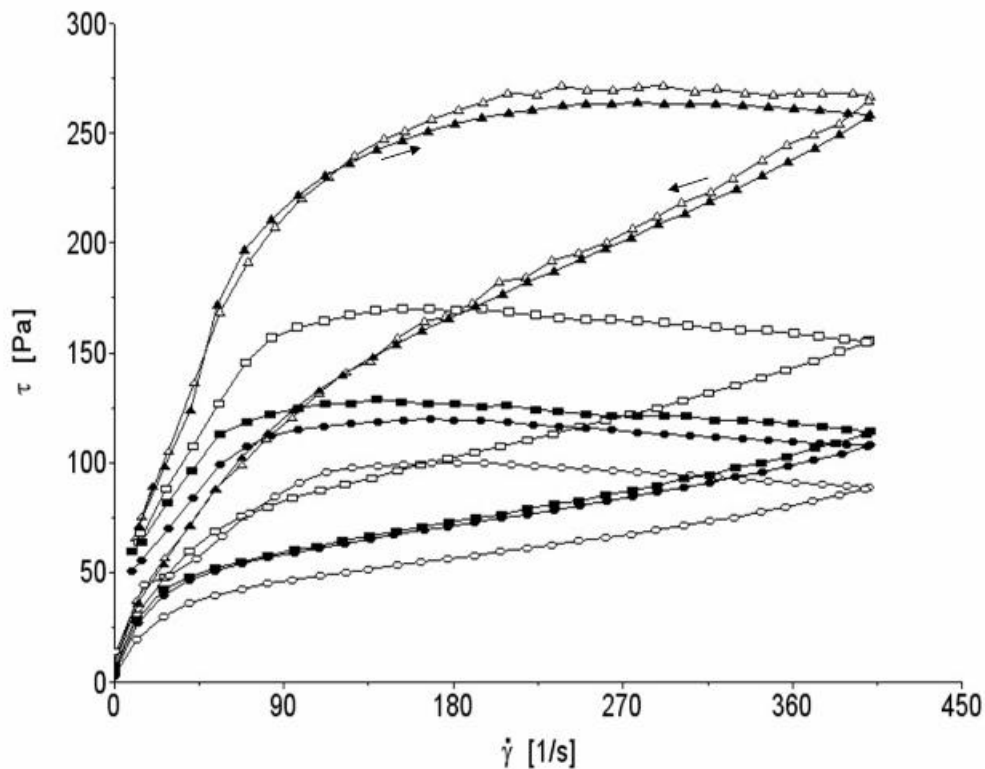
Figure 4-24:   Flow curves: without final homogenisation
△ SHT292-P02
▲ SHT292-P03

15 min final homogenisation
□ SHT292-P02
■ SHT292-P03

25 min final homogenisation
○ SHT292-P02
● SHT292-P03

From the flow curves it is also evident that final homogenisation reduces the hysteresis. The hysteresis as attribute of thixotropic flow behaviour is often accounted as measure for texturing or for mechanical degradation of structure (Rose 1999, Martin 1964). Shear stresses of homogenised creams are much lower in comparison with not homogenised creams. These creams are less structured. Where initially less structure is available obviously less structure can be degraded. This results in reduced hystereses (table 4-12). Primarily the hysteresis is dependent on the cream structures available at the outset. Increased shearing during final homogenisation lowers the apparent shear viscosity (table 4-12) of the creams. In comparison with creams which did not passed the final homogenisation step a considerable loss of viscosity was observed when the cream was homogenised for the

first 15 min. The decrease in viscosity was less distinct but noticeable if the homogenisation time was prolonged by further 10 min.

Table 4-12:   Shear viscosity and hysteresis after different circulation times;
                   Means and relative standard deviations (n=2)

Number of circulations (= Duration of homogenisation)	Viscosity [mPa*s]	Hysteresis [kPa/s]
0 (= 0 min)	555.6 ± 19.8	20.2 ± 2.7
8.1 (= 15 min)	354.4 ± 114.2	18.4 ± 4.7
13.5 (= 25 min)	287.6 ± 33.2	15.0 ± 2.3

Oscillatory tests give more detailed information about the viscoelastic properties in dependence from the homogenisation time. Within the LVE-region all creams show predominantly elastic behaviour with G' exceeding G'' and the phase shift δ below 45° (table 4-13).

Table 4-13:   Storage and loss modulus, phase shift and deformation at 10 Pa, 1 Hz

Number of circulations (= Duration of homog.)	G' [kPa]	G'' [kPa]	δ [°]	γ [%]
0 (= 0 min)	5.34 ± 0.46	2.27 ± 0.32	23.00 ± 1.15	0.15 ± 0.01
8.1 (= 15 min)	8.03 ± 0.43	2.94 ± 0.05	20.16 ± 0.64	0.12 ± 0.01
13.5 (= 25 min)	6.32 ± 0.51	2.24 ± 0.15	19.54 ± 0.28	0.15 ± 0.01

Final homogenisation leads to more elastic systems as shown by declining phase shift δ. From a declining phase shift a progressively increasing storage modulus is expected which is a measure for the elastic saved energy of the system. But as shown in table 4-13 the elastic modulus G' firstly increases but with the second homogenisation relapses.

The most prominent gain in elasticity occurs when going from no homogenisation to homogenisation in 15 min. A further extension of the final homogenisation time up to 25 min leads to a regression of both, elastic and viscous modulus. The phase shift δ (tanδ = G''/G') clearly decreases with increasing homogenisation time as the elastic modulus G' increases more strongly than the viscous modulus G''.

According G' = (t/γ)*cos δ (Rose, 1999) the elastic modulus depends on phase shift and deformation. The cosine of δ hardly changes with increasing homogenisation time (0.92-0.94-0.94). The firstly increasing and afterwards declining elastic modulus can be explained with changes of the deformation.

4.3.2.2   Verum

In the foregoing chapter the impact of the homogenisation shear on placebo was described. In the following the influence of the final homogenisation time on the API containing cream is discussed. Verum batches ## SHT056-P01/P02/P03/P05/P06/P07/P08 (40 kg) were homogenised at 25 ± 5 °C in circulation at the maximum speed (25.0 m/s) for 7.5 min, and 12.5 min respectively. A comparison with not homogenised verum could not be performed (as carried out for placebo) as final homogenisation was indispensable for dispersing homogeneously the API in the cream. Table 4-14 gives a summary of the test results.

Table 4-14:   Verum homogenised with respectively 8.1 or 13.5 circulation times (n=7)

Method	Unit	8.1 (= 7.5 min)	13.5 (= 12.5 min)
Bleeding	mm^2	935 ± 123	979 ± 132
Conductivity	µS/cm	31.7 ± 1.7	33.5 ± 1.7
Spreadability	mm^2	1531 ± 60	1666 ± 133
Micro-penetration	$mm*10^{-1}$	378 ± 35	373 ± 44
Viscosity	mPa*s	459.9 ± 26.1	449.9 ± 36.7
Hysteresis	$Pa/s*10^4$	1.46 ± 0.25	1.34 ± 0.21
Yield point	Pa	73.6 ± 21.1	65.1 ± 17.2
G'	Pa	9210 ± 1692	8384 ± 1566
G''	Pa	3400 ± 666	3074 ± 538
Phase shift	°	20.24 ± 0.57	20.18 ± 0.76
Enthalpy	J/g	58.25 ± 1.07	60.25 ± 2.67
T_{onset}	°C	62.32 ± 0.51	61.23 ± 1.67

From the summarised results in table 4-14 it becomes evident that the prolongation of the homogenisation time from 7.5 to 12.5 min does not have any effect on physical, thermo analytical or rheological properties of verum. On the basis of the very homogeneous results and low standard deviations of 7 investigated pilot scale batches, a high reproducibility of the manufacturing process was demonstrated.

4.3.2.3   *Summary and concluding results*

Through the foregoing investigation an impact of the duration of the final homogenisation on the microstructure of placebo was shown.

Water binding capacity of the hydrophilic/lipophilic gel lattice is markedly decreased and this in turn increases the amount of free bulk water. Homogenisation most likely induces an increased crystallisation of hydrophilic/lipophilic gel lattice. The more condensed matrix does not support water-binding, water gets squeezed out from it. This effect comes along with worse cream qualities. The longer the homogenisation time the more unstable the semisolid system becomes.

Final homogenisation leads to notable changes in the rheological behaviour of the cream, too. Creams not subjected to the final homogenisation are well structured and resistant to mechanical shear forces. The shear applied during final homogenisation leads to loss of viscosity and reduction of mechanical resistance to shear although enhanced elastic behaviour is observed during oscillatory measurements (refined mesh of micro structure). Reason for these changes of physical and rheological cream properties most likely is a re-organisation of hydrophilic and lipophilic gel lattice that are responsible for the flow properties and the water binding capacity.

It can be supposed that during final homogenisation the fraction of crystalline lipids is increased. This was shown by increased melting enthalpy and increased onset temperatures. These fatty phase crystals might contribute to the formation of an elastic network, the reason for the higher elasticity of homogenised creams. This gel lattice formed during homogenisation is finer and more sensitive to shearing. Its lower robustness leads to lower viscosity and reduced hysteresis. However, it can be easily destroyed by shear forces and does not support water binding.

Whereas a cold homogenisation affects directly physical, thermo analytical and rheological properties of placebo, a similar effect on verum by increasing the number of circulations was missing. Obviously, differences in the cream properties caused by different homogenisation shear get levelled by the strongly affecting amphiphilic API.

4.3.3   Cooling rate

The cooling rate is one of the most critical process parameters during cream preparation. The cooling process of creams should be performed moderately and stepwise or continuously and not excessively rapid in order to avoid a solidification of fatty phase components on the vessel walls which can lead to a less homogeneous product (Köhler, 1992). On the other hand, to slow cooling and insufficient stirring can favour the formation of large crystals of texture forming agents.

Aim of the current investigation on the cooling rate was to evaluate the effect of different cooling procedures on the physical, rheological, and thermoanalytical properties of placebo. Three different cooling profiles have been realized (table 4-15). Cooling rates of 1.0 and 0.5 °C/min have been chosen based on the abilities of the available cooling system and close to practice. Both represent an almost linear cooling process. 0.85 °C/min represents the average cooling profile (from 6 industrial scale batches) as depicted in table 4-16.

Table 4-15:   Actual cooling profiles of placebo pilot scale batches; 80 kg, n=2

Step [°C]	Cooling rate [°C/min]		
Batches ##	P02/P03	P07/P08	P09/P10
70 to 60	1,23 ± 0,05	0,49 ± 0,01	1,50 ± 0,24
60 to 45	0,82 ± 0,00	0,46 ± 0,06	0,80 ± 0,03
45 to 40	1,10 ± 0,14	0,75 ± 0,35	0,43 ± 0,10
40 to 28	1,05 ± 0,18	0,43 ± 0,01	0,41 ± 0,06
Mean: 70 to 28	**1,05 ± 0,17**	**0,53 ± 0,15**	**0,79 ± 0,51**

Table 4-16: Average cooling profile from 6 industrial scale batches; n=6

Cooling step [°C]	Cooling rate [°C/min]
70 to 60	1,7 ± 0,3
60 to 45	0,9 ± 0,2
45 to 40	0,4 ± 0,1
40 to 28	0,4 ± 0,2
Mean: 70 to 28	**0,85 ± 0,61**

4.3.3.1 Influence of different cooling rates on the cream properties

Independent from the cooling profile all creams appear smooth and homogeneous. They represent fine emulsions with globules of the internal phase = 5 µm (fig. 4-25).

a)   b)   c)
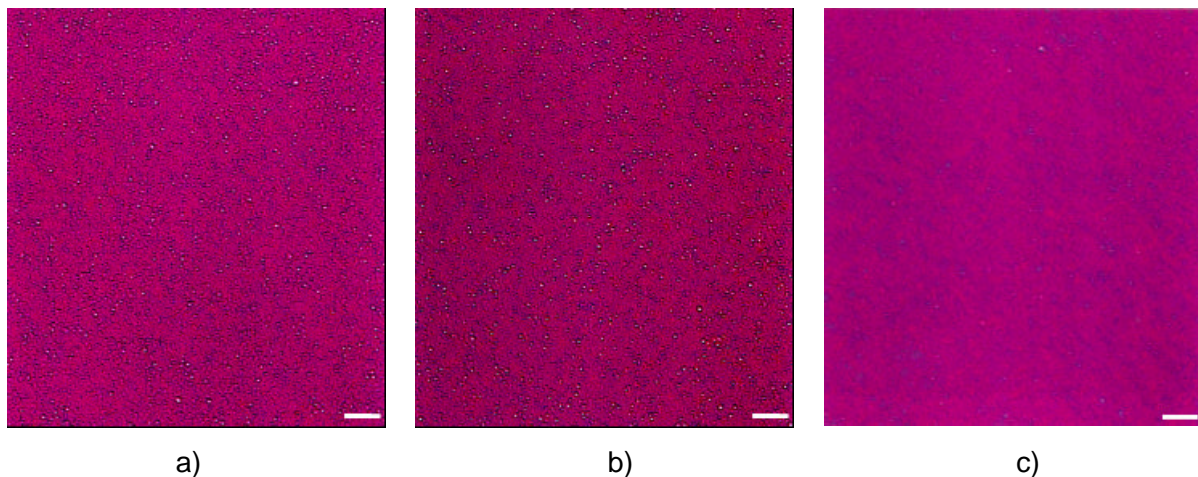
Figure 4-25: Placebo with different cooling rates, 200 times magnified, bar 32 µm
a)   1.0 °C/min, linear
b)   0.5 °C/min, linear
c)   0.85 °C/min, non-linear

4.3.3.1.1 Consistency

Slowly cooled creams (0.5 °C/min) arise more consistent as determined just by visual inspection. This was confirmed by minor spreadability and micro-penetration values (fig. 4-26a and b). Spreadability and micro-penetration are a direct measure of the cream's consistency. Aligned with higher cream consistencies are higher shear viscosities depicted in figure 4-26c.

a)

b)

c)
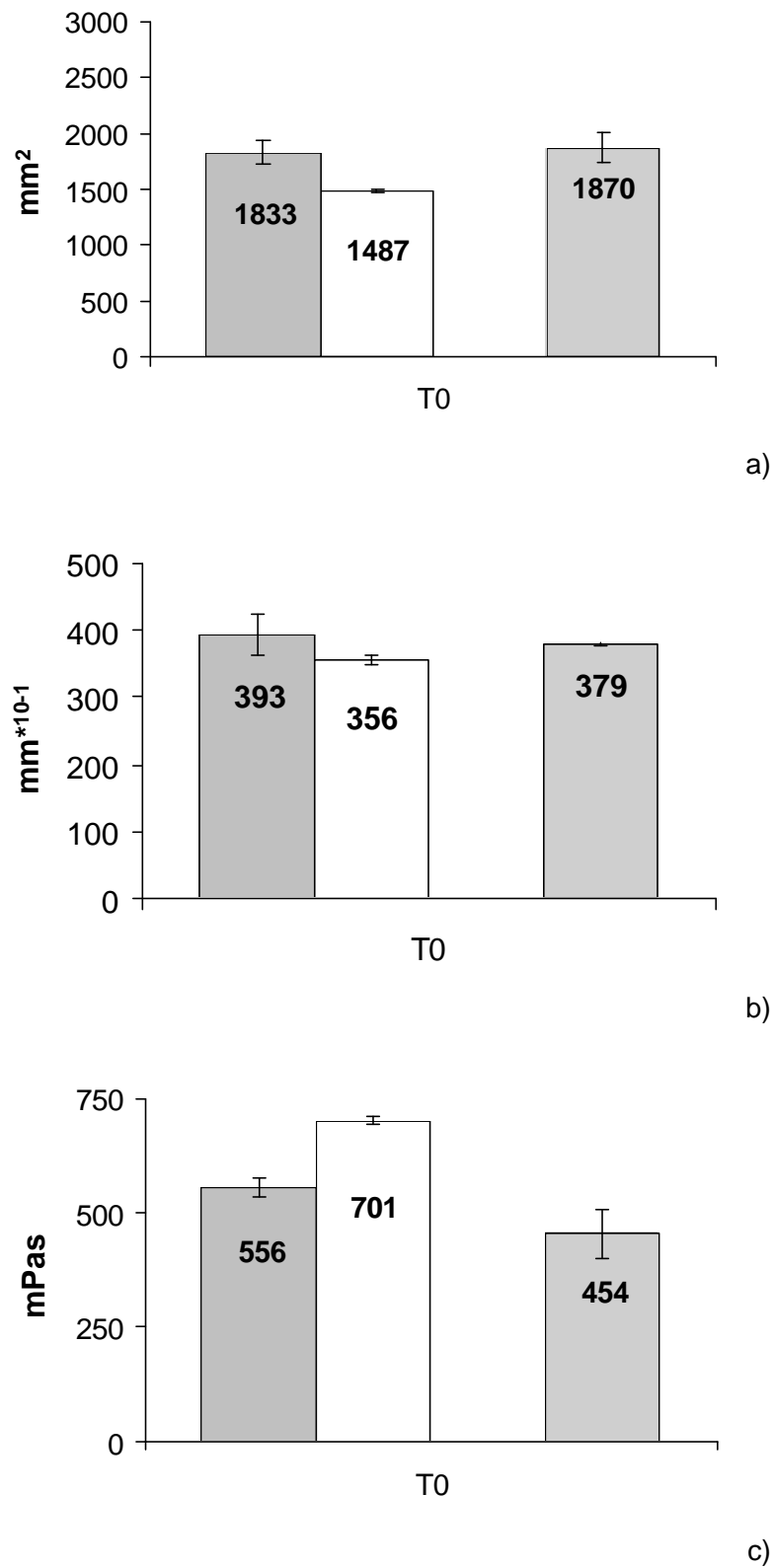
Figure 4-26:   spreadability (a), micro-penetration (b), and viscosity at 400 s^{-1} (c)

grey: 1.0 °C/min, linear
white: 0.5 °C/min, linear
striped: 0.85 °C/min, non-linear

From the foregoing results on spreadability and micropenetration it could be expected that consistencies of creams with the mean cooling rate of 0.85 °C/min range in between those profiles with the cooling rates of 1.0 °C/min and 0.5 °C/min. Actually they are more similar to the creams which are cooled faster. Shear viscosities are even lower than those of fast cooled creams.

4.3.3.1.2   Water binding capacity

For an evaluation of the water binding capacity primarily bleeding and electrical conductivity were consulted (fig. 4-27a and b).

a)

b)
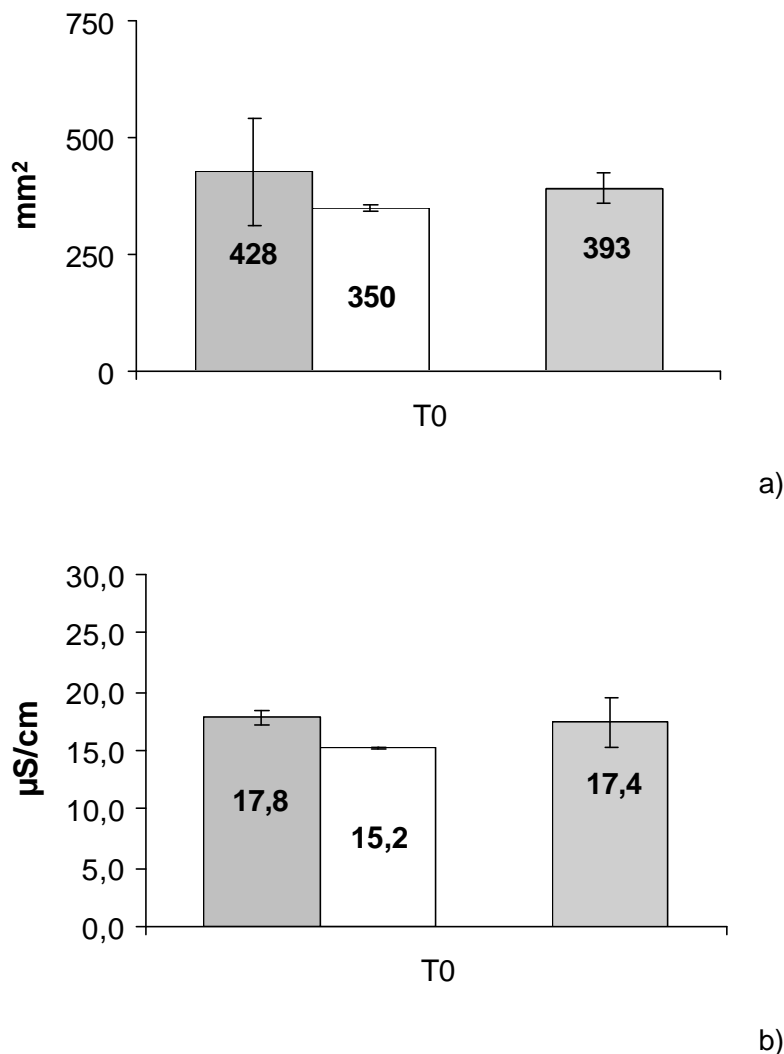
Figure 4-27:   bleeding (a), and electrical conductivity (b)

grey: 1.0 °C/min, linear
white: 0.5 °C/min, linear
striped: 0.85 °C/min, non-linear

Slower cooled creams show both less bleeding and lower electrical conductivity. Obviously slower cooling enhances water binding within the microstructure. Lower electrical conductivity confirms the smaller portion of free water. The water binding capacity of creams with non-linear cooling rate ranges in between slow and fast cooling.

Thermogravimetry was not capable to differentiate between different cooling rates as extractable from table 4-17. Independent from the cooling rate, individual free water loss varies between 7.4 and 14.1 % referring to total sample weight. This evidences the high variability of the method.

Table 4-17: :   free bulk water [%] from total sample weight; means ± sd [%]

1.0 °C/min		0.5 °C/min		0.85 °C/min*	
P02	P03	P07	P08	P09	P10
9,1	10,8	7,7	10,6	7,4	10,9
11,8	9,6	14,1	10,0	7,4	12,1
10,2	10,0	10,3	8,0	-	-
n=6		n=6		n=4	
10,3 ± 1,2		10,6 ± 2,6		9,5 ± 2,4	

*   production like, non-linear CR

4.3.3.1.3   Melting behaviour

Figure 4-28 shows melting curves of creams with different cooling rates. The curve shape of all creams is characterised by a single symmetric peak. The profound peak of the fast cooled cream (curve at the top) with the highest melting enthalpy flattens when the cream is cooled by 0.5 °C/min (curve in the middle). Non-linear cooling by 0.85 °C/min (curve at the bottom) leads to the least profound peak with the lowest melting enthalpy.
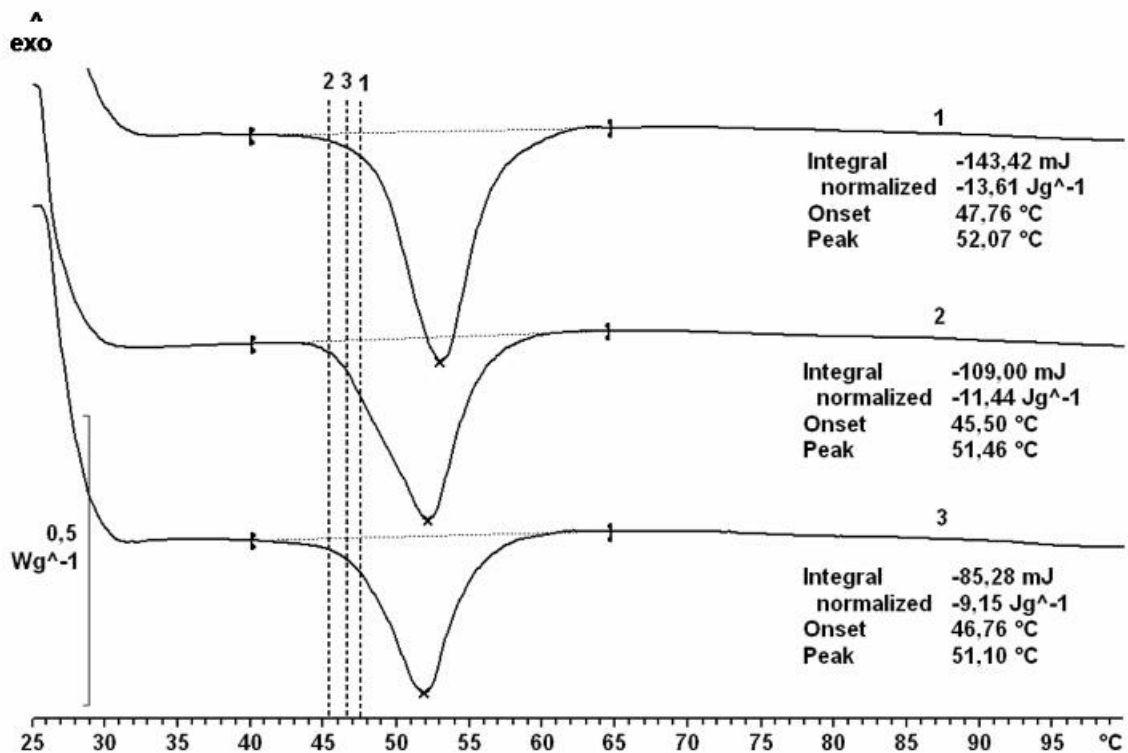
Figure 4-28:   DSC curves of creams with different cooling rates

at the top (1):   1.0 °C/min, linear
in the middle (2):   0.5 °C/min, linear
at the bottom (3):   0.85 °C/min, non-linear

DSC revealed a diminution of melting energy by slower cooling (fig. 4-29a). Melting enthalpy is the energy necessary to melt the crystalline gel framework. Consequently lower melting energy is associated with less solid cream properties. The lowest melting enthalpy was detected for non-linear cooled creams.

a)

b)
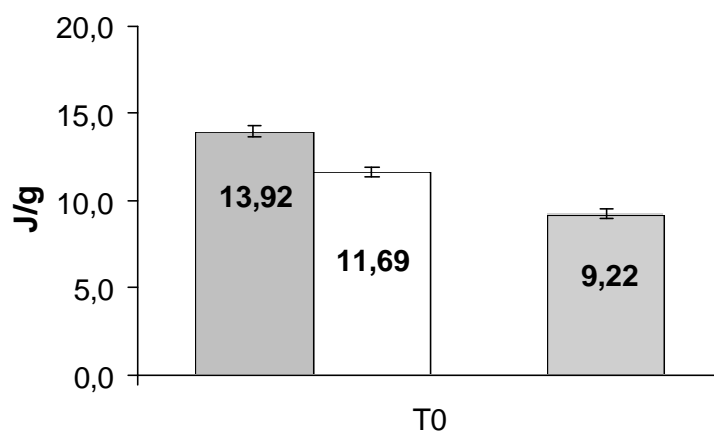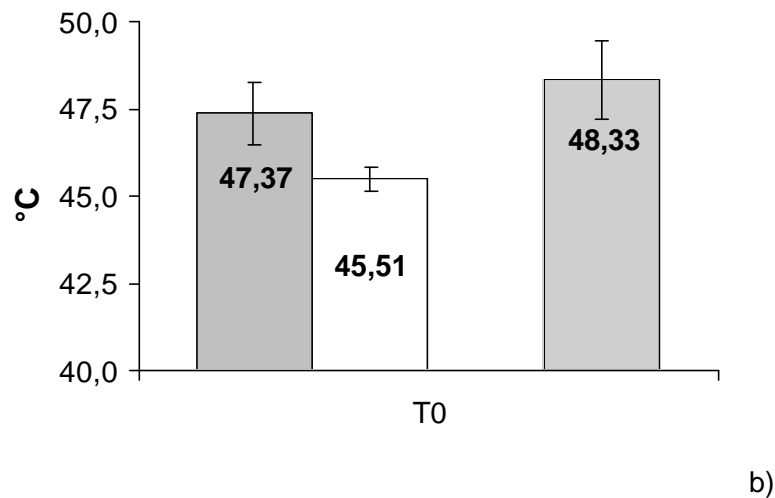
Figure 4-29:   melting enthalpy (a), and onset temperature (b)
                    integration range: 40-65 °C
                         grey: 1.0 °C/min, linear
                         white: 0.5 °C/min, linear
                         striped: 0.85 °C/min, non-linear

Indicator of the beginning phase transition is the onset temperature. Onset temperatures of creams with cooling profiles 1.0 and 0.5 °C/min are aligned with the respective melting enthalpies (fig. 4-29b). Creams with non-linear cooling which show the lowest melting enthalpies unexpectedly show high onset temperatures.

4.3.3.1.4   Rheological properties

Figure 4-30 exemplarily shows a shear stress curve for each cooling rate. Curve progressions of the shear stress τ with increasing shear rate (upwards curves) differ clearly from each other. The recover is in delay for all formulations due to their plastic thixotropic flow behaviour. At the same shear rate the cream cooled by 0.5 °C/min shows noticeable higher shear stress compared to the creams cooled by 1.0 and 0.85 °C/min. Further the progression of the upwards curve is much steeper. The shear stress plateau of the non-linear cooled cream is reached at 200 Pa while the maximum shear stress of the slower cooled cream is reached only above 300 Pa. This indicates the decrease of the structural viscosity of creams cooled non-linearly. Whereas curve progressions of 0.5 and 0.85 °C/min slightly regress above shear rates of 180 1/s, the shear stress of the cream cooled by 1.0 °C/min always rises. Slower cooled creams show higher hystereses. It points to a more pronounced rheodestruction.
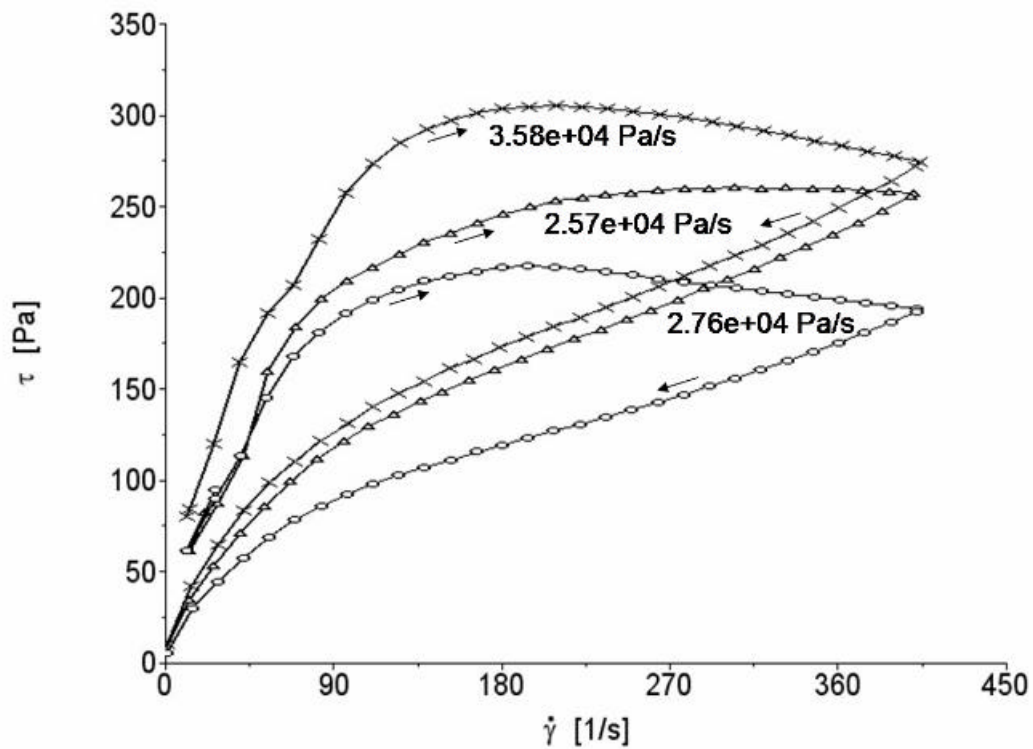
Figure 4-30:   Flow curves of placebo pilot scale with different cooling rates
-×-   0.5 °C/min, linear (# SHT292-P07)
-△-   1.0 °C/min, linear (# SHT292-P03)
-○-   0.85 °C/min, non-linear (# SHT292-P09)

Independent from the initial available framework, the structure breaks down during the shear loop resulting in almost identical downward curves when the cooling rate was linear. The downward curves of the cream cooled non-linearly shows much lower shear stresses with a much flatter upward curve. This indicates a rather low resistance to shear. The hysteresis is comparable with the hysteresis of the cream cooled by 1.0 °C/min.

The average phase shift of the creams with different cooling rates increases in the order 1.0 – 0.5 – 0.85 °C/min (table 4-18). The creams seem to loose in elasticity. However, considering the standard deviations the difference between the phase shifts is not significant.

Table 4-18: :   Phase shift δ [°]

Cooling rate [°C/min]	Phase shift δ [°]
1.0	23.0 ± 1.2
0.5	24.0 ± 0.3
0.85*	24.4 ± 0.7

*   production like, not homogeneous CR

The more structured network of slower cooled creams leads to higher storage modulus and higher loss modulus (fig. 4-31).
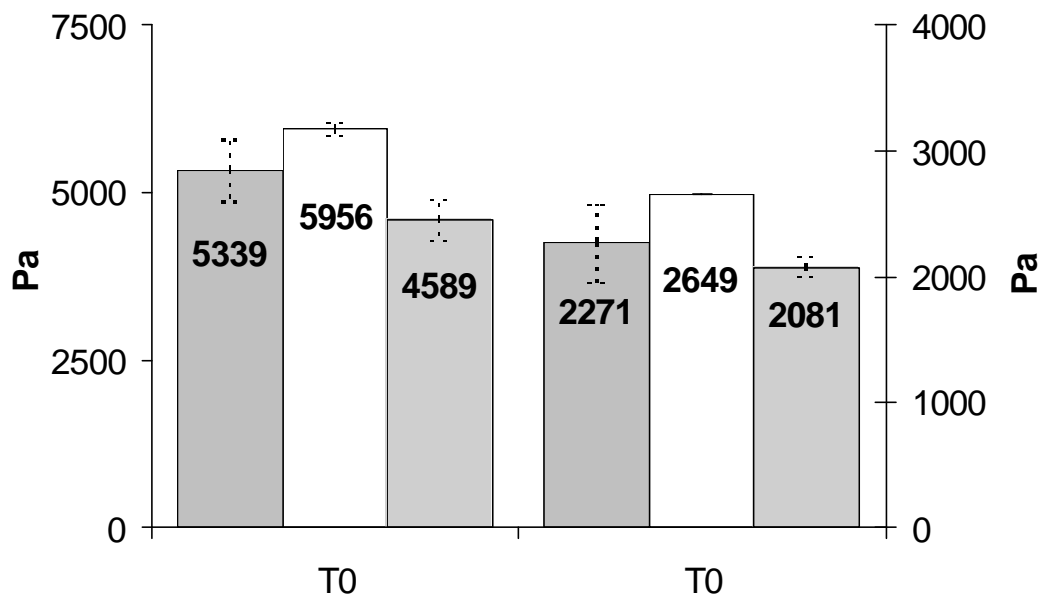
Figure 4-31:   Storage modulus (left scale); Loss modulus (right scale)
grey: 1.0 °C/min, linear
white: 0.5 °C/min, linear
striped: 0.85 °C/min, non-linear

Even though the batches of raw materials used for manufacturing of the creams cooled non-linearly were not completely identical with those utilized for manufacturing of the other creams, the differences in the cream properties seem to be exclusively related to the cooling profiles but not to the raw material batches (chapter 4.4.5).

4.3.3.2   Cooling rate in combination with a final homogenisation

In the foregoing chapter, a certain dependency of cream consistency from cooling rate could be shown. Slowly and homogeneously cooled creams are more consistent and show higher viscosity than fast cooled creams.

In the following, the combined influence of cooling rate (0.5 and 1.0 °C/min) and terminal homogenisation are assessed.

4.3.3.2.1   Consistency

Figure 4-32 shows spreadability and micro-penetration of creams with the cooling rates 0.5 and 1.0 °C/min after 0, 15 and 25 min homogenisation time.
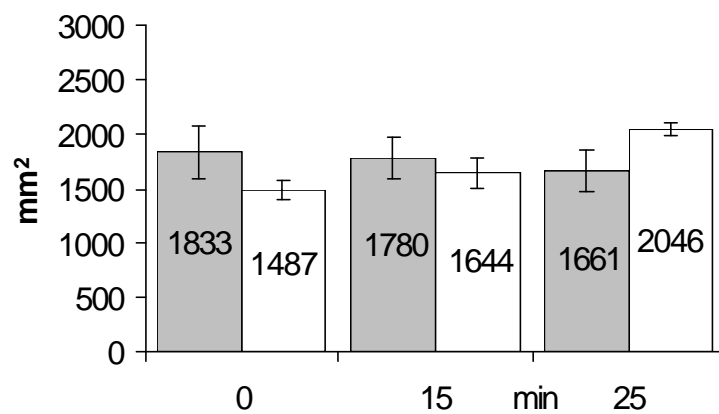
a)
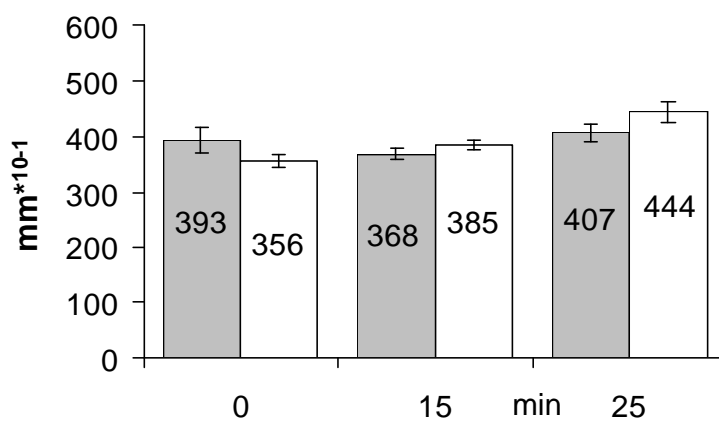
b)

Figure 4-32:   spreadability (a), micro-penetration (b)
                  grey: 1.0 °C/min, linear
                  white: 0.5 °C/min, linear

Homogenisation reverses the effect of slow cooling. The longer the final homogenisation the more fluid the creams prepared at 0.5 °C/min CR become. This can be seen from increasing spreadability and micropenetration values. Creams cooled by 1.0 °C/min do not react to sensitivity to a homogenisation. The consistency remains almost unchanged.

4.3.3.2.2   *Water binding capacity*

Homogenisation in general enhances the separation of a watery fluid from the system. This can be clearly seen from figure 4-33a and b. Bleeding and electrical conductivity increase with increasing duration of homogenisation. This phenomenon was already observed and assessed in chapter 4.4.2 on placebo with the cooling profile of 1.0 °C/min. The longer the final homogenisation the higher the water separation becomes. This is again more pronounced when creams are prepared with moderate cooling. Moderate cooled creams show a better water binding capacity only without a terminal homogenisation step. After the first homogenisation (15 min) bleeding and electrical conductivity become almost the same. And after 25 min of homogenisation the result is the reverse.

Free water loss seems to increase slightly with increasing homogenisation time. However, there is no significant difference between these values due to the high variation of the method (table 4-19).

Table 4-19:   Free water loss [%] from total sample weight, mean and sd (n=2)

Duration of homogenisation [min]	1.0 °C/min	0.5 °C/min
0	10.26 ± 0.97	10.11 ± 2.28
15	11.07 ± 1.28	9.98 ± 0.91
25	12.04 ± 1.39	11.13 ± 0.91
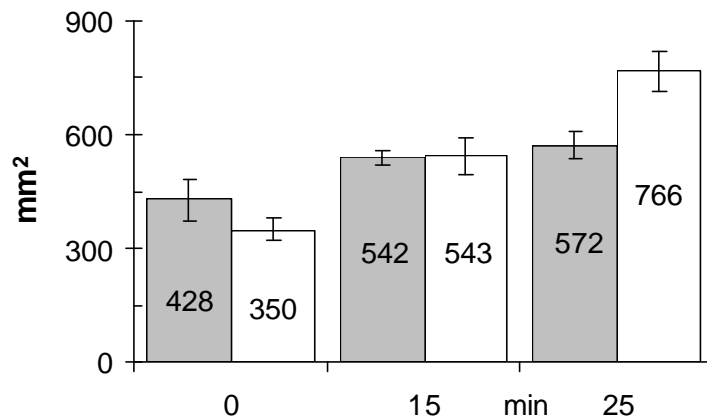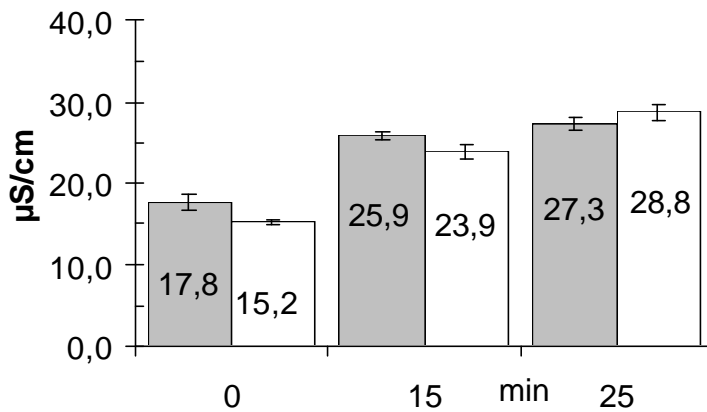
Figure 4-33: bleeding (a), conductivity (b)

grey: 1.0 °C/min, linear
white: 0.5 °C/min, linear

4.3.3.2.3   Melting behaviour

Slower cooling leads to the diminution of melting enthalpy and the shift to the lower onset temperatures (chapter 4.4.3.1). This was explained with a minor solid character and thus better cream qualities. This effect persists despite homogenisation (fig. 4-34).

An influence of the final homogenisation step on the melting behaviour of the formulation was already shown in chapter 4.4.2.1.3. The clearly noticeable effect of different cooling profiles on creams without homogenisation is not more significant between the same creams after a homogenisation time of 25 min.
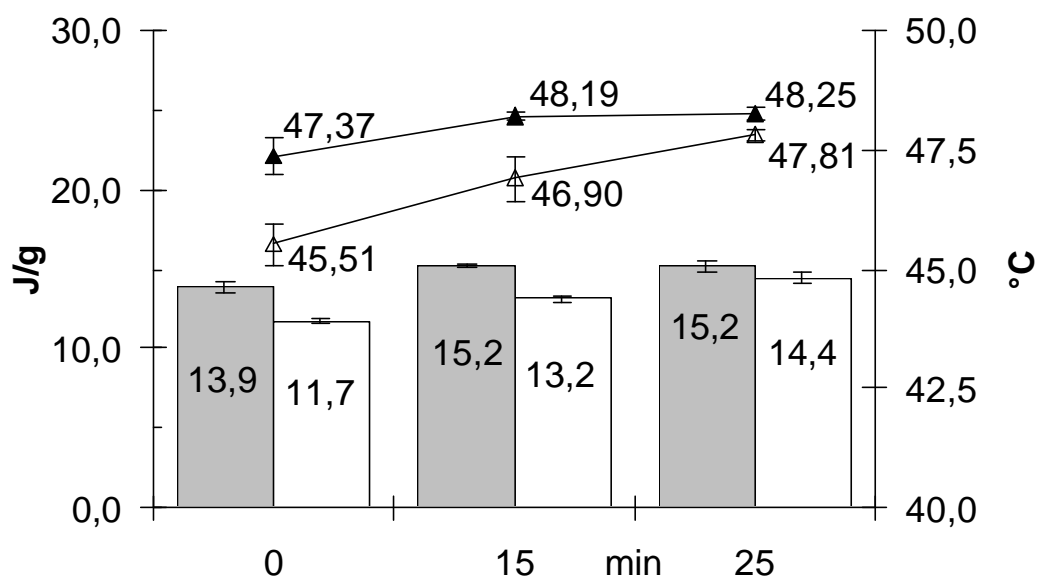
Figure 4-34:   melting enthalpy [J/g] (columns), onset temperature [°C] (lines)
                    grey/ -▲-:   1.0 °C/min, linear
                    white/-△-:   0.5 °C/min, linear

4.3.3.2.4   Rheological properties

Without final homogenisation slower cooling leads to more viscous and more structured creams. The higher hysteresis, measure for a better structured cream, results from the higher resistance to shear force during the upward flow curve. From figure 4-35 the continuous diminution of both shear viscosity a) and hysteresis b) by increasing shearing (number of circulations: 0-8-13) becomes evident. Higher viscous and more resistant creams with 0.5 °C/min CR become more and more similar to creams with a CR of 1.0 °C/min. A well visible effect from the cooling rate on the not homogenised cream base is damped after 15 min of homogenisation and even levelled after 25 min of homogenisation.

The levelling of flow behaviour and the hysteresis in particular is depicted in figure 4-36. A different progressing shear stress during upward curves between creams with different CR is visible only when the creams were not homogenised. The high reply of the shear stress τ of the moderate cooled cream indicates a robust structure resistant to shear force. Shear stress curves of creams homogenised for 25 min show a congruent progression independent from the cooling rate.
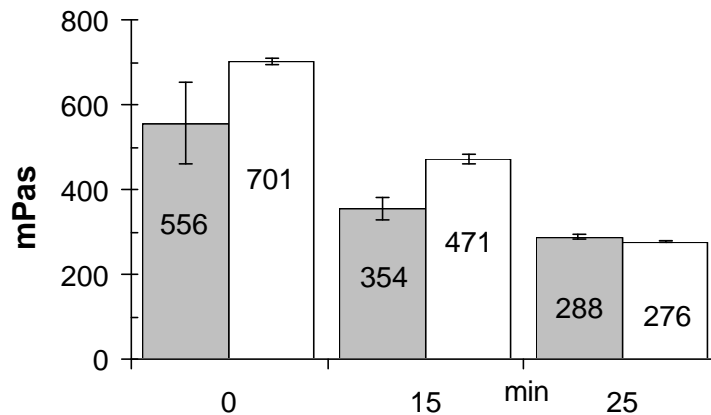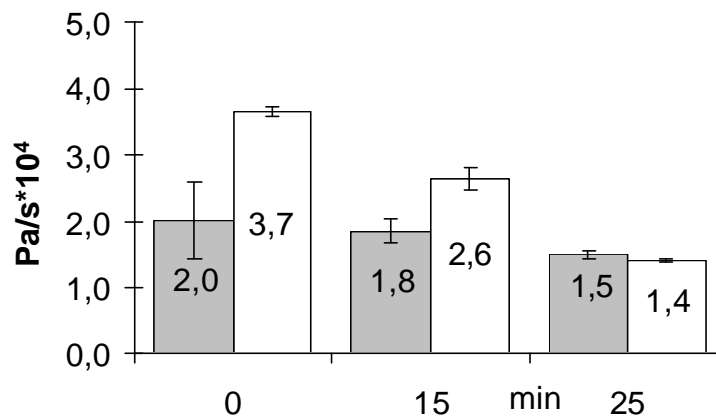
Figure 4-35:   shear viscosity (a), hysteresis (b)
grey: 1.0 °C/ min, linear
white: 0.5 °C/min, linear

Oscillatory measurements are an indicator for revealing changes in the visco-elastic behaviour of a cream. As evaluated in chapter 4.4.2.1.4, homogenisation leads to predominantly elastic creams. The phase shift declines because the ratio of G'' and G' is shifted in favour of G' (fig. 4-37). The phase shift as ratio between elastic and viscous parts in the cream do not differ significantly between creams with different cooling profiles and is almost identical after 25 min of homogenisation.
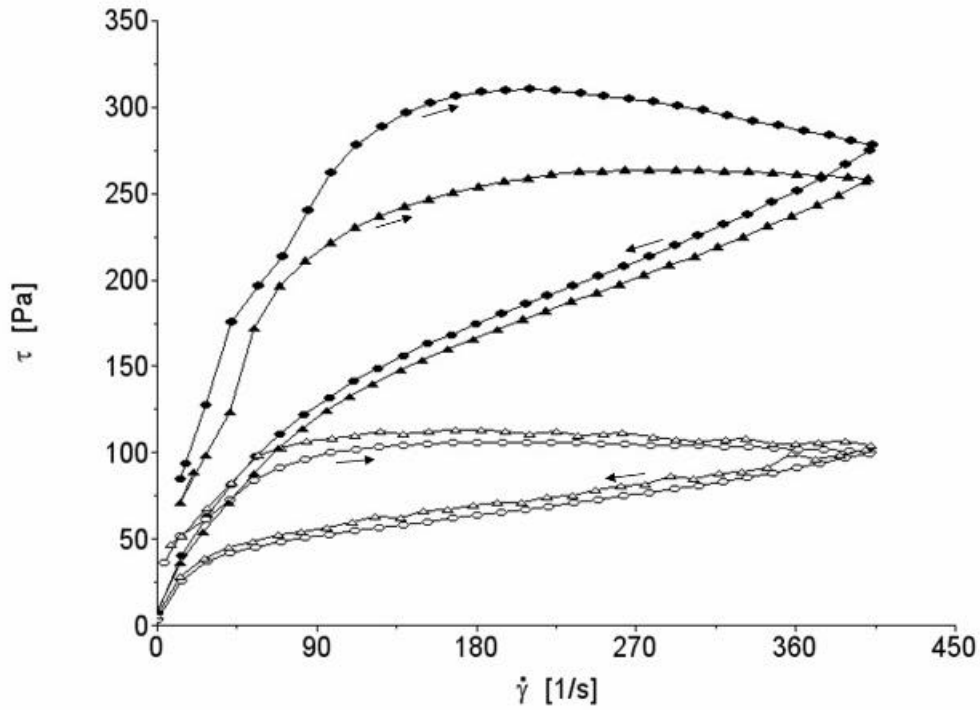
Figure 4-36:   Flow curves of placebo pilot scale with different cooling rates and after
                    different duration of homogenisation

1.0 °C/min (# SHT292-P03)   0.5 °C/min (# SHT292-P07)
-▲-   0 min   -●-   0 min
-△-   25 min   -○-   25 min
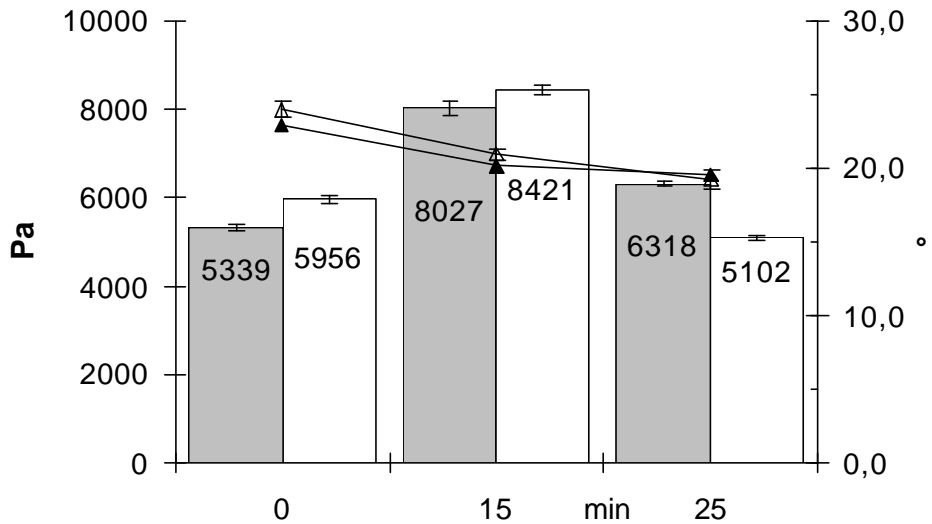
Figure 4-37:   storage modulus [Pa] (columns), phase shift [°] (lines)
                    grey/ -▲-:   1.0 °C/min, linear
                    white/-△- :   0.5 °C/min, linear

4.3.3.3   *Summary and concluding discussion*

A slow and homogeneous cooling process alters consistency and water separation of the cream. With a moderate cooling profile the resulting creams are more consistent and display higher viscosities. Results obtained from spreadability and micro-penetration are in alignment with the rheological findings. Slowly cooled creams are very resistant to shear forces at low shear rates. This was demonstrated with a much steeper curve progression of the shear stress τ by increasing shear rate. Oscillatory modules indicated differences between different cooling rates.

Cooling rate arose to be a critical parameter regarding cream quality. It seems to be likely that homogeneous and moderate cooling improve the cream qualities. Moderate cooling increases consistency and viscosity, leads to a structure which is resistant to shear force and which shows reduced water separation. Moreover, data on creams with a non-linear cooling profile as usually applied during bulk production do not fit in this scheme.

It could be evidenced that a slow and linear cooling rate forms a more defined microstructure with improved galenical cream properties. Higher melting enthalpies of faster cooled creams are a hint for crystalline structures. Lower melting enthalpies of slower (0.5 °C/min) and non-linear cooled creams on the other hand can be explained with a minor tendency to re-crystallisation of fatty phase components. The lowest melting enthalpy was determined for the non-linear cooled creams. Slow cooling between 45 °C and 28 °C (~0.4 °C/min for non-linear cooled creams compared to ~1.1 °C/min for fast cooled creams compared to ~0.6 °C/min for slow cooled creams) seems to be determinant for the formation of fatty alcohol crystals. However, this is only evident if the creams are not terminally homogenised. Fatty alcohol crystals are diminished due to the mechanical stress during final homogenisation. Furthermore it can be assumed that due to the shear force of the homogeniser the cream temperature in the homogeniser rises considerably (at least 10 °C above the temperature in the mixer). This leads to a partly melting of fatty phase fractions in the cream. These molten fatty phase fractions re-crystallise when the cream reaches the mixer with the cooler cream. This melting and re-crystallisation process probably levels thermo analytical properties (melting enthalpy, onset temperature) of the creams.

Thus, a careful control of the CR seems not to be necessary. Also the non-linear cooling process during production can be judged to be fully acceptable.

The impact of crystalline fractions formed after homogenisation on bleeding, conductivity and rheological properties of the creams has already been discussed in chapter 4.3.2.

4.3.4   Temperature during API-addition and final homogenisation

The temperature limit for API-addition and final homogenisation in commercial production is set to 28 ± 2 °C. In order to study the influence of this process step, cream batches were prepared where temperatures during API-addition and final homogenisation have been varied. Temperatures above 40 °C have not been considered because of the well-known crystal growth of the micronized API. The impact of these processing conditions was evaluated on samples of 4 groups of batches (table 4-20). A total of 12 batches was manufactured on pilot scale with a batch size of 40 kg. Each batch was sampled before final homogenisation (placebo) and respectively after 8.1 (= 7.5 min) and 13.5 (= 12.5 min) times of circulation (= duration of homogenisation).

Table 4-20:   Verum bulk batches (pilot scale): temperatures during API-addition and during final homogenisation, content of AzA (% w/w)

SHT056-	n	$T_{API-addition}$ [°C]	$T_{homogenisation}$ [°C]	Content of AzA [% w/w]
P03;P06;P08;P10	4	20	20	20.1 ± 0.3
P02;P05;P07;P09	4	30	30	19.9 ± 0.5
P12;P13	2	40	40	20.0 ± 0.2
P14;P15	2	40	30	20.0 ± 0.9
			Mean ± sd [%]	**20.1 ± 0.5**

4.3.4.1   Manufacturing procedure

The primary emulsion (chapter 2.2.4.3) was cooled down to the predetermined temperature (table 4-20). Half of the placebo was discharged. The micronized API was added by aspiration to the remainder in the mixer (~32 kg). Through this manufacturing procedure verum batches were produced with reproducible content of azelaic acid (table 4-20). The average content of all produced batches was 20.1 ± 0.5 %.

After the API-addition, residues of the powdered API were removed carefully and manually and were added to the cream. During this procedure the cream temperature was always kept at the predetermined temperature. After a short mixing and deaeration time, the cream was homogenised the 1st time. During this 1st homogenisation the total batch (40 kg) circulated 8.1 times through the homogeniser corresponding to 7.5 min of homogenisation. After 10 min

of stirring the cream was homogenised again. During this 2nd homogenisation the total batch (40 kg) circulated further 5.4 times ($\equiv$ 5 min) through the homogeniser.

Thus, the total number of circulations was 13.5 and corresponds to the duration of the homogenisation of 12.5 min. After 10 min of stirring and deaeration the verum was unloaded through the pumping homogeniser. The manufactured creams were discharged at the respective homogenisation temperatures. Samples were withdrawn while directly unloaded from the circulation tube in the appropriate containers (0.5 kg). Without further treatment samples were analysed after a holding time of 10 days at 25 °C/60 % RH.

Whereas batches # P12 and # P13 were kept at 40 °C during API-addition and final homogenisation, batches # P14 and # P15 were cooled to 30 °C after the API was added to the placebo at 40 °C. In this way a differentiation of the temperature effect during API-addition and final homogenisation was possible.

Table 4-21 summarises the actual average temperatures during API-addition, 1st, and 2nd final homogenisation respectively. Generally temperature rises slightly during homogenisation due to the enormous energy input of the homogeniser. Therefore the mixer jacket was cooled during homogenisation in order to meet the predetermined temperatures. This temperature shift can be considered as non-critical and occurs for all batches uniformly.

Table 4-21: Actual temperatures during API-addition and homogenisation (means ± sd) n: number of batches

T_{target} [°C]	n	$T_{API-addition}$ [°C]	$T_{1° \, homogenisation}$ [°C]	$T_{2° \, homogenisation}$ [°C]
20/20/20	4	19.8 ± 0.5	24.0 ± 1.4	22.3 ± 1.0
30/30/30	4	30.4 ± 0.6	31.8 ± 1.3	31.4 ± 1.1
40/40/40	2	41.0 ± 0.0	42.0 ± 0.0	42.0 ± 2.8
40/30/30	2	40.5 ± 0.7	31.5 ± 0.7	30.0 ± 0.0

4.3.4.2   Verum after the 1st final homogenisation

4.3.4.2.1   Macroscopic and microscopic appearance

The manufactured verum creams are white and shiny. API-crystals show dimensions between 5 and 20 µm (fig. 4-38 a-d). Creams homogenised at 20 °C and 30 °C respectively are homogeneous whereas creams homogenised at 40 °C represent a lot of small or large lumps. In addition they appear more consistent than the others.
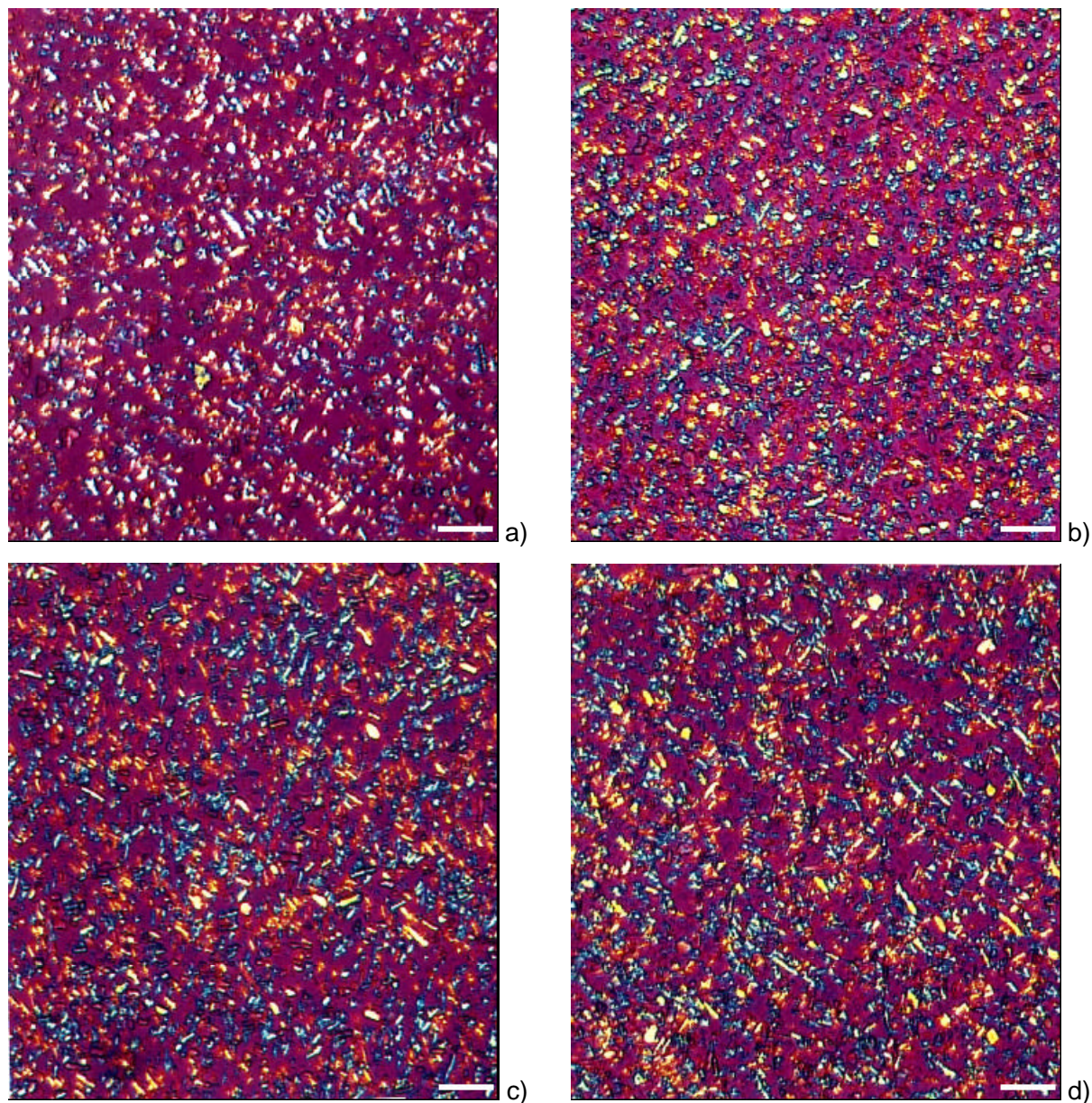
Figure 4-38:   Microscopic pictures of verum, 200x, bar 32 µm
                          Temperatures during API-addition/final homogenisation:
                          a)   20/20 °C
                          b)   30/30 °C
                          c)   40/40 °C
                          d)   40/30 °C

4.3.4.2.2 Consistency

Figure 4-39 depicts spreadability and micro-penetration data of the creams. It becomes evident that shifting the temperature from 20 to 30 °C does not affect the cream's consistency. But it also becomes evident that an increase of the temperature during API-addition or final homogenisation up to 40 °C clearly abases both, spreadability and micro-penetration of the creams. A different image arises when the API was added at 40 °C but the homogenisation of the API was performed after cooling to 30 °C. Both, spreadability and micro-penetration increase, corresponding to lower consistencies in comparison to creams prepared at 20/20, 30/30, and 40/40 °C respectively.
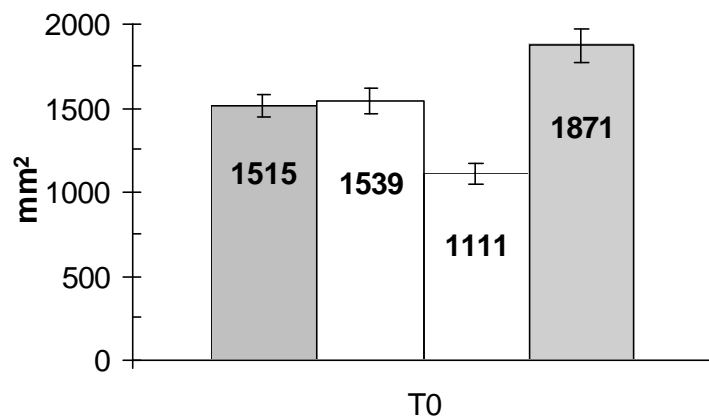
a)
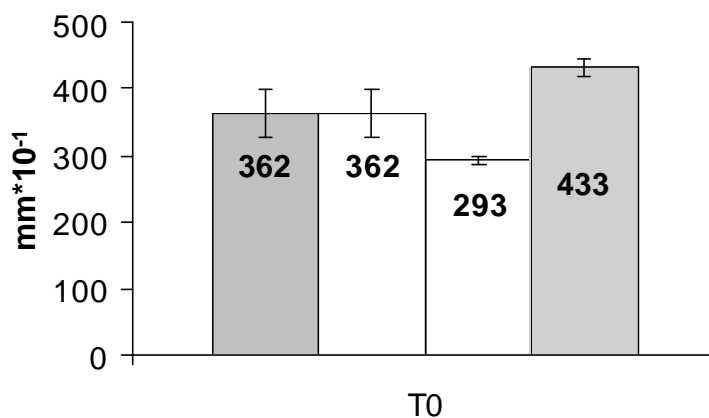
b)

Figure 4-39:   spreadability (a), micro-penetration (b)

filled:	20/20 °C
empty:	30/30 °C
shaded:	40/40 °C
striped:	40/30 °C

4.3.4.2.3   Water binding capacity

Homogenising the final cream at 40 °C seems to improve the water binding capacity. This is easily seen on the low bleeding and electrical conductivity values at t_0 (t_0 corresponds to a holding time of 10 days). Creams with the API-addition/final homogenisation temperatures 20/20, 30/30, and 40/30 °C respectively show similar bleeding and electrical conductivity values right from the beginning (fig. 4-40).
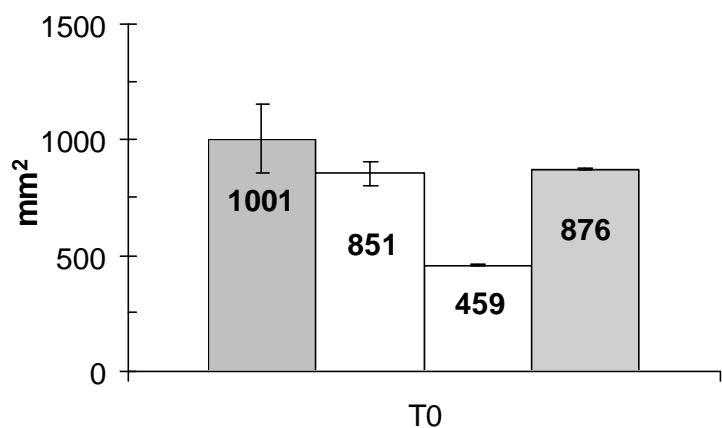
a)
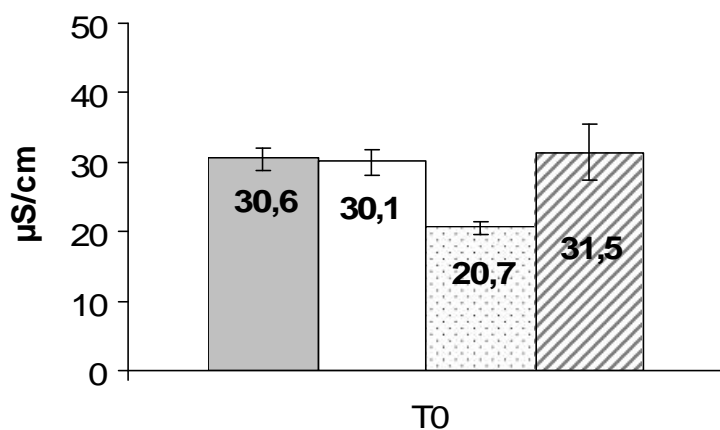
b)

Figure 4-40:   bleeding (a), electrical conductivity (b)

filled:	20/20 °C
empty:	30/30 °C
shaded:	40/40 °C
striped:	40/30 °C

4.3.4.2.4   Melting behaviour

DSC curve 1 in figure 4-41 shows exemplarily the melting profile of creams homogenised at 20 or 30 °C. The melting peak of the fatty phase forms a plateau indicating a broad melting range. The 2nd peak is much more distinctive. It shows the melting point of the API. In curve 2, representative for creams homogenised at 40 °C, the tendency of the 1st peak to form two shoulders is clearly visible. The melting peak of the API is broader and less profound compared to curve 1.
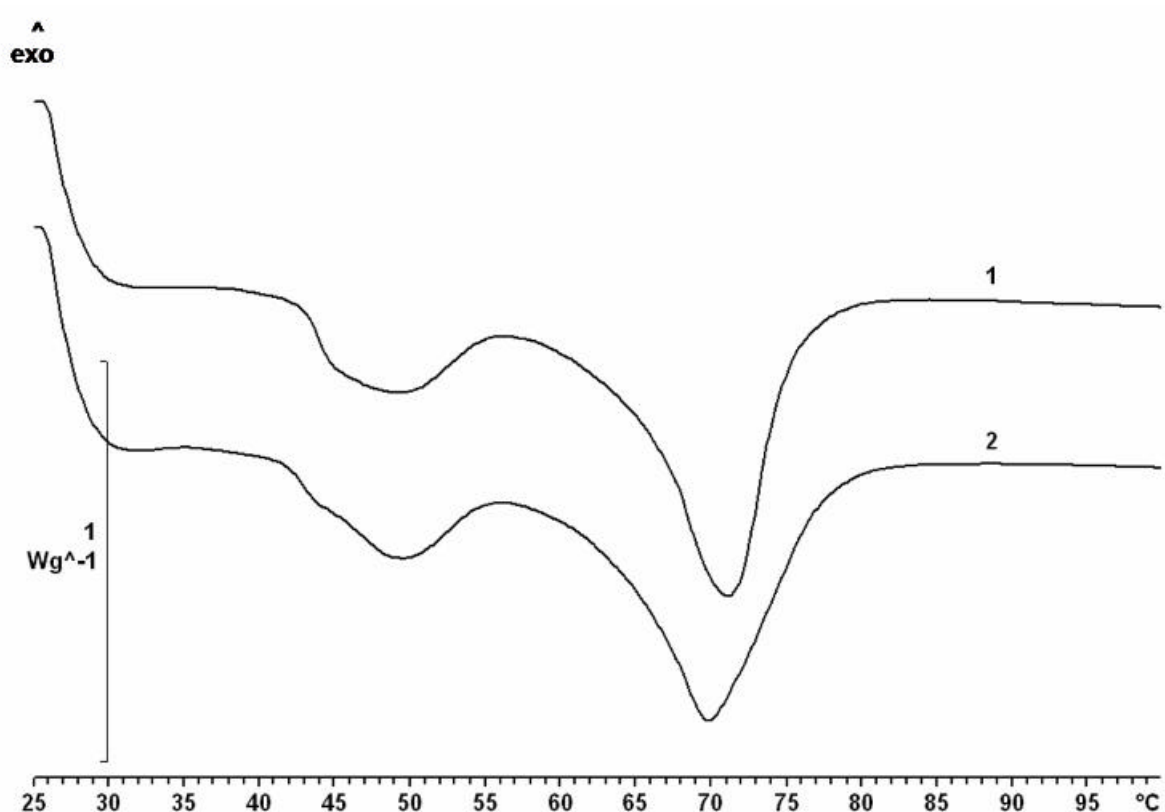
Figure 4-41:   DSC curves of verum with different homogenisation temperatures
                1:        curve example for verum homogenised at 20 °C or 30 °C
                2:        curve example for verum homogenised at 40 °C

Table 4-22 shows that melting enthalpies and onset temperatures of creams with different processing temperatures vary less than 2 °C one from another. In addition, the peaks are not completely separated from each other (fig. 441). Thus there is no significant difference within the melting behaviour between creams with various processing temperatures.

Table 4-22:   Melting enthalpies [J/g] and onset temperatures [°C], means ± sd

T_{target} [°C]	Melting enthalpy [J/g]	Onset temperature [°C]
20/20	57.86 ± 0.42	62.32 ± 0.32
30/30	58.60 ± 0.99	62.04 ± 0.83
40/40	59.62 ± 1.26	60.99 ± 0.54
40/30	59.88 ± 0.47	63.20 ± 0.29

4.3.4.2.5   Rheological properties

Flow curves exemplarily for each API-addition/ final homogenisation temperature at t_0 are depicted in figure 4-42.
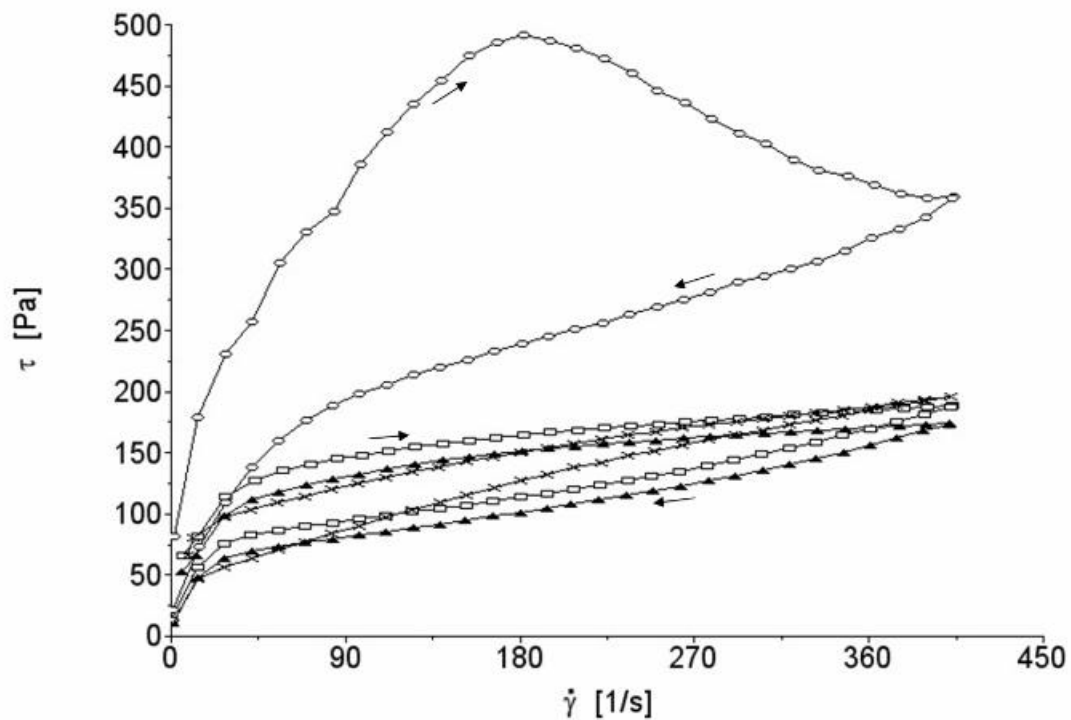
Figure 4-42:   Flow curves of verum (pilot scale) at t_0 with different temperatures during API-addition/ final homogenisation

-□-   20/20 °C (# SHT056-P08)
-▲-   30/30 °C (# SHT056-P02)
-○-   40/40 °C (# SHT056-P12)
-×-   40/30 °C (# SHT056-P14)

Flow curves of 20/20, 30/30 and 40/30 °C creams are very similar to each other. They show a continuous increase of the shear stress by increasing shear rate up to a shear stress of about 175 Pa (at the apex). Further, the even curve shapes indicate stable systems.

The shear stress of the 40/40 °C cream rises very steeply but unevenly up to approx. 500 Pa. At shear rates above 180 1/s the shear stress drops to 350 Pa (at the apex at 400 1/s).

From the different flow behaviour different hystereses and shear viscosities result (fig. 4-43a and b).
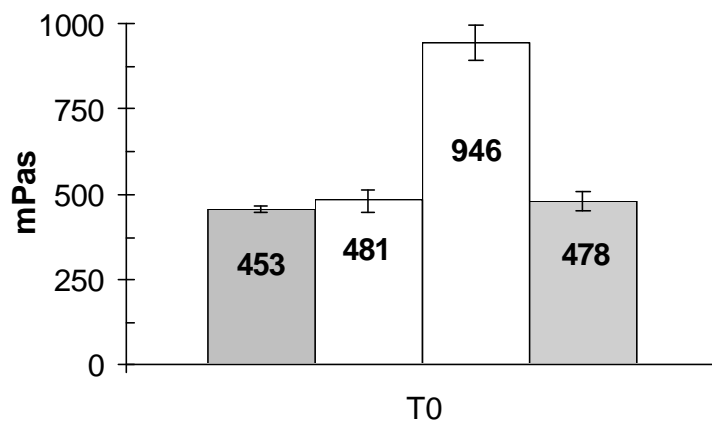
a)
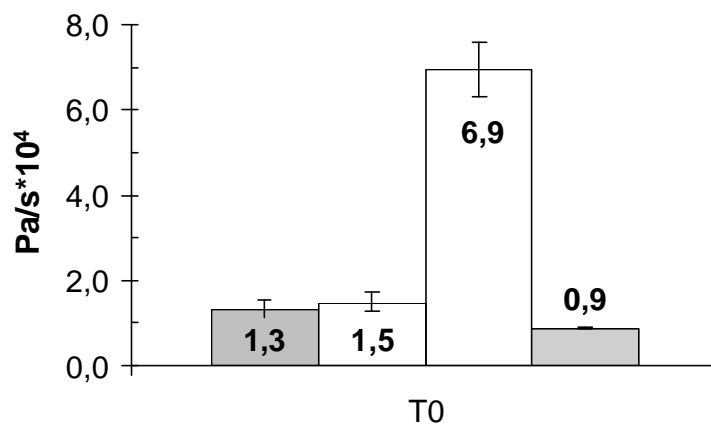
b)

Figure 4-43:   viscosity (a), hysteresis (b)

filled:	20/20 °C
empty:	30/30 °C
shaded:	40/40 °C
striped:	40/30 °C

Clearly visible and in accordance with spreadabilty and micro-penetration 40/40 °C creams show two fold shear viscosities compared to creams with lower homogenisation temperatures. The great gain in viscosity is retrieved in hystereses values. In comparison to the high hysteresis of approx. 70 kPa/s of 40/40 °C creams the very low hysteresis of about 9 kPa/s of the 40/30 °C creams becomes even more conspicuous.

Storage modulus and loss modulus as well as phase shift of 40/40 °C creams are significantly higher than those of the other creams (table 4-23). The low elastic and viscous properties of the 40/30 °C creams compared to the others are also evident whereas its phase shift is identical with the 20/20 and 30/30 °C creams.

Table 4-23:   Storage modulus G' [Pa], Loss modulus G'' [Pa] and phase shift δ [°]

T_{target} [°C]	Storage modulus G' [Pa]	Loss modulus G'' [Pa]	Phase shift δ [°]
20/20	9673 ± 2281	3652 ± 860	20.7 ± 0.2
30/30	9120 ± 1330	3350 ± 514	20.2 ± 0.3
40/40	14225 ± 1351	5928 ± 38	24.2 ± 0.3
40/30	5392 ± 951	1998 ± 343	20.3 ± 0.1

4.3.4.3   *Verum after the 2nd final homogenisation*

As explained in the foregoing chapters, all creams have been subjected to two final homogenisation steps. In chapter 4.4.4.1 it has been verified on the once homogenised cream whether API-addition and homogenisation temperature have an influence on the properties of the final cream. This aspect has been verified on creams which passed the 2nd final homogenisation. Table 4-24 gives a summary of the results from the investigation on the different creams homogenised for a 2nd time.

The results without exception are very similar to the results of the creams homogenised once. Whereas creams with homogenisation temperatures of 20 and 30 °C show very similar properties, creams homogenised at 40 °C are more consistent, show higher water binding capacity, are higher viscous and more thixotropic and show higher response of oscillating parameters (G', G'', δ).

Table 4-24: Verum twice homogenised: comparison between different temperatures during API-addition and final homogenisation (means ± sd)

Method	20/20 °C (n=4)	30/30 °C (n=5)	40/40 °C (n=2)	40/30 °C (n=1)
Consistency				
Spreadability [mm^2]	1571 ± 115	1666 ± 161	1144 ± 60	1693
Micro-penetration [mm*10^{-1}]	362 ± 48	374 ± 46	299 ± 2	424
Water binding capacity				
Bleeding [mm^2]	1102 ± 131	877 ± 46	431 ± 21	808
Conductivity [µS/cm]	33.2 ± 1.6	31.4 ± 2.3	20.5 ± 2.5	29.9
Melting behaviour				
Enthalpy [J/g]	61.8 ± 2.5	56.7 ± 4.4	60.7 ± 1.1	59.1
T_{onset} [°C]	60.7 ± 2.1	61.9 ± 0.3	60,8 ± 3.1	63.4
Rheological properties				
Viscosity [mPa*s]	427 ± 9.5	490 ± 33.6	1056 ± 49.3	454
Hysteresis [kPa/s]	12.4 ± 0.2	14.6 ± 0.2	49.9 ± 0	8.7
G' [Pa]	7870 ± 1585	8665 ± 1651	14320 ± 1146	4591
G'' [Pa]	3008 ± 571	3084 ± 537	5872 ± 16	1795
δ [°]	21.0 ± 0.2	19.7 ± 0.5	22.4 ± 1.5	21.4

4.3.4.4   Summary and concluding results

An alteration of the temperature where the API is added between 20 and 30 °C does not affect the properties of the bulk drug product neither of creams once homogenised nor of creams twice homogenised.

Creams homogenised at 40 °C (once and twice homogenised likewise) are more viscous, and thixotropic, show higher elastic and viscous modules and higher phase shifts. Bleeding and conductivity are clearly decreased which indicates a better water binding capacity. They show a different melting behaviour (peak shape) of the fatty phase. Melting enthalpy and onset temperature are similar between creams with various temperatures during API-addition/final homogenisation. Temperatures higher than 40 °C have not been subjected to the investigation because of the well known dissolution and re-crystallisation phenomenon of the API at higher temperatures. Further a manufacturing condition similar to production should be simulated.

Creams homogenised and sampled at 40 °C formed numerous big lumps after approx. 24 hours. This probably occurred because they have not been stirred while cooling to room temperature.

During cooling the primary homogeneous lipid and water phase crystallise in hydrophilic and lipophilic gel-phase separately from each other. Water is most likely entrapped mechanically within this gel-matrix. The crystallisation process has not yet finished at 40 °C. The fat alcohols cetylalcohol and stearylalcohol crystallise because of their low solubility in both phases. Lumps in the following days are the consequence. The lumps obviously contain less water and are able to absorb water. This is shown in low bleeding and electrical conductivity. The low solubility and thus crystallisation of fatty components in both gel phases changes the melting behaviour seen on the DSC curves.

Further, the uneven upwards flow curve of creams homogenised at 40 °C reflect the lumpy appearance of the creams. Crystallised fat alcohols become entangled in a manner that does not allow following the increasing shear rate.

It can be concluded that although the homogenisation at 40 °C seems to improve cream properties (consistency, water binding capacity), this however is not desirable because of the bad macroscopic appearance.

4.3.5   Raw materials

Changes of batches of raw materials should be taken into consideration when manufacturing semisolids. Problems due to the use of different batches of raw materials should possibly be excluded during development activities of the formulation or at least during scaling up to pilot scale. Target of this evaluation was to exclude the impact of the raw materials on the cream's properties during the study of manufacturing process parameters.

In table 4-25 the utilised raw materials are evaluated with respect to a possible impact on the cream's properties. From this, the possible influence of the API and the excipients Arlatone 983S and Cutina CBS was investigated. Two different batches of each of them (utilised for cream processing) did not show significant differences in their chemical-analytical properties (QC-Certificate of analysis).

Table 4-25:   Evaluation of raw materials utilised for cream processing

Raw material	Quantity	Fully completely chem. analyt. characterisation	Evaluated as critical
Azelaic acid	high	yes	+
Cutina CBS	high	no	+
Arlatone 983S	high	no	+
PCL-Liquid	low	no	-
Propylene glycol	high	yes	-
Glycerol 85 %	low	yes	-
Benzoic acid	low	yes	-

Propylene glycol can be considered as not critical as it dissolves completely in the aqueous phase whereas AzA is suspended in the lipid and in the aqueous phase and thus must be considered critical. For the evaluation of the possible influence from various batches of excipients on the cream properties the bulk drug product batches ## P01 - P10 with the API-addition at 20, 25 and 30 °C were considered. Apart from the investigated raw materials (table 4-26), the batches of all other raw materials were identical. In chapter 4.4.4 the similarity of the cream batches ## P01 - P10 has already been shown.

Table 4-26:   Verum batches (pilot scale) manufactured with different batches of AzA,
                   Cutina CBS and Arlatone 983S

SHT056-	AzA 1	AzA 2	Cutina 1	Cutina 2	Arlatone 1	Arlatone 2
P01 - P04	X		X		X	
P05; P06	X		X			X
P07; P08		X	X			X
P09; P10	X			X	X	

4.3.5.1   Cutina CBS

Cutina CBS is a complex mixture of fatty ester and fatty alcohol. It consists of 70 % glycerolmono- and distearate, 10 % cetylstearylalcohol, 10 % cetylpalmitate and 10 % cocoglycerides. The most critical property of Cutina CBS, the hydroxyl number, was 188 for both batches.

Verum batches ## P01 - P04 containing Cutina CBS batch # 1 were compared with verum batches # P09 and # P10 containing Cutina CBS batch # 2. Table 4-27 summarises the results with regard to consistency, water binding capacity, melting behaviour and rheological properties.

As Cutina CBS acts as consistency agent a change of the batch of Cutina CBS was suspected to vary the cream consistency. Apart from the lower electrical conductivity of creams containing Cutina CBS batch # 2 the creams do not show significant differences regarding water binding capacity, consistency, and melting behaviour. Viscometric parameters do not differ from each other as well comparing creams containing Cutina CBS batch # 1 with creams containing Cutina CBS batch # 2. Cream batches containing Cutina CBS batch # 1 show lower values of storage and loss modules at rather similar phase shifts.

Table 4-27:   Verum with Cutina CBS batches # 1 and # 2 (n: number of batches)

Method	Unit	batch 1 (n=4)	batch 2 (n=2)
Consistency			
Spreadability	mm^2	1546 ± 81	1508 ± 102
Micro-penetration	mm*10^{-1}	410 ± 21	321 ± 8
Water binding capacity			
Bleeding	mm^2	843 ± 37	892 ± 146
Conductivity	µS/cm	32.0 ± 1.9	27.6 ± 0.8
Melting behaviour			
Enthalpy	J/g	57.61 ± 0.54	57.70 ± 0.28
T_{onset}	°C	62.06 ± 0.96	62.09 ± 0.26
Rheological properties			
Apparant shear viscosity	mPa*s	459.5 ± 24.5	471.4 ± 31.8
Hysteresis	Pa/s*10^4	1.33 ± 0.24	1.28 ± 0.09
G'	Pa	7531 ± 919	10183 ± 1665
G''	Pa	2722 ± 281	3819 ± 643
Phase shift	°	19.9 ± 0.6	20.5 ± 0.1

4.3.5.2   Arlatone 983S

This non-ionic emulsifier consists of ethoxylated fatty acid esters of vegetable origin. With its HLB of 8.7 it is particularly suitable as oil-in-water emulsifier in creams. Arlatone batches # 1 and # 2 showed identical analytical results. Verum batches ## P01 - P04 containing Arlatone 983S batch # 1 were compared with verum batches # P05 and # P06 containing Arlatone 983S batch # 2 (table 4-28).

Table 4-28:   Verum with Arlatone 983S batches # 1 and # 2 (n= number of batches)

Method	Unit	batch 1 (n=4)	batch 2 (n=2)
Consistency			
Spreadability	mm^2	1546 ± 81	1530 ± 61
Micro-penetration	mm*10^{-1}	410 ± 21	356 ± 21
Water binding capacity			
Bleeding	mm^2	843 ± 37	1044 ± 186
Conductivity	µS/cm	32.0 ± 1.9	30.7 ± 1.8
Melting behaviour			
Enthalpy	J/g	57.61 ± 0.54	59.27 ± 1.16
T$_{onset}$	°C	62.06 ± 0.96	62.25 ± 0.56
Rheological properties			
Apparent shear viscosity	mPa*s	459.5 ± 24.5	479.1 ± 44.4
Hysteresis	Pa/s*10^4	1.33 ± 0.24	1.61 ± 0.28
G'	Pa	7531 ± 919	9907 ± 42
G''	Pa	2722 ± 281	3722 ± 120
Phase shift	°	19.9 ± 0.6	20.6 ± 0.5

Cream batches can be considered as not significantly different regarding water binding capacity, consistency (spreadability, micro-penetration), and melting behaviour using different batches of the emulsifier Arlatone 983S. As far as oscillating properties are concerned, different storage and loss modulus values can be observed.

4.3.5.3 Azelaic acid micronised

Regarding chemical properties both azelaic acid batches can be considered as equal. Mean surface tensions of azelaic acid solutions (5 %) were almost identical (59.9 ± 0.1 vs 59.3 ± 0.3 mN/m). Within the scanning electron micrographs (chapter 4.1.3) and the BET surface (2.38 ± 0.02 m^2/g vs 2.40 ± 0.05 m^2/g) there were no differences among the two azelaic acid batches.

Table 4-29: Verum with AzA batches # 1 and # 2 (n= number of batches)

Method	Unit	AzA batch 1 (n=2)	AzA batch 2 (n=2)
Consistency			
Spreadability	mm^2	1530 ± 61	1543 ± 61
Micro-penetration	mm*10^{-1}	356 ± 21	353 ± 15
Water binding capacity			
Bleeding	mm^2	1044 ± 186	946 ± 103
Conductivity	µS/cm	30.7 ± 1.3	31.6 ± 0.1
Melting behaviour			
Enthalpy	J/g	59.27 ± 1.16	58.49 ± 0.88
T_{onset}	°C	62.25 ± 0.56	62.21 ± 0.39
Rheological properties			
Apparent shear viscosity	mPa*s	479.1 ± 44.4	455.6 ± 17.9
Hysteresis	Pa/s*10^4	1.61 ± 0.28	1.53 ± 0.05
Yield point	Pa	77.5 ± 3.6	87.0 ± 41.8
G'	Pa	9907 ± 42	10930 ± 127
G''	Pa	3722 ± 120	4068 ± 88
Phase shift	°	20.6 ± 0.5	20.4 ± 0.2

As summarised in table 4-29, it could be shown that the two different azelaic acid batches used did not lead to differences in the cream properties.

4.3.5.4   Summary of investigations on raw materials

The use of different batches of the most critical components of the formulation, the consistency agent Cutina CBS, the emulsifier Arlatone 983S, and the API did not lead to substantial changes in the cream properties during these studies.

A critical review of the data acquired in this work revealed that it could be excluded that different batches of raw materials had an interference with the assessment of critical process parameters within this study.

4.3.6   Batch size

Amongst other factors also different batch sizes can influence the properties of a cream. This normally has to be considered during scaling up from pilot to industrial scale. During this study it has been verified whether different batch sizes influence the final cream properties when manufacture on the same plant (RW 125). Manufacturing of smaller quantities than 80-100 kg on the RW 125 for instance is required for clinical trial studies.

Therefore verum bulk batches # P02 (40 kg) and # P04 (80 kg) have been compared with each other. Respective results are summarised in table 4-30.

Both batches were manufactured on the pilot plant Becomix RW 125 using identical batches of raw materials. The API was added at 30 °C. For batch # P02 placebo was halved before adding the API. Due to the halved batch size the homogenisation time of the final homogenisation was halved accordingly from 15 min to 7.5 min. The homogeniser speed remained unchanged at 25.0 m/s. Thus the circulation times for 80 kg were 0.54/min whereas 1.08/min for 40 kg. This guaranteed that in both cases the product was circulated approx. 8.1 times when the homogeniser speed was hold constant at 25 m/s.

As far as consistency concerns a slightly better spreading cream was detected with the large batch size. This difference in spreadability is negligible considering the very similar viscosities of both batch sizes. As far as the result for just one batch can be considered as relevant and representative, all other cream parameters show very homogeneous results as well.

Table 4-30: Verum batches # P02 (40 kg) and # P04 (80 kg)

Method	Unit	P02 (40 kg)	P04 (80 kg)
Water binding capacity			
Bleeding	mm^2	873	809
Conductivity	µS/cm	31.5	31.1
Consistency			
Spreadability	mm^2	1430	1610
Micro-penetration	mm*10^{-1}	386	406
Melting behaviour			
Enthalpy	J/g	57.7	58.2
T_{onset}	°C	63.2	60.9
Rheological properties			
Apparent shear viscosity	mPa*s	470.3	488.1
Hysteresis	Pa/s*10^4	1.64	1.35
G'	Pa	8550	7328
G''	Pa	3078	2665
Phase shift	°	19.8	20.0

4.3.6.1 Summary of investigations on the batch size

Comparing the data from the manufacturing of 40 and 80 kg batch sizes respectively, results give clear hints that adapting the homogenisation time to the batch size and thus maintaining identical the number of circulations yields comparable products.

4.3.7   Holding time

In previous chapters the shear sensitivity of the model formulation has already been shown. In case of the model cream shearing is necessary in order to disperse homogeneously the API after cooling was finished. This shear can considerably alter the colloidal structure of the vehicle especially when it is required after crystallisation of the molten lipid phase. The structural changes caused by this may be partly reversible and the structure might be restored after a certain period (HT) where the product is kept at rest.

Based on previous studies on the model cream during development the holding time of the bulk cream was stated at 10 days.

Usually, holding time before filling semisolids is limited in order to warrant an excellent microbiological quality of the pharmaceutical finished product. On the other hand a minimum holding time before filling might be recommended for shear sensitive products. In case of the model cream the holding time describes the recommended rest period of the bulk before filling into the primary packaging material.

The objective within the course of this thesis was to reinvestigate this rest period immediately after manufacturing which is presumed to be critical for the physical properties of the model cream. Based on the structure findings of this study the target was to explain in more detail the cream behaviour and to verify the duration of this rest period.

Rheological flow and oscillating properties of the model cream were assessed during the course of 10 days after cream preparation. The impact of the API on changes in flow behaviour and visco-elastic properties of verum during the holding time was assessed. Bulk creams from industrial and from pilot scale as well as finished product from pilot scale have been subject of this study (table 4-31).

4.3.7.1   Sample preparation

Samples were taken before the addition of the API (placebo), after the addition of the API and after the subsequent homogenisation (verum). Samples were gently filled into single 500 g jars and stored in a climatic chamber at 25 °C/60 % RH. Analyses were carried out right after sampling and after every 10 days, using a different jar every day.

Table 4-31:   Bulk batches from pilot and industrial scale

Manufacturing scale	Batch #	Temperature during API-addition/ final homogenisation [°C]
Ind	53179, 53180, 53181	28 ± 2
Pilot	SHT056-P12/P13	40/40
Pilot	SHT056-P14/P15	40/30

4.3.7.2   *Bulk product from industrial manufacturing*

Placebo and verum bulk product of 3 industrial scale batches were subjected to this evaluation.

4.3.7.2.1   *Viscosimetry*

Figure 4-44 shows apparent shear viscosities of verum and placebo during a holding time of 10 days after cream processing.
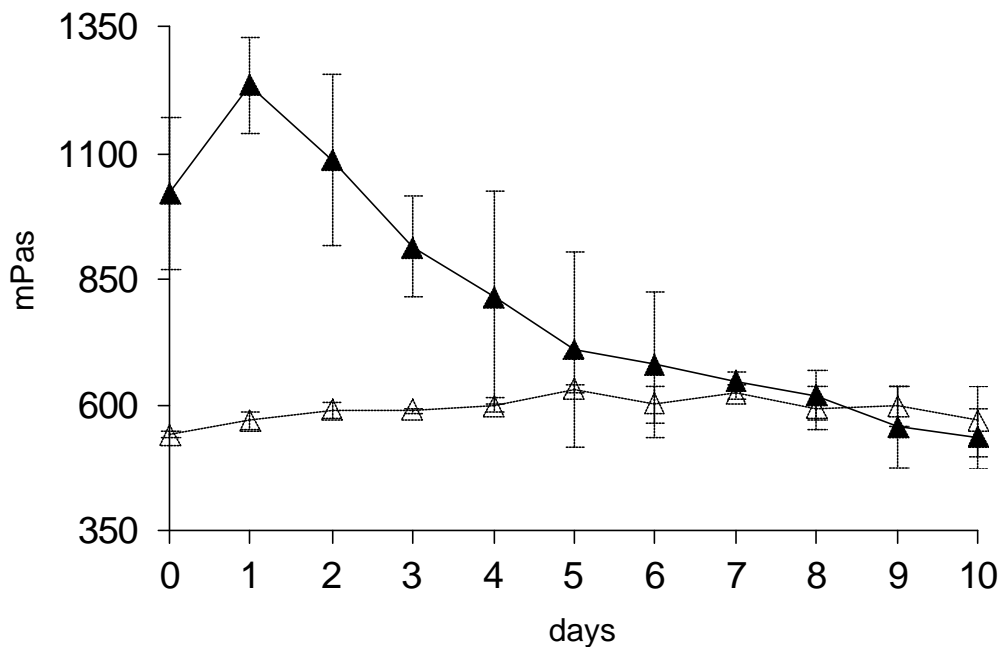
Figure 4-44:   Apparent shear viscosity η_a [mPas] at 400 ^{1}/s (n=3), ind scale
                        -▲-   verum
                        -△-   placebo

At first a much higher viscous verum is evident shortly after manufacturing and the huge drop of viscosity of verum compared to the stable viscosity of placebo during the overall holding time afterwards. After a remarkable drop of the verum's viscosity during the first five days it reaches a stable plateau value comparable to the corresponding placebo's viscosity. This behaviour of verum is rather particular. It shows the loss of consistency shortly after cream manufacturing although verum contains 20 % solid fraction. The varying standard deviations immediately after manufacturing are interesting. Verum viscosities in decrease show high standard deviations. With increasing holding time, shear viscosities become more reproducible and similar to placebo.

Figure 4-45 shows viscosity curves of verum and placebo at different holding times. The apparent shear viscosities are determined at the apex of the flow curves at 400 1/s.
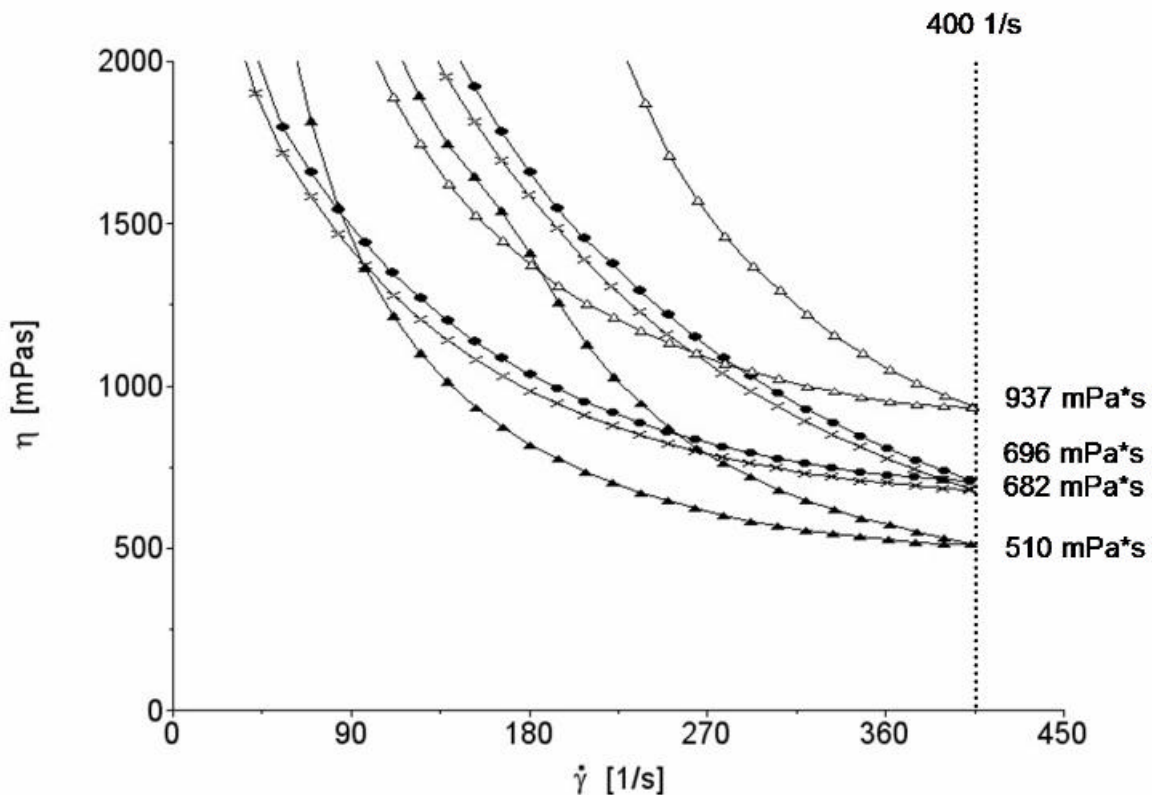
Figure 4-45:   Shear viscosities, # 61003 (ind scale) after different HT

Placebo   Verum
-×-   1 d   -△-   1 d
-●-   10 d   -▲-   10 d

The section around the apex of the flow curves with linear plotted viscosity on the y-axis and linear plotted shear rate on the x-axis is depicted. During increasing shear rate viscosities drop. With decreasing shear rate during the backward curves viscosities are regained only partially. At the same shear rate viscosities of backward curves are distinctly lower compared to viscosities of the forward curves. This structure and viscosity break down is typical for creams that show plastic thixotropic behaviour.

The almost congruent viscosity curves of placebo after 1 day and after 10 days holding time respectively with apparent shear viscosities at the apex of 682 mPa*s and 696 mPa*s are evident. The courses of upward and downward curves of verum after different holding times differ distinctively from each other. At the same shear rate verum after 1 day holding time shows markable higher shear viscosity compared to verum after 10 days of holding time. The apparent shear viscosities at the apex are 937 mPa*s and 510 mPa*s, respectively.

Figure 4-46 shows hystereses of verum and placebo during the course of the holding time. Verum's hysteresis increases within the first 3 days of holding time from approx. 15 kPa/s to 30 kPa/s. Afterwards hysteresis falls below the placebo value and stabilises at approx. 20 kPa/s. Placebo in comparison shows continuously increasing hysteresis up to 5 days. Then it remains constant on the plateau value of approx. 25 kPa/s.
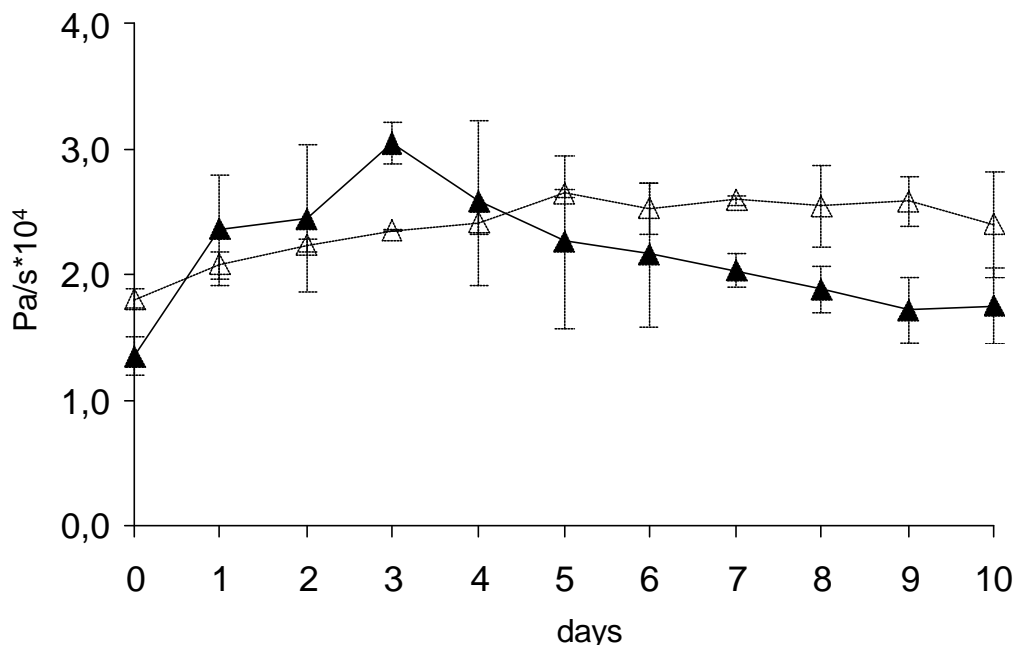
Figure 4-46:   Hystereses [Pa/s*10^4] (n=3), ind scale
-▲-   verum
-△-   placebo
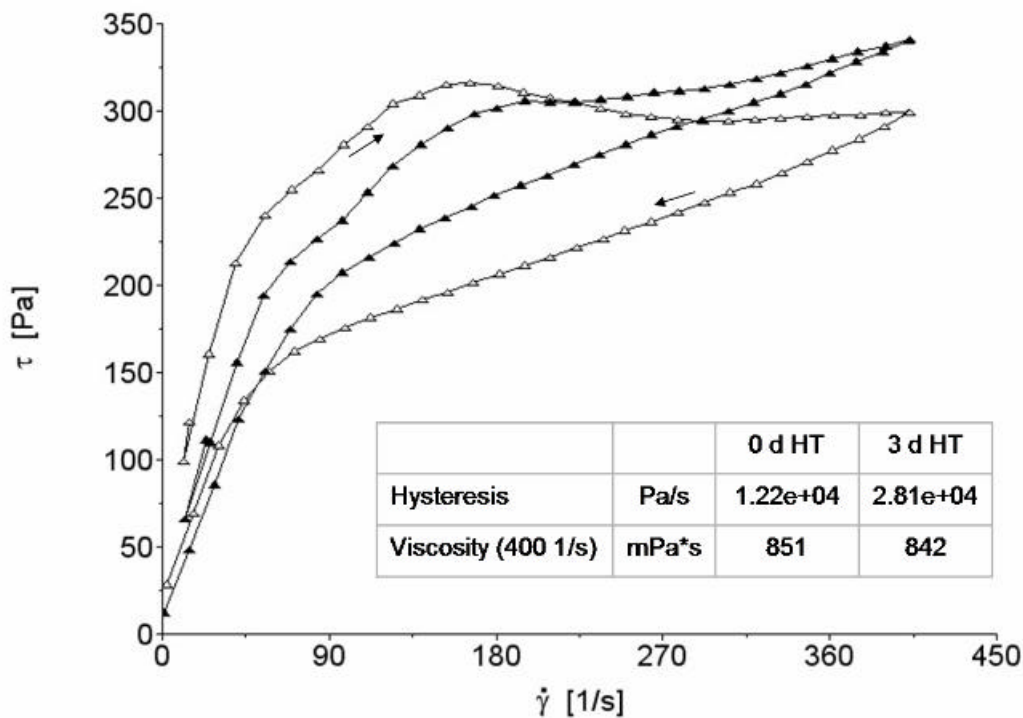
Figure 4-47:   Flow curves of verum, # 53181 (ind scale)

-▲-   immediately after cream processing

-△-   3 days after cream processing

The changed flow curve-profiles of verum in the initial period after manufacturing are shown in figure 4-47. Easily seen is the relative small hysteresis between the upward and downward curve immediately after manufacturing. Within the first three days of rest the hysteresis rises up to more than the double and the shear stress τ rises more steeply by increasing shear rate. It demonstrates the recovery of the microstructure of the cream. However, this structure seems to be very fragile and shear sensitive.

Storage and loss modules (fig. 4-48) and the phase shift δ (table 4-32) are very sensitive parameters to visualise changes in the microstructure. Both, verum and placebo show predominantly elastic behaviour with G' exceeding G''. By incorporation of the API the microstructure clearly gains on elasticity (G' of verum). Demonstrative is the varying storage modulus of verum accompanied by high standard deviations. In contrast, standard deviations of placebo are negligible. Placebo shows a stable structure (constant G' and G'') right after manufacturing.
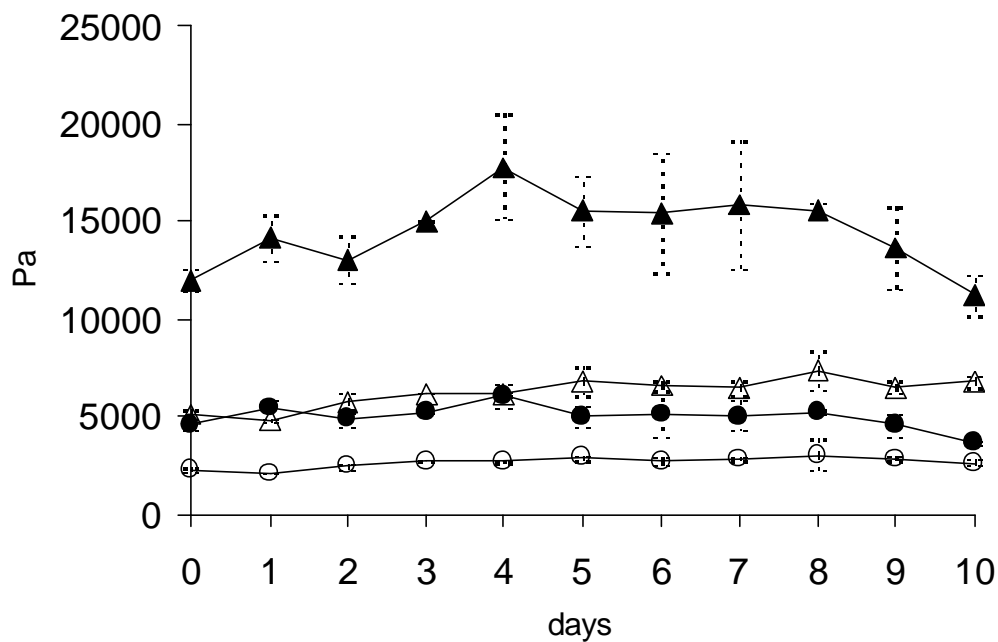
Figure 4-48:   Storage modulus G' [Pa] (n=3), ind scale
                    -▲-   verum
                    -△-   placebo
                    Loss modulus G'' [Pa] (n=3), ind scale
                    -●-   verum
                    -○-   placebo

The verum phase shift (table 4-32) decreases during the first 4 days of holding time. After 4 days the phase shift reaches a constant level corresponding to a stable and more elastic structure. Placebo on the contrary shows constant phase shifts and a high reproducibility just from the beginning and over the entire term of the holding time.

Table 4-32:   Phase shifts δ during holding time (means ± sd [°]), n=3

Phase shift δ [°] ± sd [°] (n=3)		
days	verum	placebo
0	21.20 ± 0.37	23.73 ± 0.07
2	20.69 ± 0.91	23.37 ± 0.16
4	18.92 ± 1.59	23.55 ± 0.23
8	18.56 ± 0.81	23.68 ± 0.21

4.3.7.2.2   DSC

The API's influence on the cream properties was additionally checked by DSC as an additive method. The typical melting profile of verum is shown in figure 4-49. After a broad endotherm peak between 42 °C and 57 °C corresponding to the melting of the fatty phase, the phase transition of the API occurs with a melting point at approx. 70 °C. The pure API by comparison melts at 108.12 °C.
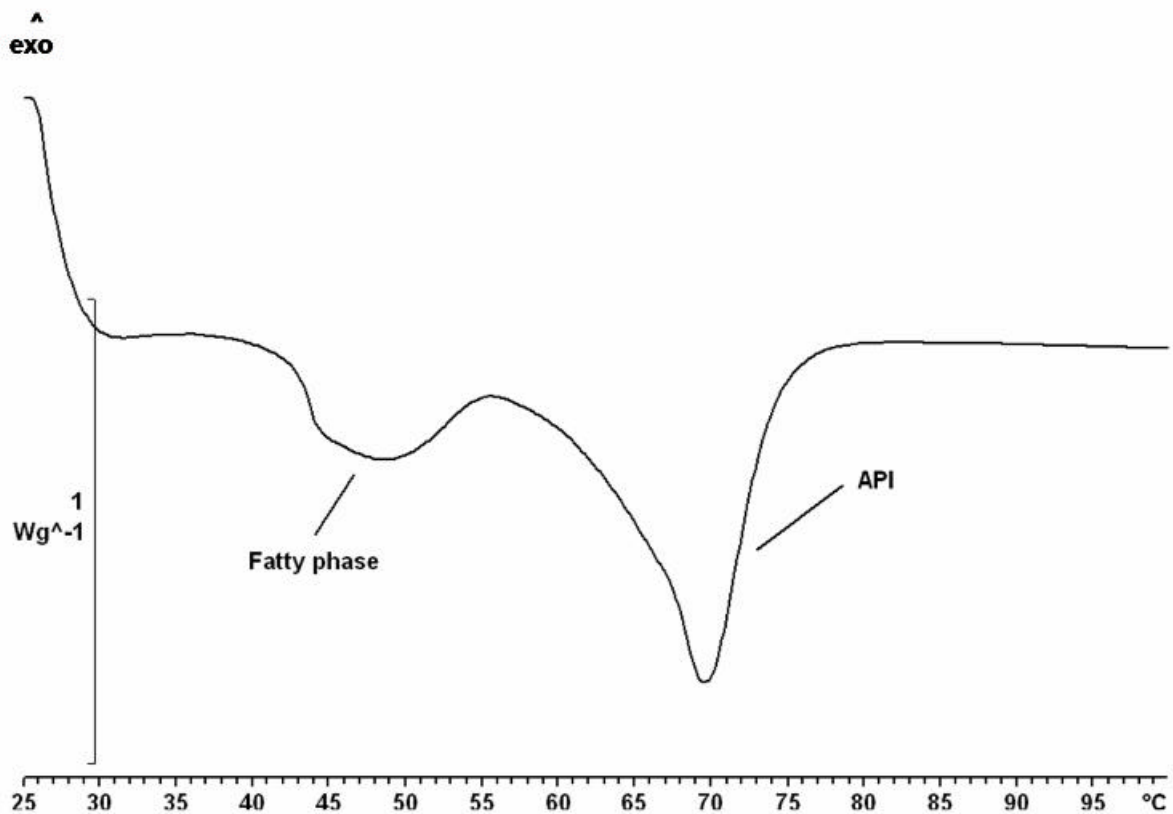
Figure 4-49:   DSC-curve of verum, # 63001 (ind scale)

Figure 4-50 shows the melting enthalpies of the fatty phase and the API in the verum cream. It is obvious that the melting enthalpy measured for the API decreases constantly during the first 5 days of the holding time. After that a plateau value seems to be obtained. Otherwise, when drawing a line between 0 day and 10 days then it points to a continuous dissolution process. In contrast, the melting enthalpy of the fatty phase marginally increases before it reaches a stable plateau value likewise after 5 days.
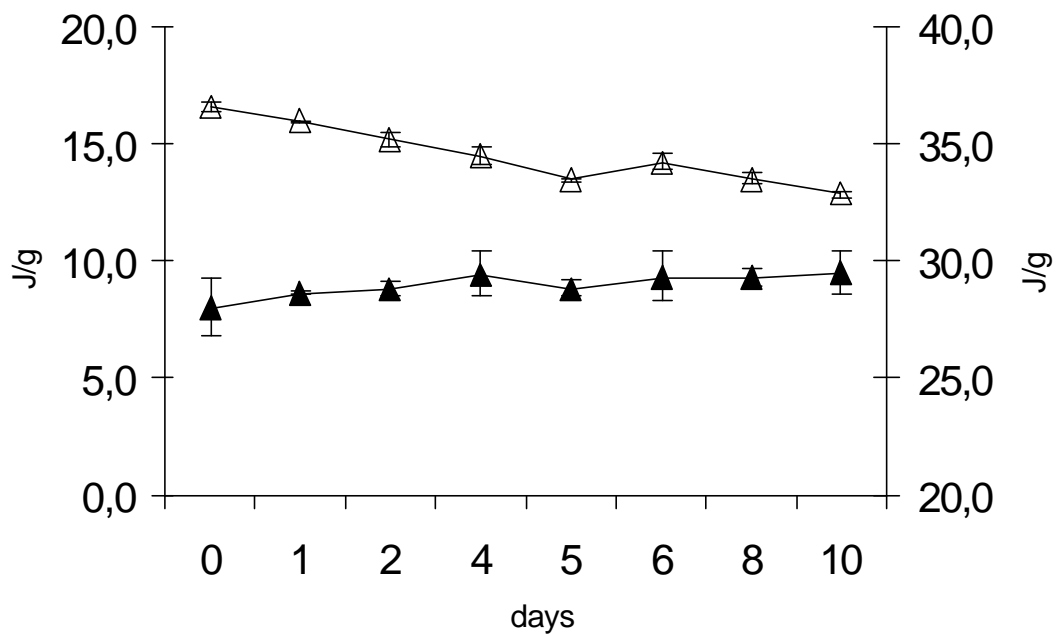
Figure 4-50:   Melting enthalpies [J/g] of verum (n=2)
-▲-   1st melting peak (fatty phase), left scale
-△-   2nd melting peak (API), right scale

4.3.7.2.3   Electrical conductivity of aqueous API solution

The aqueous solution consisting of propylene glycol, glycerol 85 % and purified water is quantitatively composed as the aqueous phase in the cream. Table 4-33 shows the electrical conductivity of an API suspension during time under continuous stirring. From this the dissolution of the API in the cream is once again possible. The aqueous API-dissolution obtains its equilibrium under continuous stirring after approx. 5 hours.

Table 4-33:   Electrical conductivity [µS/cm] of an AzA-suspension (5 % w/w) at 25 °C

Time [min]	0	5	10	15	20	25	30	45	60	120	180	240	300	360
Cond. [µS/cm]	92.9	93.5	94.1	94.5	94.6	94.8	94.7	94.8	95.3	95.6	96.6	97.1	97.3	97.3

4.3.7.3   Holding time of homogenised placebo

So far placebo and verum have been compared where only the verum was subjected to terminal homogenisation at 28 ± 2 °C. In order to clarify the influence from the final homogenisation on the cream properties during holding time two placebo pilot scale batches (# P09 and # P10) either not homogenised or homogenised respectively for 15 and 25 min were investigated by rheological methods during the first 10 days after manufacturing. Exemplarily for the rheological parameters the course of the average shear viscosities during holding time are depicted in figure 4-51.
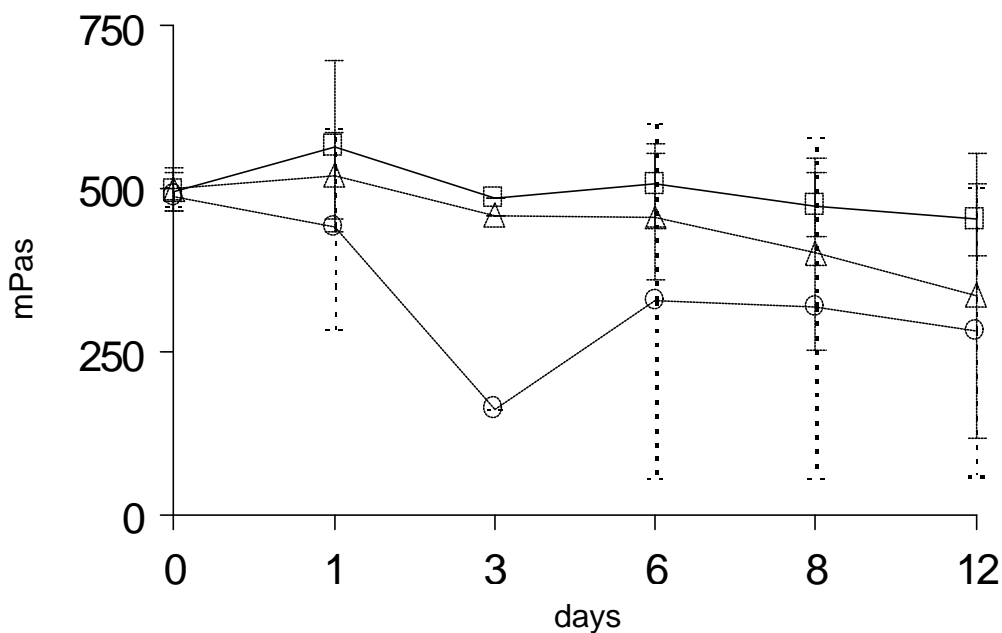
Figure 4-51:   Shear viscosities [mPas] of placebo (n=2), 3 days (n=1)
                    -□-   0 min homogenised
                    -△-   15 min homogenised
                    -○-   25 min homogenised

Placebo creams homogenised for different durations show the same shear viscosities immediately after production. Shear viscosities of non-homogenised creams do not decrease during holding time whereas viscosities of homogenised creams decrease substantially and show high standard deviations after a holding time of 12 days (table 4-34).

Table 4-34:   Mean shear viscosities ± sd [mPa*s], n=2

Holding time [days]	Duration of homogenisation [min]		
	0	15	25
0	496.3 ± 28.1	499.8 ± 32.0	489.1 ± 15.9
12	453.7 ± 53.9	337.7 ± 217.4	283.0 ± 222.4

4.3.7.4   Summary of holding time on the bulk cream (ind scale)

The current investigation on the model cream revealed that amongst various parameters within the complex manufacturing process of a semisolid formulation the holding time of the bulk product must be considered as a critical parameter for the cream quality.

The initial viscosity and hysteresis increase of verum clearly point to an impact of the shear applied during manufacturing. Increasing storage modules during the first days after manufacturing are in accordance with increasing hystereses. Obviously the cream needs a period of rest shortly after manufacturing in order to recover and re-organize its proper gel-structure. Both indicate a re-organisation of the gel-structure. A possible explanation for the decreasing verum viscosity/hysteresis possibly is an interaction between API and hydrophilic/lipophilic gel-phase. This can be supported by decreasing melting enthalpy of the API in the cream. This lets assume a solubilization of the API in the gel-phase. After approx. 5 days the saturation level was obtained. Slightly increasing melting enthalpy of the fatty phase can be explained with re-crystallisation processes.

Placebo on the contrary, shows a stable plateau value which characterises a robust structure. As placebo is sampled before the final homogenisation the hysteresis increase is less significant and shear viscosity even remains constant.

It has been further proven that the influencing factor is the API but not the final homogenisation. The only difference within the manufacturing process between verum and placebo is the final homogenisation step which is missing for placebo. Homogenisation time notably influences the cream properties. This was discussed in detail in chapter 4.4.2. On the other hand it has only a secondary effect on the cream properties during holding time.

4.3.7.5   Bulk product with API-addition at 40 °C

Pilot scale batches with API-addition at 40 °C have been investigated on holding time. It should be assessed how creams manufactured at an elevated temperature (40 °C) show similar behaviour during holding time as creams manufactured close to production parameters. Compared to standard creams where the API was added and dispersed homogeneously at 28 ± 2 °C the here investigated creams were homogenised at 40 °C (# P12, # P13) or at 30 °C (# P14, # P15) respectively after the API was added at 40 °C.

4.3.7.5.1   Viscosimetry

Figure 4-52a shows viscosities and figure 4-52b shows hysteresis of 40/40 °C and 40/30 °C creams compared to standard creams (ind scale). Verum viscosity of standard creams immediately after manufacturing is twice as much compared to placebo viscosity. 40/40 °C creams show similar placebo and verum viscosities immediately after manufacturing and reach a plateau value after 3 day. Noteworthy is the drop in shear viscosities of 40/30 °C creams to the halve viscosities within two days (placebo) and within six days (verum). The verum viscosity declines clearly below the placebo viscosity.

Placebo and verum hystereses (fig. 4-52 b) of creams homogenised at 30 °C show identical course during holding time. Their hysteresis values are similar to the standard creams. But they are clearly lower compared to the hysteresis values of creams homogenised at 40 °C. After a considerable initial drop, hysteresis values approach a plateau value after six days. In contrast thereto, creams homogenised at 40 °C show almost constant hystereses right from the start. Creams homogenised at 40 °C were unloaded at 40 °C and filled immediately in jars without cooling to ambient while stirring. These creams showed rather lumpy appearance after few days.
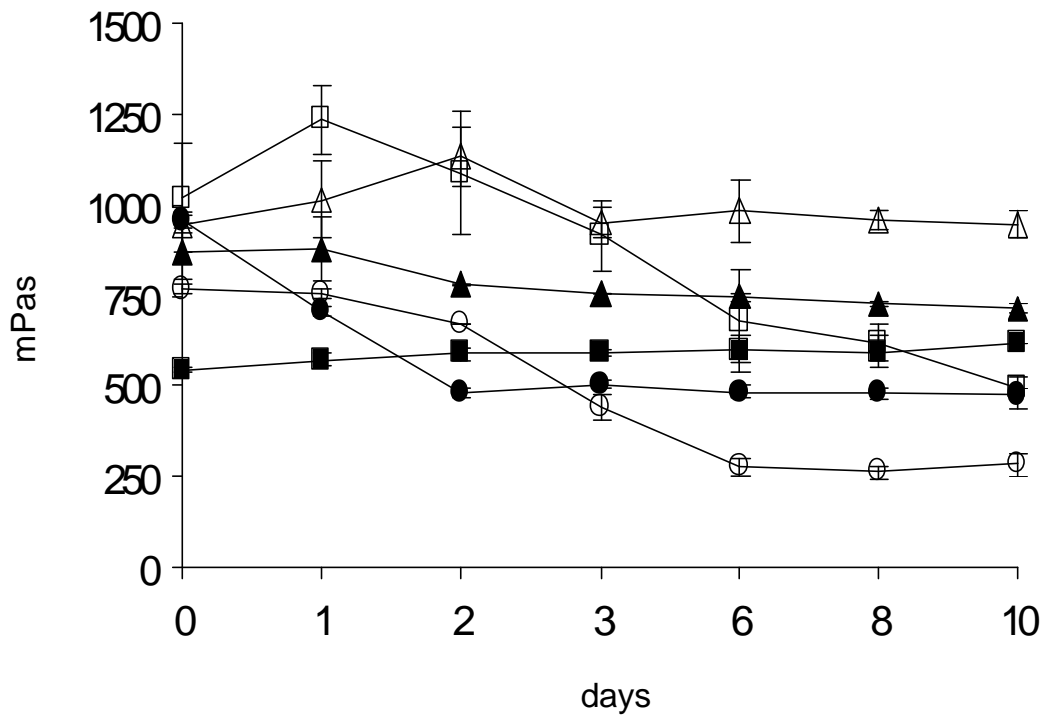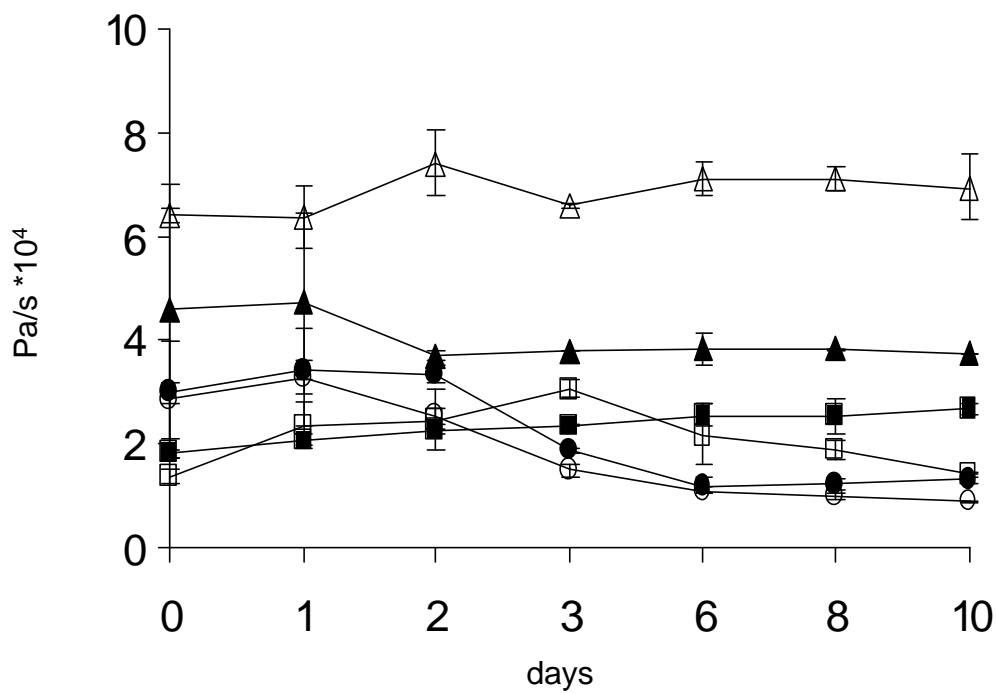
Figure 4-52:   Shear viscosity [mPas] (a), hysteresis [Pa/s*10^4] (b)

-□- verum std   -■- placebo (n=3)
-△- 40/40 °C   -▲- placebo (n=2)
-○- 40/30 °C   -●- placebo (n=2)

4.3.7.5.2   Oscillation

Phase shifts (fig. 4-53) show rather different behaviour. Creams homogenised at 30 °C are more elastic whereas creams homogenised at 40 °C show lower elasticity with an initial drop up to 3 days followed by an increase to the initial value. Standard creams in comparison show continuously slightly decreasing phase shift during the first 5 days, afterwards almost stable values.
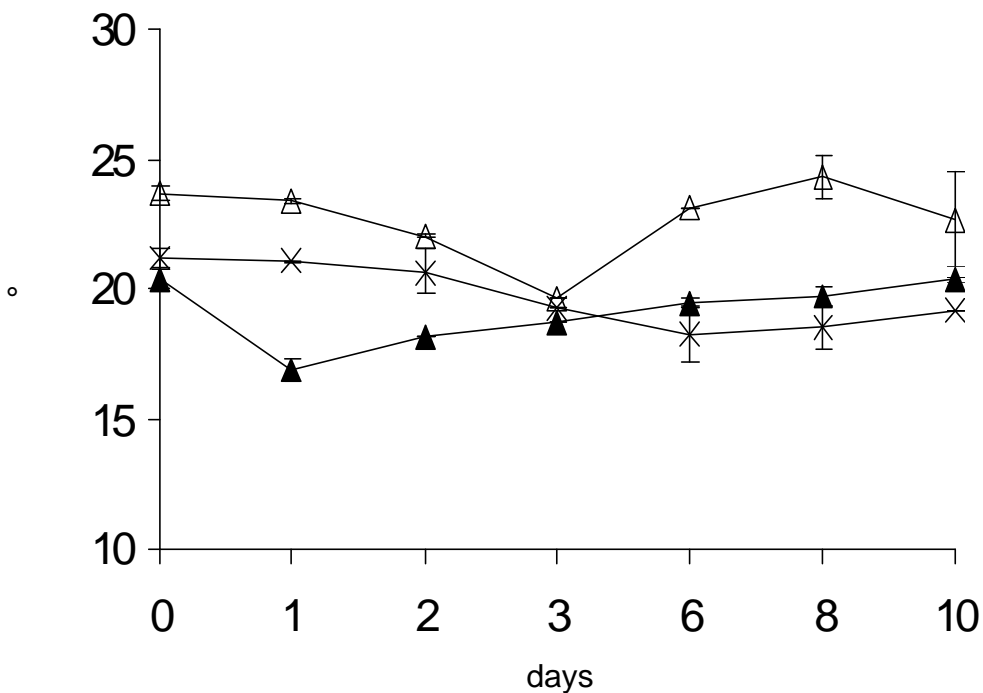
Figure 4-53:   Phase shift δ [°] during holding time (n=2)
-△-   40/40 °C
-▲-   40/30 °C
-×-   verum bulk std (ind scale)

4.3.7.6   Summary of holding time on bulk with API-addition at 40 °C

Different homogenisation temperatures caused different rheological behaviour during holding time. A loss in verum viscosity was detected for creams homogenised at 30 °C as well as for creams manufactured under standard conditions. But API-addition and homogenisation likewise at 40°C clearly lead to the levelling of verum and placebo properties as well as to stable rheological properties after a short holding time. Interactions between API and hydrophilic/lipophilic gel phase seem to be reduced to a minimum. From this point of view the addition of the API at 40 °C and following homogenisation at 40 °C might be favourable and might allow reduce the holding time to 3 days.

Creams of this type showed rather lumpy appearance after 1-2 days. These lumps probably formed by separately crystallised fat alcohols do not contribute to an elastic network and thus showed lower elastic properties. From esthetical point of view consequently API-addition and homogenisation at 40 °C is not recommended at least if the cream is unloaded without further stirring during cooling to ambient.

4.3.7.7   Finished drug product

Apart from the process parameters during the manufacturing of a semisolid cream also the filling process must be taken in consideration and in particular the shear effect which is applied to the cream from the pumping tool as well as from the filling injector. 30 g aluminium tubes were filled on the filling line Tonazzi Colibri (chapter 2.2.4.8) after transferring the bulk cream manually from the bin into the hopper of the filling machine (table 4-35). A pump transfer system as is usually used for the filling activities during industrial manufacturing was not utilised because of the small amount of bulk cream (15 kg each batch). Therefore an impact from the pumping stress to the cream during the transfer from the bin to the hopper was not subject of the current investigation.

About 200 tubes of the pilot scale batch # P15 and the industrial scale batch # 64009 have been filled immediately after manufacturing and after 10 days holding time of the bulk drug product respectively. During manufacturing batch # P15 the API was added at 40 °C and the cream was homogenised at 30 °C whereas batch # 64009 was manufactured by the standard procedure (28 ± 2 °C). The actual temperatures were determined with 28.8 ± 0.1 °C during API-addition and with 29.1 ± 0.6 °C during final homogenisation. The creams were monitored rheologically during the first 10 days after filling and manufacturing.

Table 4-35:   Finished drug product (FP) and corresponding bulk drug product (BP)

FP batch # (30 g)	BP batch #	Temperature API-addition/final homogenisation [°C]
CF058/06*	SHT056-P15 (pilot scale)	40 ± 1
CF059/06^		
CF060/06*	64009 (ind scale)	28 ± 2
CF061/06^		

*   filled immediately

^   filled after 10 days HT

The result of viscometric and oscillatory parameters of finished products (30 g tubes) either filled immediately or filled after a holding time of the bulk product of 10 days during an analysing period of 10 days and the corresponding bulk drug product (batch # SHT056-P15) are depicted In figures (4-54, 4-55, 4-56 and 4-57). The shear viscosities of bulk as well as of FP filled immediately decrease in the first days half as much as before, they reach a stable plateau value after 5-6 days. In comparison, the FP filled after 10 days of rest (# CF059/06) shows stable viscosity and hysteresis results (fig. 4-54 and fig. 4-55) right after the filling activity. After 10 days analysing period its shear viscosity coincides with the viscosity values of bulk and FP filled after 0d HT.
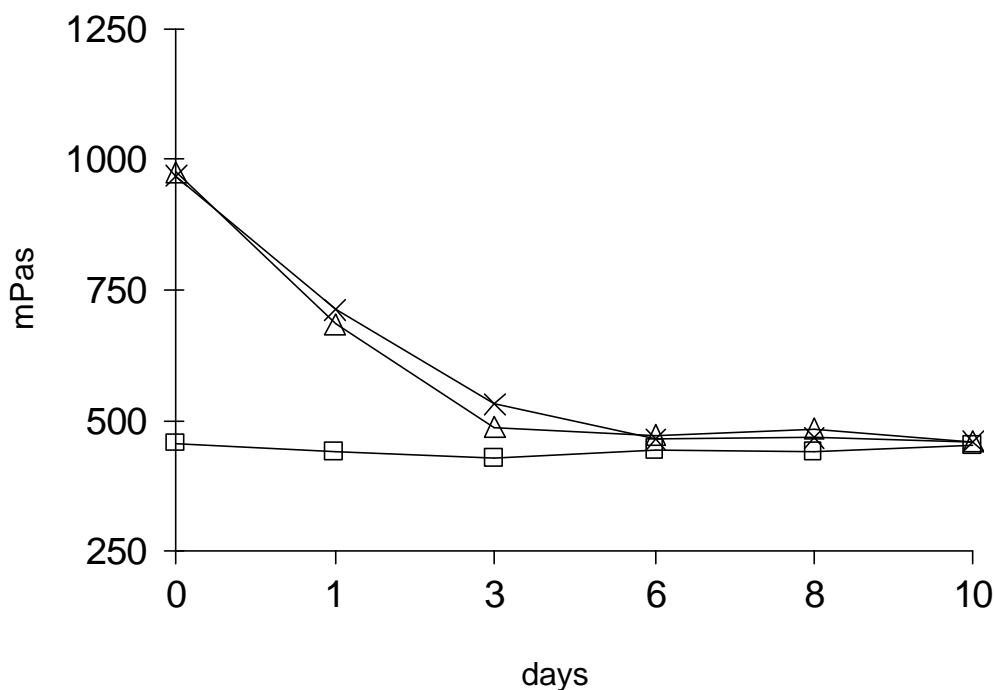
Figure 4-54:   Shear viscosity [mPas] during analysing period of 10 days
-△-   0 d HT (# CF058/06)
-□-   10 d HT (# CF059/06)
-×-   bulk (# SHT056-P15)

The hysteresis of batch # CF059/06 is lower than terminal hystereses of batch # CF058/06 and the bulk (fig. 4-55). Similar to viscosity tendency the hysteresis decreases half as much, up to 6 days when the cream had not had a rest period after manufacturing. Afterwards it reaches a stable plateau value.
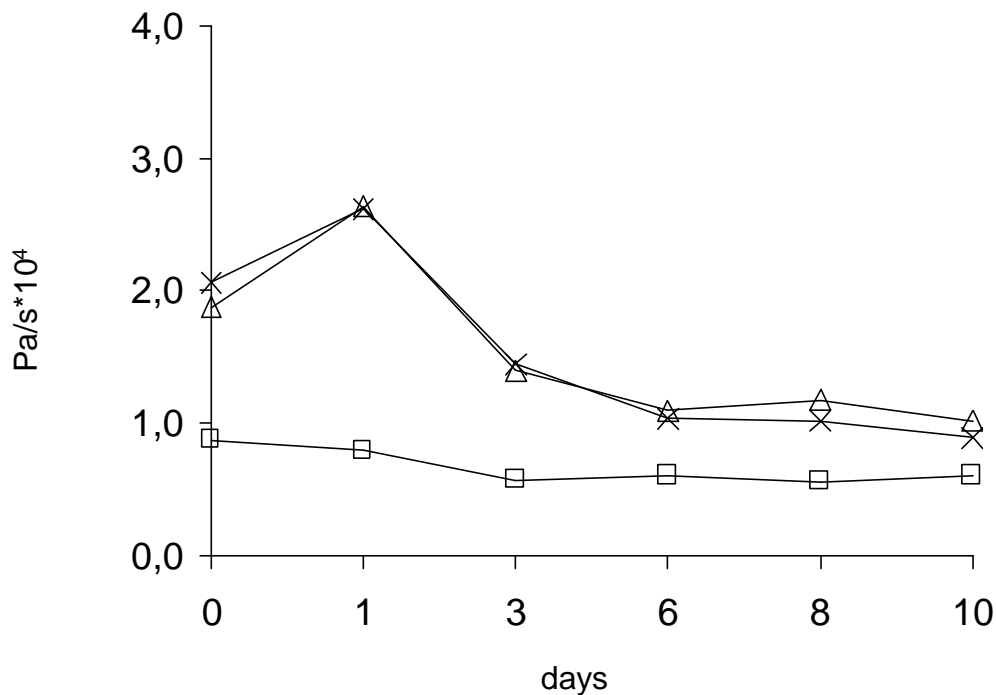
Figure 4-55:   Hysteresis [Pa/s*10^4] during analysing period of 10 days

-△-   0 d HT (# CF058/06)
-□-   10 d HT (# CF059/06)
-×-   bulk (# SHT056-P15)

Figure 4-56 evidences the different flow behaviour of creams filled immediately after manufacturing, or maintaining a rest period of 10 days before filling respectively. Shear stress τ rises steeply up to almost 400 Pa (# CF058/06 and bulk) compared to 175 Pa (# CF059/06) measured each at the apex of the flow curve. Flow curve progressions of the finished products are even and always rising. In comparison, bulk shows uneven flow curve profile with regressing flow curve above shear rates of 180 1/s. The filling evidently has a light pre-shear effect (uneven vs even flow curve profile). But the shear applied during filling does not influence the reply of the shear stress.

Flow curves of both batches (# CF058/06 and # CF059/06) recorded again after 10 days after first analysing are congruent to one other and identical to the flow curve of batch # CF059/06 recorded at filling date.
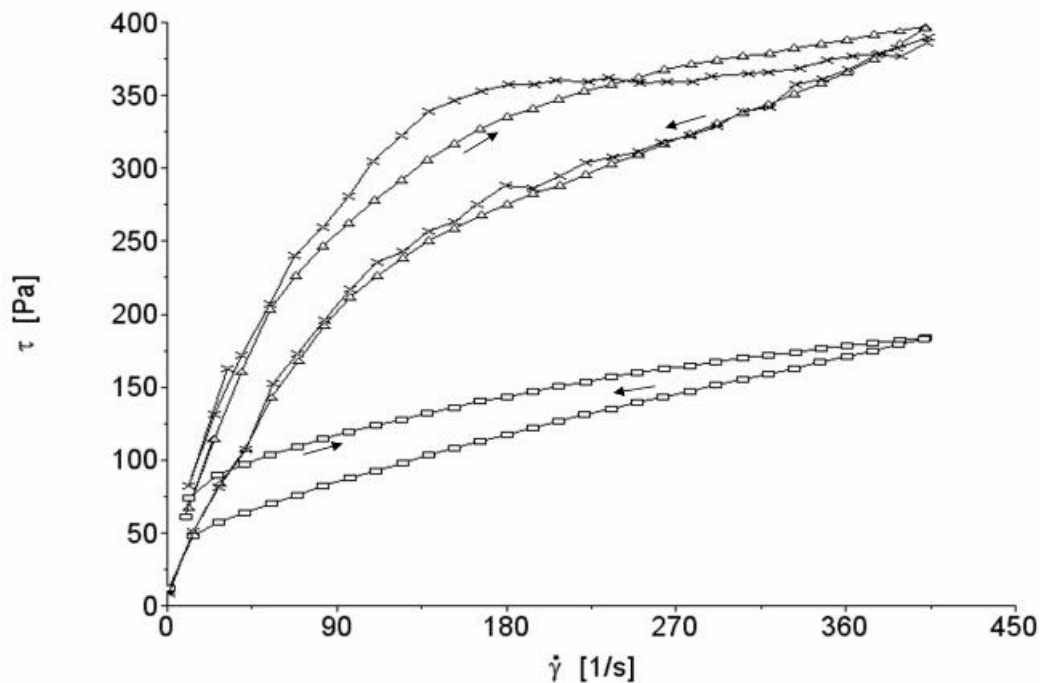
Figure 4-56:   Flow curves, # SHT056-P15 (pilot scale), FP analysed at filling date

-△-   FP filled after 0 d HT (# CF058/06)
-□-   FP filled after 10 d HT (# CF059/06)
-×-   bulk immediately after manufacturing

The progress of the storage modulus G' confirms the foregoing results regarding the insensitivity of the cream properties to the filling stress. Easily noticeable is the decreasing elastic modulus during the first 3 days after filling or manufacturing respectively (fig. 4-57). During remaining holding time batch # CF058/06 and bulk show constant storage modulus G'. Worthwhile to mention, is the low elastic behaviour of batch # CF059/06 which is in line with the low hysteresis.

Finally, fig. 4-58 shows the comparison of viscosities between pilot and industrial scale batches. The similarity in the flow behaviour between pilot and industrial scale batches is visible. After 10 days all samples of finished product approach a uniform viscosity value.
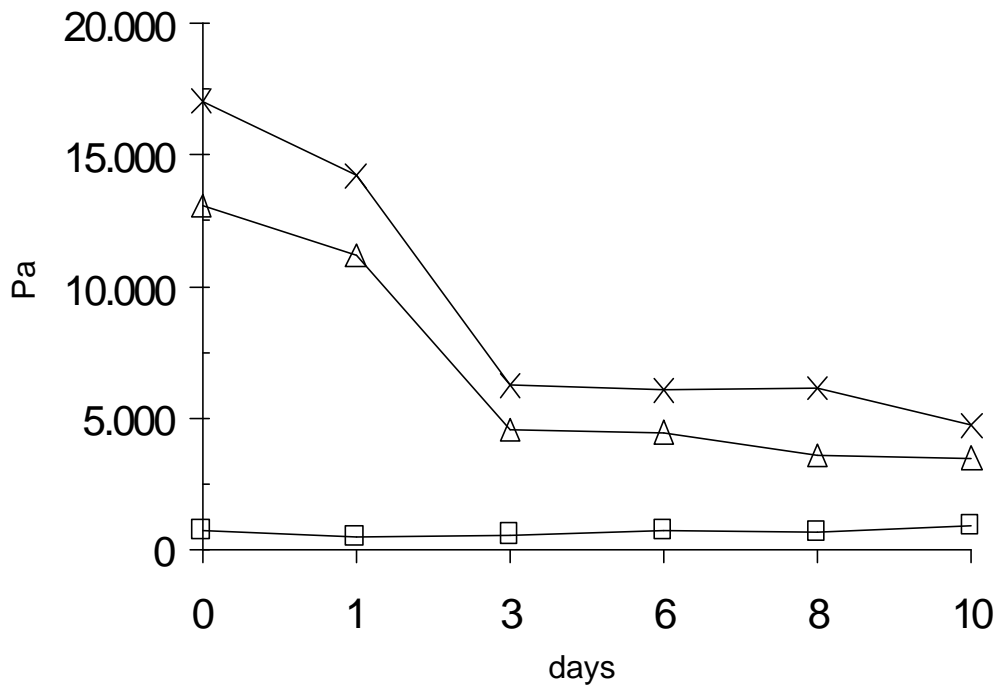
Figure 4-57:   Storage modulus G' [Pa], n=1
-△-   0 d HT (# CF058/06)
-□-   10 d HT (# CF059/06)
-×-   bulk (# SHT056-P15)
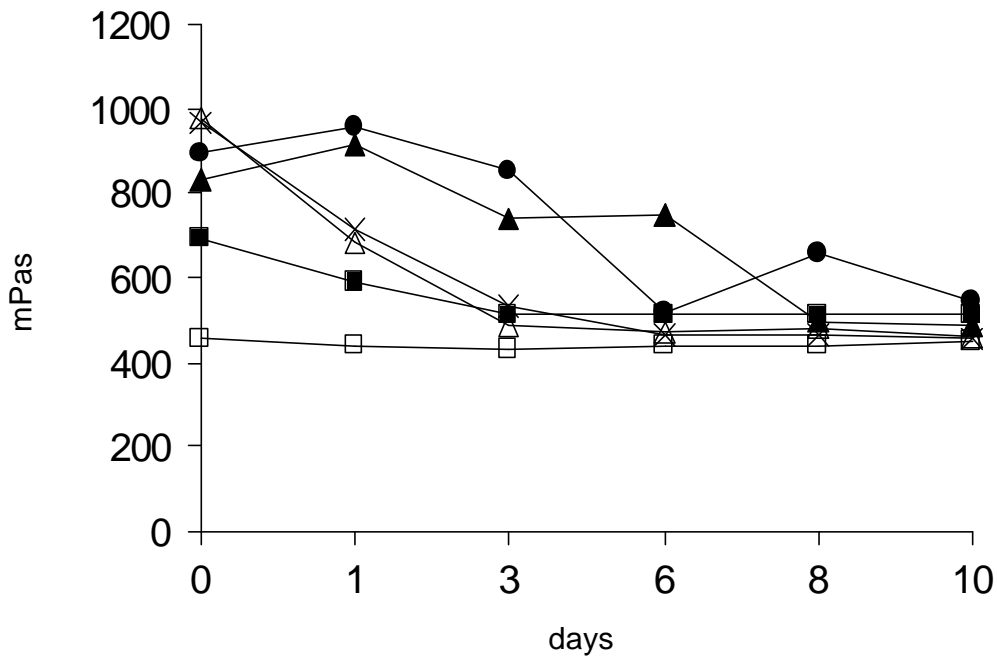
Figure 4-58:   Shear viscosity [mPas] of FP samples from pilot and ind scale
-△-   0 d HT pilot (# CF058/06)   -▲-   0 d HT ind (# CF060/06)
-□-   10 d HT pilot (# CF059/06)   -■-   10 d HT ind (# CF061/06)
-×-   bulk (# SHT056-P15)   -●-   bulk (# 64009)

4.3.7.8   Summary of holding time of finished drug product

Creams (pilot scale 40/30 °C) filled into final packaging material shortly after manufacturing show rheological behaviour similar to the corresponding bulk cream. After 3 to 6 days the microstructure and consequently the rheological parameters reach stable plateau values. The shear stress applied to the cream by the injector during the filling process showed no influence in the rheological cream properties.

Creams (pilot scale 40/30 °C) filled after a holding time of 10 days showed stable rheological properties right from analysis start and different from bulk and finished product immediately filled. This underlines the changes taking place in the re-organisation of the microstructure during the first days. The found values coincide with the ones found after 3 to 6 days (when become stable) for bulk and finished product immediately filled.

Investigations showed for pilot and industrial scale trials likewise that it is indifferent if the holding time is carried out on the bulk or directly in the tube. In light of this, immediately filling and 5 to 10 days rest afterwards appear recommendable.

4.3.7.9   In vitro release tests

Drug release from semisolid dosage forms is highly influenced by vehicle properties (Benninger, 1977). Drug substances in diluted solutions are released according the 1st Ficks' law of diffusion (equation 4-1).

$$J = -D^* \, \Delta C/\Delta x \qquad \text{(Eq. 4-1)}$$

J   mass flux
D   diffusion coefficient
C   concentration of the solute
x   distance into the substrate

In case where the vehicle is a semisolid system the diffusion is hindered by interactions between vehicle and drug substance. For such semisolid systems an apparent diffusion coefficient can be determined. Release from ointments containing suspended drug substance can be described by the equation according to Higuchi (1967).

$$Q = A^* \, (2^*D_s{}^*C_0{}^*C_s{}^*t)^{\frac{1}{2}} \qquad \text{(Eq. 4-2)}$$

Q   cumulative API-amount released [mg]
A   diffusion area [cm^2]
C_0 initial concentration [mg/cm^3]
D_s apparent diffusion coefficient [cm^2/s]
t   time [min]
C_s saturation concentration within donor [mg/cm^3]

The following prerequisites have to be met in order to apply Higuchi's equation:

- speed of diffusion changes only slightly after a initial phase
- linear concentration gradient between vehicle and membrane
- sufficient high speed of dissolution, the dissolution must not be speed determinant
- particles of drug substance must be much smaller than the vehicle layer
- there is only one diffusing drug substance
- acceptor medium meets sink conditions, concentration of drug substance in the acceptor must not exceed 10 % of the saturation concentration
- C_0 of the donor is much higher than C_s

Viscosity is one of the key attributes of semisolid dosage forms. As shown on 3 investigated bulk batches from production (Fig. 4-44 in chapter 4.4.7.2) the viscosity of the verum bulk decreases significantly during the first days after processing the cream. Target of the current in vitro release tests on the model cream was to verify, if the decrease of viscosity during holding time influences the release of the API from the cream.

Therefore in-vitro-release tests of a further bulk batch from production were carried out 1 day and 8 days after manufacturing respectively. After 1 day the cream showed its maximum viscosity. After 8 days the viscosity decreased by 400 mPa*s (table 4-36).

Table 4-36:   Viscosities of # 61003 during HT (n=2 measurements)

days	η [mPa*s]
1	**962.3**
2	944.7
5	832.3
6	709.5
7	612.6
8	**560.7**
9	523.7
12	517.3

The release profiles of the API from the o/w cream can be extracted from figure 4-59. Both curves show a linear release profile and almost identical slopes. The flux of the different viscous creams and the total amount released are shown in table 4-37. They do not show significant differences. The average flux of the API from the model cream is approx. 420 $\mu g/cm^2/min^{1/2}$.

Table 4-37:   Average flux for investigational cream at different viscosities

η [mPa*s]	flux* [$\mu g/cm^2/min^{1/2}$]	Total amount released after 6 h [mg/cm^2]
962.3	426.6	7.36
560.7	414.6	7.11

*   average slope of the line where square root of time [min1/2] is the x-axis and
       cumulative amount released [µg/cm2] is the y-axis
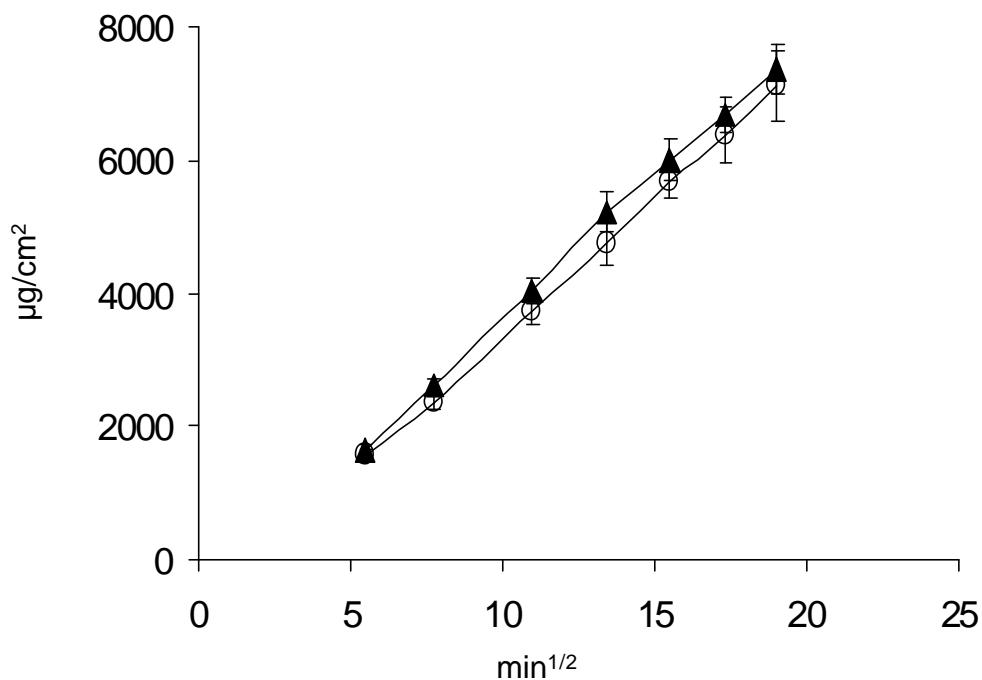
Figure 4-59:   API-amount released from the bulk cream [µg/cm^2]

-▲-   after 1 day HT, R^2 0.9986
-○-   after 8 day HT, R^2 0.9994

4.3.7.10   Summary of in vitro release tests

A viscosity change of approx. 400 mPa*s does not affect the release rate of the API from the model cream. The decisive release factor is most likely the API amount. Within 6 hours approx. 7 mg/cm^2 API were released from the model cream. Compared to other formulations with other sparingly water soluble API's the released AzA amount is relatively high (Franke et. al, 1996, Frigoli, 2001). However, this was expectable because of the high API concentration of 20 % (w/w). Hence it can be presumed that the release rate is only marginally dependent on the cream's microstructure.

An effect of changes in process parameters and in viscosity on the release rate could be shown for other formulations by different authors. Thakker (2003) observed a significant impact of viscosity changes on the release of retinoic acid from semisolid formulations. He varied the viscosity builder between 0, 5 and 10 % and showed that the release of retinoic acid was inversely proportional to the amount of viscosity builder in the formulation.

Franke (1996) showed increasing release rates of metylprednisolone aceponate (MPA) from Advantan in the sequence fatty ointment < ointment < cream corresponding to decreasing viscosity of the Advantan vehicles. Kaca (2007) showed on sparingly soluble corticosteroids that viscosity does not influence the release rate.

4.3.7.11   Concluding results of holding time

A remarkable impact of the API on flow and oscillating properties of the formulation could be verified. The rheological monitoring of verum bulk product cream clearly points to structural changes taking place after processing the cream. Obviously, these changes are triggered by the API and might be attributed to an incorporation of the amphiphilic API into hydrophilic and /or lipophilic gel-phases. Results from this investigation suggested that the holding time before filling into primary packaging materials can be shorted to a minimum of 5 days. Further it could be shown that final homogenisation does not affect the cream properties during holding time. Actually it has no influence on placebo properties.

API-addition and homogenisation likewise at 40°C clearly lead to the levelling of verum and placebo properties as well as to stable rheological properties after a short holding time (approx. 3 days). This processing condition (40 °C) seems to be favourable for the cream quality. On the other hand these samples exhibited unacceptable aesthetic properties (lumpy appearance). This proved that it is necessary to stir during cool down to room temperature for a homogeneous formation of hydrophilic and lipophilic gel-phases (disordered state).

Investigations on pilot and industrial scale trials likewise showed that holding time is a critical parameter for verum but it is indifferent if this holding time is applied to the bulk or to the FP (tube). Thus immediately filling appears recommendable. The shear stress applied by the injector during the filling process does not influence the rheological cream properties.

Finally it could be shown that the viscosity loss during holding time does not affect the API in-vitro-release rate and thus it is hardly dependent on the cream's microstructure.

4.4 Assessment of storage stability

All produced batches (placebo and verum) were investigated on their macroscopic and microscopic appearance, consistency, water binding capacity, melting behaviour and rheological properties during different storage times and conditions. Samples were stored at 25 °C/ 60 % RH and 40 °C/ 75 % RH for 1; 3, and 6 months respectively. Further a stress test comprising 3 cycles changing from +5 °C to +40 °C was performed as well.

4.4.1 Placebo

4.4.1.1 Placebo with different cooling rates

4.4.1.1.1 25 °C/60 % RH

Placebo samples with different cooling rates (table 4-38) showed a uniform tendency during storage at room temperature. The separation of water from the system increased with increasing storage time. This was visible on higher bleeding and conductivity values. All creams loss in consistency/viscosity and hysteresis independent from the performed cooling rate. The samples also lost in elasticity (increasing phase shift). Regarding the melting behaviour a general increase of melting enthalpy and onset temperature were observed, a hint for the formation of lipid crystals. Creams cooled by 0.5 °C/min showed improved properties shortly after manufacturing compared to the more rapidly cooled creams. This benefit of lower bleeding and spreadability, higher viscosity and hysteresis as well as lower melting enthalpy disappeared during storage. The cream properties of different placebo became similar on storage at 25 °C/60 % RH.

4.4.1.1.2 40 °C/75 % RH

Comparison of stability data of placebo with different cooling rates did not reveal significant differences during storage at 40 °C/75 % RH (table 4-39). The increasing phase shift became evident, and likewise viscosity for all batches whereas the batches with 0.5 °C/min and 0.85 °C/min cooling rates showed a loss in hysteresis compared to increasing hysteresis of placebo cooled with 1.0 °C/min. Also the melting enthalpies could not be interpreted unambiguously. The homogeneously cooled cream batches showed increasing water binding capacity whereas electrical conductivity and bleeding values were constant for placebo cooled non-linearly. Spreadability and micro-penetration increased for both.

4.4.1.1.3 Cycle test

The cycle test (table 4-40) indicated few changes within the cream properties of the batches with linear cooling rates. In contrast, creams homogenised non-linearly showed clear worsening properties. These creams were less stable than the others.

Table 4-38:   Placebo pilot scale - different cooling rates - 25 °C/60 % RH

Method	CR 1.0 °C/min Mean (n=2) sd				CR 0.5 °C/min Mean (n=2) sd				CR 0.85 °C/min Mean (n=2) sd			
Months	T0	1	3	6	T0	1	3	6	T0	1	3	6
Conductivity µS/cm	17.8 0.7	18.0 6.7	19.8 1.2	20.7 1.5	15.2 0.4	18.5 0.3	18.7 1.7	21.2 0.8	17.4 2.1	18.4 2.1	18.3 0.6	23.0 4.6
Bleeding mm^2	428 115	503 69	548 14	539 58	350 28	527 51	469 48	500 25	392 33	471 34	439 96	571 127
Spreadability mm^2	1833 109	1752 194	2526 274	2241 190	1487 24	2093 51	1845 180	2563 180	1870 136	2001 21	2286 370	2543 189
Micro-penetration mm*10^{-1}	393 31	450 1	489 25	528 4	356 11	499 21	472 27	443 42	379 2	392 9	415 34	498 119
Enthalpy J/g	13.92 0.34	14.67 0.33	14.46 0.37	15.43 0.25	11.69 0.26	13.92 0.93	15.09 0.38	15.34 0.24	9.22 0.30	11.28 0.94	12.79 0.94	12.13 1.87
T_{onset} °C	47.37 0.89	48.60 0.74	50.03 0.13	49.71 0.05	45.51 0.32	48.12 1.10	49.14 0.09	49.81 0.21	48.33 1.14	48.44 0.34	48.76 0.20	48.86 1.00
Viscosity mPa*s	556 20	354 30	277 3	245 9	701 9	419 68	349 161	362 68	454 54	396 110	405 52	338 56
Hysteresis Pa/s	2.02 0.27	1.39 0.07	1.23 0.01	1.25 0.23	3.66 0.07	2.08 0.05	1.65 0.87	1.54 0.36	2.62 0.19	1.94 0.49	1.95 0.08	1.52 0.19
Phase shift °	23.0 1.2	24.3 1.5	24.3 1.2	31.2 5.8	24.0 0.3	25.0 0.0	25.5 0.3	26.6 1.3	24.4 0.7	25.4 0.7	25.8 0.1	26.5 0.4

Table 4-39:　　　Placebo pilot scale - different cooling rates - 40 °C/75 % RH

Method	CR 1.0 °C/min Mean (n=2) sd				CR 0.5 °C/min Mean (n=2) sd				CR 0.85 °C/min Mean (n=2) sd			
Months	Months	1	3	6	T0	1	3	6	T0	1	3	6
Conductivity µS/cm	17.8 0.7	16.3 0.5	11.5 1.1	11.0 0.3	15.2 0.4	14.5 0.4	13.1 1.4	11.5 0.5	17.4 2.1	15.4 0.0	17.3 0.3	17.2 2.3
Bleeding mm^2	428 115	416 65	248 33	259 20	350 28	303 27	312 27	251 18	392 33	330 8	442 33	351 54
Spreadability mm^2	1833 109	1773 30	1946 179	1843 98	1487 82	1801 173	1790 91	2073 152	1870 136	2167 86	2788 235	2403 138
Micro-penetration mm*10^{-1}	393 31	417 10	392 6	383 24	356 11	447 11	383 8	353 13	379 2	413 64	483 8	446 27
Enthalpy J/g	13.92 0.34	12.47 0.12	13.64 0.28	11.07 0.14	11.69 0.26	12.80 1.02	12.83 0.47	11.24 0.45	9.22 0.30	10.58 0.16	10.18 0.94	10.55 1.08
T_{onset} °C	47.37 0.89	47.38 0.30	48.56 0.24	48.81 0.15	45.51 0.32	47.39 0.10	47.65 0.33	49.29 0.15	48.33 1.14	49.00 0.45	49.19 0.45	49.04 0.88
Viscosity mPa*s	556 20	728 78	858 6	898 114	701 9	787 28	793 2	849 34	454 54	549 22	446 22	530 113
Hysteresis Pa/s	2.02 0.27	2.37 0.49	2.80 0.27	2.79 0.23	3.66 0.07	3.15 0.06	2.96 0.06	3.15 0.01	2.62 0.19	2.03 0.05	1.37 0.10	1.80 0.49
Phase shift °	23.0 1.2	24.6 1.2	27.2 0.3	28.6 0.3	24.0 0.3	26.3 0.2	27.3 0.1	27.7 0.2	24.4 0.7	26.7 0.6	28.0 0.1	28.0 0.1

Table 4-40:   Placebo pilot scale - different cooling rates – Cycle test

Method	CR 1.0 °C/min Mean (n=2) sd				CR 0.5 °C/min Mean (n=2) sd				CR 0.85 °C/min Mean (n=2) sd			
Cycle	T0	1	2	3	T0	1	2	3	T0	1	2	3
Conductivity µS/cm	17.8 0.7	18.0 1.5	16.2 0.1	17.5 0.8	14.0 0.8	17.0 4.4	14.4 0.7	18.5 0.4	17.4 2.1	17.0 2.5	17.6 1.2	25.0 0.0
Bleeding mm^2	428 115	502 42	446 71	406 91	350 7	443 12	336 69	428 12	392 33	398 43	471 93	384 28
Spreadability mm^2	1833 109	1677 64	1523 17	1816 266	1942 148	1783 21	1630 105	2175 54	1870 136	2279 209	2747 173	2299 296
Micro-penetration mm*10^{-1}	393 31	392 1	360 10	369 3	356 6	370 19	359 15	360 1	379 2	427 13	480 69	677 78
Enthalpy J/g	13.92 0.34	13.31 0.10	12.97 0.40	13.56 0.18	13.04 0.04	14.56 0.02	14.00 1.43	13.83 1.11	9.22 0.30	11.46 0.09	12.49 0.83	11.29 0.44
T_{onset} °C	47.37 0.89	46.74 0.57	47.18 0.02	47.20 0.07	46.46 0.19	48.02 0.25	47.48 0.72	47.11 0.39	48.33 1.14	48.74 0.01	49.04 0.41	49.04 0.20
Viscosity mPa*s	556 20	656 23	648 12	653 39	660 43	590 136	650 91	632 18	454 54	474 22	280 55	343 69
Hysteresis Pa/s	2.02 0.27	3.11 0.30	2.76 0.27	2.56 0.32	3.66 0.07	2.80 0.76	3.08 0.63	3.17 0.06	2.62 0.19	2.60 0.08	1.29 0.24	1.77 0.55
Phase shift °	23.0 1.2	22.9 0.2	22.6 1.6	24.3 0.5	24.9 0.4	24.2 1.6	24.7 0.5	23.5 1.8	24.4 0.7	25.4 0.4	26.1 0.6	28.1 1.9

4.4.1.2   Placebo with different duration of final homogenisation

4.4.1.2.1   25 °C/60 % RH

Placebo with different homogenisation times (table 4-41) showed similar trends during storage at ambient temperature as placebo with different cooling rates (table 4-38). They lost in consistency/viscosity. The more fluid and less consistent appearance was visible by eye. Elastic properties decreased whereas melting enthalpies increased. The microscopic appearance of the creams remained unchanged. Creams without final homogenisation showed increasing bleeding and conductivity. The contrary could be observed for creams homogenised for 15 or 25 min respectively. Enthalpies of homogenised creams were constant.

At t_0 creams without final homogenisation dearly showed improved cream properties. They showed lower electrical conductivity and bleeding values as well as higher viscosities and hystereses. These differences disappeared during storage. The homogenised creams did not change their viscosities considerably. The final values of all samples converged to one other. The initial disadvantage of non- homogenisation got lost during storage.

4.4.1.2.2   40 °C/75 % RH

Initially, the better properties of the non homogenised creams became similar with the ones of the homogenised creams during storage at 40 °C/75 % RH (table 4-42). Non homogenised creams showed higher viscosities at t_0 and during the entire storage program. Creams homogenised for 25 min showed the lowest initial values of hysteresis but highest gain in hysteresis during storage. In general a sandy appearance was typical for storage at higher temperature.

4.4.1.2.3   Cycle test

During cycle test, creams exhibited higher stability compared to isothermal storage. Creams remained smooth during temperature change. The comparison of different homogenisation durations revealed better storage stability for the not homogenised creams which showed only few changes in their properties (table 4-43).

Table 4-41:   Placebo pilot scale - different final homogenisation times - 25 °C/60 % RH

Method	0 min Mean (n=2) sd				15 min Mean (n=2) sd				25 min Mean (n=2) sd			
Months	T0	1	3	6	T0	1	3	6	T0	1	3	6
Conductivity µS/cm	17.8 0.7	18.0 6.7	19.8 1.2	20.7 1.5	25.9 1.6	22.7 2.3	23.0 0.4	22.9 0.5	27.3 0.6	24.3 1.0	23.2 0.5	21.5 1.4
Bleeding mm^2	428 115	503 69	548 14	539 58	542 29	513 36	496 16	526 12	572 38	554 32	533 63	557 17
Spreadability mm^2	1833 109	1752 194	2526 274	2241 190	1780 276	1917 31	2509 62	2105 124	1661 123	2272 281	2757 393	2180 161
Micro-penetration $mm*10^{-1}$	393 31	450 1	489 25	528 4	368 1	458 25	486 18	535 13	407 20	486 42	510 6	538 3
Enthalpy J/g	13.92 0.34	14.67 0.33	14.46 0.37	15.43 0.25	15.16 0.12	15.62 0.25	15.13 0.57	15.65 0.72	15.22 0.39	15.39 1.00	14.52 0.09	15.41 0.45
T_{onset} °C	47.37 0.89	48.60 0.74	50.03 0.13	49.71 0.05	48.19 0.45	49.07 0.30	49.82 0.17	49.69 0.08	48.25 0.25	49.17 0.18	50.04 0.10	49.61 0.11
Viscosity mPa*s	556 20	354 30	277 3	245 9	354 114	283 9	270 10	259 3	288 33	281 23	254 26	255 9
Hysteresis Pa/s	2.02 0.27	1.39 0.07	1.23 0.01	1.25 0.23	1.84 0.47	1.44 0.15	1.28 0.06	1.15 0.07	1.50 0.23	1.13 0.11	1.41 0.04	1.15 0.00
Phase shift °	23.0 1.2	24.3 1.5	24.3 1.2	31.2 5.8	20.2 0.6	22.9 0.5	24.8 0.40	31.6 5.3	19.5 0.3	23.3 0.4	24.2 1.9	33.2 6.0

Table 4-42:   Placebo pilot scale - different final homogenisation times - 40 °C/75 % RH

Method	0 min Mean (n=2) sd				15 min Mean (n=2) sd				25 min Mean (n=2) sd			
Months	T0	1	3	6	T0	1	3	6	T0	1	3	6
Conductivity µS/cm	17.8 0.7	16.3 0.5	11.5 1.1	11.0 0.3	25.9 1.6	19.8 0.3	16.3 0.1	10.8 1.3	27.3 0.6	20.0 2.6	17.9 0.2	10.9 0.6
Bleeding mm^2	428 115	416 65	248 33	259 20	542 29	475 0	299 25	236 10	572 38	452 69	325 62	218 20
Spreadability mm^2	1833 109	1773 30	1946 179	1843 98	1780 276	1792 96	1651 129	1738 132	1661 123	1820 93	1987 134	1730 61
Micro-penetration mm*10^{-1}	393 31	417 10	392 6	383 24	368 1	430 33	406 0	373 5	407 20	446 13	382 19	388 25
Enthalpy J/g	13.92 0.34	12.47 0.12	13.64 0.28	11.07 0.14	15.16 0.12	13.62 0.05	13.77 0.03	11.05 0.47	15.22 0.39	13.83 0.08	14.04 0.37	11.38 010
T$_{onset}$ °C	47.37 0.89	47.38 0.30	48.56 0.24	48.81 0.15	48.19 0.45	47.29 0.06	48.16 0.30	48.54 0.26	48.25 0.25	47.23 0.20	48.52 0.11	48.83 0.25
Viscosity mPa*s	556 20	728 78	858 6	898 114	354 114	356 45	550 82	597 442	288 33	345 15	496 2	550 20
Hysteresis Pa/s	2.02 0.27	2.37 0.49	2.80 0.27	2.79 0.23	1.84 0.47	1.78 0.11	2.52 0.29	2.95 0.44	1.50 0.23	1.81 0.01	2.44 0.02	4.13 0.22
Phase shift °	23.0 1.2	24.6 1.2	27.2 0.3	28.6 0.3	20.2 0.6	23.4 0.9	25.1 0.0	28.4 0.2	19.5 0.3	23.7 0.4	24.9 1.8	26.6 3.6

Table 4-43:   Placebo pilot scale - different final homogenisation times – Cycle test

Method	0 min Mean (n=2) sd				15 min Mean (n=2) sd				25 min Mean (n=2) sd			
Cycle	T0	1	2	3	T0	1	2	3	T0	1	2	3
Conductivity µS/cm	17.8 0.7	18.0 1.5	16.2 0.1	17.5 0.8	25.9 1.6	23.3 0.3	21.9 0.2	22.9 0.7	27.3 0.6	24.5 1.0	23.3 1.7	23.5 1.5
Bleeding mm^2	428 115	502 42	446 71	406 91	542 29	532 18	550 58	522 76	572 38	570 60	613 110	573 14
Spreadability mm^2	1833 109	1677 64	1523 17	1816 266	1780 276	1663 266	1451 139	1507 61	1661 123	1476 115	1338 52	1423 174
Micro-penetration mm*10^{-1}	393 31	392 1	360 10	369 3	368 1	368 1	366 6	339 6	407 20	368 1	365 0	350 4
Enthalpy J/g	13.92 0.34	13.31 0.10	12.97 0.40	13.56 0.18	15.16 0.12	13.96 0.19	14.32 0.07	14.21 0.11	15.22 0.39	13.82 0.01	14.40 0.07	13.97 0.17
T_{onset} °C	47.37 0.89	46.74 0.57	47.18 0.02	47.20 0.07	48.19 0.45	46.11 0.31	46.36 0.32	46.70 0.26	48.25 0.25	46.13 0.33	46.51 0.21	46.51 0.91
Viscosity mPa*s	556 20	656 23	648 12	653 39	354 114	506 133	432 36	515 50	288 33	602 25	339 105	453 47
Hysteresis Pa/s	2.02 0.27	3.11 0.30	2.76 0.27	2.56 0.32	1.84 0.47	4.45 0.28	2.93 0.48	3.27 0.23	1.50 0.23	4.41 0.82	3.03 0.72	3.28 0.05
Phase shift °	23.0 1.2	22.9 0.2	22.6 1.6	24.3 0.5	20.2 0.6	22.0 0.3	20.9 0.1	21.3 0.2	19.5 0.3	22.0 0.6	20.6 0.0	21.3 0.1

4.4.1.3   Placebo with different melting parameters

4.4.1.3.1   25 °C/60 % RH

At t_0 both creams did not show significant differences in their physical properties (table 4-44). But stability data during storage at 25 °C/60 % RH showed that cream properties of both batches diverged from each other. The electrical conductivity of batch # P04 was rising at constant bleeding values compared to constant electrical conductivity of the cream melted at 90 °C. Both creams lost in viscosity/consistency. This loss is clearly more pronounced for the cream melted for 30 min at 65 °C. Further it is accompanied by a huge loss in hysteresis. The very similar oscillating parameters of # P04 and # P06 at t_0 become quite different during storage. The collapse of elastic and viscous modules of batch # P04 led to rising phase shift up to a value of 41 ° and the cream becomes rather fluid. Batch # P06 on the other hand conserved very well its elastic and viscous energies.

4.4.1.3.2   40 °C/75 % RH

Storage at 40 °C/75 % RH led to more stable creams than in storage at room temperature. Water binding capacity of the creams increased and batch P04 showed even increasing viscosity and hysteresis (table 4-45).

4.4.1.3.3   Cycle test

Cream properties of the creams with different melting temperatures showed an opposite behaviour as far as DSC and rheology results are concerned. The water binding capacity remained almost unchanged for both. But thermoanalytical and rheological data clearly pointed to worsening cream properties (increasing enthalpy and decreasing viscosity and hysteresis) for the cream with the lower melting temperature and time (table 4-46).

Table 4-44: Placebo Lab - different melting parameters - 25 °C/60 % RH

Method	30 min/65 °C (# P04) Mean* sd				210 min/90 °C (# P06) Mean* sd			
Months	T0	1	3	6	T0	1	3	6
Conductivity µS/cm	18.5 1.0	25.3 0.8	24.5 1.5	23.9 0.4	21.5 1.3	19.2 0.6	21.7 1.0	18.8 1.5
Bleeding mm^2	568 92	669 55	594 19	528 23	450 30	595 47	521 27	404 19
Spreadability mm^2	1731 157	1556 87	2307 179	2717 571	1842 67	1797 57	2188 182	2215 179
Micro-penetration mm*10^{-1}	395 42	523 19	680 41	547 20	357 14	507 18	428 11	429 23
Enthalpy J/g	13.66 0.45	16.69 0.11	14.56 0.57	16.08 0.28	13.51 0.44	16.11 0.20	15.43 0.39	16.09 0.25
T_{onset} °C	46.22 0.54	49.09 0.06	49.03 0.13	49.55 0.03	47.54 1.17	49.17 0.06	48.57 0.04	49.76 0.35
Viscosity mPa*s	569 86	316 59	232 21	221 14	714 62	406 24	300 5	351 21
Hysteresis Pa/s	1.84 0.51	1.14 0.13	0.76 0.09	0.78 0.04	2.32 0.07	1.57 0.13	1.30 0.03	1.73 0.12
Phase shift °	24.1 0.9	27.9 0.6	33.2 0.7	41.1 2.0	22.3 0.7	22.0 1.3	24.3 0.4	26.4 0.3

* measurements of each batch in triplicate

Table 4-45:   Placebo Lab scale - different melting parameters - 40 °C/75 % RH

Method	30 min/65 °C (# P04) Mean* sd				210 min/90 °C (# P06) Mean* sd			
Months	T0	1	3	6	T0	1	3	6
Conductivity µS/cm	18.5 1.0	15.1 0.6	13.4 1.2	15.1 0.6	18.4 0.5	13.9 0.3	13.6 0.1	11.8 0.4
Bleeding mm^2	568 92	365 59	274 18	372 34	450 30	281 4	301 12	239 20
Spreadability mm^2	1731 157	2097 77	1991 141	1881 157	1842 67	1940 164	1699 79	1952 120
Micro-penetration $mm*10^{-1}$	395 42	354 21	397 35	373 30	357 14	429 5	366 3	355 5
Enthalpy J/g	13.66 0.45	15.50 0.54	12.49 0.45	11.92 0.06	13.51 0.44	13.69 0.11	14.08 0.67	17.39 1.22
T_{onset} °C	46.22 0.54	48.02 0.66	48.01 0.42	48.45 0.01	47.54 1.17	47.55 0.30	46.98 0.65	48.74 0.00
Viscosity mPa*s	569 86	802 1	733 4	745 3	714 62	984 9	1020 34	985 22
Hysteresis Pa/s	1.84 0.51	2.61 0.00	2.37 0.17	2.28 0.04	2.32 0.07	3.22 0.02	3.13 0.18	3.22 0.05
Phase shift °	24.1 0.9	27.4 1.3	28.5 0.5	28.2 0.1	22.3 0.7	26.8 0.6	27.5 0.5	28.0 0.1

* measurements of each batch in triplicate

Table 4-46:   Placebo Lab - different melting parameters – Cycle test

Method	30 min/65 °C (# P04) Mean* sd				210 min/90 °C (# P06) Mean* sd			
Cycle	T0	1	2	3	T0	1	2	3
Conductivity µS/cm	18.5 1.0	22.2 0.5	23.7 0.5	20.6 2.1	18.4 0.5	20.5 1.1	20.1 0.2	18.3 0.1
Bleeding mm^2	568 92	587 38	528 27	501 26	469 58	335 32	517 6	472 35
Spreadability mm^2	1731 157	2116 259	3172 819	2148 220	1605 272	1710 238	1733 202	1837 149
Micro-penetration mm*10^{-1}	395 42	497 11	382 23	608 38	377 47	326 30	376 15	327 3
Enthalpy J/g	13.66 0.45	15.47 0.12	15.94 0.13	14.67 0.04	15.03 0.14	14.52 0.25	14.69 0.78	13.65 0.64
T_{onset} °C	46.22 0.54	49.00 0.12	48.76 0.06	48.35 0.24	47.22 0.07	47.32 0.55	46.89 0.34	46.37 0.25
Viscosity mPa*s	569 86	228 14	264 1	126 143	421 8	739 55	683 6	817 12
Hysteresis Pa/s	1.84 0.51	1.23 0.1	0.96 0.04	1.09 0.01	1.64 0	3.02 0.38	2.64 0.12	3.40 0.14
Phase shift °	24.1 0.9	27.8 0.3	30.0 0.6	25.8 0.4	21.6 2.2	22.7 1.0	22.5 0.7	23.7 0.9

* measurements of each batch in triplicate

4.4.1.4   Summary of placebo stability testing

Placebo with different cooling rates, different homogenisation times and different melting procedures were assessed regarding different storage conditions. In general, placebo creams loss in consistency/viscosity during long time storage at room temperature at 60 % RH. On the other hand, they became more consistent during storage at 40 °C and 75 % RH and they appeared sandy and matt compared to t_0. Microscopic appearance remained unchanged for all samples. There was no coarsening of emulsion observed.

Placebo showed the best properties of all during cycle test, whereas worst storage stability during storage at 25 °C and 60 % RH was observed. This rather unusual behaviour can be explained by dissolving hydrophilic and lipophilic microstructures at 40 °C which then re-crystallize at 25 °C. Temperature changes from 25 °C to 40 °C and back led to a continuous swelling and regeneration of network structures separating more and more the two gel-phases. This divergence resulted in a better water binding capacity.

A temperature cycle (25-40-25 °C) also occured in the course of the storage program at 40 °C/75 % RH and hence explains the better cream properties at the storage temperature of 40°C. At room temperature more and more liquid gel-phase crystallised. Hydrophilic and lipophilic gel-phases became closer to each other and more compact, thus water binding capacity got reduced. None of the different cooling rates applied during cream processing showed any clear advantage over the others.

A low and homogeneous cooling gradient as well as non-homogenising cold creams did not show advantages during long time storage and accelerated storage.

The influence from melting time/temperature on the cream properties was shown by data from different stability programs whereas immediately after manufacturing a substantial difference between both creams could not be seen. The cream with the higher melting temperature and time showed better cream properties during isotherm storage and during cycle test. It seems to be likely that a melting temperature near the solidification point of the fatty phase components Cutina CBS and Arlatone 983S negatively affected the cream properties. On the other hand an impact from the effective melting time was unlikely.

4.4.2   Verum

4.4.2.1   Different temperatures of API-addition/final homogenisation

In the following the storage stability of verum creams with different temperatures of API-addition/final homogenisation under different isotherm conditions and under stress conditions is evaluated. All creams loss elasticity during isotherm storage at 25 °C and 40 °C as well as during stress test.

4.4.2.1.1   25 °C/60 % RH

Macroscopically the creams were similar to each other. The different creams showed similar microscopic appearance which did not change during storage time. In general storage at 25 °C/60 % RH led to less consistent and better spreadable creams even if the viscosity remained constant during time (table 4-47). Creams homogenised at 40 °C showed a remarkable loss in viscosity and hysteresis. The initially more consistent creams became similar to the others after several months.

Creams where the API was added at 20 °C and 30 °C showed the same behaviour during long time storage at ambient temperature. As far as water binding capacity is concerned, these creams showed stable electrical conductivity and bleeding values. The very low initial bleeding and conductivity of creams homogenised at 40 °C increased considerably during 6 months and finally reached values of the other creams.

4.4.2.1.2   40 °C/75 % RH

During storage at 40 °C the water binding capacity clearly increased visible on decreasing conductivity and bleeding results (table 4-48). Creams became more spreadable. This has already been described for the placebo with different cooling rates. Worth mentioning is the different behaviour in hysteresis. Creams homogenised at 20 and 30 °C showed a clear increase in hysteresis whereas creams homogenised at 40 °C loss about 70 % of hysteresis during 6 months and became similar to the others.

4.4.2.1.3   Cycle test

During stress test cream properties changed less than during isothermal storage (table 4-49). Contradictory were the slight increase in viscosity for creams homogenised at 20 and 30 °C and the clear decreasing viscosity and hysteresis of creams homogenised at 40 °C. The water binding capacity of 40 °C creams decreased (increasing electrical conductivity and bleeding) compared to increasing water binding capacity of 20 and 30 °C creams. DSC-results and consistency/spreadability values showed less significant changes.

Table 4-47: Verum pilot scale – different temperatures of API-addition - 25 °C/60 % RH

Method	20/20 °C (n=4) Mean sd				30/30 °C (n=6) Mean sd				40/40°C (n=2) Mean sd			
Months	T0	1	3	6	T0	1	3	6	T0	1	3	6
Conductivity [μS/cm]	30.6 1.7	28.1 2.4	28.0 0.6	28.9 2.7	30.9 2.6	28.3 1.7	28.5 1.3	28.0 1.3	20.7 1.1	23.6 1.7	29.5 1.3	27.8 0.2
Bleeding [mm^2]	1001 148	831 205	815 20	911 165	856 47	810 101	813 104	818 165	459 4	820 15	869 11	953 18
Spreadability [mm^2]	1515 61	1874 119	1839 57	1947 93	1547 72	1729 197	1749 91	2023 305	1111 63	1531 82	1653 194	2072 67
Micro-penetration [$mm*10^{-1}$]	362 36	351 57	389 16	426 28	375 44	377 49	372 22	415 16	293 7	341 31	447 8	432 54
Enthalpy [J/g]	57.86 0.42	58.78 1.79	59.62 1.55	59.78 2.07	58.32 1.12	60.00 2.01	61.31 1.06	60.80 1.43	59.62 1.26	59.01 0.71	59.93 0.19	58.87 4.74
T_{onset} [°C]	62.32 0.32	61.88 0.88	61.65 2.57	61.32 2.07	62.00 0.75	61.66 1.77	62.79 1.30	61.75 1.28	60.99 0.54	61.74 0.49	61.09 1.63	62.25 0.38
Viscosity [mPa*s]	453 10	468 16	477 60	431 33	464 31	473 22	473 43	453 67	947 35	633 40	421 6	345 20
Hysteresis [Pa/s]	1.34 0.21	1.10 0.19	1.07 0.37	0.93 0.10	1.46 0.23	1.27 0.22	0.95 0.13	0.94 0.09	6.93 0.64	2.51 0.52	0.92 0.02	0.73 0.01
Phase shift [°]	20.7 0.2	22.7 0.5	24.0 0.4	24.8 1.8	20.0 0.4	21.9 0.6	24.0 0.4	26.7 1.4	24.2 0.3	21.7 0.3	22.9 0.1	29.8 0.1

* 20 °C P03;P06;P08;P10   ^ 30 °C P01;P02;P04;P05;P07;P09   # 40 °C P12;P13

Table 4-48:   Verum pilot scale – different temperatures of API-addition - 40 °C/75 % RH

Method	20/20 °C (n=4) Mean sd				30/30 °C (n=6) Mean sd				40/40°C (n=2) Mean sd			
Months	T0	1	3	6	T0	1	3	6	T0	1	3	6
Conductivity [µS/cm]	30.6 1.7	22.9 1.1	229 1.5	23.5 1.6	30.9 2.6	21.0 1.2	20.7 0.6	20.8 2.5	20.7 1.1	16.2 1.1	9.5 11.3	16.6 1.5
Bleeding [mm^2]	1001 148	852 92	653 83	617 68	856 47	784 118	580 170	517 39	459 4	431 11	508 13	509 1
Spreadability [mm^2]	1515 61	1779 81	1694 133	1702 191	1547 72	1819 191	1780 144	1751 126	1111 63	1600 37	1599 133	1900 92
Micro-penetration [mm*10^{-1}]	362 36	348 38	357 14	361 32	375 44	367 30	355 29	371 17	293 7	324 11	333 6	332 6
Enthalpy [J/g]	57.86 0.42	59.12 2.41	59.21 3.06	55.80 1.99	58.32 1.12	58.12 2.54	57.84 2.13	55.82 1.44	59.62 1.26	56.51 0.10	55.69 0.80	56.41 1.34
T$_{onset}$ [°C]	62.32 0.32	60.08 0.93	60.49 2.50	58.31 1.20	62.00 0.75	59.68 1.66	60.31 1.82	58.68 0.80	60.99 0.54	59.18 0.57	59.98 0.49	59.44 2.75
Viscosity [mPa*s]	453 10	576 32	527 82	450 78	464 31	548 59	517 41	568 174	947 35	591 69	448 28	539 28
Hysteresis [Pa/s]	1.34 0.21	1.32 0.19	2.36 0.71	2.99 1.32	1.46 0.23	2.06 1.11	1.89 0.52	3.00 1.02	6.93 0.64	3.54 1.75	2,75 0,42	2.25 0.39
Phase shift [°]	20.7 0.2	24.3 0.5	25.3 0.6	26.6 0.4	20.0 0.4	24.4 1.9	25.7 0.6	27.6 1.0	24.2 0.3	26.5 0.5	27.2 1.3	28.2 0.3

* 20 °C   P03;P06;P08;P10   ^ 30 °C   P01;P02;P04;P05;P07;P09   # 40 °C   P12;P13

Table 4-49:   Verum pilot scale – different temperatures of API-addition – Cycle test

Method	20/20 °C (n=4)* Mean sd				30/30 °C (n=6)^ Mean sd				40/40°C (n=2)[#] Mean sd			
Cycle	T0	1	2	3	T0	1	2	3	T0	1	2	3
Conductivity [µS/cm]	30.6 1.7	27.5 2.0	28.4 1.2	26.4 1.1	30.9 2.6	28.9 1.9	26.6 1.8	27.3 2.0	20.7 1.1	26.4 4.1	24.7 0.9	22.7 2.9
Bleeding [mm^2]	1001 148	1065 301	856 39	939 145	856 47	922 101	809 77	857 141	459 4	865 68	782 81	828 3
Spreadability [mm^2]	1515 61	1566 71	1623 25	1669 126	1547 72	1430 53	1454 154	1534 74	1111 63	1733 250	1235 55	1379 88
Micro-penetration [$mm*10^{-1}$]	362 36	379 24	375 35	371 36	375 44	372 18	375 32	372 20	293 7	347 6	352 1	346 23
Enthalpy [J/g]	57.86 0.42	58.49 0.87	58.06 0.90	58.59 0.48	58.32 1.12	57.22 1.34	57.42 1.42	56.72 1.22	59.62 1.26	57.88 0.76	59.34 3.75	59.41 0.66
T_{onset} [°C]	62.32 0.32	60.24 2.61	62.40 1.93	62.20 0.74	62.00 0.75	61.74 1.07	61.62 0.90	60.10 1.30	60.99 0.54	60.90 0.45	59.59 1.40	59.69 0.41
Viscosity [mPa*s]	453 10	570 100	565 96	546 85	464 31	460 42	483 56	485 57	947 35	494 6	507 7	585 196
Hysteresis [Pa/s]	1.34 0.21	1.53 0.19	1.45 0.29	1.30 0.26	1.46 0.23	1.98 0.41	1.77 0.47	1.68 0.45	6.93 0.64	1.39 0.01	3.02 0.46	3.67 2.51
Phase shift [°]	20.7 0.2	22.8 1.0	21.7 2.0	23.3 1.4	20.0 0.4	22.0 2.3	22.1 2.2	22.1 2.6	24.2 0.3	21.7 0.8	23.5 0.2	23.6 1.2

* 20 °C   P03;P06;P08;P10   ^ 30 °C   P01;P02;P04;P05;P07;P09   # 40 °C   P12;P13

4.4.2.2   Verum with different duration of final homogenisation

In general, creams with different final homogenisation times showed similar behaviour during isothermal storage and during stress test.

4.4.2.2.1   25 °C/60 % RH

The water binding capacity increased and the creams became easier to spread. The declining hysteresis for both types of creams (table 4-50) was evident.

4.4.2.2.2   40 °C/75 % RH

The cream behaviour with regard to water binding capacity and spreadability (table 4-51) during storage at 40 °C was similar to that during storage at 25 °C. Whereas the phase shift always increased the gain in hysteresis was different. The gain in hysteresis at a storage temperature of 40 °C is a typical observation for the cream (placebo and verum).

4.4.2.2.3   Cycle test

Creams are more stable when alternate the temperatures between +5 and +40 °C. Changes during storage are only visible in electrical conductivity and in hysteresis (table 4-52).

Table 4-50: Verum pilot scale - different homogenisation times - 25 °C/60 % RH, n=10

Method	8.1 circulation times (7.5 min) Mean sd				13.6 circulation times (12.5 min) Mean sd			
Months	T0	1	3	6	T0	1	3	6
Conductivity µS/cm	38.8 2.2	28.2 1.9	28.3 1.1	28.3 1.9	32.5 2.3	29.0 1.2	29.5 1.2	27.9 0.0
Bleeding mm^2	914 119	818 141	814 78	855 163	954 123	890 113	952 9	780 5
Spreadability mm^2	1534 66	1787 179	1785 89	1992 237	1644 150	1938 144	1955 79	2154 532
Micro-penetration $mm*10^{-1}$	370 40	366 51	379 21	419 21	374 46	420 8	1955 79	453 31
Enthalpy J/g	58.14 0.91	59.51 1.92	60.64 1.48	60.39 1.49	59.77 2.32	59.27 1.36	60.07 0.78	60.82 1.97
T_{onset} °C	62.13 0.61	61.75 1.42	62.33 1.87	61.58 1.49	61.38 1.37	61.92 0.55	63.23 0.22	61.06 1.03
Viscosity mPa*s	460 25	471 19	475 47	444 55	450 34	444 32	439 47	482 28
Hysteresis Pa/s	1.41 0.22	1.20 0.21	1.00 0.24	0.93 0.09	1.32 0.21	1.05 0.25	0.93 0.16	0.99 0.14
Phase shift °	20.3 0.5	22.2 0.7	24.0 0.4	26.0 1.8	20.2 0.7	22.5 0.4	23.4 0.1	27.4 1.1

Table 4-51:   Verum pilot scale - different homogenisation times - 40 °C/75 % RH, n=10

Method	8.1 circulation times (7.5 min) Mean sd				13.6 circulation times (12.5 min) Mean sd			
Months	T0	1	3	6	T0	1	3	6
Conductivity µS/cm	38.8 2.2	21.8 1.4	21.6 1.5	21.9 2.5	32.5 2.3	21.9 1.8	19.8 0.1	20.1 3.2
Bleeding mm^2	914 119	811 109	609 140	557 71	954 123	911 185	664 66	517 74
Spreadability mm^2	1534 66	1803 151	1746 140	1731 147	1644 150	1749 111	1727 23	1627 92
Micro-penetration $mm*10^{-1}$	370 40	359 33	355 23	367 23	374 46	379 26	322 8	350 15
Enthalpy J/g	58.14 0.91	58.52 2.40	58.39 2.48	55.81 0.93	59.77 2.32	58.78 2.76	54.88 3.83	57.09 0.01
T_{onset} °C	62.13 0.61	59.84 1.36	60.38 1.98	58.54 0.93	61.38 1.37	60.93 1.07	61.27 1.22	58.74 1.33
Viscosity mPa*s	460 25	559 50	521 57	521 150	450 34	489 174	538 30	493 18
Hysteresis Pa/s	1.41 0.22	1.77 0.61	2.07 0.61	3.00 1.08	1.32 0.21	2.36 1.85	1.56 0.21	2.91 0.25
Phase shift °	20.3 0.5	24.4 1.5	25.5 0.6	27.2 1.0	20.2 0.7	24.8 0.6	25.7 0.1	27.4 1.4

Table 4-52: Verum pilot scale - different homogenisation times – Cycle test; n=10

Method	8.1 circulation times (7.5 min) Mean sd				13.6 circulation times (12.5 min) Mean sd			
Cycle	T0	1	2	3	T0	1	2	3
Conductivity µS/cm	38.8 2.2	28.3 1.9	27.3 1.8	26.9 1.7	32.5 2.3	30.1 1.4	29.6 1.7	28.3 1.5
Bleeding mm^2	914 119	976 193	827 66	888 138	954 123	872 83	943 81	983 91
Spreadability mm^2	1534 66	1481 90	1517 146	1585 112	1644 150	1501 45	1540 91	1548 151
Micro-penetration mm*10^{-1}	370 40	375 20	375 32	371 26	374 46	372 21	368 16	379 25
Enthalpy J/g	58.14 0.91	57.73 1.30	57.67 1.23	57.47 1.36	59.77 2.32	57.23 1.35	57.89 1.82	57.73 1.86
T_{onset} °C	62.13 0.61	61.14 1.87	61.93 1.36	60.94 1.52	61.38 1.37	62.31 0.94	61.22 2.57	61.09 1.61
Viscosity mPa*s	460 25	504 87	516 81	509 72	450 34	449 15	462 46	456 23
Hysteresis Pa/s	1.41 0.22	1.77 0.92	2.08 0.61	3.00 1.08	1.32 0.21	1.82 0.48	1.66 0.31	1.52 0.14
Phase shift °	20.3 0.5	22.3 1.9	21.9 2.0	22.6 2.2	20.18 0.70	20.1 0.9	20.4 0.6	20.1 0.9

4.4.2.3   Summary of verum stability testing

Stability results could not be interpreted unambiguously and not always in analogy with previous conclusions about the impact of single process parameters on the cream properties.

It could be observed, that cream properties changed only rarely during stress test compared to isothermal storage conditions. Actually, the worst stability was revealed at 25 °C/60 % RH, both for placebo and verum which was rather unexpected. Storage at 40 °C/75 % RH showed better stabilities than creams stored at 25 °C/60 % RH but lower stabilities than creams under cycle test.

Whereas creams during storage at room temperature became more spreadable, at elevated temperature (40 °C) they showed decreasing spreadability.

The water binding capacity during storage at 40 °C increased compared to storage at 25 °C. This rather unusual behaviour can be explained by the cream's microstructure. At ambient temperature hydrophilic and lipophilic gel-phases continued to crystallise. Thus they got more compact/elastic exhibiting higher melting enthalpies.

The water entrapped mechanical within the gel-phases was 'squeezed out', and water binding capacity is reduced. Samples stored at 40°C passed at least 1 cycle from 25 to 40 and back to 25 °C. Structures renewed by dissolving and swelling processes at elevated temperature. Water is entrapped in between the gel-phases. Thus water binding capacity was improved. Back to 25 °C both gel-phases crystallised and turned to starting point. Stability data from 40 °C/75 % RH and cycle test showed even after 6 month and 3 cycles respectively an advantage for the 40/40 °C creams in particular in water binding capacity.

Also rheological properties changed during storage. Whereas creams during storage at ambient temperature became less viscous and showed lower hystereses, at elevated temperature they tended to be more viscous showing increasing hystereses. However, the phase shift as an indicator for the elasticity of the system increased independently from the storage condition. The formulation lost in elasticity. At isotherm storage obviously the gel network looses its mechanical stability. Hydrophilic and lipophilic gel-phases were pressed together which resulted in the squeezing out of water. During cycle test rheological properties rarely changed. Dissolution and re-crystallisation processes which regenerated the gel structures most likely led to an improved mechanical stability.

API-addition/final homogenisation at 40 °C caused clearly different cream properties compared to API-addition /final homogenisation at 20 and 30 °C immediately after manufacturing. But as stability data showed, the supposedly improved consistency and robustness of the creams with API-addition/ homogenisation temperature of 40 °C were levelled out during storage. During storage, physical test results and macroscopic appearance became more and more similar to the other creams and even became identical after 3 months. These creams loss consistency and water binding capacity.

The primary homogeneous lipid and water phases, during cooling crystallised in hydrophilic and lipophilic gel-phases separately from each other. In other words hydrophilic and lipophilic gel-phases segregate. This crystallisation process has not yet finished at 40 °C. Water is most likely is entrapped mechanically within this gel-matrix. Cetearyl alcohol crystallised because of its low solubility in either of the phases. Lumps in the following days were the consequence. Lumps obviously contained less water and thus led to a higher water binding capacity of the cream (less bleeding and electrical conductivity). With time these lumps swelled more and more by binding water and disappeared/dissolved. Finally, after 3 months the 40/40 °C creams appeared smooth and similar to the others.

Different temperatures of API-addition and final homogenisation did not significantly influence the physical cream properties in a long-term comparison. The duration of final homogenisation in the comparison 8.1 vs 13.5 times of circulation was not critical, neither immediately after production nor after different storage programs.

5   CONCLUDING DISCUSSION

The impact of the processing conditions on the properties of semi-solid preparations is well known. Deviations in the production scheme are frequently the reason for OOS results and stability problems. Very few studies, however, that address this challenging field were reported in literature. Thus the overall objective of this study was to evaluate systematically the influence of the different manufacturing steps on the resulting product quality. More specifically the goals of this study were to evaluate the effect of melting, cooling, homogenisation, filling procedure, and holding time after production on the properties of a hydrophilic cream which contains 20 % (w/w) azelaic acid as the active pharmaceutical ingredient. Characterisation of the model cream was accomplished by a series of methods. Hence, secondary aim of this study was to assess these methods in terms of their cost-benefit ratio.

The proper interpretation of the diverse test results requires at least a rough structural characterization of the semi-solid preparation. The o/w cream consists of a gel-matrix comprised by the visco-elastic hydrophilic gel-phase and the lipophilic gel-phase which crystallize separately from each other to a fine and complex network immobilizing small oil droplets. This network forms a disordered liquid-crystalline structure of lamellar type, placed either at the border of the oil droplets or widespread towards the continuous phase. The gel-matrix comprises different water phases: inter-lamellarly bound water, water mechanically entrapped in the lipophilic gel phase, water fixed between lipid layers in liquid-crystalline state, and free bulk water.

From literature it could be expected that the structure might be explained by the bi-lamellar four-phase system as described for the non-ionic hydrophilic cream DAC by Junginger et al. (1984) or by a complex gel-matrix model as described by Savic et al. (2005). WAXD, SAXD, DSC, DTG and microscopy revealed, that the cream can be most likely described as a complex gel-matrix of hydrophilic and lipophilic crystalline phases with randomly oriented multilayer that contributes to the oil droplets immobilization.

The semi-solid character is largely provided by a lipohilic gel consisting predominantly of cetearyl alcohol hemi-hydrate as supported by the findings from SAXD and DSC. The oily phase forms small droplets surrounded by a lamellar liquid-crystalline layer of the emulsifier. It becomes visible in the polarized light microscope from the maltesian crosses which can be seen at the oil water inter-phase. Interestingly, there are no signals in the SAXD diagrams which give a hint for the existence of lamellar structures other than the fatty alcohol hemi-hydrate crystals.

Obviously, the amount is not sufficient to give a signal or the inter-lamellar spacing in this complex mixture is not as well defined as to show sharp interferences in the SAXD.

Due to the results from DTG measurements water seems to be incorporated as either free (unbound) water or water which is entrapped within the gel network. As SAXD measurements on model mixtures of emulsifier and lipid components with different water content gave no evidence for a swelling of a lamellar phase, it was not possible to further decide in which form - either inter-lamellarly or mechanically bound - water is entrapped within the gel network. Furthermore, in verum creams it was not possible to clearly differentiate between the fraction of bound and unbound water.

The API is only partially soluble in the cream base and thus the main fraction is found as finely suspended crystals. With increasing temperature the solubility of azelaic acid in the cream increases dramatically. The onset temperature of the phase transition from solid to liquid was reached at approx. 70 °C in the cream formulation. This is 38 °C below the melting temperature of the pure API.

The dominance of the cetearyl alcohol crystals in the framework of the cream is also visible in the mechanical properties of the cream. It is very shear sensitive when the shear stress exceeds a certain limit. At low shear stress the o/w cream behaves predominantly elastic. However, as soon as structural break down started, the cream showed profound shear thinning. As the recovery of the structure required at least hours and even when it was incomplete, the rheograms showed largely hysteresis during the first shear cycle. Subsequently, the creams show plastic flow behaviour with low yield stress, little shear thinning and negligible hysteresis.

These general findings concerning the properties of the investigated cream were the starting point to analyse how changes in the processing conditions change the cream quality. The following steps were identified as to be eventually critical: the effect of melting, cooling, homogenisation, filling procedure, and holding time after production.

The melting parameters of the fatty phase were expected to be of minor importance. Supposed the fatty phase was completely molten and no chemical decomposition occurs this should not have an impact on the cream properties. This was confirmed by the data obtained immediately after processing (t_0). However, during storage creams prepared at a high melting temperature and melting time (90 °C and 210 min) became more often favourable regarding consistency, hysteresis, viscous/elastic properties and water binding capacity. Actually, a melting temperature of 65 °C for 30 min led to a considerable loss in consistency/viscosity with strongly increasing conductivity and even collapsing oscillatory parameters, not

immediately after manufacturing but after storage. Maintaining a melting temperature at the upper limit (75 °C) of the default range (65-75 °C) in order to avoid occurrence of solidification of lipids when melting near the solidification temperature of surfactant and amphiphile could be an advantage. On the other hand, the melting time should be kept short in order to save energy and time and in order to minimize the instance of chemical decomposition.

From the rheological characterization it was seen that mild or moderate shear stress as applied during filling activities affected the structure of the cream only marginally. Evaluating the changes of the rheological behaviour the days after preparation showed that there was no difference if the cream was stored in bins before filling or if it was filled into tubes and stored afterwards. That means that the time point of filling is not decisive for the final cream properties and it does not matter if holding time is applied on the bulk cream or on the finished product. Hence, from an economical point of view (i.e. saving time for keeping of deadlines) it appears recommendable to fill the cream quickest possible after manufacturing. A holding time of the finished product (tube) of 5 days is necessary before a stable product is obtained and the maximum API-solubilization level is reached.

Furthermore rheology impressively documented the sensitivity of the formulation to high shear forces after the gel network was established. This behaviour could be easily explained by the colloidal structure of the cream. By exceeded shearing, in particular after cold homogenisation the gel-network of the two separately crystallised gel-phases (the hydrophilic and the lipophilic one) becomes partially irreversibly destroyed. It takes at least several months to completely recover the gel-structure. Homogenisation is accompanied by strong temperature increase which most likely induces a partly melting of the lipophilic gel-lattice. It re-crystallises forming a more compact gel-lattice where water gets squeezed out from it. For this reason it is suggested to reduce the final homogenisation time in order to alter the cream-framework as less as possible but to conserve available microtextures formed by crystallisation after cooling. With reference to earlier investigations a high level of API-homogeneity was shown just after a single total batch circulation. A security margin of 5 min appears to be sufficient for a homogeneous dispersion of the API.

An alternative proposal to the cooling process which is generally performed in non-linear mode is a more moderate and in particular steady cool down which allows a regular formation of both crystalline gel-structures and consequently even in the gel-matrix distributed different water phases. A cooling in non-linear mode may add to the risk of a 'shock'-crystallisation which inhibits the unbothered build-up of a well structured network widespread towards the continuous phase or immobilizing the oil droplets.

A higher API-addition/ final homogenisation temperature (40 °C instead of 26-30 °C) was thought to improve applications (e.g. spreadability and viscosity increase) and physical cream properties (e.g. increase of water binding capacity). The API-dissolution process within the gel-matrix which slowly occurs after normal manufacturing may be accelerated at 40 °C. As DSC results showed the API gets most likely solubilized within the gel-phases. Unfortunately, storage stability data showed that the initially improved cream properties do not last for a long time.

The initially appeared lumps (caused by a final cooling without stirring) confirmed the idea of two gel-networks which organize separately from each other entrapping the water in the system in different modes. Homogeneously separation of hydrophilic and lipophilic gel phases (disordered system) is hindered when stirring during cool down to room temperature is absent. Namely, during storage these lumps swelled and formed a gel-network belatedly. For that reason, a temperature change between 20 and 30°C does not cause microstructural and hence physical changes because dissolution processes do not or occur rarely.

In contrast to storage recommendations (< 30 °C) are stability data. Namely, cream samples have shown to be more stable during storage at temperatures above 30 °C as well as by applying temperature changes of 35 °C within the positive region. Cream samples stored at ambient temperature generally loss clearly in viscosity. Hydrophilic and lipophilic gel-phases crystallise squeezing out water with decreasing water binding capacity in consequence.

From available data we suggest an alternative proposal for manufacturing the model cream:

Melting time: $\leq$ 30 min; Melting temperature: $\geq$ 70 °C

Steady cooling rate: 0.5 – 0.75 °C/min

Temperature during API-addition: < 40 °C

Temperature during final homogenisation: < 40 °C

Duration of final homogenisation: 5 min (1st); 2 min (2nd if necessary)

Filling: immediately after manufacturing

Holding time: 5 days in the tube (no HT in bulk)

Concerning the suitability and relevance of the characterisation methods the following conclusions can be drawn:

Water binding and phase separation within the cream can be easily evaluated by bleeding measurements and electrical conductivity measurements. In contrast, TGA measurements were less worthwhile. Here the cost-benefit ratio was less favourable because the information was sparse and the measurements were hardly reproducible. DSC on the other hand could provide valuable results on the stability of the formulation.

Spreadability and micropenetration proved to be important clues for the application properties of the cream. In particular bleeding, electrical conductivity and spreadability provided the possibility of a quick and easy operation, gave reliable information on the cream quality immediately after manufacturing as well as stability data during storage.

Rheology undoubtedly provided the most informative and detailed results. It was an indispensable tool to get valuable insight into the cream structure as well as to visualize changes in the flow and viscous/elastic cream behaviour as reaction on modification of process parameters for instance as consequence of increased shear force. Relevant parameters from shear measurements were flow curve with viscosity and hysteresis. Oscillatory rheology provided information about the visco-elastic properties expressed as elastic and viscous modulus, and phase shift. To determine the yield stress from shear rheology was less valuable as far as it was less reproducible. A better alternative might be to extract the yield stress from the cross over in stress sweep curves in the oscillatory mode.

X-ray diffraction was the most sophisticated technique used in this study. This method is far away from routine and is only necessary where more detailed insights in the colloidal structure are required.

However, even none of the other methods can be used as a real 'In process control' or is suited as process analytical technology (PAT), which gives continuous information about the process and can be integrated into control loops.

Nevertheless, the selected methods were able to distinguish physical cream properties in dependency of the manufacturing process and allowed to explain possible causes of cream deficiencies.

6 LITERATURE

Alberg, U. 1998. Wasserhaltige hydrophile Salbe DAB mit suspendiertem Hydrocortisonacetat - Einfluß von Ethanol auf die Mikrostruktur der Cremes, Arzneistofffreigabe und Arzneistoffpermeation durch humanes Stratum corneum. Dissertation, TU Braunschweig.

Asche, H., D. Essig, and P. C. Schmidt. 1984. Technologie von Salben, Suspensionen und Emulsionen. Paperback APV. **10:** WVG mbH Stuttgart.

Ash, M., and I. Ash. 1994. Handbook of cosmetic and personal care additives. Gower Publishing Limited, Aldershot.

Attwood, D., P. H. Elworthy, and M. J. Lawrence. 1990. Effect of structural variations of non-ionic surfactants on surface properties: surfactants with semi-polar hydrophobes. *J. Pharm. Pharmacol.* **42:** 581-583.

Barnes, H. A. 1999. A brief history of the yield stress. *Applied Rheology* **9** (6)**:** 262-266.

Barry, B. W. 1974. Rheology of pharmaceutical and cosmetic semisolids. *Adv. Pharm. Sci.* **4:** 1-72.

Barry, B. W., and G. M. Eccleston. 1973. Influence of gel networks in controlling consistency of o/w emulsions stabilised by mixed emulsifiers. *J. Texture Stud.* **3:** 53-81.

Barry, M. D., and R. C. Rowe. 1989. The characterisation by small-angle X-ray scattering of a pharmaceutical gel with a lamellar structure. *Int. J. Pharm.* **53:** 139-143.

Bauer, K., K.-H. Frömming, and C. Führer. 1991. Pharmazeutische Technologie. 3. Auflage. Georg Thieme Verlag, Stuttgart.

Becomix. Instruction manual. Berents GmbH & Co KG, Stuhr.

Beiersdorf AG. 1999. Conference Report IV: DGK Workshop 'The rheology of cosmetic emulsions'. *Applied rheology* **9** (6)**:** 272-273.

Bouwstra, J.A., G. S. Gooris, J. A. van der Spek, and W. Bras. 1991. Structural investigations of human stratum corneum by small-angle X-ray scattering. *The Journal of Investigative Dermatology* **97:** *1005-1012.*

Bouwstra, J.A., G. S. Gooris, A. Weerheim, J. Kempenaar, and M. Ponec. 1995. Characterization of stratum corneum structure in reconstructed epidermis by X-ray diffraction. *Journal of lipid research* **36:** 496-504

Brämer, A. 2004. Direktdampfinjektion - ein Verfahren zur Herstellung halbfester Zubereitungen. Dissertation, TU Braunschweig.

EMEA, CPMP. 2003. Guideline on stability testing: Stability testing of existing active substances and related finished products. EMEA. Public CPMP/QWP/122/02 rev 1.

Daniels, R., and U. Knie. 2007. Galenics of dermal products - vehicles, properties and drug release. *JDDG* **5:** 367-382.

Davis, S. S. 1969. Viscoelastic properties of pharmaceutical semisolids: II. Creams. *J. Pharm. Sci.* **58** (4)**:** 418-421.

De Vringer, T., J. G. H. Joosten, and H. E. Junginger. 1986. A study of the gel structure in a non-ionic o/w cream by differential scanning calorimetry, *Coll. Polym. Sci*. **264:** 691-700.

De Vringer, T., J. G. H. Joosten, and H. E. Junginger. 1987. A study of the gel structure in a non-ionic o/w cream by X-ray diffraction and microscopic methods. *Coll. Polym. Sci.* **265:** 167-179.

De Vringer, T., J. G. H. Joosten, and H. E. Junginger. 1987. A study of the ageing of the gel structure in a non-ionic o/w cream by X-ray diffraction, differential scanning calorimetry and spin-lattice relaxation measurements. *Coll. Polym. Sci.* **265:** 448-457.

De Vringer, T., J. G. H. Joosten, and H. E. Junginger. 1984. Characterization of the gel structure in a non-ionic ointment by small angle X-ray diffraction. *Coll. Polym. Sci.* **262:** 50-56.

Eccleston, G. M. 1986. Application of emulsion stability theories to mobile and semisolid o/w emulsions *Cosmet. & toilet.* **101:** 73-92.

Eccleston, G. M. 1977. Influence of long chain alcohols (or acids) and surfactants on the stabilities and consistencies of cosmetic lotions and creams. *Cosmet. & toilet.* **92:** 21-28.

Eccleston, G. M. 1990. Multiple-phase oil-in-water emulsions. *J. Soc. Cosmet. Chem.* **41:** 1-22.

Eccleston, G. M. 1986. The microstructure of semisolid creams. *Pharm. Intern*. **3:** 63-70.

Eccleston, G. M. 1976. The structure and rheology of pharmaceutical and cosmetic creams. *J. Coll. Interf. Sci.* **57** (1)**:** 66-74.

Eccleston, G. M., and L. Beattie. 1988. Microstructural changes during the storage of systems containing cetostearyl alcohol/polyethylene alkyl ether surfactants. *Drug Dev. Ind. Pharm.* **14:** 2499-2518.

Eccleston, G. M., L. Beattie. 1989. The influence of emulsifier composition on the microstructure of non-ionic semisolids. *J. Pharm. Pharmacol.* **40**.

Eccleston, G. M., M. K. Behan, G. R.Jones, and E. Towns-Andrews. 1988. Swelling properties of emulsifying wax-water gel phases. *J. Pharm. Pharmacol.* **39**.

Eccleston, G. M., M. K. Behan, G. R. Jones, and E. Towns-Andrews. 2000. Synchrotron X-ray investigations into the lamellar gel phase formed in pharmaceutical creams prepared with cetrimide and fatty alcohols. *Intern. J. of Pharm.* **203** (1-2)**:** 127-139.

Eros, I., M. Konya, and I. Csoka. 2003. Study of the structure of coherent emulsions. *Intern. J. of Pharm.* **256:** 75-84.

European pharmacopoeia (Ph. Eur.) 2005. 5th edition with 3rd supplement. Council of Europe, Strasbourg. 135-136.

Folger, M. 1994. Einfluss der Herstellungstechnologie auf die Stabilität flüssigkristalliner Strukturen in topischen Zubereitungen. Dissertation, TU Braunschweig.

Ford, J. L., and P. Timmins. 1989. Pharmaceutical thermal analysis, techniques and applications. Ellis Horwood Limited, Chichester.

Franke, P., K. Hoffmann, U. Täuber, and S. Keipert. 1996. In-vitro-Liberationsstudien aus Steroidsalben. *Pharm. Ind.* **58** (12)**:** 1152-1156.

Frigoli, C. 2001. Sviluppo e convalida di un metodo di determinazione del rilascio in vitro del principio attivo da forme farmaceutiche semisolide per uso topico. thesis for a degree, University of Milan.

Führer, C. 1971. Gelgerüste von Fettalkoholen in Salbengrundlagen. *Pharmazie.* **26:** 43-45.

Führer, C. 1981. Systematik der Dermatika. *Acta Pharm. Technol*. **27** (2)**:** 67-75.

Führer, C., J. G. H. Junginger, and S. Friberg. 1978. Strukturuntersuchungen von Salben 1. Mitteilung: Röntgenuntersuchungen an der Hydrophilen Salbe DAB 7. *J. Soc. Cosmet. Chem.* **29:** 703-716.

Fukushima, S., M. Takahashi, and M. Yamaguchi. 1976. Effect of cetostearyl alcohol on stabilization of oil-in-water emulsion: I. Difference in the effect by mixing cetyl alcohol with stearyl alcohol. *J. Coll. Interf. Sci.* **57:** 201-206.

Fukushima, S., M. Yamaguchi, and F. Harusawa. 1977. Effect of cetostearyl acohol on stabilization of oil-in-water emulsion: II. Relation between crystal form of the alcohol and stability of the emulsion. *J. of coll. Interf. Sci.* **59** (1)**:** 159-165.

Funke, K. 1972. Die Verkürzung der Herstellzeiten kosmetischer Emulsionen durch Kaltemulgierung. *Seifen – Öle – Fette – Wachse.* **98** (14)**:** 457-459.

Gedde, U. W. 1990. Thermal analysis of polymers. *Drug devel. Ind. Pharm.* **16** (17)**:** 2465-2486.

Girod, S., F. Rodriguez, and J. L. Grossiord. 2005. Formulation strategy for semi-solid forms (ointments, creams): contribution of rheology. *STP Pharma Pratiques.* **15** (3)**:** 255-263.

Griffin, W. C. 1949. Classification of surface-active agents by HLB. *J. Soc. Cosmet. Chem.* 311-326.

Grimm, W. 1998. Extension of the international conference on harmonization tripartite guideline for stability testing of new drug substances and products to contries of climatic zones III and IV. *Drug Devel. And Ind. Pharm*. **24:** 313-325.

Grimm, W. 1985. Storage conditions for stability testing-long term testing and stress tests. *Drugs made in Germany: Part I*. **28:** 196-202.

Grimm, W. 1986. Storage conditions for stability testing-long term testing and stress tests. *Drugs made in Germany: Part II*. **29:** 39-47.

Haake Rheowin Pro. 2004. Instruction manual. Thermo Electron Corporation. Karlsruhe.

Hadjistamov, D. 2003. The yield stress – a new point of view. *Applied rheology* **13** (4)**:** 209-211.

Haighton, A. J. 1959. The measurement of the hardness of margarine and fats with cone penetrometers. *J. Amer. Oil Chem. Soc.* **36:** 345-348.

Junginger, H. E. 1984. Colloidal structures of o/w creams. *Pharmaceut. Weekblad.* **6:** 141-149.

Junginger, H. E. 1987. Kristalline Gelstrukturen in Cremes. *DAZ.* **131:** 1933-1941.

Junginger, H. E. 1984. Strukturuntersuchungen an Stearatcremes. *Pharm. Ind.* **46** (7)**:** 758ff.

Junginger, H. E. 1984. Verhältnis von freiem und interlamellar fixiertem Wasser als Qualitätskriterium für O/W Cremes. *Pharmazie.* **39:** 610-614.

Junginger, H., A. A. M. D. Akkermans, and W. Heering. 1984. The ratio of interlamellary fixed water to bulk water in o/w crèmes. *J. Soc. Cosmet. Chem.* **35:** 45-57.

Junginger, H. E., C. Führer, A. Beer, and J. Ziegenmeyer. 1979. Polymorphie bei Salben. *Pharm. Ind.* **41** (4)**:** 380-385.

Junginger, H. E., C. Führer, J. Ziegenmeyer, and S. Friberg. 1979. Strukturuntersuchungen von Salben, 2. Mitteilung: Strukturuntersuchungen an der Wasserhaltigen hydrophilen Salbe DAB 7. *J. Soc. Cosmet. Chem.* **30:** 9-23.

Junginger, H., and W. Heering. 1983. Hydrophile Gelstrukturen in O/W Cremes, Charakterisierung mit Hilfe mikroskopischer Verfahren. *DAZ.* **42:** 1988-1992.

Junginger, H., W. Heering, C. Führer, and I. Geffers. 1981. Elektronenmikroskopische Untersuchungen über den kolloidchemischen Aufbau von Salben und Cremes. *Coll. Polym. Sci.* **259:** 561-567.

Kallioinen, S, K. Helenius, and J. Yliruusi. 1994. Influence of storage time and temperature on the stability of some emulsion creams. *Pharmazie* **49** (7)**:** 500-505.

Kallioinen, S, K. Helenius, and J. Yliruusi. 1995. Structure of non-ionic emulsion creams studied by analytical methods. *Pharmazie.* **50** (7)**:** 478-481.

Kiessig, H. 1942. Röntgenuntersuchungen großer Netzebenenabstände und Untersuchung strömender Lösungen. *Kolloid – Z.* **98:** 213-217.

Köhler, H. J. 1992. Herstellung im Produktionsmaßstab. *In* Dermatika: Therapeutischer Einsatz, Pharmakologie und Pharmazie. Niedner, Ziegenmeyer. Wissenschaftliche Verlagsgesellschaft mbH, Stuttgart.

Kònya, M., M. Sorrenti, F. Ferrari, S. Rossi, I. Csòka, C. Caramella, G. Bettinetti, and I. Eròs. 2003. Study of the microstructure of oil-in-water creams with thermal and rheological methods. *J. Therm. Anal. & Calor.* **73:** 623-632.

Krischner, H. 1974. Einführung in die Röntgenfeinstrukturanalyse. Vieweg & Sohn Verlagsgesellschaft mbH, Braunschweig.

Kudlek, B. 1996. Kolloidstruktur und Entstehungsmechanismus von Produktvarianten einer halbfesten Zubereitung, Dissertation, TU Braunschweig.

Laba, D. 1993. Rheological properties of cosmetics and toiletries. *Cosmet. Sci. and techn. Series.* **13:** Marcel Dekker, New York.

Lashmar, U. T., and J. Beesley. 1993. Correlation of rheological parameters of an oil in water emulsion with manufacturing procedures and stability. *Int. J. of Pharm.* **91:** 59-67.

Lashmar, U. T., J. P. Richardson, and A. Erbod. 1995. Correlation of physical parameters of an oil in water emulsion with manufacturing procedures and stability. *Int. J. of Pharm.* **125:** 315-325.

Leuenberger, H. 2002. Martin Physikalische Pharmazie. 4. Auflage. Wissenschaftliche Verlagsgesellschaft mbH, Stuttgart.

Liebermann, H. A. 1998. Pharmaceutical Dosage forms: Disperse Systems. **3** (2).

List, P. H. 1985. Arzneiformenlehre. 4. Auflage. Wissenschaftliche Verlagsgesellschaft mbH Stuttgart.

Maue, R., F. Moll. 1987. Stabilisierung und Destabilisierung von Emulsionen unter Einwirkung von Mikrowellen. *Acta Pharm. Technol.* **33** (4)**:** 225-230.

Marini, A. 2003. Eccipienti farmaceutici: Compatibilità farmaco-eccipiente, Caratterizzazione chimico-fisica di principi attivi: a case study, Master universitario di 2° livello in preformulazione e sviluppo galenico, Università degli studi di Pavia.

Marini, A. 2003. Eccipienti farmaceutici: Compatibilità farmaco-eccipiente, Parte I – tecniche chimico fisiche di indagine, Master universitario di 2° livello in preformulazione e sviluppo galenico, Università degli studi di Pavia.

Martin, A., G. S. Banker. 1964. Rheology. Advances in Pharmaceutical Sciences. Academic Press London, New York **1:** 1 ff.

Mettler Toledo. 1995. Collected applications thermal analysis: Pharmaceuticals, Schwerzenbach.

Mettler Toledo. 1995. Operating Instructions TA 4000 System, Schwerzenbach.

Metzger, T. 2000. Das Rheologie-Handbuch, Vincentz Verlag, Hannover.

Mitchell, D. J., J. T. Tiddy, and L. Waring. 1983. Phase behaviour of polyoxyethylene surfactants with water. *J. Chem. Soc.* Faraday Trans. I, **79:** 975-1000.

Moore, W. S., and P. O. Hummel. 1986. Viskosität von Polymerlösungen, Physikalische Chemie Wd Gruyter Verlag. 1170-1174.

Müller-Goymann, C. C., M. Folger, and T. Rades. 1991. Salben, Cremes, Gele, Pasten *In*: Nürnberg, E., Surmann, P. Hagers Handbuch der Pharmazeutischen Praxis. 5. Auflage. Springer Verlag, Berlin-Heidelberg-New York. 871ff.

Müller-Goymann, C. C., and B. Usselmann. 1989. Mikrostruktur von 4-Komponenten-Cremes, *Acta Pharm. Technol.* **35** (3)**:** 116-120.

Niedner R., and J. Ziegenmeyer. 1992. Dermatika: Therapeutischer Einsatz, Pharmakologie und Pharmazie. Wissenschaftliche Verlagsgesellschaft mbH, Stuttgart.

Niemi, L., and E. Laine. 1991. Effect of water content on the microstructure of an oil-in-water cream. *Intern. J. of Pharm.* **68:** 205-214.

Nürnberg, E., and R. Muckenschnabel. 1982. Hydrophile und ambiphile Cremesysteme. *DAZ.* **122:** 2093-2106.

Ohwaki, T., R. Machida, H. Ozawa, Y. Kawashima, T. Hino, H. Takeuchi, and T. Niwa. 1993. Improvement of the stability of water-in-oil-in-water multiple emulsions by the addition of surfactants in the internal aqueous phase of the emulsions. *Int. J. Pharm.* **93:** 61-74.

O'Laughlin, R., C. Sachs, H. Brittain, E. Cohen, P. Timmins, and S. Varia. 1989. Effects of variation in physicochemical properties of glycerol monostearate on the stability of an oil-in-water cream. *J. Soc. Cosmet. Chem.* **40:** 215-229.

Park, B. D., J. K. Youm, S. K. Jeong, E. H. Choi, S. K. Ahn, and S. H. Lee. 2003. The characterization of molecular organization of multilamellar emulsions containing pseudoceramide and type III synthetic ceramide. *Journal of Investigative Dermatology* **121:** 794-801.

Paspaleeva-Kühn, V., and E. Nürnberg. 1992. Participation of macrogolstearate 400 lamellar phases in hydrophilic creams and vesicles. *Pharm. Res.* **9** (10)**:** 1336-1340.

Patel, H. K., R. C. Rowe, J. Mc Mahon, and R. F. Stewart. 1985. A comparison of the structure and properties of ternary gels containing cetrimide and cetostearyl alcohol obtained from both natural and synthetic sources. *Acta Pharm. Technol.* **31** (4)**:** 243-247.

Patel, H. K., R. C. Rowe, J. Mc Mahon, and R. F. Stewart. 1985. An investigation of the structural changes occurring in a cetostearyl alcohol/cetrimide/water gel after prolonged low temperature (4 °C) storage. *J. Pharm. Pharmacol.* **37:** 899-902.

Physika Meßtechnik GmbH. 1991. Applikationstag: Pharma und Kosmetik, Stuttgart.

Physika Meßtechnik GmbH. 1991. Ein kleiner Rheologiekurs, Teil 2: Oszillation, Stuttgart.

Remington. 2005. The Science and Practice of Pharmacy. 21st ed. Lippincott Williams & Wilkins, Baltimore.

Ries, R., and F. Moll. 1991. Thermoanalytische Charakterisierung von Wachsen, Fetten und verwandten Formulierungshilfsstoffen. *PZ Wissen* **136** (4)**:** 167-172.

Rose, C. 1999. Stabilitätsbeurteilung von O/W Cremes auf Basis der Wasserhaltigen Hydrophilen Salbe DAB 1996. Dissertation, TU Braunschweig.

Rose, C, and R. Daniels. 1999. Grundlagen der Rheologie - Anwendungsbeispiele zur Stabilitätsprüfung von Dermatika. *PZ Prisma.* **2:** 129-139.

Rose, C, and R. Daniels. 2000. Stabilitätsbeurteilung von O/W-Cremes mit Hilfe der Oszillationsrheologie Teil 1. *Pharm. Ind.* **62** (9)**:** 726-729.

Rose, C, and R. Daniels. 2000. Stabilitätsbeurteilung von O/W-Cremes mit Hilfe der Oszillationsrheologie Teil 2. *Pharm. Ind.* **62** (10)**:** 811-815.

Rowe, R. C. 1987. Water distribution in creams prepared using cetostearyl alcohol and cetrimide. *J. Pharm. Pharmacol*. **39:** 642-643.

Rowe, R. C., and H. K. Patel. 1985. The effect of temperature on the conductivity of gels and emulsions prepared from cetrimide and cetostearyl alcohol. *J. Pharm. Pharmacol.* **37:** 564-567.

Savic, S., G. Vuleta, R. Daniels, and C.C. Müller-Goymann. 2005. Colloidal microstructure of binary systems and model creams stabilized with an alkylpolyglucoside non-ionic emulsifier. *Colloid Polym Sci*. **283:** 439-451.

Savic, S., G. Vuleta, J. Milic, S. Tamburic, R. Daniels, and C.C. Müller-Goymann. 2005. Structural characterisation of multiphase emulsion systems based on an alkylpolyglucoside non-ionic emulsifier. *La rivista italiana delle sostanze grasse.* **LXXXII:** 236-244.

Schambil, F. 1985. Neue Methoden zur Charakterisierung der Stabilität von W/O- und O/W-Emulsionen. *Seifen – Öle – Fette – Wachse*. **115** (15)**:** 515.

Sepulveda, E, D. O. Kildsig, and E. S. Ghaly. 2003. Relationship between internal phase volume and emulsion stability: the cetyl alcohol/stearyl alcohol system. *Pharm. Develop. and Techn.* **8** (3)**:** 263-275.

Shinoda, K., H. Saito, and H. Arai. 1971. The effect of the size and the distribution of the oxyethylen chain lenghts of nonionic emulsifiers on the stability of emulsions. *J. Coll. Int. Sci.* **35:** 624.

Schramm, G. 1995. Einführung in die Rheologie und Rheometrie. Gebrüder Haake GmbH, Karlsruhe.

TA Instruments. Thermal solutions: separation of free and bound water in pharmaceuticals. TA Instruments Thermal Analysis & rheology. http://www.tainst.com.

Tadros, Th. F. 1994. Fundamental principles of emulsions: rheology and their applications. *Coll. Surfaces A. Physicochem. and Engin. Aspects*. **91:** 39-55.

Taleb, A., and I. Eròs. 1996. Rheological studies of creams, **I**. Effect of water content on rheological characteristics. *Acta. Pharm. Hungarica* **66:** 71-76.

Taleb, A., and I. Eròs. 1996. Rheological studies of creams. III. Effect of lipophilic phase on consistency. *Acta. Pharm. Hungarica* **66:** 77-82.

Thakker, K. D., and W. H. Chern. 2003. Development and validation of In vitro release tests for semisolid dosage forms – case study. *Dissolution Technologies* 10-15.

The Merck Index. 2001. 13th ed. Merck Research Laboratories Division of Merck & Co, Whitehouse Station.

Timmins, P., I. Browning, and N. I. Payne. 1990. Differential scanning calorimetry characterization of process-induced variations in an ointment base. *J. Pharm. Pharmacol*. **42:** 583-585.

USP 29. NF 24. 2006. The United States Pharmacopeial Convention, Rockville.

Virtanen, S., J. Yliruuse, and E. Selkainaho. 1993. Effect of the amount of nonionic emulsifier and cooling rate on the rheological properties of some emulsions, *Pharm. Technol. Europe*. Oct. 40-50.

Virtanen, S., J. Yliruuse, E. Selkainaho, M. Niskanen, and T. Niskanen. 1993. Effect of different storage temperatures on the rheological characteristics and droplet size of non-ionic emulsifier containing emulsions. *Pharmazie*. **48:** 48-53.

Voigt, R. 1993. Pharmazeutische Technologie für Studium und Beruf, Ullstein Mosby.

Weipert, D., H. D. Tscheuschner, and E. Windhab. 1993. Rheologie der Lebensmittel, Behrs Verlag.

Wells, J. I. 1988. Pharmaceutical preformulation: the physicochemical properties of drug substances. Ellis Horwood Limited, Chichester.

Wood, J. H. 1986. Pharmaceutical Rheology *In*: Lachman, L., Lieberman, H. A., Kanig, J. L., eds. The theory and practice of industrial pharmacy. Lea & Febinger. Philadelphia, 123-145.

Zografi, G. 1982. Physical stability assessment of emulsions and related disperse systems: a critical review. *J. Soc. Cosmet. Chem.* **33:** 345-358.

Freie Universität Berlin:

Prof. Dr. Dr. W. Schunack

Prof. Dr. M. Schäfer-Korting

Prof. Dr. E. Eich

Prof. Dr. Roland Bodmeier

Prof. Dr. R.H. Müller

Prof. Dr. S. Elz

Prof. Dr. H. Kolodziej

Prof. Dr. H.H. Pertz

Prof. Dr. W. Löwe

Prof. Dr. Ronald Gust

Prof. Dr. B. Kleuser

Eberhard-Karls-Universität Tübingen:

Prof. Dr. R. Daniels

Curriculum vitae

Name:	Anja Großmann
Date of birth:	10.11.1976
Place of birth	Räckelwitz, Germany
Nationality:	German
Marital status:	Single

Education:	1983 - 1991 Unified comprehensive school 'Erich-Weinert', Kamenz
	1991 - 1995 Grammar school 'Lessinggymnasium', Kamenz *Qualification*: Entrance requirement for higher education
Training:	08/1995 - 03/1998 Training college of pharmacy, Leipzig *Qualification*: Pharmaceutical assistant (PTA)
Higher education:	04/1998 - 06/2002 University pharmaceutics course, Freie Universität, Berlin
	08/2002 - 01/2003 Practical training, Schering AG, Berlin
	02/2003 - 07/2003 Practical training, pharmacy 'Prenz'l Apotheke', Berlin
	08/2003 Degree in pharmaceutics Licence to practise as a pharmacist
Experience:	08/1998 - 06/2000 Employed as PTA, pharmacy 'Neukölln Apotheke', Berlin
	07/2000 - 12/2001 Employed as PTA, pharmacy 'Ahorn-Apotheke', Schwepnitz
	09/2003 - 12/2003 Employed as pharmacist, pharmacy 'Prenz'l Apotheke', Berlin
	01/2004 - 12/2006 Doctoral thesis (PhD), pharmaceutical production, Schering S.p.A./ Intendis Manufacturing S.p.A. (Bayer group), Milan, Italy
	Since 01/2007 Employee, System qualification (QA), Intendis Manufactuirng S.p.A., Milan, Italy